Report on Amur-Okhotsk Project

No.4

February 2007

Research Institute for Humanity and Nature

Contents

Contents

Contents

PROGRESS REPORT OF THE AMUR-OKHOTSK PROJECT 2006

SHIRAIWA TAKAYUKI
Research Institute for Humanity and Nature
Leader of the Amur-Okhotsk Project

1. OBJECT AND CONTENTS OF THE PROJECT

The object of the project is to elucidate role of the Amur river on the primary productivity in the Sea of Okhotsk and northern North Pacific, then to evaluate possible human impacts such as land surface disturbances in the Amur river basin on the marine ecosystem of the ocean (Narita and Shiraiwa, 2003, 2004; Shiraiwa, 2005a, 2005b, 2006a, 2006b). In this study, we try to answer following five questions; 1) How the dissolved iron is transported from the Amur river basin to the Sea of Okhotsk and the northern North Pacific through the Amur river and by ocean current ?; 2) To what extent the supply of dissolved iron is regulating the primary production in the Sea of Okhotsk and the northern North Pacific ?; 3) How the land surface disturbance affects on the material circulation in the Amur-Okhotsk system ?; 4) How the human impacts will change the system in the future ?; and 5) How we can conserve this environmental system which expands across the international boundaries ? By solving these five questions, we will propose a new global environmental concept "*Giant" Fish-Breeding Forest*" to conserve the system as collaborative efforts between China, Russia, Mongolia and Japan (Shiraiwa, 2006b).

The Amur-Okhotsk Project consists of nine research groups; 1) physical oceanographic processes; 2) chemical and biological oceanographic processes; 3) biogeochemical process in river; 4) biogeochemical process at land surface; 5) sociological and economical background behind land-use changes; 6) land-use monitoring; 7) atmospheric transport; 8) hydrological processes; and 9) numerical modeling of marine ecosystem. Research groups 1-4 and 7-9 study the production, transport and utilization of the dissolved iron. The groups 5 and 6 analyze historical processes in the land-use changes and background behind the land-use changes occurring in the Amur river basin.

The main target of the project is lower half of the 2.05 million km^2 basin of Amur river and the Sea of Okhotsk plus western part of the northern North Pacific (so-called Oyashio region). The project conducts various types of field observation/research, analyses on biogeochemical samples, satellite monitoring and image interpretation, analyses on historical data, and interviewing from local residents. The collected data will be used for terrestrial hydrogeochemical and marine ecosystem models to simulate how the changing land use affects on the marine ecosystem through iron flux for the future.

The Amur-Okhotsk Project is trying to create a new global environmental concept "Giant" Fish-Breeding Forest by expanding Japanese indigenous idea called "Uotsuki-Rin (Fish Breeding Forest)" which relates upstream forest with coastal ecosystem both physically and spiritually. The idea called "Uotsuki-Rin" has been developed in Japan first as material

linkage between the upstream forest and the coastal ecosystem. The idea was then expanded further to the linkage in humanities inside the system which included fishermen in the coast and foresters and farmers in the upstream. With this idea in mind, fishermen started afforestation in their drainage basin to protect their fishery zone. This movement expanded all over Japan and now it is well known as one of the social movement to conserve local environment.

The physical linkage inside the "Uotsuki-Rin" has not fully established yet, although the humanistic aspects of "Uotsuki-Rin" has been developed further since 1970s. The Amur-Okhotsk Project tries to establish the physical linkage between the Amur river basin and the Sea of Okhotsk and the northern North Pacific with respect to the transport of dissolved iron. The outcome of the project is significant because this will be the first attempt to relate nearly 2 million square km of land surface with open ocean ecosystem much beyond the scale of "Uotsuki-Rin". The proposed system encompasses international boundaries such as Russia, China, Mongolia and Japan. People living in and depending on the system have deferent perspectives on their natural environment. Our project will seek a way how we conserve this vast linkage by studying various flows in the system, which include export and import in economics, cultural interaction, information, and governmental regulations.

2. PROGRESS REPORT

The project aims at clarifying linkage between the Amur river basin and the ocean ecosystem with respect to dissolved iron transport. Role of humanities is essential to conserve this system. We discussed this point in 2006 and decided to consider this topic under the new concept "Giant" Fish-Breeding Forest. Because the materials including dissolved iron flow downward only and there is no transport towards reverse direction. Therefore, the lower end of this system suffers every impact from upward regions. In such one-way flows system, benefit and risk tend to be distributed unevenly. Such inequality can be compensated by introducing different flows beside materials. By looking at various flows among stakeholders in the system, we will propose a conceptual background on which every stakeholder can collaborate for the conservation of the system.

Followings are individual progresses of each group in 2006.

a) Groups 1 and 2

These groups conducted a research cruise in the Sea of Okhotsk in August/September. They succeeded in measuring concentrations and distributions of various types of iron in the Sea of Okhotsk. The observed results showed that "Intermediate-Water Iron Hypothesis" was basically the main mechanism how the dissolved iron from the Amur river was transported to the Sea of Okhotsk and even to Oyashio region. It was supposed in the beginning that transported iron was once deposited in the estuary area of Amur river. However, our bottom-sea coring showed that the transported iron can hardly deposit on the estuary and continental shelf region due to strong tidal current there. This suggests that the transported

iron through the Amur river can immediately be transported into intermediate water layer in offshore region of the Sea of Okhotsk together with dense shelf water.

It was also confirmed that most of the dissolved iron in the Amur river was actually precipitated in the estuary area before penetrating into offshore intermediate layer as particulate iron. We speculated that some part of dissolved iron could be transported to the surface water of the Sea of Okhotsk directly as a complex with terrestrial organic matters, but this direct input of riverine dissolved iron into surface water of the Sea of Okhotsk might not be significant as we anticipated at least in the southern region of the Sea of Okhotsk. Long-range transport into the North Pacific Intermediate Water (NPIW) was found to be the most important process carrying the iron from Amur river to the Sea of Okhotsk and Oyashio region.

b) Groups 3 and 4

These groups conducted routine measurements on the concentration of iron in river water, soil water and ground water at Great and Little Khingan Mountains, Sanjiang Plain, Gassi Lake basin, and Anuy river basin, respectively. Spatial distribution of the concentrations in the dissolved iron was also measured in the Gassi Lake drainage basin where the concentrations of the dissolved iron in the lake and the adjacent wetland was significantly higher than those observed in nearby streams in forested area.

We studied the impact of land-use changes on the production of dissolved iron. In Sanjiang Plain, concentrations of dissolved iron in the interstitial water in the soil horizons were measured repeatedly from May to November in 2006. The highest concentration was always found in natural wetland whereas the lowest was in cultivated dry land. Paddy field showed intermediate concentrations. The concentration of dissolved iron was found to be related with water table too even in the same land-use type. In paddy field, water table solely decides the concentration.

We succeeded in carrying out a research cruise at Amur Liman (mouth of the Amur river) for the first time for foreigners since the beginning of 1800. The team collected water samples at various points of the Amur Liman and Sakhalin Bay. The samples are stored at the Institute of Water and Ecological Problems at Khabarovsk for future analyses.

c) Group 5

Group 5 studied mechanism on forest management and forest industry in Russia and their impacts on the present situation of the mixed forest in the Far East. It was found that the Far Eastern timber cutting is now accelerated by investments both from Russia and overseas and the illegal cutting of deciduous forest was still a serious problem. They also compiled a statistics on export of timber at trading stations between China and Russia.

In order to know the present situation of farming in the Sanjiang plain, group 5 made extensive interview to 76 farmers in Sanjiang plain. Preliminary results show that the farming in this region is not fully sustainable due to shortage of irrigated water, lowering of ground water table, and employment problems. These factors will be examined when we simulate how possible land-use changes affect on the marine ecosystem for the future.

d) Group 6

This group succeeded in compiling electric layers on landform, geology, hydrology, vegetation and land-uses for the whole Amur river basin with a scale of 1/1,000,000. The basic GIS products tell us the present situation of the land surface of the basin. It also shows anthropogenic land-surface disturbances such as dry lands, paddy fields, deforestation, forest fires, huge dams all of which may affect the production of dissolved iron. They also made several field observations as ground-truth for their monitoring of land-use changes by satellite data interpretations. By combining the GIS products and satellite observations, we were able to show recent land-use changes in the Amur river basin.

e) Group 7

Atmospheric transport of iron was quantified from the continuous monitoring by Automatic Aerosol sampler installed at Kamchatka peninsula. We also made an 131-m ice core drilling at the summit of Ichinsky volcano in Kamchatka to reconstruct a longer time record of iron deposition from the atmosphere over the Sea of Okhotsk. The samples are under analyses at present.

f) Group 8

This group started to construct a numerical model to simulate the production and transport of dissolved iron in the Amur river basin. The model consists of three sub-models describing soil water movement, solutes transport and chemical equilibrium. In 2006, we started to develop the sub-model of soil water movement by using a commercial software "GETFLOWS". This model simulates both water velocity and residence time in the Amur river basin.

g) Group 9

Group 9 developed a numerical model to simulate primary production in the Sea of Okhotsk and Oyashio region with special reference to the dissolved iron. They succeeded to simulate distribution of biomass productivity in these regions. However, the ocean model lacks the process of intermediate water transport of iron and thereby the model failed to simulate the actual distributions which are mainly determined by the contributions of intermediate water transport of iron. They will revise the model by including the process in the following years.

We have been carrying out this project as we planed initially but there is a major concern with respect to transport of samples from Russia to Japan. Russian Federation prohibits foreigner to take any samples out from their territory since 2005. We collected so many samples from river, land-surfaces and glacier in 2006. They are currently stocked in our collaborative research institutes. In spite of serious arrangement between Russia and Japan, we have not solved this problem yet. There was no good sign for this issue so far, and we decided last year that we asked related Russian institutes to analyze these samples in Russia.

This will increase our project expenses but we will mange it by reducing other expenses for the future.

3. FUTURE SCHEDULE

As we already mentioned in the previous section, our project is currently carried out as we planed initially. In the remaining 3 years from 2007 to 2009, we will attempt;

1) to quantify the flux of iron from wetlands extending at the middle reach of the Amur river. We need to clarify the present mechanism "how" and "how much" iron is produced in the Amur river basin and "how much" iron is discharged to the Sea of Okhotsk. Then we will predict how human impact will affect on this mechanism;
2) to clarify the mechanism how dissolved iron is incorporated in the river water from various types of land cover. We will conduct several intensive observations in relation to flooding in the Amur river. It is also important to clarify the biogeochemical processes occurring in the river water with respect to dissolved iron. We will quantify the fluxes not only of dissolved iron but also labile iron in the river;
3) to quantify the biogeochemical processes such as aggregation and precipitation in the estuary region of the Amur river;
4) to quantify the mass balance of iron in the continental shelf in the Sea of Okhots;
5) to quantify the transport, precipitation and dissolution of iron in the intermediate water layer in the Sea of Okhotsk and Oyashio regions. This will be an important issue related to solution chemistry controlling solubility of iron by organic ligand in the Intermediate water;
6) to quantify fluxes of iron input through atmospheric transport;
7) to unveil the relationship between dissolved iron and primary production in the Sea of Okhotsk and Oyashio region;
8) to conduct numerical simulations to evaluate the impacts of land-surface disturbance on oceanic primary productivity by means of a terrestrial iron transport model and a ocean ecosystem model including dissolved iron cycle;
9) to compile historical GIS on the land-use changes in the Amur river basin;
10) to unveil background behind intensive land-use changes in the Amur river basin in the 20th century;
11) to construct a framework of *"Giant" Fish-Feeding Forest* to better understand the conservation strategy of the Amur-Okhotsk system;
12) to find a way to conserve the Amur-Okhotsk system for the sustainable use of the marine and terrestrial ecosystems.

REFERENCES

Narita, H. and Shiraiwa, T. (2003) Report on Amur-Okhotsk Project No. 1, Narita, H. and Shiraiwa, T. (eds), RIHN, 88pp (In Japanese).

Narita, H. and Shiraiwa, T. (2004) Report on Amur-Okhotsk Project No. 2, Narita, H. and Shiraiwa, T. (eds.), RIHN/ILTS, 166pp.

Shiraiwa, T. (2005a) Report on Amur-Okhotsk Project No.3, Shiraiwa, T. (ed.), RIHN, 147pp.

Shiraiwa, T. (2005b) The Amur-Okhotsk Project, The Japan Journal, 2 (2), 30.

Shiraiwa, T. (2006a) World heritage, SHIRETOKO, as a part of Pan-Okhotsk view., Chiri、4、27 (In Japanese).

Shiraiwa, T. (2006b) The Amur-Okhotsk Project: Trilateral cooperation to protect a shared environment, GAIKO FORUM, Fall, 6 (3), 36-42.

PARTICLE TRACKING EXPERIMENT ON A MODEL OF THE OKHOTSK SEA: SPREADING OF THE AMUR ORIGIN WATER

OHSHIMA KAY I. [1] **AND SIMIZU D.** [2]

1 Institute of Low Temperature Science, Hokkaido University, Sapporo, Japan

2 Japan Sea National Fisheries Research Institute, Fisheries Research Agency

INTRODUCTION

In November 2005, the Amur River was severely polluted by the contaminants due to a chemical plant explosion at the upper river in China. If such contaminants flowed out from the mouth of the Amur River and were dissolved or suspended in sea water without removal, they would eventually come to Hokkaido coast via the East Sakhalin Current (ESC). On the other hand, in February and March 2006, thousands of dead seabirds were found in massive amounts of oil on the shores of Hokkaido, including part of a UNESCO World Heritage site. Although the cause of this incident has not been clarified, these birds were likely transported from the north via the ESC. If an oil spill incident occurred around the Sakhalin oil field, spilled oil would be brought southward along the Sakhalin east coast and finally to Hokkaido coast.

It is very important to predict the drifting and spreading of these contaminants or spilled oil. The ocean current is the most important component for their drifting (Varlamov et al., 1999). However, the prediction models that have been developed so far do not include appropriate currents. This is just because the current system in the Sea of Okhotsk had not been well understood before the recent international Japan-Russia-U.S. joint study of the Sea of Okhotsk.

Surface drifter observations (Ohshima et al., 2002) suggested the cyclonic circulation and clearly revealed the existence of the ESC, which is consistent with the schematics of Moroshkin (1966) and Luchin (1998). The ESC is strongly controlled by the bottom topography. Ohshima et al. (2002) showed that the ESC consists of two cores: the nearshore core on the shelf and the offshore core over the shelf slope. Mizuta et al.(2003) clarified the structure and seasonal variations of the ESC based on long-term moored current measurements. They showed that the transport and velocity of the ESC exhibit large seasonal variations with the maximum in winter and minimum in summer. Simizu and Ohshima (2006) showed that the nearshore core (branch) is mainly driven by the alongshore wind stress through the onshore component of Ekman flux trapped over the shelf. On the other hand, Ohshima et al. (2004) showed that the offshore core (branch) of the ESC is regarded as the western boundary current of the cyclonic circulation driven by a positive wind stress curl.

In this study, toward the development of a prediction model for the drift/diffusion of the contaminants or spilled oil, we make a particle tracking experiment using the general circulation ocean model. Specifically, we run an experiment on drifting and spreading of water originating from the Amur mouth. This experiment is also useful for examining the drift

and diffusion of suspended and dissolved matters from the Amur, which may be important ingredients for biological productivity (Nakatsuka et al., 2004).

1. MODEL

We used the Okhotsk Sea model of Simizu and Ohshima (2006). The model is a Princeton Ocean Model incorporating the realistic bottom topography and density stratification. Zonal and meridional grid spacings are 1/6 degree. The vertical grid uses 21σ

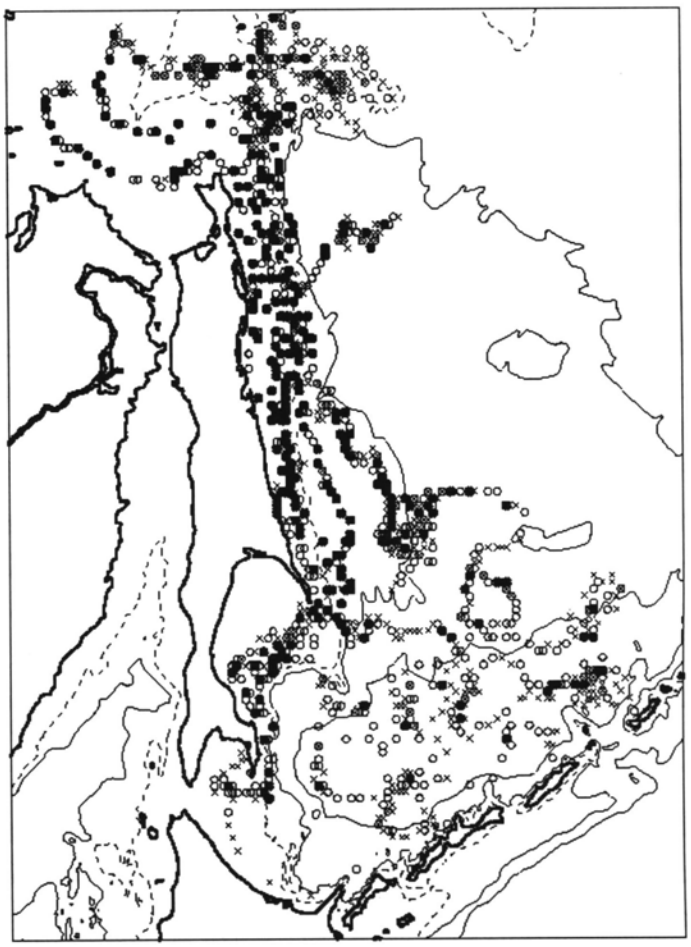

Figure 1: Map of fitting between the model and buoy velocities on 3-day running mean basis. Good fitting (R<0.5: solid circles), moderate fitting (0.5<R<1.0: open circles), and bad fitting (R>1.0: crosses)

levels. The model was spun up for 11 years with the climatological monthly mean wind stress, and subsequently run by the daily wind forcing from ERA-40 and by the monthly heat flux from Ohshima et al., (2003). The effects of sea ice and salt/fresh water flux were not included in the model. A second-moment turbulent closure scheme is adopted to calculate the vertical eddy viscosity and diffusivity. At initial state the ocean is at rest and density stratification is horizontally uniform. The initial profiles of temperature and salinity are typical values of the Okhotsk Sea. All straits are closed and thus inflow and outflow are neglected.

To examine the reproducibility of the model, we compare the model velocity at a depth of 15m with the velocity of the Argos drifting buoys deployed in 1999 (Ohshima et al., 2002): the buoys have large holey sock drogue centered at 15 m depth. Figure 1 is a map of fitting between the model and buoy velocities on 3-day running mean basis. The difference between the two velocity vectors are calculated and categorized into three classes using a ratio of the difference to the buoy velocity (R): good fitting (R<0.5: indicated by solid circles), moderate fitting (0.5<R<1.0: indicated by open circles), and bad fitting (R>1.0: indicated by crosses). The figure shows that the model can roughly reproduce the buoy velocity in the shelf and slope regions with water depths shallower than 1000m, while cannot reproduce it at all in the deep basin.

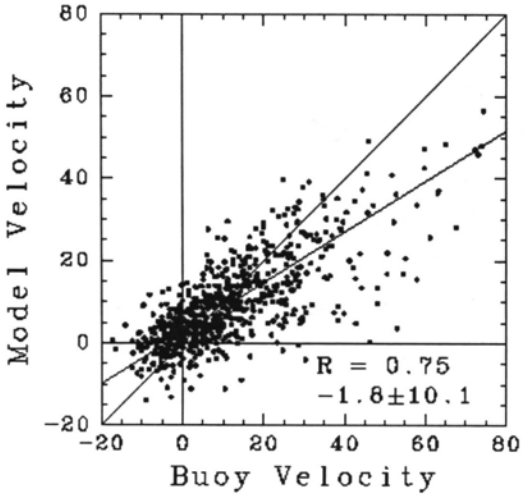

Figure 2: Comparison between the buoy and model north-south velocities in 3-day running mean over the east and north Sakhalin shelves with a water depth shallower than 1000m. Southward direction is taken positive.

Figure 2 shows the comparison between the buoy and model velocities (north-south component) in 3-day running mean over the east and north Sakhalin shelves with a water depth shallower than 1000m. The model velocity is smaller by ~2 cm s^{-1} on average, and the standard deviation of the difference between them is ~10 cm s^{-1}. The correlation coefficient between them is 0.75. Although the principal component line shows some bias (see thick line in Fig.2), the agreement between them is overall good. As long as the simulation of the ESC, the model can work to some degree.

The particle tracking method in the model is similar to that of Awaji (1982). Labeled particles are tracked by the interpolated velocity of the model result. The turbulent velocities caused by tidal currents etc. are incorporated using random-walk on the assumption of a Markov-chain model, where the horizontal turbulent diffusivity and the integral time scale are set to 10^6 cm^2 s^{-1} and 1 day, respectively.

2. RESULTS

In this study, we present the results of the particle tracking experiment in the case of 1998 as an example. 8 particles have been released from the Amur mouth every day from May to October, when the Amur discharge is large (Ogi et al., 2001). Contaminants or spilled oil would usually drift within the upper 0-15 m layer of the sea. Thus we make the particle tracking at the surface and a depth of 15 m.

Figure 3 shows the simulated time series of the particle distribution at a depth of 15 m. At that depth, the current is hardly affected by the wind and the movement of a particle is mostly determined by the ocean current, specifically the ESC in this case. Since the ESC is very weak during May-September, most of the particles are stagnant around the Amur mouth and move southward only slightly during summer. They start to move swiftly southward after October in accordance with the abrupt intensification of the ESC, and finally reach offshore of Hokkaido in December. The particle can reach offshore of Hokkaido in a similar time, regardless of the deployment month.

Figure 4 shows the simulated time series of the particle distribution at the surface. Movement of a particle at the surface is partly affected by the wind drift in addition to the ocean current. During May-September when the ESC is very weak, the particles are diffused offshore due to the wind drift. The particles that were deployed in May-July have been diffused and out of the ESC mainstream before the onset of the ESC intensification, and thus most of them can not be transported to offshore of Hokkaido. While, the particles that were deployed in August and September remain in the ESC mainstream and move swiftly southward after October in accordance with the intensification of the ESC, finally reaching offshore of Hokkaido in December. Dominance of northwesterly wind in fall makes the surface particles drifted offshore. Thereby, the particle distribution at the surface is shifted offshoreward when compared to that at a depth of 15 m (compare Fig. 3d with Fig. 4d).
We also made experiments for other years. For the case of a depth of 15m, the results are insensitive to year. Most of the deployed particles finally reach offshore of Hokkaido via the ESC. For the case of the surface, the results are somewhat different from year to year, due to the effect of the wind drift. In some years, most of the particles were out of the mainstream of the ESC due to the strong offshore-ward wind drift and the only small portion is transported to offshore of Hokkaido.

Watanabe (1963) and Itoh and Ohshima (2000) showed that low salinity water originating from the Amur River is advected to offshore of Hokkaido in the upper 50 m in November or December via the ESC. The particle distribution shown in Figs. 3d and 4d and the timing of the arrival at offshore of Hokkaido are roughly consistent with these previous observations except that the timing of the arrival in the model is delayed slightly, by about 0.5-1.0 month. This suggests that the water originating from the Amur mouth is transported southward mostly by the wind-driven component and that the density driven component is not large. The delay of 0.5-1.0 month is likely due to the lack of density current due to the Amur River flux in the model.

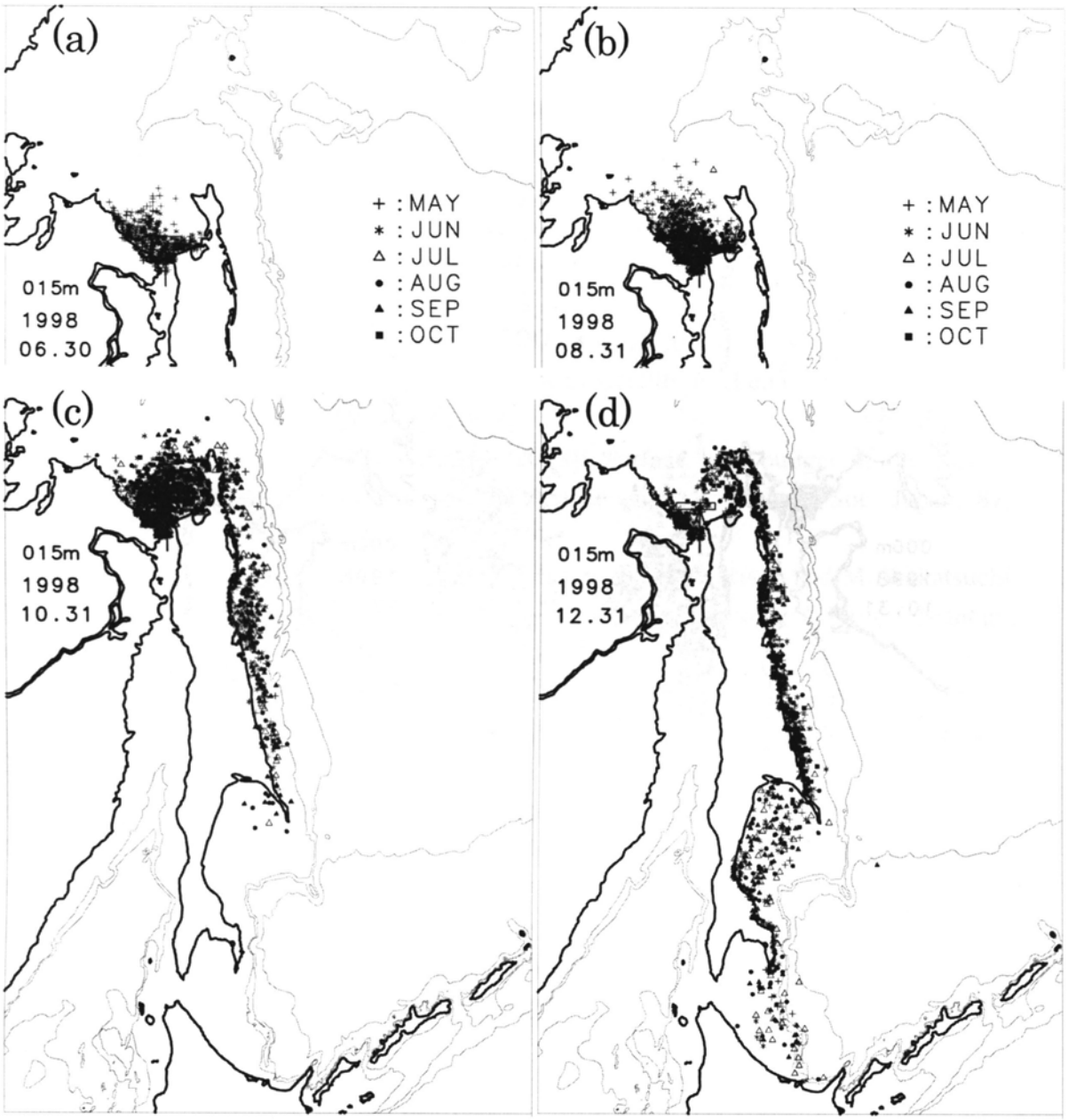

Figure. 3: Simulated time series of the particle distribution at a depth of 15 m at intervals of two months, when 8 particles have been released from the Amur mouth (designated by the rectangular and arrow) every day from 1 May to 31 October, 1998: (a) June 30, (b) August 31, (c) October 31, and (d) December 31. Deployment month of each particle is discriminated by the symbol.

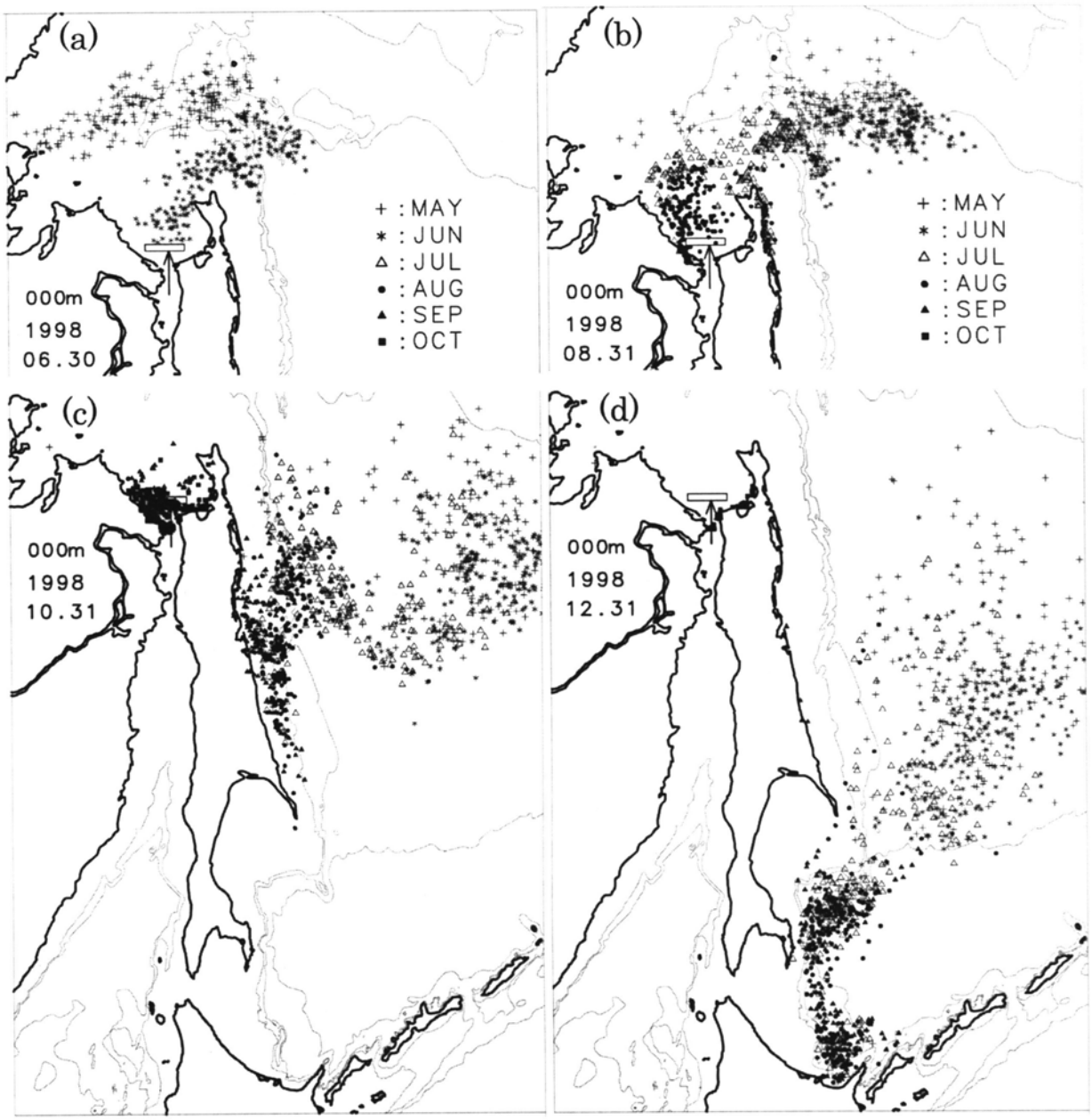

Figure. 4: The same as Fig. 3 except for the distribution at the surface.

REFERENCES

Awaji, T. (1982): Water mixing in a tidal current and the effect of turbulence on tidal exchange through a strait. J. Phys. Oceanogr., **12**, 501-514.

Itoh, M. and K. I. Ohshima (2000): Seasonal variations of water masses and sea level in the southwestern part of the Okhotsk Sea, J. Oceanogr., **56**, 643-654.

Luchin, V. A. (1998): Hydrometeorological condition: Steady current (in Russian) in Hydrometeorology and Hydrochemistry of the Seas. Vol. **9**, The Okhotsk Sea, 233-256, Hydrometeoizdat, Saint Petersburg.

Mizuta, G., Y. Fukamachi, K. I. Ohshima, and M. Wakatsuchi (2003): Structure and seasonal variability of the East Sakhalin Current. J. Phys. Oceanogr., 33, 2430-2445.

Moroshkin, K. V. (1966): Water masses of the Sea of Okhotsk. Joint Pub. Res. Serv., 43942, 98, U.S. Dept. of Commerce, Washington, D.C.

Nakatsuka T., T. Toda, K. Kawamura, and M. Wakatsuchi (2004): Dissolved and particulate organic carbon in the Sea of Okhotsk: Transport from continental shelf to ocean interior, J. Geophys. Res., **109**, C09S14, doi:10.1029/2003JC001909.

Ogi, M., Y. Tachibana, F. Nishio, and M. A. Danchenkov (2001): Dose the fresh water supply from the Amur River flowing into the Sea of Okhotsk affect sea ice formation?, J. Meteorol. Soc. Jpn., **79**, 123-129.

Ohshima, K. I., M. Wakatsuchi, Y. Fukamachi and G. Mizuta (2002): Near-surface circulation and tidal currents of the Okhotsk Sea observed with satellite-tracked drifters. J. Geophys. Res., **107**, 3195, doi:10.1029/2001JC001005.

Ohshima, K. I., T. Watanabe, and S. Nihashi (2003): Surface heat budget of the Sea of Okhotsk during 1987-2001 and the role of sea ice on it, J. Meteor. Soc. Japan, **81**, 653-677.

Ohshima, K. I., D. Simizu, M. Itoh, G. Mizuta, Y. Fukamachi, S. C. Riser, and M. Wakatsuchi (2004): Sverdrup balance and the cyclonic gyre in the Sea of Okhotsk, J. Phys. Oceanogr., **34**, 513-525.

Simizu, D. and K. I. Ohshima (2006): A model simulation on the circulation in the Sea of Okhotsk and the East Sakhalin Current, Journal of Geophysical Research, **111**, C05016, doi:10.1029/2005JC002980

Varlamov, S. M., J.-H. Yoon, N. Hirose, H. Kawamura and K. Shinohara (1999): Simulation of the oil spill processes in the Sea of Japan Sea with regional ocean circulation model. Journal of Marine Science and Technology, **4**(3), 94-107.

Watanabe, K (1963): On the reinforcement of the East Sakhalin Current preceding to the sea ice season off the coast of Hokkaido; Study on the sea ice in the Okhotsk Sea (IV). Oceanogr. Mag., **14**, 117-13.

DECREASE OF SEA ICE PRODUCTION IN THE OKHOTSK SEA CAUSES WEAKENING OF OVERTURNING IN THE NORTHWESTERN NORTH PACIFIC ?

OHSHIMA KAY I., NAKANOWATARI T. AND WAKATSUCHI M.
Institute of Low Temperature Science, Hokkaido University, Sapporo, Japan

INTRODUCTION

It is known that North Pacific Intermediate Water (NPIW), characterized by a salinity minimum at $26.8\sigma_\theta$, is a major water mass at the intermediate level of the North Pacific (e.g., Reid, 1965). Figure 1 shows the distribution of potential temperature on the $27.0\sigma_\theta$ isopycnal surface in the North Pacific. Cold water seems to originate from the Sea of Okhotsk. High oxygen content (Talley, 1991) and high CFC concentration (Warner et al., 1996) also originate from the Sea of Okhotsk. These distributions suggest that the ventilation source of intermediate water in the North Pacific, including NPIW, is the Sea of Okhotsk.

Then where is the specific region of the ventilation in the Sea of Okhotsk? Figure 2 shows the distributions of potential temperature and oxygen content on the $26.8\sigma_\theta$ isopycnal surface in and around the Sea of Okhotsk. Cold and high oxygen water appears to originate from the northwestern shelf region, suggesting that the ventilation occurs there. Figure 3 shows the annual mean cumulative sea ice production calculated from the microwave ice information and heat budget (Ohshima et al., 2003). The northwestern shelf is found to be the far highest ice production region in the Sea of Okhotsk. Over the northwestern shelf, a large amount of

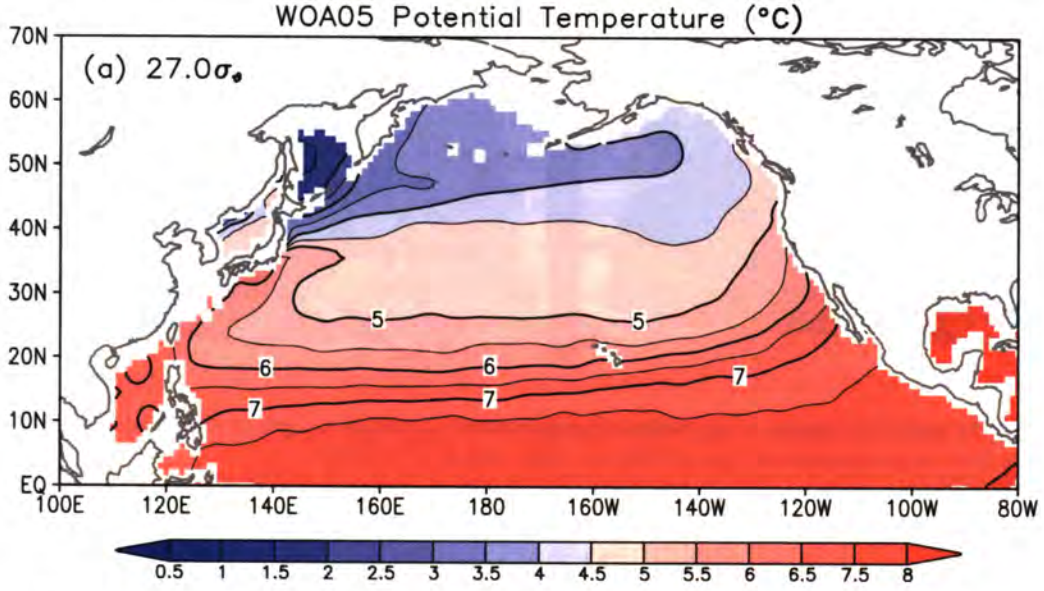

Figure 1: Horizontal distribution of potential temperature on the $27.0\sigma_\theta$ isopycnal surface in the North Pacific.

sea ice is produced due to severe winds from northeastern Eurasia in winter. The sea ice production leads to production of cold, oxygen-rich dense shelf water (DSW) with densities of up to 27.0σ_θ (Shcherbina et al., 2003). The DSW is transported southward (Fig. 2) into the intermediate layer of the deep Okhotsk basin in the southern Okhotsk Sea, and mixed with intermediate water coming from the North Pacific.This mixing forms the coldest, freshest and oxygen-richest water in the North Pacific in the density range of 26.8-27.4σ_θ (Talley, 1991), which is called Okhotsk Sea Mode Water (Yasuda, 1997) or Okhotsk Sea Intermediate Water (OSIW) (Itoh et al., 2003). The signal of OSIW extends downward to 27.4σ_θ owing to diapycnal mixing caused by strong tidal currents around the Kuril Straits (Wong et al., 1998).

The OSIW outflows to the North Pacific through the Kuril Straits, mainly Bussol' Strait (Talley, 1991), and then mixes with East Kamchatska Current Water, which flows southwestward along the northern Kuril Islands, forming the Oyashio water. The Oyashio water extends to the intermediate layer, flowing southwestward along the Kuril Island chain as the western boundary current of the subarctic gyre. The Oyashio water reaches the confluence of the subtropical and subarctic gyres, and then part of the Oyashio water flows northeastward as the Subarctic Current (SAC), bounding the subarctic gyre on the south.

In this study, through the trend analyses of temperature and oxygen in the intermediate water, we suggest that the weakening of ventilation (overturning) in the northwestern North Pacific during the past 50 years, caused by a decrease in sea ice production in the Sea of Okhotsk.

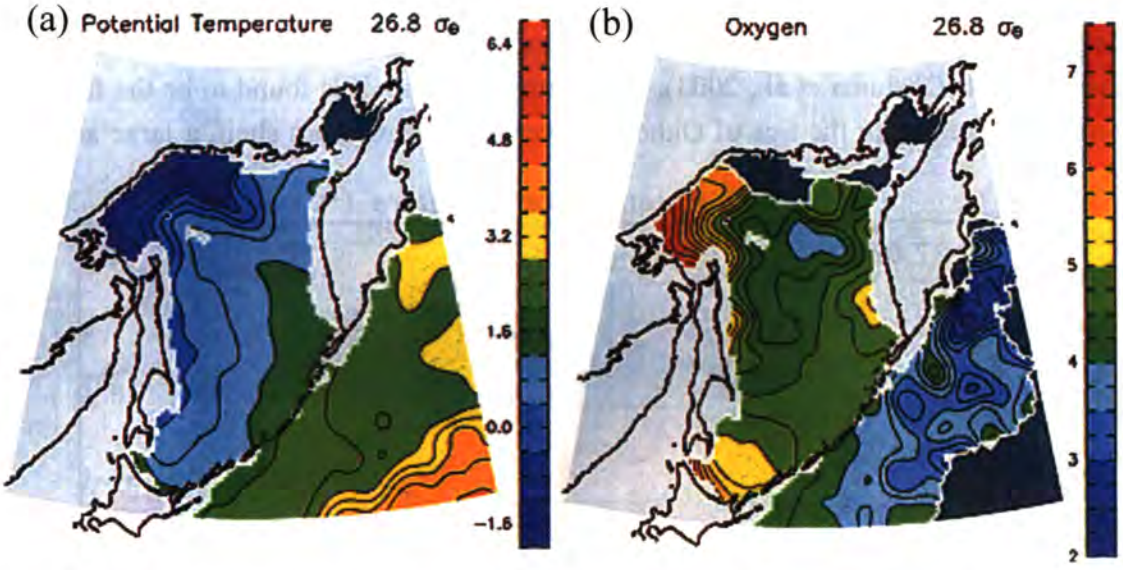

Figure 2: Horizontal distributions of (a) potential temperature (C) and (b) oxygen content (mL/L) on the 26.8σ_θ isopycnal surface in and around the Sea of Okhotsk. After Itoh et al. (2003).

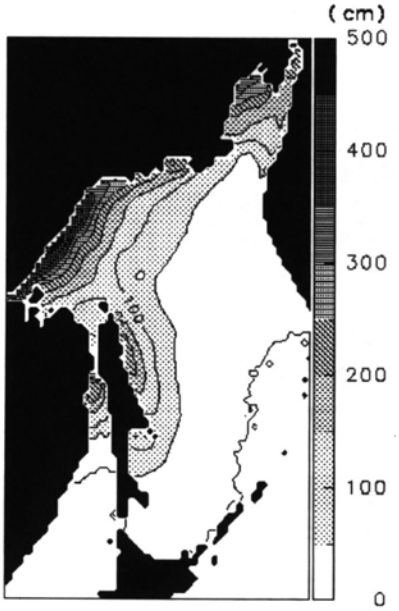

Figure 3: Annual mean cumulative sea ice production, represented by the ice thickness (cm). Estimation is based on the sea ice information from the satellite microwave and heat budget calculation. After Ohshima et al. (2003).

1. WARMING AND OXYGEN-DECREASE TRENDS

For the trend analyses, we have used all available data of temperature, salinity and dissolved oxygen, taken from the World Ocean Database (WOD01), observational data obtained by the Japan-Russia-United States international joint study of the Sea of Okhotsk from 1998 to 2004, data archived by the Japan Oceanographic Data Center, and profiling float data obtained by the international Argo program from 2000 to 2004. After the quality control, a gridded dataset of potential temperature anomalies on isopycnal surfaces was then prepared for the period 1955-2004, and one of dissolved oxygen for the period 1960-2004.

Figure 4a shows linear trend maps of intermediate water temperature on the $27.0\sigma_\theta$ isopycnal surface for the last 50 years. Significant warming trends are observed in the northwestern North Pacific and the Sea of Okhotsk. The warming trend in these regions is most prominent at density $27.0\sigma_\theta$, and the largest warming area exists in the western part (47.5°-55°N, 145°-147.5°E) of the Sea of Okhotsk with an average of 0.68°C/50-yr. The warming trend at $27.0\sigma_\theta$ seems to extend along the pathway of the OSIW. Climatology of the acceleration potential at $27.0\sigma_\theta$ (Figure 4b) shows that the western subarctic gyre, which consists of the Oyashio and Subarctic Current (SAC), extends to the intermediate depth of $27.0\sigma_\theta$. A significant warming trend is observed in the Oyashio and SAC regions, but not in the East Kamchatska Current region, i.e., upstream of the Sea of Okhotsk. Since the intermediate water masses in the Oyashio and SAC regions are largely affected by the OSIW

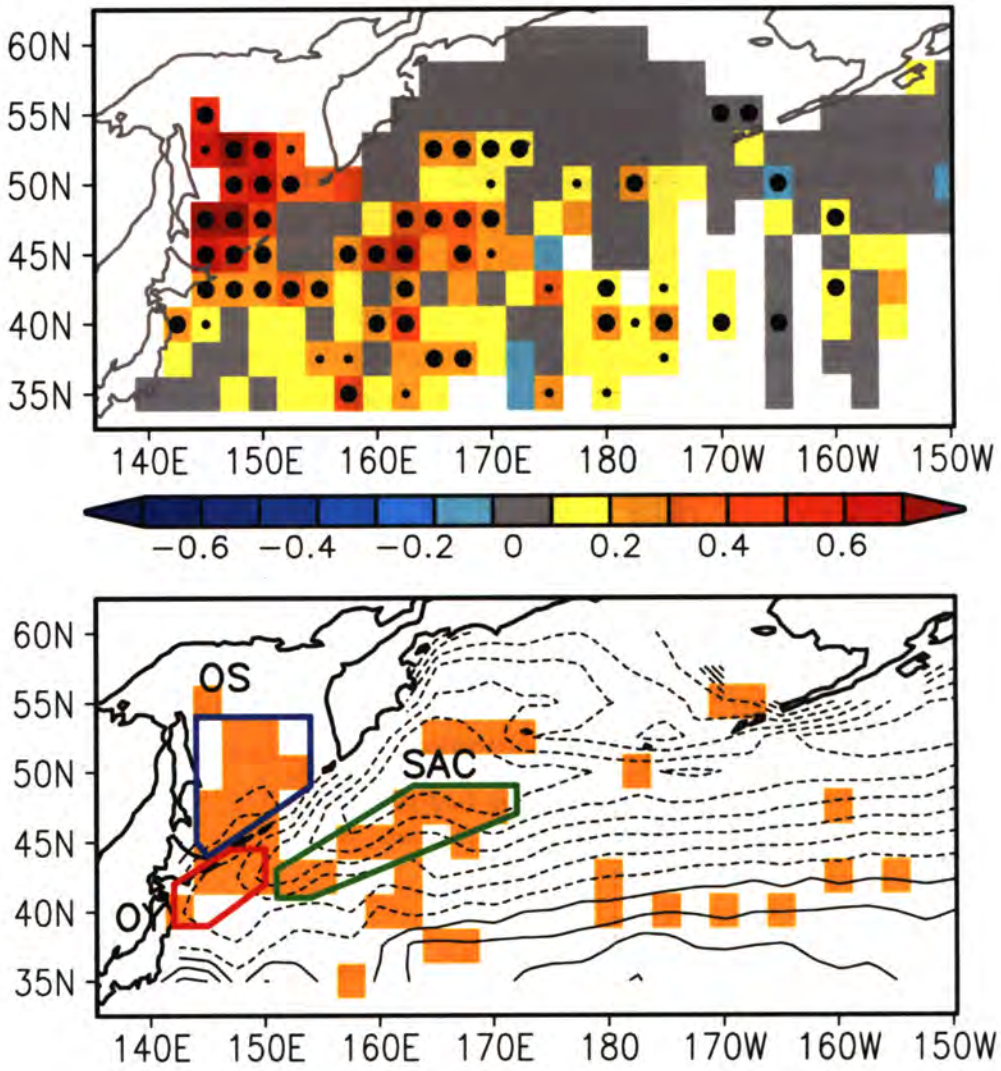

Figure 4: (a) Linear trends (colors in °C/50-yr) of potential temperature anomalies at density 27.0σ_θ from 1955-2004 in the northwestern North Pacific. Large and small dots indicate grid boxes in which the linear trend is significant at the 95% and 90% confidence levels, respectively. White color indicates the grid boxes where yearly temperature anomalies are not available for more than 10 years throughout the respective periods. The significance of the linear trend estimate is based on a Student t distribution. (b) Map of acceleration potential (contours) at 27.0σ_θ relative to 2000 dbar, derived from our dataset. Boundaries of the Sea of Okhotsk (blue), Oyashio (red), and SAC regions (green), for which area-averaged quantities are displayed in Figure 3, are indicated. Shading (yellow) indicates areas where the positive linear trend of potential temperature at 27.0σ_θ exceeds the 95% confidence level. After Nakanowatari et al. (2007).

(Yasuda, 1997), these results indicate that the warming trend in the northwestern North Pacific may be caused by advection of warmed OSIW.

Figure 5a shows the time series of temperature anomalies at 27.0σ_θ for the Sea of Okhotsk, Oyashio and SAC regions (Figure 4b). A positive linear trend is the most significant feature in all three regions. The temperature has increased by 0.62±0.18°C (significant at 99% confidence interval) in the Sea of Okhotsk during the past 50 years from 1955 through 2004. The magnitude of the warming trend in the other two regions is about half of that.

We next examine the linear trend of dissolved oxygen content. For all three regions, significant negative trends are found (Figure 5b). Decreasing trend of dissolved oxygen content in the Oyashio is consistent with Ono et al. (2001). The decrease of dissolved oxygen is most prominent at 26.9-27.0σ_θ, where the warming trend is most prominent. At 27.0σ_θ, the linear trend in the Sea of Okhotsk is -0.58±0.34ml/l (significant at 95% confidence interval) for the past 45 years. The Oyashio and SAC regions have the value less than that for the Sea of Okhotsk.

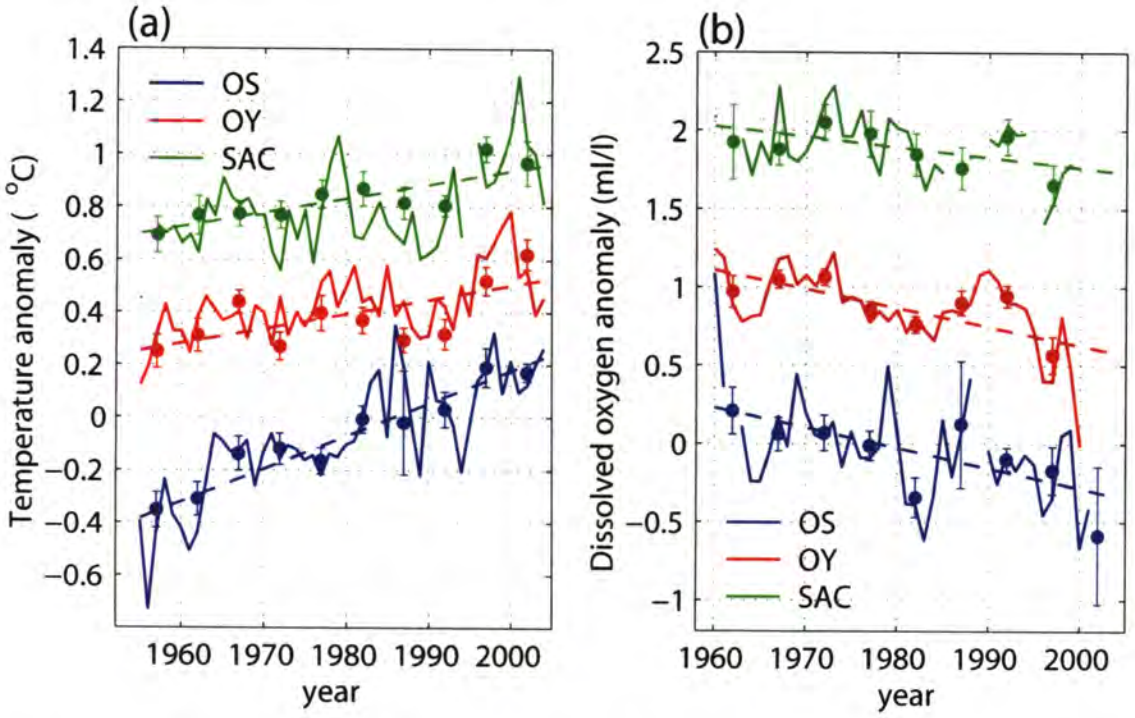

Figure 5: Time series of (a) potential temperature (°C) and (b) dissolved oxygen (ml/l) anomalies at 27.0σ_θ averaged over the Sea of Okhotsk (blue), Oyashio (red), and SAC (green) regions, respectively (see Figure 2 for locations of these three areas). Closed circles show 5-yr averaged anomalies with errors at the 95% confidence interval for the 5-yr averages. Linear regression line for each time series is also indicated by a dashed line. Note that in panel a (b) 0.4°C (1.0 ml/l) and 0.8°C (2.0 ml/l) has been added to the time series for the Oyashio and SAC regions, respectively. After Nakanowatari et al. (2007).

2. POSSIBLE SCENARIO

It is shown that warming and oxygen-decreasing trends in the intermediate water are most prominent in the Sea of Okhotsk. Moreover, these trends appear to extend to the northwestern North Pacific along the pathway of the water mass originating from the Sea of Okhotsk. These facts suggest that trends in the northwestern North Pacific are due to preceding changes of water-mass properties in the Sea of Okhotsk. Intermediate water in the Sea of Okhotsk retains its cold and oxygen-rich properties by mixing with dense shelf water (DSW) associated with sea ice production in the coastal polynya of the northwestern shelf. The largest warming trend occurs in the western Sea of Okhotsk (Figure 4a), to which DSW is transported from the northwestern shelf (Fukamachi et al., 2004). Therefore, we suppose that

the main cause of the warming and oxygen-decreasing trends is the weakening of DSW production.

Although reliable estimation of DSW production is not yet available, there is some indirect evidence for a decrease trend in DSW production. Figure 6 shows the time series of surface air temperature anomaly in the cold season averaged over northeastern Eurasia, which is upwind of the Sea of Okhotsk; this air temperature can be an index of sea ice extent. This air temperature has increased considerably during the past 50 years (2.0±1.4°C/50-yr, significant at 99% confidence level). Sea ice extent in the Sea of Okhotsk derived from satellite measurements, which is highly correlated with this air temperature (r=-0.61, significant at 95% confidence level), has decreased (-9.2%/27-yr) (Figure 6). Although satellite measurements have only been available since the 1970's, visual observations at Hokkaido coast, located on the southern boundary of sea ice extent in the Sea of Okhotsk, show the decreasing trend of sea ice season length during the past 100 years (Aota, 1999). These trends of air temperature and sea ice season suggest that sea ice extent, accordingly sea ice production, have likely decreased during the past 50 years. During the current global warming, the surface air temperature anomaly in autumn and winter is particularly large over northeastern Eurasia (Serreze et al., 2000). The DSW production area of the northwestern shelf in the Sea of Okhotsk is located where the winter monsoon from northeastern Eurasia directly transports cold air masses. Therefore, intermediate water in the Sea of Okhotsk which

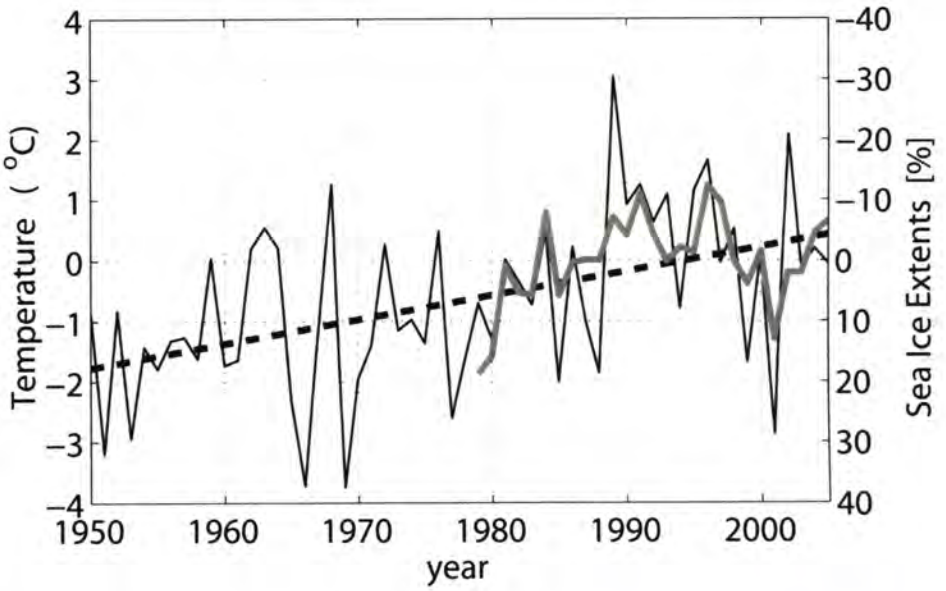

Figure 6: Time series of surface air temperature anomaly in the cold season (October to March) and the linear trend over northeastern Eurasia (50º65N, 110º140E) from 1950 to 2005 (solid and dashed lines, respectively), and the annual sea ice extent anomaly in the entire Okhotsk Sea from 1979 to 2005 (blue line). The scale of the sea ice extent anomaly is indicated on the right axis and inverted. The surface air temperature anomaly is derived from (Jones, 1994), and the sea ice extent anomaly is derived from the Met Office Hadley Centre's sea ice data set (Rayner et al., 2003). The surface air temperature anomaly with respect to the 27-yr average from 1979 to 2005 is shown for the benefit of comparison with the sea ice extent anomaly. After Nakanowatari et al. (2007).

is ventilated through DSW may be sensitive to the global warming.

Recent studies suggest that OSIW has a significant role in material circulation of the intermediate layer in the North Pacific. (Hansell et al., 2002) indicated that dissolved organic carbons in NPIW originate from the Sea of Okhotsk. (Nakatsuka et al., 2004) showed that large amounts of dissolved and particulate organic carbons are exported from the highly productive northwestern shelf into the intermediate layer in the Sea of Okhotsk through the outflow of DSW. Moreover, recent observational data show that in the northwestern North Pacific, iron, which is an essential micronutrient for phytoplankton, may come from the intermediate water of the Sea of Okhotsk (Nishioka, 2004). The co-occurrence of warming and decrease in dissolved oxygen concentration in the northwestern North Pacific, originating from the Sea of Okhotsk, implies that overturning in the northwestern North Pacific has weakened in the sense of material cycle. Therefore, such a trend has a possibility of substantial impacts on the material cycle and biological productivity in the North Pacific.

Figure 7 summarizes our proposal with schematics. Because the Sea of Okhotsk is a sensitive area to the current global warming, production of sea ice and dense shelf water in the northwestern shelf has decreased during the past 50 years. This possibly causes a decrease in supply of iron in the intermediate layer in the Sea of Okhotsk and further in the North Pacific. Finally, this might induce the decrease in primary biological production, fishery resources, and capacity of CO2 absorption.

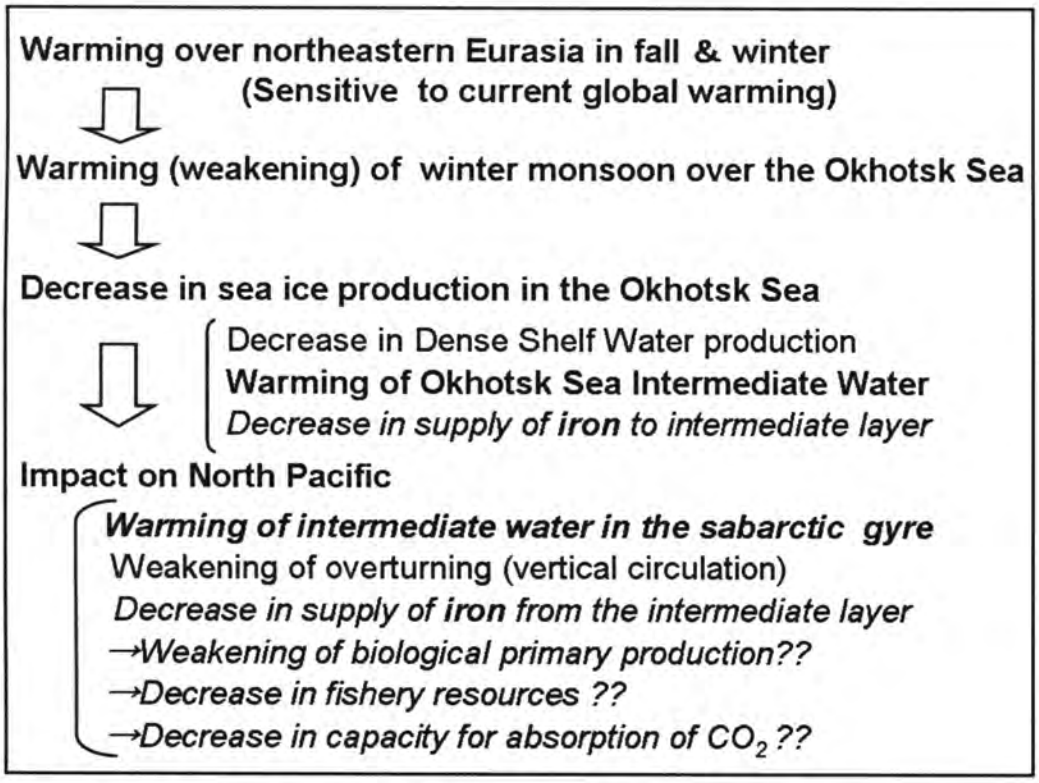

Figure 7: Schematics for impact of the Okhotsk Sea on the North Pacific through global warming. Thick letters indicate a fact evidenced by observations and analyses. Italic letters indicate a hypothesis. Larger number of question mark indicates larger uncertainty.

ACKNOWLEDGMENTS

The Argo float data used in this study were collected and made freely available by the International Argo Project and the national programs that contributes to it. Part of the hydrographic data in the Okhotsk Sea were obtained under the cooperation with Far Eastern Regional Hydrometeorological Research Institute, Scripps Institute of Oceanography, and S. C. Riser of University of Washington. We wish to thank M. Itoh and K. Ono for data processing.

REFERENCES

Aota, M. (1999): Long-term tendencies of sea ice concentration and air temperature in the Okhotsk Sea coast of Hokkaido, PICES Sci. Rep., 12, 1-2.

Fukamachi, Y., G. Mizuta, K. I. Ohshima, L. D. Talley, S. C. Riser, and M. Wakatsuchi (2004): Transport and modification processes of dense shelf water revealed by long-term moorings off Sakhalin in the Sea of Okhotsk, J. Geophys. Res., 109, C09S10, doi:10.1029/2003/JC001906.

Hansell, D. A., C. A. Carlson, and Y. Suzuki (2002): Dissolved organic carbon export with North Pacific Intermediate Water formation, Global Biogeochem. Cycles, 16 (1), 1007, doi:10.1029/2000GB001361.

Itoh, M., K. I. Ohshima, and M. Wakatsuchi (2003): Distribution and formation of Okhotsk Sea Intermediate Water: an analysis of isopycnal climatology data, J. Geophys. Res., 108, 3258, doi:10.1029/2002JC001590.

Jones P. D. (1994): Hemispheric surface air temperature variations: a reanalysis and an update to 1993, J. Climate, **7**, 1794-1802.

Nakanowatari T., K. I. Ohshima, M. Wakatsuchi: Warming and oxygen-decrease of intermediate water in the northwestern North Pacific, originating from the Sea of Okhotsk, 1955-2004. Geophys. Res. Lett., 34, doi:10.1029/2006GL028243 (in press)

Nakatsuka T., T. Toda, K. Kawamura, and M. Wakatsuchi (2004): Dissolved and particulate organic carbon in the Sea of Okhotsk: Transport from continental shelf to ocean interior, J. Geophys. Res., 109, C09S14, doi:10.1029/2003JC001909.

Nishioka J. (2004): Iron study in the Sea of Okhotsk: comparison to the subarctic Pacific, Rep. on Amur-Okhotsk project, 2, 103-109.

Ohshima, K. I., T. Watanabe, and S. Nihashi (2003): Surface heat budget of the Sea of Okhotsk during 1987-2001 and the role of sea ice on it, J. Meteor. Soc. Japan, 81, 653-677.

Ono, T., T. Midorikawa, Y. W. Watanabe, K. Tadokoro, and T. Saino (2001): Temporal increases of phosphate and apparent oxygen utilization in the surface waters of western subarctic Pacific from 1968 to 1998, Geophys, Res. Lett., 28, 3285-3288.

Rayner, N. A., D. E. Parker, E. B. Horton, C. K. Folland, L. V. Alexander, and D. P. Rowell (2003): Global analyses of sea surface temperature, sea ice, and night marine air temperature since the late nineteenth century, J. Geophys. Res., 108, D14,4407,

doi:10.1029/2002JD002670.

Reid, J. L. (1965): Intermediate water of the Pacific Ocean, Johns Hopkins Oceanogr. Stud., 2, 85.

Serreze M., et al. (2000): Observational evidence of recent change in the northern high-latitude environment, Climatic Change, 46, 159-207.

Shcherbina A. Y., L. D. Talley, D. L. Rudnick (2003): Direct observations of North Pacific ventilation: brine rejection in the Okhotsk Sea, Science, 302, 1952-1955.

Talley, L. D. (1991): An Okhotsk Sea water anomaly: implications for ventilation in the North Pacific, Deep Sea Res., Part A, 38, suppl., 171-190.

Warner, M. J., J. L. Bullister, D. P. Wisegraver, R. H. Gammon, and R. F. Weiss (1996): Basin-wide distributions of chlorofluorocarbons CFC-11 and CFC-12 in the North Pacific, J. Geophys. Res., 103, 2849-2865.

Wong, C. S., R. J. Matear, H. J. Freeland, F. A. Whitney, and A. S. Bychkov (1998): WOCE line P1W in the Sea of Okhotsk: 2. CFCs and the formation rate of intermediate water, J. Geophys. Res., 103, 15625-15642.

Yasuda, I. (1997): The origin of the North Pacific Intermediate Water, J. Geophys. Res., 102, 893-909.

HOW CAN THE IRON FROM AMUR RIVER SUPPORT THE PRIMARY PRODUCTIVITY IN NORTH PACIFIC OCEAN ?

-*"INTERMEDIATE-WATER IRON HYPOTHESIS" AND ITS EVIDENCES FROM THE RESEARCH CRUISE IN 2006-*

NAKATSUKA TAKESHI AND ALL MEMBERS OF RESEARCH GROUPS 1 AND 2
Institute of Low Temperature Science, Hokkaido University and Others

INTRODUCTION

Before 20 years ago, most of oceanographers thought that marine ecosystem in open oceans are not influenced by short-term variability in land surface conditions, especially not affected by environment changes at inland areas. About 10 years ago, many oceanographers began to believe that ecosystem in open ocean is connected with environment of inland areas, because they have found that growth of phytoplankton at open ocean is often regulated by limitation of dissolved iron and long-distance transport of aerosols from arid continental regions to open ocean may supply significant amounts of iron into open ocean surface. After the proposal of this "Airborne Iron Hypothesis", many studies have been carried out to clarify the direct relationship between atmospheric iron inputs and primary productions in the open ocean. However, the connection between them is still unclear because we do not have sufficient information on the solubility of aerosol iron and we have seldom observed the sequential evidences of aerosol supply and phytoplankton bloom in the open ocean.

Another important background of "Airborne Iron Hypothesis" is the fact that iron can be hardly dissolved in the seawater. This intrinsic nature of iron inevitably suggests that riverine iron cannot reach the open ocean, because it must precipitate on bottom sediments near the river mouth. Therefore, most of oceanographers have been assuming that atmospheric transport is the only one way supplying iron into the surface water of open ocean. Here, we propose a new hypothesis, which connect the land surface conditions of inland areas and the primary production in open oceans by the iron transport through river and ocean flows. That is "Intermediate-Water Iron Hypothesis". Briefly to say, most of the riverine iron actually precipitates on the continental shelf and slope sediments, but parts of them are resuspened and transported to open ocean through intermediate layers and eventually supplied into the surface layer as dissolved forms of iron by upwelling and/or diffusion processes.

In this paper, first, we explain the details of this "Intermediate-Water Iron Hypothesis" based on previous our geochemical and oceanographic knowledge around the Sea of Okhotsk. Second, we show the direct evidences for this hypothesis obtained at Research Expedition of the Sea of Okhotsk during August-September 2006. Third, we discuss the implication of this hypothesis to the relationship between the human impacts on the land surface condition in Amur River basin and the biological productivity of the North Pacific Ocean.

"INTERMEDIATE-WATER IRON HYPOTHESIS" -(1) IT'S FINDING

Oyashio current is the subarctic western boundary current of Pacific Ocean, flowing southwestward just outside of the southeastern rim, Kuril archipelago, of the Sea of Okhotsk. Because of its nutrient-rich nature, Oyashio is the mother water mass for fishes growing in Pacific Ocean near Japan and brings huge benefits to Japanese fishery and Japanese people. This water mass is characterized by occurrence of large spring phytoplankton bloom (Saito et al., 2002), which is about ten times larger, on the basis of maximum amount of phytoplankton pigment (Chl-a), than that observed in eastern subarctic Pacific (Alaska bay) (Harrison et al., 1999). Because both of Oyashio region and Alaska bay are the High Nutrient and Low Chlorophyll (HNLC) regions where large amounts of nitrogenous and phosphorous nutrients remain unutilized in mid-summer surface water, the size of spring phytoplankton bloom at both regions are regulated by the amount of iron supplies into the surface layers just before spring. Therefore, this east-west contrast of the size of spring phytoplankton bloom in the subarctic Pacific inevitably suggest that there is much larger iron source in western region (Oyashio) than in eastern region (Alaska bay).

In fact, the "Airborne Iron Hypothesis" may explain the large iron supply to Oyashio region because the Oyashio current is located near Northeast Asia where large amounts of aerosol are originating and transported eastward by strong westerly wind. However, there are some mismatches between the Asian aerosols and the phytoplankton blooms. Although the strength of Asian dust event varies large interannually, the phytoplankton bloom occurs regularly every spring in Oyashio region. While the Asian dust event occurs mostly in spring, the dissolved iron in Oyashio surface water reaches its highest concentration in winter (Nishioka, unpublished data).

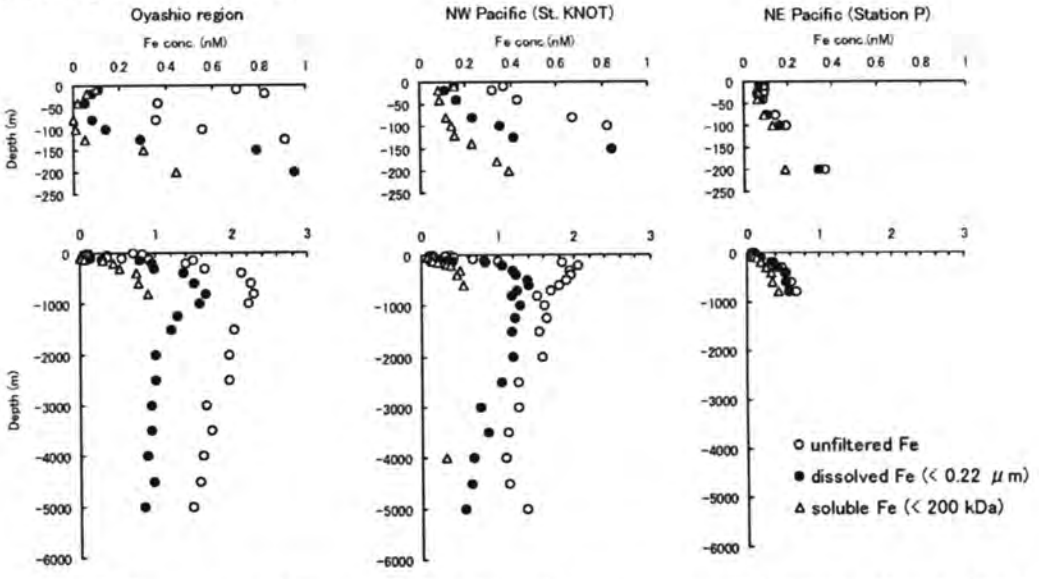

Figure 1. Comparison of vertical profiles of iron between western and eastern subarctic Pacific

Nishioka et al. (2003) found another big source of iron at the intermediate water layer in Oyashio region. Figure 1 shows the vertical distributions of "dissolved" and "unfiltered (total acid-dissolvable)" iron at Oyashio region together with those at western and eastern

subarctic Pacific Ocean. Obviously, the water columns in Oyashio region and western subarctic Pacific have predominant peaks of dissolved and particulate iron at intermediate depths just below surface water, although there is not such a feature in eastern subarctic Pacific. This iron-rich subsurface water mass can be entrained into surface layer during winter convective mixing and may support the primary productivity there. Nishioka et al. (2007) actually calculated that the upward flux of dissolved iron from the intermediate layer can support the spring phytoplankton bloom in Oyashio region.

What is source of the iron in the intermediate water of Oyashio and western subarctic Pacific ? Nishioka et al.(2007) suggested that the iron in the intermediate layer comes from the Sea of Okhotsk based on the comparison of iron concentrations along the isopycnal surfaces between the Sea of Okhotsk and Pacific Ocean (Figure 2). At all of three regions (Southern basin of the Sea of Okhotsk, Oyashio and western subarctic Pacific), there are large increases in iron concentration at common density layers corresponding to the intermediate depths. In the case of total acid-dissolvable iron (Figure 2-a), the concentration at intermediate layer is much higher in the Sea of Okhotsk than in Pacific side. Because the southern basin of Sea of Okhotsk and Pacific Ocean is connected by deep straits among Kuril archipelago, this characteristic feature in the iron distribution clearly indicates that the iron in the intermediate layer comes from the Sea of Okhotsk to the Pacific Ocean. In contrast to the "total acid-dissolvable iron", the "dissolved iron" shows almost equivalent increases at the intermediate layers among the three regions (Figure 2-b). This difference of horizontal gradients between total and dissolved iron concentrations suggests that the main form of iron in the intermediate water of Sea of Okhotsk is particle, but it may be continuously dissolved through the dissolution equilibrium which makes the dissolved iron concentration constant during the course of transport of intermediate water mass from the Sea of Okhotsk to the Pacific Ocean.

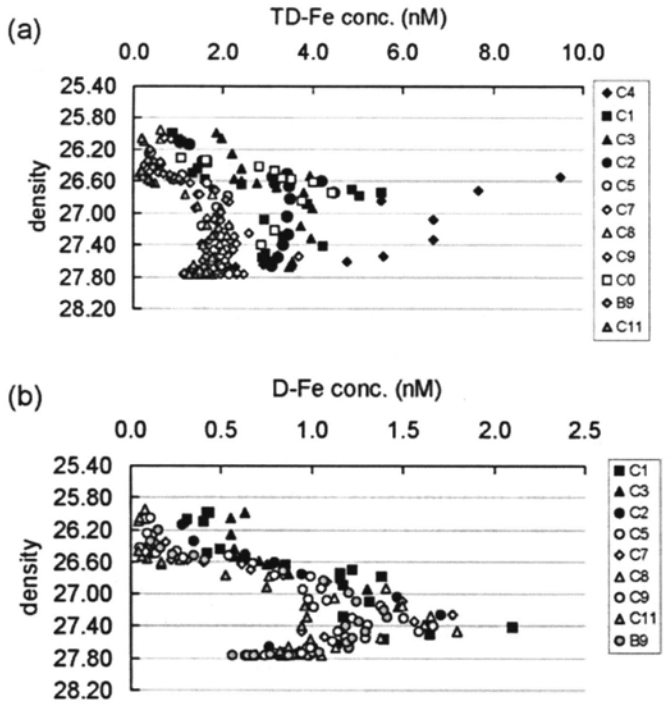

Figure 2. Iron distributions along isopycnal surfaces (Solid:Okhotsk; Open:Oyashio; Gray Western subarctic)

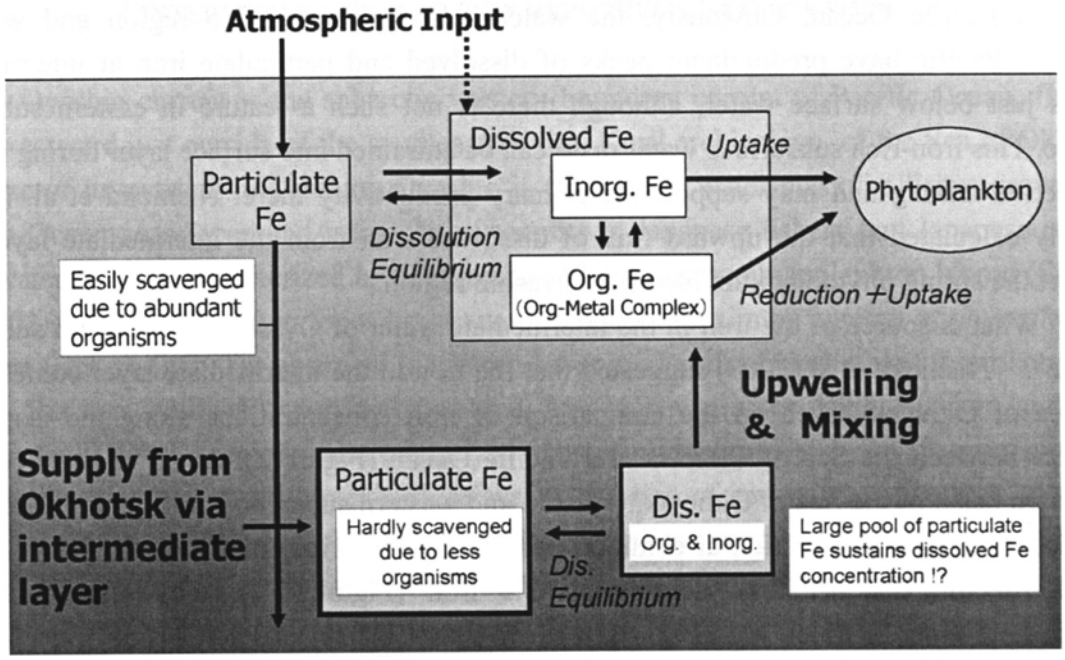

Figure 3. Possible iron sources in Oyashio & western subarctic Pacific regions

Figure 3 shows the possible schema of iron dynamics in the Oyashio region. In fact, large amount of iron must be supplied onto surface water from atmosphere as aerosol particles intermittently. However, it may be scavenged downward very rapidly because a lot of planktonic organisms in the surface water uptake and/or adsorb the aerosol particles and settle down as large sinking particles. In contrast, the particles containing iron in the intermediate layer of the Sea of Okhotsk must be very fine and cannot be scavenged easily because there are scarce numbers of organisms in the intermediate water. During the course of intermediate water transport, the particulate iron is dissolved partly according to the dissolution equilibrium and finally entrained into surface water by winter convective mixing and/or upwelling of water. Of course, iron can be hardly dissolved in the seawater. In order to make the concentration of dissolved iron in the intermediate layer as high as seen in Figure 2-b, there must be some organic ligands, which increase the solubility of iron in this water mass. Previous study on the iron solubility in the Sea of Okhotsk reported that there are plenty of autochthonous organic ligands of iron (Tani et al., 2003).

"INTERMEDIATE-WATER IRON HYPOTHESIS" -(2) IT'S MECHAMISMS

If the intermediate water of the Sea of Okhotsk contains large amounts of fine iron particles that can be dissolved easily, what is the source of this particulate iron? Our previous studies can suggest the potential mechanisms to bring huge amounts of fine iron particles to the intermediate layer of the Sea of Okhotsk.

Nakatsuka et al. (2002) found extremely turbid (particle-rich) intermediate water masses in the depth ranges of 200-500m around northeast slope of Sakhalin Island. These water masses also had another predominant feature that is very cold. The Sea of Okhotsk is characterized as the lowest latitudinal area of seasonal sea-ice cover in the world, and main

part of sea ice is created along the continental shelf on the northwest of Sakhalin Island. Because sea ice consists of pure water crystals, extremely saline water, so-called brine water, is rejected during the formation process of sea ice. The brine water has higher density than surrounding waters. Therefore it settles down onto the bottom of continental shelf and eventually flows out into the intermediate layer of offshore basin. That is the cause of very cold temperature of the intermediate water masses there.

The continental shelf on the northwest of Sakhalin has another physical oceanographic characteristic. That is the existence of very large tidal current (Kowalik and Polyakov, 1998). After precipitation of the brine water on the bottom of northwestern continental shelf of the Sea of Okhotsk, the dense shelf water (DSW) is created by continuous tidal mixing of brine water and surrounding bottom waters. During the DSW formation, bottom sediment particles are resuspended and entrained into the DSW and finally involved in the formation of extremely turbid intermediate water masses. Nakatsuka et al. (2002) called the mechanisms which create extremely turbid intermediate water as "Tidal and Brine Pump". In this area, the collaboration between tidal current and sea ice formation on the continental shelf brings large amounts of sedimentary particles into the intermediate layer in offshore region.

Amur River mouth is located at the very adjacent place to the source area of this extremely turbid and cold intermediate water mass. Huge amounts of dissolved iron, about 1.5 x 10^{11} gFe/yr (0.5 mgFe/L x 300 km^3/yr), are transported into the Amur River mouth. Almost all of them must precipitate around the river mouth by flocculation due to the contact with sea water. However, the particulate iron may not stay there, because strong tidal current prevents any fine particles from settling down there. Most of newly produced fine iron particles must be discharged onto the continental shelf on the north of Amur River mouth and join the formation of the DSW. This is the potential cause of the existence of abundant fine iron particles that may be easily dissolved again in the intermediate layer of the Sea of Okhotsk.

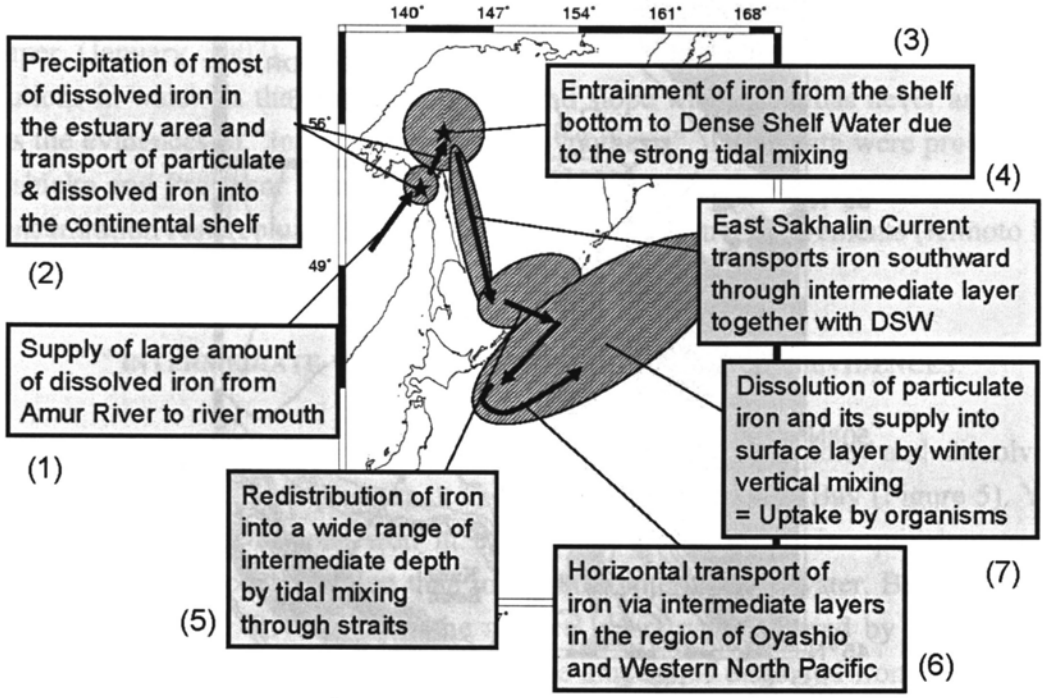

Figure 4. Iron transport from Amur River to Western Subarctic Pacific (Intermediate-Water Iron Hypothesis)

Figure 4 shows a schematic illustration of the potential processes which bring iron from the Amur River to Oyashio surface water. It contains some additional physical oceanographic features in the Sea of Okhotsk. (1) Amur River brings huge amount of dissolved iron to its river mouth, (2) Most of the dissolved iron precipitate around river mouth, but the iron particles are eventually discharged into continental shelf region due to strong tidal current there, (3) Dense shelf water entrains fine iron particles and penetrates into the intermediate layer of offshore basin, (4) East Sakhalin Current, the southward-flowing western boundary current, transports the iron-rich intermediate water mass rapidly to the southern Sea of Okhotsk, (5) The iron-rich particles are redistributed into the wider depth range due to strong tidal vertical mixing during passage through a narrow deep strait in Kuril archipelago, (6) The water currents distribute the iron-rich intermediate water masses into the wider horizontal area around western subarctic Pacific, (7) The particulate and re-dissolved iron are finally entrained into the surface water of Oyashio and western subarctic Pacific areas, and support the primary productivity there.

RESEARCH EXPEDITION IN THE SEA OF OKHOTSK DURING AUGUST-SEPTEMBER 2006

In order to prove this "Intermediate-Water Iron Hypothesis" and clarify the relating geochemical, biological and physical processes in the Sea of Okhotsk, we have conducted a research cruise in the Sea of Okhotsk in collaboration with a Russian institute (Far Eastern Regional Hydrometeorological Research Institute, Vladivostok, Russia). The research cruise was carried out from 13 August to 14 September using R/V Professor Khromov along the cruise track shown in Figure 5.

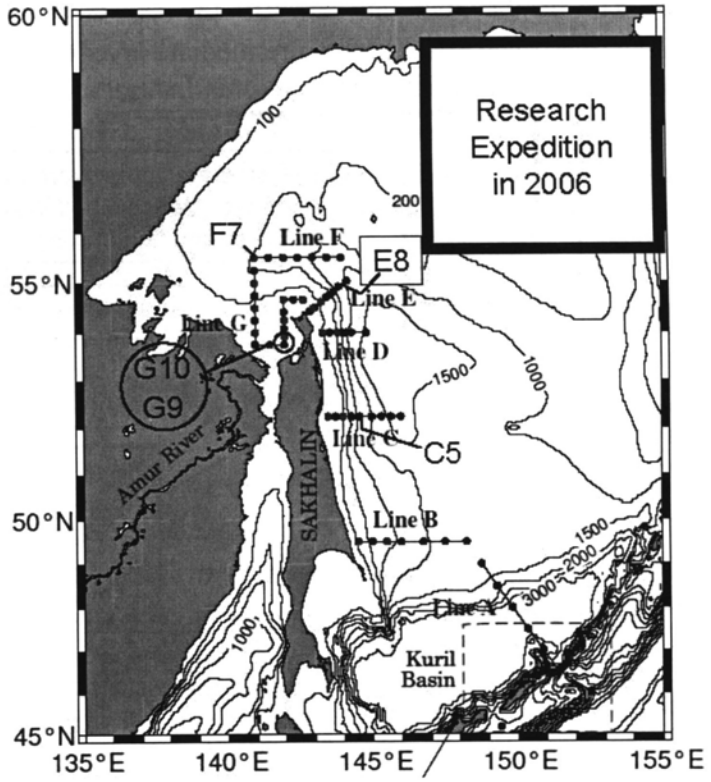

Figure 5. Cruise track of the Research Expedition in the Sea of Okhotsk in August-September 2006

Main purpose of this research expedition was to clarify following subjects.

(1) Three-dimentional iron distribution in the Sea of Okhotsk and Pacific Ocean, including Amur River mouth area and intermediate layers off east coast of Sakhalin.
(2) Budget of iron on the continental shelf around Amur River mouth, especially how much % of Amur River iron is discharged into offshore intermediate layers
(3) Limitation factors of primary productivity in the Sea of Okhotsk, whether it is limited by iron or not.
(4) Other important processes relating the iron transportation and its consequences such as "Riverine iron remaing in the surface water of the Sea of Okhotsk", "Iron flux from atmosphere", "Vertical dispersion of iron due to tidal mixing at Kuril strait", "Ecological situations of Okhotsk Sea Intermediate Water" etc.

At all of the stations shown in Figure 5, CTD observations (vertical measurements of conductivity (salinity), temperature, depth, turbidity and dissolved oxygen using wired in-situ sensors) and water samplings were carried out. Water samples were distributed on board for many chemical and biological measurements, such as dissolved oxygen, salinity, nutrients, dissolved and total iron, carbonate systems, dissolved organic matter, chlorophyll-a, bacteria, primary productivity and so on, using ultra-clean water treatment techniques. At several sites on the continental shelf and slope, bottom sediment cores were collected using a kind of multiple corer for measurements of major metal concentrations and sedimentation rates as well as the chemical compositions of pore waters. Zooplankton samples were also collected from subsurface and intermediate water depths using plankton nets at many stations along the cruise track. Turbulence caused by tidal mixing was measured by free-falling "Shear Probe Sensor" at the area around Bussol strait and the northwestern continental shelf. On the cruise track, radiosonde observation of atmosphere, aerosol samplings and bio-optical measurements were continuously conducted every day.

Because only parts of the collected samples have been analyzed by the time of writing this paper (January 2007), we would like to show here the most important data, iron distributions in water on the continental shelf and slope where iron has never analyzed until now, as the evidences of "Intermediate-Water Hypothesis". Those data were provided by Dr. Jun Nishioka and Professor Kenshi Kuma in Group 2 using "Iron Analyzer" equipped with iron concentration resin column for ultra-trace amount of iron measurements (Kimoto Electric Co., EN-701).

"INTERMEDIATE-WATER IRON HYPOTHESIS"- (3) IT'S EVIDENCES

Figure 6 shows vertical distributions of total (acid-dissolvable) and dissolved iron together with salinity and temperature at G-9 and G-10 in Sakhalin Bay (Figure 5). You can find enormous amounts of total iron in the bottom water, which is equivalent to several hundreds times higher concentration than in Oyashio intermediate water. Because these sites are very close to Amur River mouth, the surface layers were covered by fresh water from Amur River, which originally contains very large amount of dissolved iron (~10000nM-Fe). However, higher concentrations of total iron are not detected in the surface layer but observed

in the bottom layer. Concentrations of dissolved iron in surface layer were actually higher than those in bottom layer or offshore surface layer (Figure 7). But, they were much less than the particulate (acid-dissolvable) iron at G-9 and G-10. These facts inevitably suggest that most of riverine dissolved iron had precipitated by flocculation due to contact with sea water and settled down into the bottom layer of Sakhalin Bay, illustrating the proposed iron transport mechanisms (1) and (2) shown in Figure 4.

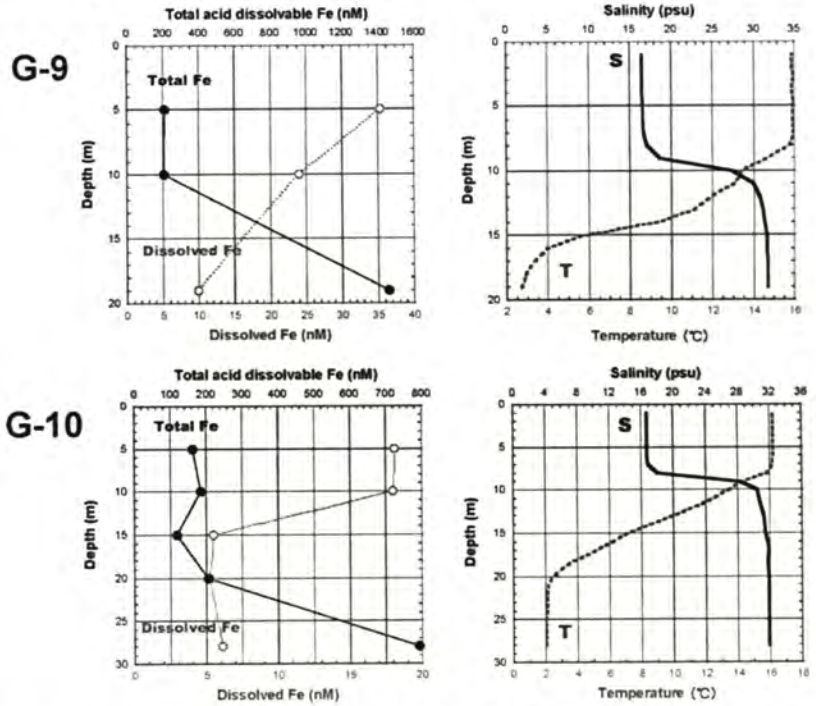

Figure 6. Vertical profiles of total and dissolved iron, salinity and temperature at G-9 & G-10 (Sakhalin Bay)

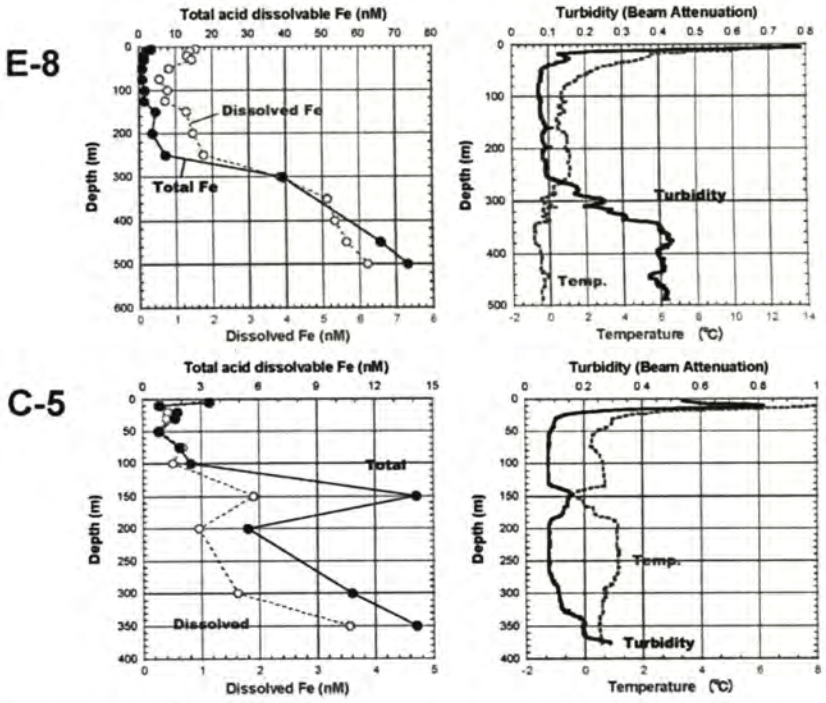

Figure 7. Vertical profiles of total and dissolved iron, turbidity and temperature at E-8 & C-5 (Continental Slope off northeast Sakhalin)

Figure 7 illustrates vertical profiles of total (acid-dissolvable) and dissolved iron concentrations together with those of water temperature and turbidity (beam-attenuation) at E-8 and C-5 on the continental slope near northeast Sakhalin (Figure 5). You can find very cold and turbid water masses in the intermediate water depths at both sites, indicating the outflows of Dense Shelf Water from the northwestern continental shelf region. Interestingly, both of total and dissolved iron show remarkable high concentrations at the corresponding layer, indicating that iron is actually transported into the offshore intermediate layer together with the DSW outflows. Total iron concentrations in these layers are equivalent to dozens times higher than those at Oyashio intermediate water and prove the proposed iron transport mechanisms (3) and (4) in Figure 4.

Both of Figure 6 and 7 are no more than snapshots of the iron transport mechanism from Amur River to Oyashio region, illustrated in Figure 4. In order to understand the role of Amur River for variations of ocean productivity in Oyashio region, it is necessary to clarify each step of the iron transport mechanisms more quantitatively. Especially, it is very important to estimate how much percentage of Amur River iron is transported into the offshore intermediate layer and how long it stays on the continental shelf. Those estimations critically affect the time lags between changes in land surface conditions and ocean productivity. If all the iron discharged from Amur River quickly penetrates into the offshore intermediate layer without significant residence time on the shelf, changes in Amur River can potentially affect the ocean productivity immediately. However, if the residence time of iron on the shelf is very long such as 1000 years, we cannot anticipate any influences in the near future on ocean productivity from human alterations of Amur River basin.

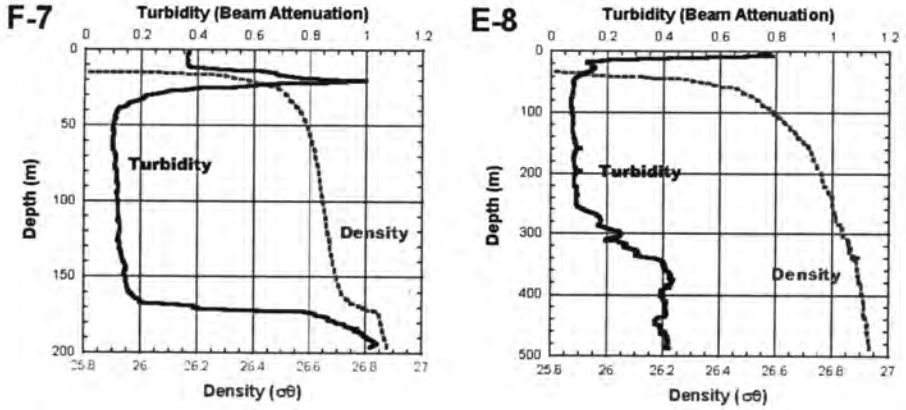

Figure 8. Vertical profiles of turbidity and water density at F-7 & E-8

Because we know approximate input of dissolved iron from Amur River (1.5 x 10^{11} gFe/yr), it is necessary to estimate outcomes of iron for the establishment of iron budget on the continental shelf near Amur River mouth. There are two potential outcomes from the shelf. One is sedimentation on the shelf bottom. The other is outflow with DSW. Unfortunately, at present, we have not finished the measurements of sedimentation rates. Therefore, we try to calculate the outflow of iron with DSW. In fact, there are not cold and dense water masses (DSW) at G-9 and G-10 sites (Figure 6), because their water depths are too shallow. On the other hand, at E-8, DSW had been already diluted by mixing with offshore intermediate water

(Figure 7). We can find the purely cold and dense, $\sigma\theta > 26.8$, water (DSW) at the bottom of F-7 on the continental shelf (Figure 8), where the iron concentration has not been analyzed yet. In order to calculate the outflow of iron into the offshore intermediate layer tentatively, we assume that turbidity and total iron concentrations are proportional between the DSW at F-7 and diluted DSW at E-8. Because the values of turbidity (beam attenuation) in the corresponding layers are 1.0 and 0.4 at F-7 and E-8, respectively (Figure 8), and the total iron concentration at the corresponding layer of E-8 is about 70 nM (Figure 7), we can estimate the total iron concentration of bottom water (DSW) at F-7 as 175 nM.

Multiplying this value, 175 nM, by the previously reported flow rate of DSW into offshore intermediate layer, 0.5×10^6 m^3/s (Gladyshev et al., 2000), we can calculate the approximate flow rate of total (acid-dissolvable) iron into the intermediate layer as 1.5×10^{11} gFe/yr. Surprisingly, this estimate is very equal to the discharge rate of dissolved iron from Amur River. Of course, this is a very tentative rough estimate, but this coincidence suggests that almost all of the Amur River iron can enter into the offshore intermediate layer together with DSW outflow and the residence time of iron on the shelf is very short, possibly less than 1 year. The reason why Amur River iron does not deposit on the shelf must be attributable to the very strong tidal current there (Kowalik and Polyakov, 1998). These tentative explanations should be checked in details by further measurements of the iron sedimentation rates on the shelf and the spatial distributions of iron in the water columns, using the collected samples in 2006, within several months.

PERSPECTIVES OF THE "INTERMEDIATE-WATER IRON HYPOTHESIS"

At first, we must integrate all data which can be provided by analyses of all samples collected in 2006 together with many physical parameters as soon as possible, and check the "Intermediate-Water Iron Hypothesis" in details. But, there remains some question which cannot be answered by the analyses of samples obtained in 2006. It is the fate of particulate iron discharged into the intermediate layer of the Sea of Okhotsk. Part of them must settle down on the deep basin and part of them may be dissolved again with the help of organic ligands. Therefore, we must examine the iron budget in the intermediate water layer at the next chance of observation by collecting sediment cores of deep basin, sinking particles by sediment traps and large volume waters for electrochemical analyses and so on.

While there remain some unrevealed mechanisms in this "Intermediate-Water Iron Hypothesis", it has many important implications for Amur-Okhotsk Project. Based on the previous and current observations of material transport system, including iron, in the Sea of Okhotsk, we can conclude that Amur River iron can be actually transported into North Pacific, and potentially support the primary productivity especially in Oyashio and western subarctic Pacific region. Because of the highly effective outflow of Amur River iron from the shelf to the offshore intermediate layer, this system may transfer impacts of the land use changes in Amur River basin to the biological productivity in North Pacific very rapidly.

On the other hand, what can the "Intermediate-Water Iron Hypothesis" suggest for global scale? Of course, this iron transport system is supported by combination of many

intrinsic natures of the Sea of Okhotsk and surrounding areas, such as iron-rich Amur River water, sea-ice formation on the continental shelf, strong tidal current near Amur River mouth, existence of southward-flowing western boundary current (East Sakhalin Current), deep and narrow straits among Kuril archipelago, vast HNLC region in subarctic Pacific and so on. Therefore, it may be difficult to find the same situation of land-ocean linkage elsewhere in the world. However, the finding of intermediate-water iron transport system suggests the potential importance of riverine iron for open ocean primary productivity. The vertical profile of iron is similar to major nutrients, such as nitrogen and phosphorous, and higher concentrations of iron are always detected in the intermediate layer than in surface layer. Parts of riverine iron deposited on the shelf and slope sediment can be re-suspended and/or re-dissolved there and parts of them are transported into open ocean areas more or less in the global scale. Because oceanographers have not clarified the direct relationship between atmospheric iron input and marine phytoplankton activity yet, it is worth reconsidering the iron budget of surface water in the world open ocean in combination with upward iron supply from the intermediate water depth.

REFERENCES

Gladyshev, S., Martin, S., Riser, S. & Figurkin, A (2000): Dense water production on the northern Okhotsk shelves: comparison of ship-based spring-summer observations for 1996 and 1997 with satellite observations. *J. Geophys. Res.* **105**, 26,281-26,299.

Harrison P.J., P. W. Boyd, D. E. Varela & S. Takeda (1999): Comparison of factors controlling phytoplankton productivity in the NE and NW subarctic Pacific gyres. *Progress in Oceanogr.* **43**, 205-234.

Kowalik, K. & Polyakov, I. (1998): Tides in the Sea of Okhotsk. *J. Phys. Oceanogr.* **28**, 1389-1409.

Nakatsuka, T., C. Yoshikawa, M. Toda, K. Kawamura & M. Wakatsuchi (2002): An extremely turbid intermediate water in the Sea of Okhotsk : Implication for the transport of particulate organic carbon in a seasonally ice-bound sea. *Geophys. Res. Letter*, **29**, 10.1029/2001GL014029

Nishioka, J., S. Takeda, I. Kudo, D. Tsumune, T. Yoshimura, K. Kuma & A. Tsuda, (2003): Size-fractionated iron distributions and iron-limitation processes in the subarctic NW Pacific, *Geophys. Res. Letters*, **30**, 14, 1730, doi:10.1029/2002GL016853.

Nishioka, J., T. Ono, H. Saito, T. Nakatsuka, S. Takeda, T. Yoshimura, K. Suzuki, K. Kuma, S. Nakabayashi, D. Tsumune, H. Mitsudera, W. K. Johnson, & A. Tsuda (2007): Iron supply to the western subarctic Pacific: Importance of iron export from the Sea of Okhotsk, *J. Geophys. Res.* (Submitted)

Saito H, A. Tsuda, & H. Kasai (2002) Nutrient and plankton dynamics in the Oyashio region of the western subarctic Pacific Ocean. *Deep-Ses Res. Part II*, **49**, 5463-5486.

Tani H, J. Nishioka, K. Kuma, H. Takata, Y. Yamashita, E. Tanoue & T. Midorikawa (2003): Iron(III) hydroxide solubility and humic-type fluorescent organic matter in the deep

water column of the Okhotsk Sea and the northwestern North Pacific Ocean. *Deep-Sea Res. Part I*, **50**, 1063-1078.

MIGRATION BEHAVIOR OF FE IN THE AMUR RIVER BASIN

NAGAO S.[1], TERASHIMA M.[2], KODAMA H.[3], KIM V. I.[4], SHESTERKIN P. V.[4] AND MAKHINOV A. N.[4]

[1]*Faculty of Environmental Earth Science, Hokkaido University*
[2]*Resreach Institute for Humanity and Nature,* [3]*Saga University*
[4]*Institute of Water Ecological Problems (IWEP),*
Far Eastern Branch of Russian Academy of Sciences, Russia

1. STUDY ITEMS OF RESEARCH GROUP-3

Iron is an essential nutrient known to limit primary productivity in HNLC regions of the oceans (Martin et al., 1994, Gervais et al., 2002, Tsuda et al., 2003, Boyd et al., 2004). The key element supporting the biomass production in the Sea of Okhotsk is considered to be iron, especially "dissolved iron" from the Amur River. The Amur River drainage was historically developed after the end of 19th century in the Russian Part. Accelerated human impacts became more obvious after the middle of 20th century in Russian and Chinese side of the Amur River (Zhang et al., 2004, 2005, Kakizawa et al., 2005). The area is being disturbed currently by various anthropogenic and natural impacts. Land-use change in the Amur River drainage might have caused significant changes in the flux of dissolved iron. We will understand the relationship between watershed environments and land-use in the Amur River basin and present ecosystem in the Sea of Okhotsk. One of goal of the project is to elucidate the mechanism how the dissolved iron and fulvic acids are formed and transported to the ocean by the Amur River, and how the flux changes will affect the phytoplankton production in the Sea of Okhotsk.

In this sub-theme (Research Group 3), we make a research plan to understand migration behavior of iron throughout the Amur River and Amur-Liman as follows:

1) Seasonal water sampling at monitoring stations along the Amur River;
2) The research cruise throughout the Amur River;
3) The research cruise at the estuary of Amur River, Amur Liman and Sakhalin Bay.

2. TRANSPORT OF DISSOLVED IRON IN RIVER WATERS FROM THE AMUR RIVER SYSTEM

2.1 Spatial and temporal variations of iron concentration in the Amur River system

Figure 1 shows dissolved iron concentration in the waters from Amur River together with water discharge at Khabarovsk in 2002. The iron concentration was almost constant at Cherniaevo (0.11±0.13 mg/l) in the upper Amur and at Blagoveschensk (0.41±0.09 mg/l) in the middle Amur. On the other hand, the iron concentration at Khabarovsk had large variation ranging from 0.38 mg/l to 1.12 mg/l. There were three peaks before increasing water discharge. The similar variation was found at Amursk, Komsomrisk-na-Amure, and Nikolaevsk-na-Amure in the lower Amur River, though the maximum value was lower than

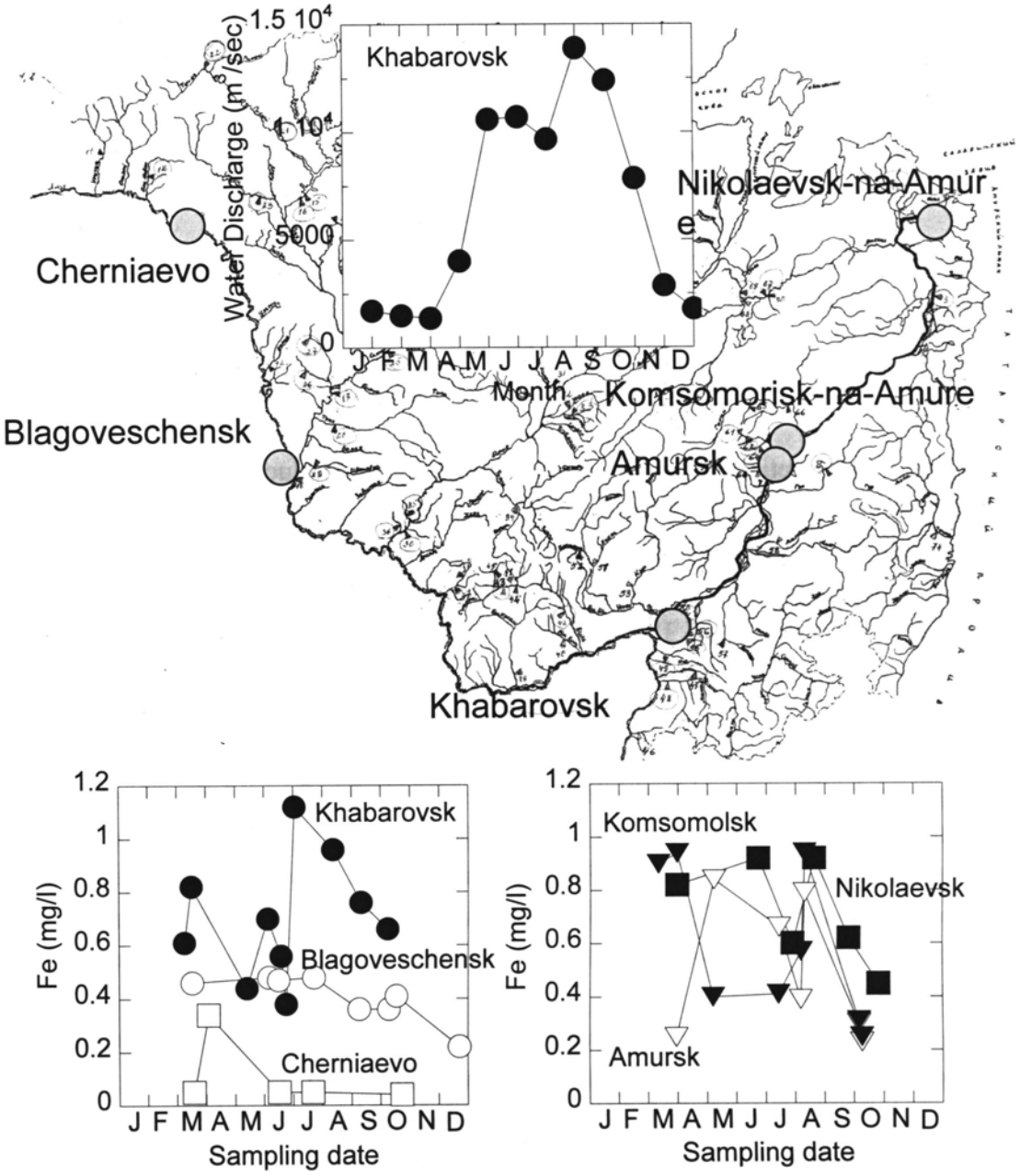

Fig.1 Monitoring observation points in the Amur River, water discharge and dissolved iron concentration in river waters in 2002. The water discharge is monthly mean value.

the Khabarovsk site.

Figure 2 shows dissolved iron concentration in river waters from main tributaries of the Amur River in 2002. The Zeya River, a major tributary of the Amur River, had the variation patterns as follows: 1) maximum concentration in July at St. 45 and, 2) in spring at St.15 and St.17, 3) almost constant at other stations. The iron concentration of Bureya River ranged from 0.13 mg/l to 0.73 mg/l. In the small rivers at St. 32-St. 35 in wetland near Khabarovsk, maximum of dissolved iron concentration was found in March and July. This is similar variation pattern with the Khabarovsk site. These results suggest that wetland near Khabarovsk may be one of important source area for dissolved iron in river waters from the

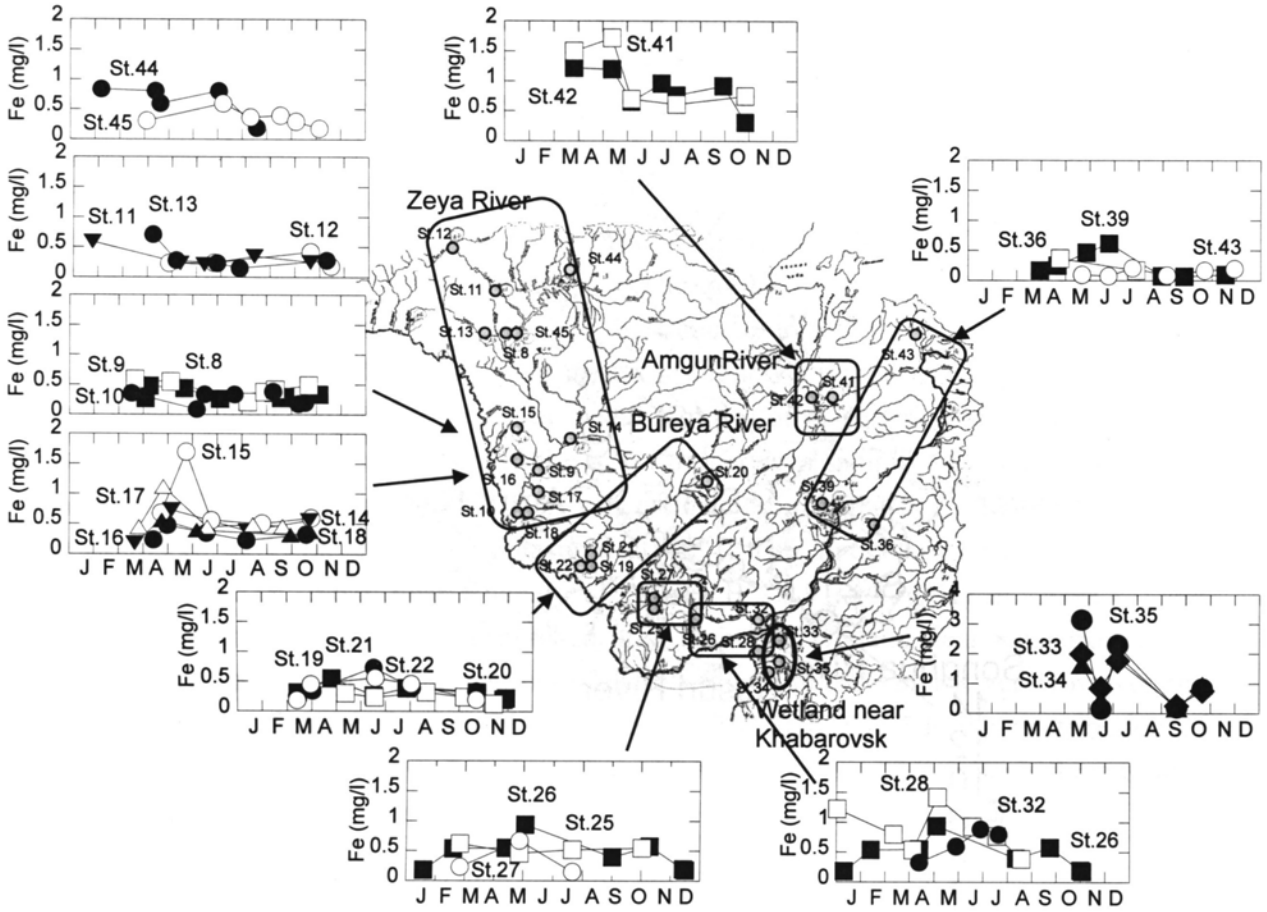

Fig.2 Dissolved iron concentration in river waters from the Amur River system in 2002.

lower Amur.

2.2 Dissolved iron concentration of the lower Amur River

Figure 3 shows sampling points at the research cruise of Lower Amur River in August 16-24. Water samples were collected during cruise of R/V *Radoga* in collaboration with the IWEP. We performed research and sampling at the Amur River, its tributaries and surrounding wetland. From August 8 to 11, our Chinese collaborators collected river water samples from the Amur River, Songhua River, Ussuri River and their tributaries in Sanjiang Plain. They also collected agricultural drainage and groundwater samples. The water samples were filtered with Whatman GF/F glass fiber filters and acidified to pH<2 with HCl for analyses of trace elements. Dissolved iron was determined by inductively coupled plasma atomic emission spectroscopy.

The lower panel of Fig. 3 shows pH and dissolved iron concentration in river waters collected at the research cruises. The Amur River water samples in lower part of the middle Amur had iron concentration of 0.33 mg/l at St.21 and 0.27 mg/l at St.14. In the Ussuri River, not shown in figure, dissolved iron concentration increased from 0.17 mg/l at the upstream to 0.44 mg/l at the downstream. On the other hand, the Songhua River had high iron concentration from 0.68 mg/l to 0.73 mg/l. As shown in Fig. 3, the iron concentration ranged from 0.55 mg/l to 0.70 mg/l at the lower Amur River. It appears that the iron concentration increases from 0.27 mg/l at St.14 to 0.68 mg/l at St.G. The maximum concentration was found

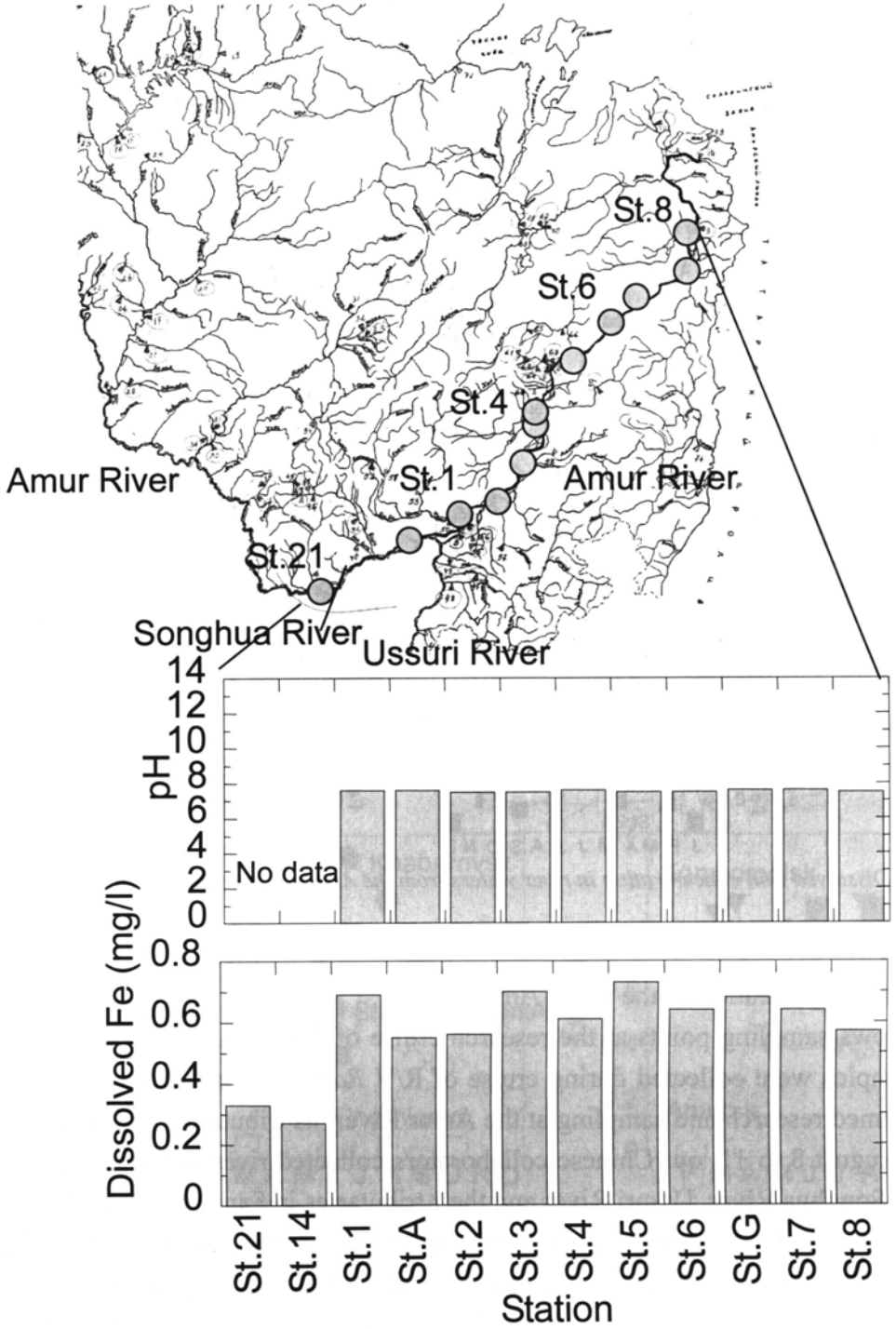

Fig.3 Variations in pH anddissolved iron concentration in river waters from the middle and lower Amur River in August, 2005. Closed circles indicate sampling stations in the Amur River.

Table 1 Iron concentration of the Amur River waters and iron flux during the research cruise in August, 2005.

Station	Water discharge ($x10^3 m^3$/sec)	Fe conc. (mg/l)	Fe flux ($x10^8$g/day)
St.1	11.0	0.57	5.41
St.4	12.0	0.61	6.32
St.6	15.5	0.64	8.57
St.8	17.4	0.57	8.57

at the sampling points of St.1, St. 3 and St.5. These sampling points are placed in the wetland area. The river waters collected from wetland extended around rivers indicate 2-3 times higher than the Amur River waters. Therefore, these results indicate the supply of dissolved iron from wetland area.

Flux of dissolved iron at each sampling point in the Amur River was estimated by averaged iron concentration from cross-section observation and water discharge at each sampling date. The results are shown in Table 1. The iron flux increased from 5.41×10^8g/ day at St.1 to 8.57×10^8g/day from St.6 to St.8. The difference in iron flux at St. 1 and St.4 suggests the supply of iron from watershed to river waters in the lower Amur River, and it apparently keeps a steady state condition for the supply and removal of dissolved iron in the watershed area at St. 6 and St.8. The differences in the iron flux between sampling stations is estimated and shown in Fig. 4. The iron flux at St.14 was estimated on the basis of the assumption for water discharge of 11.0×10^3 m^3/sec measured at St. 1. The amount of iron supplied from watershed is 2.56×10^8 g/day near Khabarovsk, "Area B", 0.91×10^8 g/day at "Area C" and 2.25×10^8 g/day at "Area D". The watershed area including wetland near Khabarovsk and Nitzhnetambovskoe is important as sources of dissolved iron in the Amur River. However, the upper and middle of Amur River with larger watershed area also has the contribution of supply of dissolved iron because of the iron flux of 2.86×10^8 g/day. This value is three to four order magnitude higher than the lower Mississipi River reported by Shiller (1997).

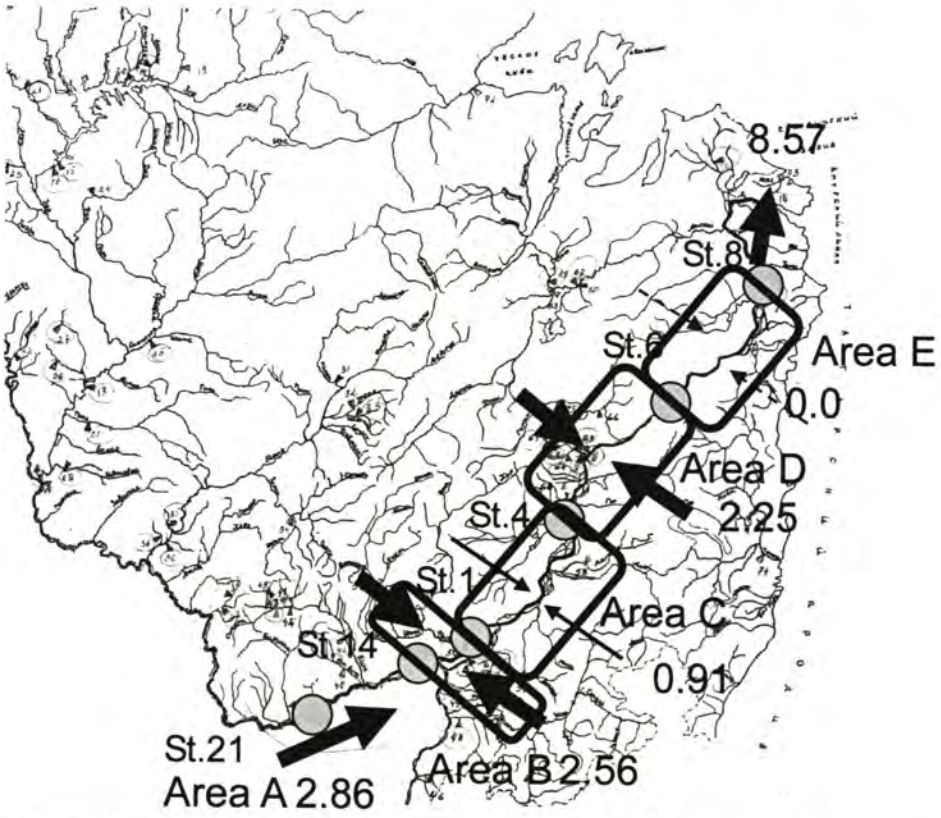

Fig.4 Flux of dissolved iron from watersheds to river waters in the Amur River during the research cruise in August, 2005.The unit is x10^8g/day. In this study, we describe each area to "Area A" to "Area E".Area E is apparently no iron supply from watersheds to river.

Figure 5 shows relationship between dissolved organic carbon (DOC) and dissolved iron concentrations in the lower Amur River. There is a positive correlation between iron and DOC concentrations. These results indicate that major part of iron is dissolved as organic complexes. Figure 6 shows iron concentration versus DOC concentration in river waters from tributaries of the Amur River in Sanjiang Plain together with the results for drainage and groundwater samples. There is no correlation with iron and DOC concentrations for the river water samples because of different watershed environments at four rivers (Usuri River, Songhua River, Yalu River, and Nangjing River). The iron and DOC concentrations for drainage and groundwater samples are higher than the Amur River and shows positive correlations.

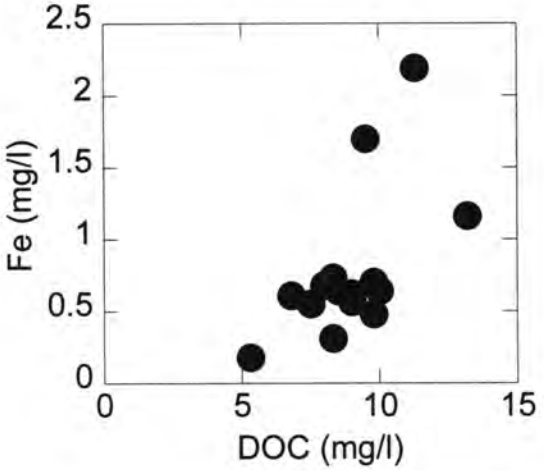

Fig.5 Variations in concentrations of dissolved iron and dissolved organic carbon (DOC) in river waters from the lower Amur River during the river research cruise from Khabarovsk to Nikolaevsk-na-Amure in August, 2005.

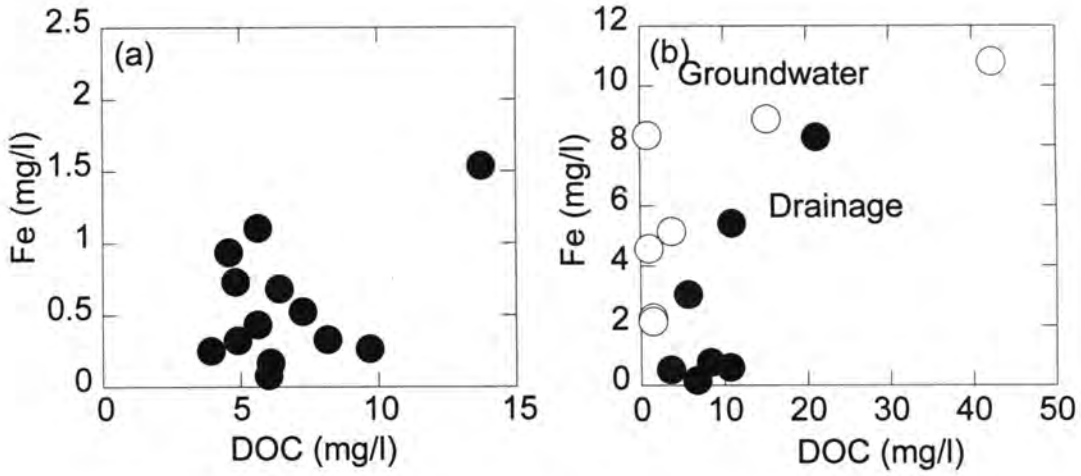

Fig.6 Variations in concentrations of dissolved iron and DOC in river waters from the tributaries of Amur River (a), and in drainage and groundwaters (b) in Sanjiang Plain in August 2005.

2.3 Temporal variations in dissolved iron concentration and its flux at Khabarovsk from 1960 to 2000

Time series of dissolved trace elements in rivers are important for flux calculation and for understanding the mechanisms controlling the concentrations of these elements in rivers. Monthly water samplings at the Khabarovsk monitoring site were conducted by the Hydromet from 1960 to 2002. Figure 7 shows time series results of iron determined in these samples. The iron concentration ranged from 0.04 mg/l to 1.28 mg/l. There was a maximum in summer in 1975, 1980, 1995 and 2002.

Flux of dissolved iron at Khabarovsk site was estimated using water discharge weighted mean value of dissolved iron from 1960 to 2002. These results are shown in Table 2 and Fig. 8. The dissolved iron flux increases with increasing time from 1960 to 1975, and then has some variations ranging from 0.56×10^{11}g/yr to 1.57×10^{11}g/yr. The iron flux can be divided into three groups as follows:

1) 1960, 1965, 1980, 1990 average annual Fe flux $0.62 \pm 0.08 \times 10^{11}$g/yr;
2) 1970, 1985, 2000 average annual Fe flux $1.1 \pm 0.1 \times 10^{11}$g/yr;
3) 1975, 1995, 2002 : average annual Fe flux $1.5 \pm 0.04 \times 10^{11}$g/yr;

As shown in Fig.8, there is no relationship between annual water discharge and iron flux.

3. BEHAVIOR OF IRON IN ESTUARINE ENVIRONMENTS

Estuarine mixing reduces the dissolved iron flux to the ocean by 70-95% because of the scavenging of iron (Chester, 2000). It has been demonstrated that iron-humate complexes stimulate the growth coastal marine phytoplankton in laboratory cultures and contribute to the phytoplankton bloom in marine coastal waters (Graneli and Moreira, 1990, Carlsson and Granet, 1993, Matsunaga et al., 1998). Therefore, the concentration and forms of dissolved iron has an important role in the limitation of the production of phytoplankton in estuary, costal sea and pelagic ocean.

3.1 Research cruise at the estuary, Amur-Liman and Sakhalin Bay

The research cruise was conducted in August 16-24, 2006. The sampling stations are shown in Fig. 9. Water samples from estuary of the Amur River were taken at three stations (St.1-3) by a speed boat. Water samples were also collected at four stations (St.4-St.7) from the Amur-Liman and at two stations (Stns. 8 and 9) in Sakhalin Bay during cruises of research vessel of Russian Navy in collaboration with the IWEP. These samples were filtered with Whatman GF/F filters for DOC analyses and 0.22 μm cartridge filter for trace element analyses. The fundamental analyses such as DOC, trace elements, nutrients etc. will be finished at the end of March in 2007.

3.2 Study on coagulation of iron in laboratory experiment

3.3 Association forms of iron in the river and estuarine environments

The results of above research items are present by Terashima and Nagao in this report.

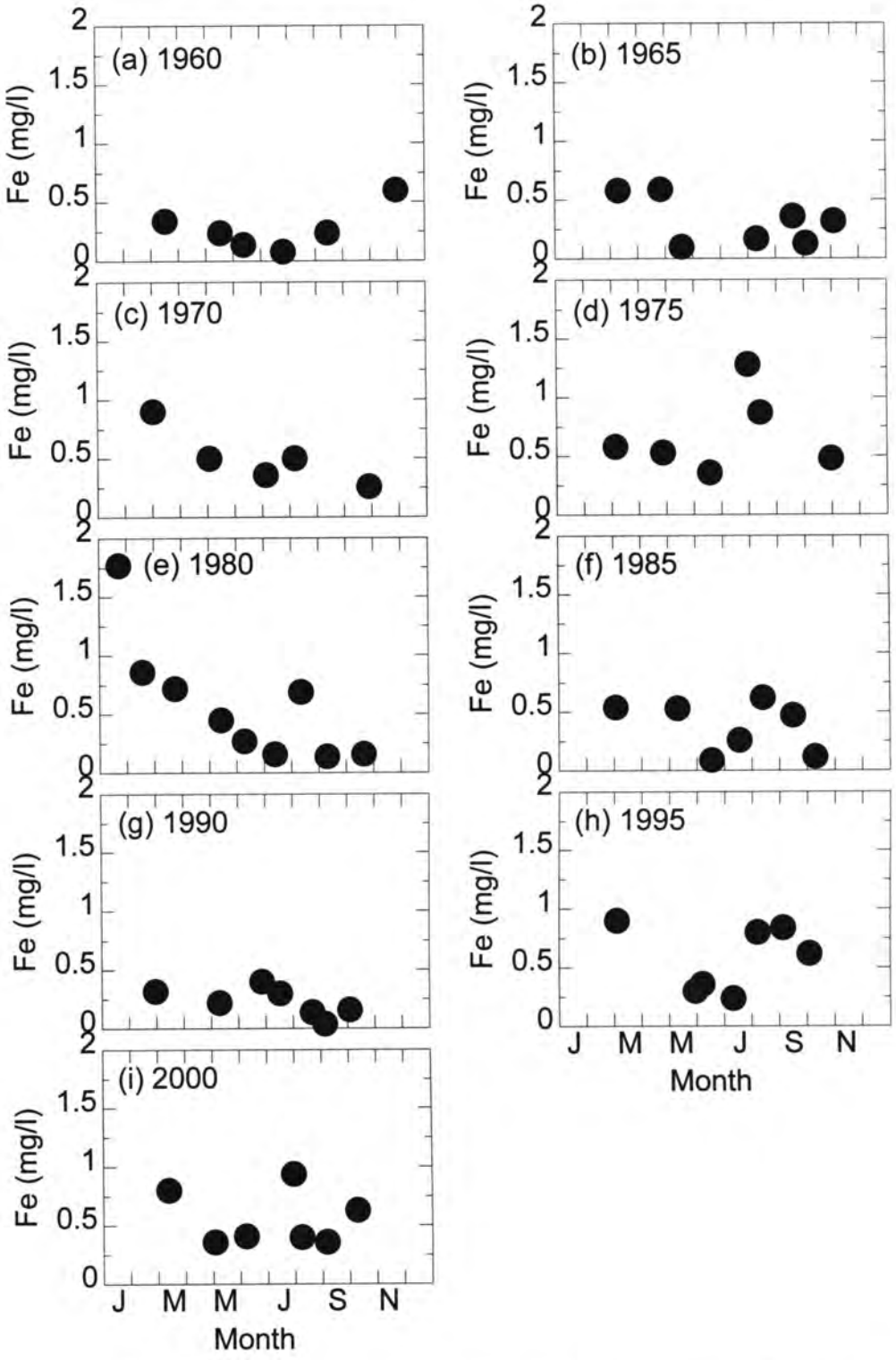

Fig.7 Dissolved iron concentration in the Amur River waters from 1960 to 2000. The water samples were collected at monitoring station near Khabarovsk.

Table 2 Iron flux at Khabarovsk monitoring station from 1960 to 2002.

Year	Water discharge ($x10^{11}m^3$/year)	Mean Fe conc.* (mg/l)	Fe flux ($x10^{11}$g/year)
1960	3.92	0.17	0.67
1965	2.47	0.23	0.56
1970	2.43	0.42	1.00
1975	1.96	0.76	1.50
1980	2.04	0.34	0.70
1985	3.17	0.38	1.21
1990	2.84	0.19	0.54
1995	2.76	0.55	1.51
2000	2.16	0.48	1.04
2002	2.07	0.76	1.57

*Water discharge weighted mean value.

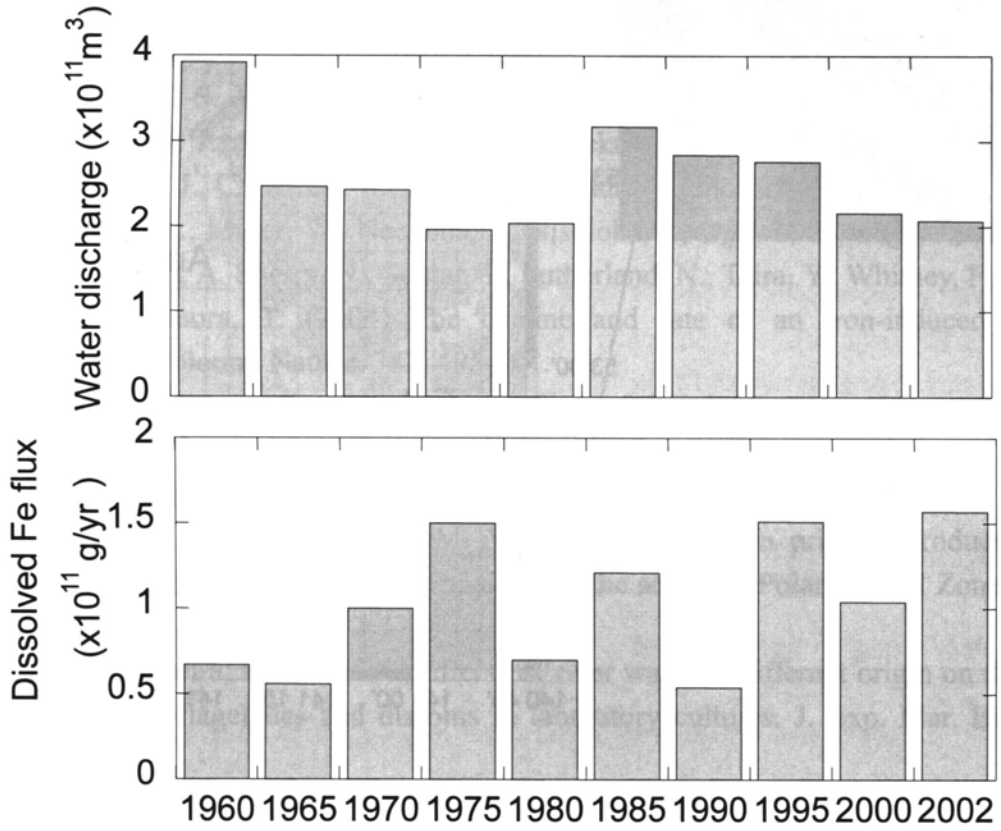

Fig.8 Annual water discharge and dissolved iron flux of the Amur River at Khabarovsk station.

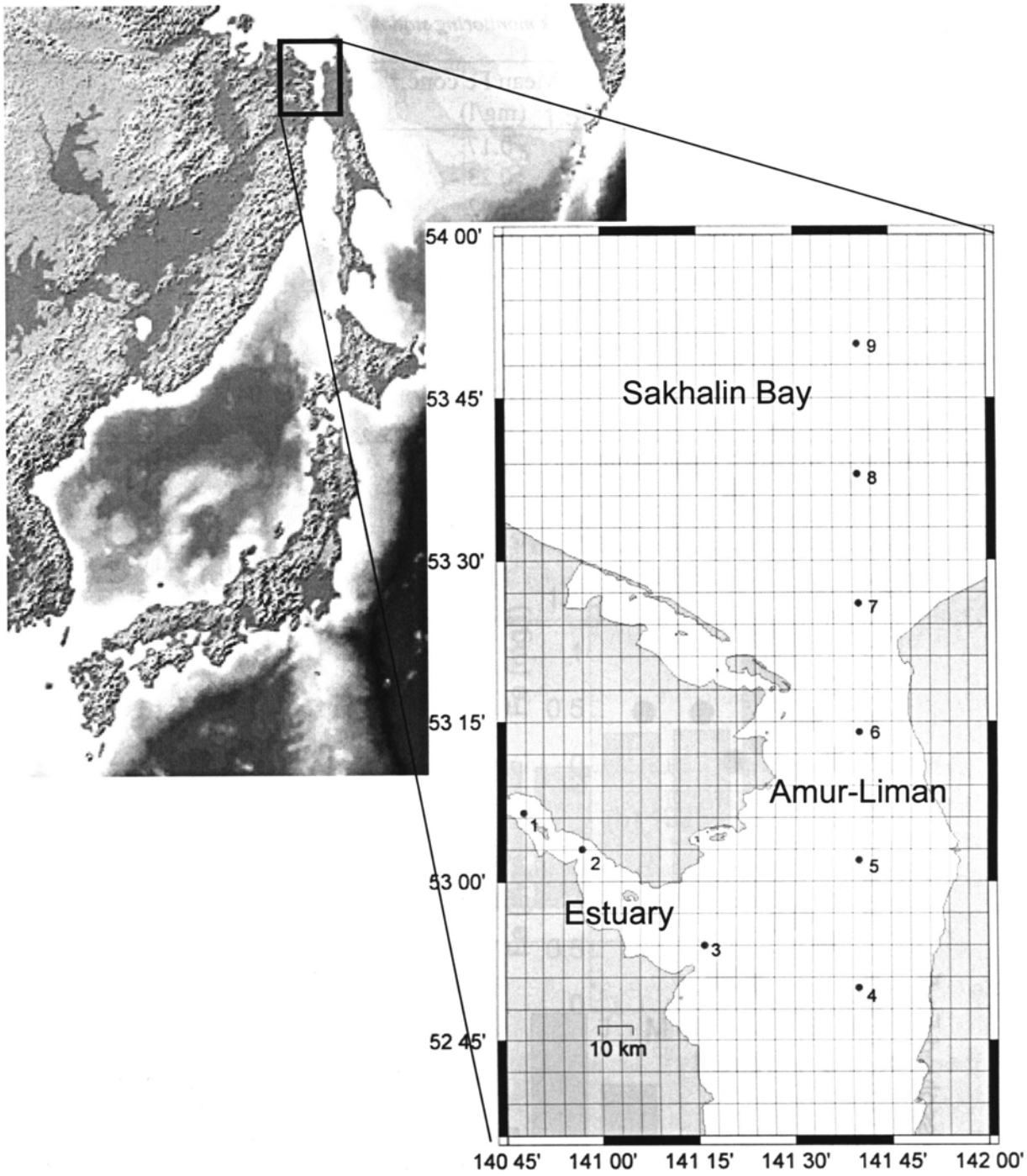

Fig.9 Sampling stations in estuary of the Amur River, Amur-Liman and Sakhalin Bay during the research cruise in August 2006.

4. FUTURE RESEARCH PLAN

We have plans for research cruises throughout the lower Amur River, its estuary and Amur-Liman, Sakhalin Bay at higher water discharge conditions in summer in 2007. We set up same sampling stations to compare the results with previous data in 2005 to understand

transport behavior of iron in the Amur River system. We also continue to perform monitoring study at Khabarovsk and Bogorodtskoe, and will add the monitoring stations at estuary of the Amur River.

ACKNOWLEDGEMENTS

We thank Mr. Y. Nakamura, Mr. Andrey Krasnenko (Hokkaido University) as well as the crew of the R/V *Radoga* for their effort in sampling of the river cruise in 2005. We also thank Dr. V. D. Kozlovski (Nature Protection Agency of the Nokolaevsk City and District Adminiatration: NPANCDA) and the crew of speed boat (NPANCDA) and research vessel of Russian Navy for their help in sampling of the cruise in 2006.

REFERENCES

Boyd, P. W., Law, C. S., Wong, C. S., Nojiri, Y., Tsuda, A., Levasseur, M., Takeda, S., Rivkin, R., Harrison, P. J., Stzepek, R., Gower, J., Mckay, R. M., Abraham, E., Arychuk, M., Barwell-Clark, J., Crawford, W., Hale, M., Harada, K., Jhonson, K., Kiyosawa, H., Kudo, I., Marchetti, A., Miller, W., Needoba, J., Nishioka, J., Ogawa, H., Page, J., Robert, M., Saito, H., Sastri, A. Sherry, N., Soutar, T., Sutherland, N., Taira, Y., Whitney, F., Wong, S. E. and Yoshimura, T. (2004) The decline and fate of an iron-induced subarctic phytoplankton bloom. Nature, 383, 495-501.

Carlsson, P. and Granet, E. (1993) Availability of humic bound nitrogen for coastal phytoplankton. Estur. Coast. Shelf Sci., 36, 433-447.

Chester, R. (2000) Marine Geochemistry, 2nd edition, Blackwell, London.

Gervais, Riebesell, U. and Gorbunov, M. Y. (2002) Changes in primary productivity and chlorophyll a in response to iron fertization in the southern Polar Frontal Zone. Limnol. Oceanogr., 47, 1324-1335.

Graneli, E. and Moreira, M. O. (1990) Effects of river water of different origin on the growth of marine dinoflagellates and diatoms in laboratory cultures. J. Exp. Mar. Biol. Ecol., 136, 89-106.

Kakizawa, H., Sakashita, A. and Park, H. (2005) Underlying causes of land use change and degradation of natural resources in the Amur Basin. Report on Amur-Okhotsk Project. Vol. 3, pp.133-139.

Matsunaga, K., Nishioka, J., Kuma, K., Toya, K. and Suzuki, Y. (1998) Riverine input of bioavailable iron supporting phytoplankton growth in Kesennuma Bay. Wat. Res., 32, 3436-3442.

Martin, J. H., Coale, K. H., Johnson, K. S., Fitzwater, S. E., Gordon, R. M., Tanner, S. J., Hunter, C. N., Elrod, V. A., Nowicki, J. L., Coley, T. L., Barber, R. T., Lindley, S., Watson, A. J., van Scoy, K., Law, C. S., Liddicoat, m. I., Ling, R., Station, T., Stockel, J.,

Collins, C., Anderson, A., Bidigare, R., Ondrusek, M., Latasa, M., Millero, F. J., Lee, K., Yao, W., Zhang, J. Z., Friederich, G., Sakamoto, C., Chavez, F., Buck, K., Kolber, Z., Green, R., Falkowski, P., Chisholm, S. W., Hoge, F., Swift, R., Yangel, J., Turner, S., Nightingale, P., Hatton, A., Liss, P. and Tindale, N. W. (1994) Testing the iron hypothesis in ecosystems of the equatorial Pacific Ocean. Nature, 371, 123-129.

Shiller, A. M. (1997) Dissolved trace elements in the Mississipi River: Seasonal, interannual, and decadal variability. Geochim. Cosmochim. Acta, 61, 4321-4330.

Tsuda, A., Takeda, S., Saito, H., Nishioka, J., Nojiri, Y., Kudo, I., Kiyosawa, H., Shiomoto, A., Imai, I., Ono, T., Shimamoto, A., Tsumune, D., Yoshimura, T., Aono, T., Hinuma, A., Kinugasa, M., Suzuki, K., Sohrin, Y., Noiri, Y., Tani, H., Deguchi, D., Tsurushima, N., Ogawa, H., Fukami, K., Kuma, K. and Saino, T. (2003) A mesoscale iron enrichment in the western subarctic Pacific induces large centric diatom bloom. Science, 300, 958-961.

Zhang, B., Wang, Z. and Duan, H. (2004) A study of the land use in Songhua River Basin of China. Report on Amur-Okhotsk Project. Vol. 2, pp.153-159.

Zhang, B., Wang, Z., Ki, J. and Li, F. (2005) Land cover change in Heilongjiang farm group company of China. Report on Amur-Okhotsk Project. Vol. 3, pp.111-116.

ASSESSMENT OF THE DISCHARGE OF SOME CHEMICAL SUBSTANCES FROM THE AMUR INTO THE SEAS OF JAPAN AND OKHOTSK

MAKHINOV A.N., KIM V.I., KUZNETSOV A.M. AND RUZHOV D.A.

Institute of Water and Ecology Problems,
Far Eastern Branch of the Russian Academy of Sciences

The Amur river today is one of the most polluted rivers in Russia due to a complex impact of different natural and anthropogenic processes in its basin that influence river water quality. Multi-component disturbance of natural landscapes in the drainage area, industrial, agricultural and community wastewater discharge into the river from Russian and China coupled with river regime changes accelerated the formation of a disastrous ecological situation in Priamurje. Most intensive changes of water quality take place in the Lower Amur [2] mostly caused by the anthropogenic pollution of the Sungari river.

Still mixing pattern of water from the Amur and Sungari in different parts of the Amur varies, thus causing uneven distribution of various chemical substances along and across the river. Seasonal changes of chemical discharge ion both rivers are also registered. All these factors make it rather difficult to assess the total volume of various chemical substances discharge from the Amur into the Seas of Okhotsk and Japan.

The Institute of Water and Ecology Problems, FEB RAS (IWEP) carried out river water quality studies in the Lower Amur from Khabarovsk to Bogorodskoe during of the seasons of 2005 and 2006. The main sampling took place near the villages Nizhneleninskoe, Petrovskoe, Nizhnespasskoe, Bogorodskoe, the cities of Khabarovsk and Komsomolsk-on-Amur and the low reaches of the Amgun river.

Water samples were analyzed in the laboratories of IWEP FEB RAS, The Analytic Center of the Institute of Tectonics and Geophysics, FEB RAS, research institutes in Ufa and Obninsk cities. Trace metals were analyzed with ICP-MS Elan DRC II Perkin Elmer (USA) mass spectrometer with inductively coupled plasma.

The data collected and combined with previous data serve a good basis for deep analysis of the present state and conditions that form Amur water quality, which, in its turn, determines the current state of freshwater, watershed and seawater ecosystems.

The Amur run-off is formed in a vast area (1 855 000 km^2), characterized with diverse natural conditions, which determine a complex background for water chemical composition. Significant run-off irregularities between the seasons and in perennial regime produce high dynamics of major indicators of water qualitative characteristics. Economic activities in the river basin also have a big impact on water quality in the Amur.

The Amur is classified as a Far Eastern river type with a prevailing precipitation-formed run-off as its specific feature. The annual share of precipitation in run-off formation reaches 90% and provides water abundance in a warm period. Snow source is of secondary importance and spring high water is observed at the end of April and the beginning of May.

Average perennial water discharge in the river mouth is 10 900 m^3/sec. Maximal registered discharge near Khabarovsk was 40 000 m^3/sec (September 1897) and minimal discharge was 153 m^3/sec (March 1922). Within the year discharge rate greatly fluctuates. In the cold period (November – March) it is minimal. In spring owing to snow melting the water level rises. The lowest water level in non-freezing period is usually registered at the beginning of summer. Maximal levels and discharge is observed in summer-autumn time (July – October), owing to frequent rain storms brought by typhoons and cyclones from East-Asian seas [5].

Morphological specifics of the riverbed of the Lower Amur passage (1 200 km from the Sungary juncture to the river estuary) include current directed accumulation. Lots of narrowings and expansions here determine riverbed structure and dynamics [3]. In wide valley parts the stream is split into numerous big and small sub-streams, spreading in a fan-like pattern down the river and forming extremely complicated hydrographic drainage. Wide sub-streams (0.8-1.5 km) form a river drainage frame, rather stable in time. These sub-streams split and merge with dozens smaller sub-streams to form permanent or temporary existing streams.

In the mountainous areas the Amur valley becomes narrow and steep mountainous slopes limit riverbed deformation development. The river there has a single stream with gentle meanders. Still due to substantial alluvial flows and their intensive sedimentation the stream dynamic axis often changes its position, thus changing the location of the waterway.

The Lower Amur has three big tributaries: the Ussuri, 897 km long and having drainage area of 193 000 km^2, the Tunguska River, 544 km long and having drainage area of 30 200 km^2, the Amgun River, 723 km long and having drainage area of 193 000 km^2.

The Amur is characterized with significant run-off fluctuations between the years. In some years the river water content may be small, medium and large. Water content differences are more evident in summer. In winter the river water content is more stable. In recent 10 years the smallest water content was observed in 2002, medium content was in 2004 and the largest was in 1998. In 2006 it can be described as close to medium.

In 2005-2006 winter period low water level fluctuated near Khabarovsk from –127 to – 150 cm. In spring 2006 a small flood tide was observed on the Amur, which in May reached 197 cm. A bigger flood happen later and had two peaks (June 30 – 327 cm and August 14 – 342 cm). Summer low water period was not long (7-10 days) with minimal water levels of 15 cm. A stable water level decrease up to – 92 cm was observed in autumn before river freezing began (Fig. 1).

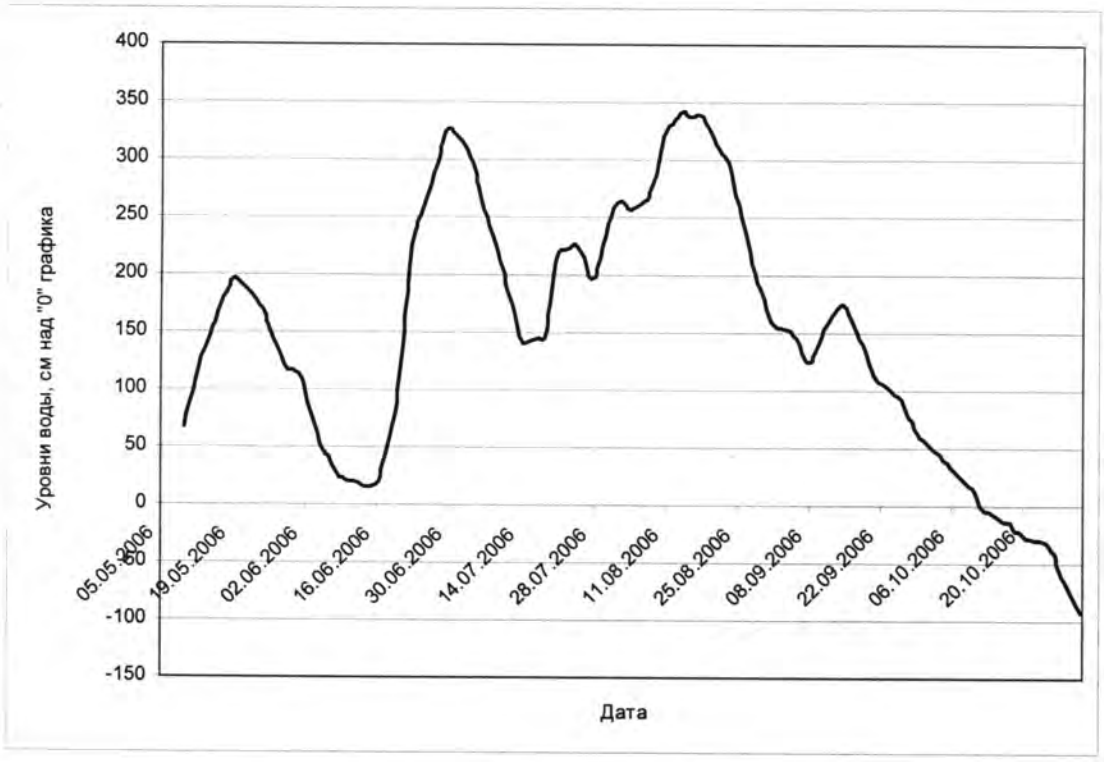

Fig. 1. Amur water levels near Khabarovsk in summer 2006.

The Amur near Khabarovsk has very specific and complicated conditions, which determine mixing of water masses that come from upstream regions. There are several main factors that form chemical distribution pattern across and along the stream. The first one is that the Amur here has many sub-streams and water run-off distribution between the sub-streams fluctuates in volume in different phases of water regime.

Secondly, The Ussuri River joins one of the Amur sub-streams upper Khabarovsk. Ussuri water mixes with Amur water in two places. The first time it partially mixes at the juncture of the Ussuri and the sub-stream and the second time it mixes with the Amur mainstream. Depending on water abundance in the river the rate and scope of water mixing changes significantly.

The third factor is that the Amur riverbed from the Sungari juncture to Khabarovsk has strongly marked specific morphological features as the river width exceeds (hundred times) its depth. Due to intensive stream turbulence and rapid vertical mixing of water masses (from the surface to the bottom), mixing of water across the river proceeds extremely slowly. Besides, in summer time this mixing process is even more slowed due to the appearance of extensive net of long and water abundant sub-streams.

Perennial regime of the Amur run-off is characterized with well-marked interchange of low and high water content periods of 8-15 years. Last 10 years the Amur water content is low. Besides, in the summers of 2000, 2001 and 2003 the river water level was extremely low and record-breaking.

In winter special conditions are created. Due to a substantial decrease of water levels and deep freezing of several sub-streams the distribution of chemical substances across the

river becomes more even much quicker than in summer. Sharp decrease of water run-off in winter accelerates water velocity irregularities along the river. The river current in long river reaches significantly slows down and mean water velocity decreases more than twice compared to summer rates. Thus, in December 2005 and January 2006 it fluctuated from 30 to 50 km/day, whereas in summer it is usually 70-80 km/day.

Detail studies of cross section distribution of the main hydrochemical characteristics showed stable differences from one bank to the other in the Amur main stream. Moreover, in various parts of the river near Khabarovsk they were of different character.

Trace metals showed most uneven distribution in cross section.

Trace metal distribution revealed a certain regularity resulting from evident impact of Sungari discharge (Tables 1-3). This impact is mostly observed in the Amur main stream lower the Sungari juncture.

At Nizneleninskoe sampling station most trace metals (Cu, Zn, Cd, Hg, Pb) have increased concentrations in water close to the right bank or in the river middle. Cr and As reveal more complicated behavior as at different times high concentrations are observed either at one bank or the other.

Much contrast in trace metal concentrations between the right and left banks was observed in the Amurskaya sub-stream due to closeness to the Ussuri juncture and poor mixing of Ussuri and Amur waters. Higher trace metal concentrations in summer were observed close to the left bank the Amurskaya sub-stream, where Amur water dominates. But some metal contents (Cu, Zn, Pb) in spring and at the beginning of summer were significant at the right bank of the sub-stream.

Seasonal fluctuations of trace metal content in Amur water were observed. Relatively low quantitative records were registered in May and September and much higher records were in June that may be explained with the surface run-off in the drainage basin resulting from precipitation.

Average perennial Amur run-off is 369.1 km^3 [4]. Its maximum of 459 km^3 in the observation period was recorded in 1985 and its minimum record was 250.8 km^3 in 1979. Thus, maximal run-off exceeds the minimal one in 1.8 times.

Perennial regime of the Amur run-off is characterized with strongly marked interchange of low and high water content periods, which last 8-15 years. High water content periods occurred in 1890-ies, 1910-teens, 1930-ies, 1950-ies and 1980-ies. Moreover, water content gradually increased from period to period and reached its maximum in the 1950-ies, when disastrous floods caused severe damage to regional economy. The last high water content period in1980-ies was not severe compared to previous ones due to significant anthropogenic impact of recently constructed hydropower energy facilities and increased consumption of water for industrial and agricultural use. Still, water levels at maximal floods in this cycle (1984 and 1991) nearly reached their historic maximum.

Low water content periods occurred in 1920-ies, 1940-ies, 1970-ies and 1990-2000. In the last low water cycle a slight decrease of the run-off was observed, which is probably also caused by the anthropogenic impact. Extremely low levels were registered in summer in 2000, 2001 and 2002 and they were very close to record-breaking in all the observation period.

All these observations indicate an evident increase of the degree of contrast in main hydrological characteristic indicators, such as water levels, run-off, turbidity and suspended matter discharge. Amur hydrological regime changes mostly due to anthropogenic impact result in the acceleration of irregularities in the river run off and discharge of dissolved and solid substances into the Okhotsk and Japan Seas.

Generally, it is estimated that the Amur water content has increased by 10-12% in 100-year period of observations. It is explained by the increase of atmospheric precipitation in the Amur River basin, especially in its lower reaches. Annual precipitation in the cold season (November – March) has increased nearly twice in recent 112 years (from 1891 till 2003). Warm season increase (April – October) is estimated as 1.2 times [1]. Total moistening of the Amur basin territory in the period of observations has increased by 31%. The Amur water content has increased not that much due to the increase of evaporation, caused by the average annual temperature rise in the region, but due to the consumption of surface water for economic development purposes.

Numerous natural and anthropogenic factors influence the formation of terrigenous and chemical matter discharge into the sea. Most part of the discharged terrigenous matter is accumulated in the Middle Amur. The biggest tributaries Zeya, Bureya, Sungari and Ussuri join the Amur in this passage of less than 1 000 km. Their accumulate 65% of the Amur run off and over 90% of suspended matter discharge. Unconsolidated clayey sediments, abundant in the basing of these tributaries and highly intensive riverbed processes cause significant suspended sediment discharge and increased water turbidity (up to 400-500 μg/l) within the Amur middle and lower reaches.

Suspended sediment discharge from the tributaries into the Amur mainstream has general geographic regularities. In the Russian part of the river basin its module fluctuates from 8 to 32 tons/km^2 per year with maximum volumes in the Zeya-Bureya plain (20 – 32 tons/km^2). Suspended sediments bring along significant amount of pollutants, especially trace metals and organic substances.

A general correlation between perennial sediment discharge and river water run off is observed. In 1960-ies was a period of increased sediment discharge, changed by the period of low sediment discharge in 1970-ies. In 1980-ies again the increase in sediment discharge was quite evident, and in 1990-ies volumes of sediment discharge were relatively small. This period is being continued now.

The following regularity in suspended sediment discharge along the river towards its lower reaches has been observed: average size of suspended particles becomes smaller. The share of particles less than 0.005 mm in size near Khabarovsk is 20% of the total amount of suspended matter, whereas near Bogorodskoe this share grows to 60%.

Permafrost rocks, widely spread in the northern part of the Amur basin, much determine the Amur chemical discharge. In the mountainous regions its layer can be 300 m thick, having temperature –5^{0}C. Such rocks significantly limit the underground flow and thus the flow of dissolved substances. Bogs and swampy areas are the other factors that influence dissolved matter discharge.

Amur run off irregularities, especially in summer cause significant fluctuations in organic matter discharge. In time of extremely summer low water, observed in 200 and 2001 vegetation started to grow at the bottom of dried lakes and sub-streams. Then later they were filled with water and a great amount of decomposed biomass was discharged from those lakes and sub-streams into the river main stream. This discharge could be compared to a instantaneous release.

The total volume of organic matter discharge from the Amur into the Okhotsk and Japan Seas is estimated 5.5 million tons [6]. Most of the organic matter amount is discharged in the second half of the warm period, predominantly in the July – October period.

Total dissolved matter discharge from the Amur into the Okhotsk and Japan Seas is 18.3 million tons per year [6]. The following ions compose the biggest share of this discharge (in million tons per year): calcium - 2.34, magnesium – 0.74, natrium and potassium – 1.60, hydrocarbons – 10.4, sulfates – 2.1, chlorides – 1.1. It is rather difficult to calculate the discharge of other elements because the discharge has a very irregular pattern and insufficient data collected in various water regime phases. Thus, only approximate estimates are possible at present to be specified with further studies.

Using the data provided by the Far Eastern Agency of Hydrometeorology and Environmental Monitoring, a quantitative analysis of phosphates and nitrite and nitrate nitrogen has been carried out. The data on average annual concentrations of these elements in the period from 1981 till 2003 were used. Mean content of nitrite nitrogen in Amur water in the multi-year period of observation is 0.016 mg/l. Based on annual average Amur run off 369.1 km^3, annual average discharge of nitrite nitrogen from the Amur into the sea is approximately 5 900 tons.

Nitrate nitrogen content in Amur water is estimated 0.110 mg/l based on annual average data on its content collected in 23 years of research. Annual average discharge of nitrate nitrogen from the Amur into the sea is approximately 41 000 tons.

Mean content of phosphates in Amur water in the multi-year period of observation is 0.050 mg/l. Annual average discharge of phosphates from the Amur into the sea is calculated as approximately 18 500 tons.

Based on perennial irregularities of the Amur run off, which maximal records exceed its minimal records 1.8 times, we can conclude that perennial biogenic matter discharge will also fluctuates within this range.

The reported data need further research and correlation to reveal dynamic regularities of Amur water quality in seasonal and perennial regimes.

Table 1. Trace metal content in water, μg/l, in September 2006 at Khabarovsk.

Element	Left bank, Surface	Left bank, Bottom	296 meters from the left bank, surface	296 meters from the left bank, bottom	571 meters from the left bank, surface	571 meters from the left bank, bottom	841 meters from the left bank, surface	841 meters from the left bank,	1021 meters from the left bank, surface	1021 м meters from the left bank, bottom	Right bank, surface	Right bank, bottom
Cr	2.37	2.37	0.67	1.93	1.08	1.02	0.68	0.86	2.01	1.02	0.87	0.90
Cu	4.72	4.22	5.32	1.38	72.75	2.20	7.32	3.07	2.31	15.28	4.00	4.05
Zn	0.35	1.14	18.18	–	56.67	–	23.98	–	–	85.63	1.68	0.03
Cd	0.02	0.05	0.06	0.01	0.09	0.01	0.10	0.01	0.09	0.71	0.10	0.06
Hg	–	–	–	–	–	–	–	0.17	0.10	–	–	–
Pb	0.88	0.87	1.08	0.78	2.34	0.82	1.72	0.79	0.85	2.73	2.04	1.32
Mn	43.40	47.55	39.09	48.43	35.90	56.82	53.14	55.98	49.41	61.65	71.37	75.77
Fe	957.58	1325.91	892.08	1112.54	796.96	1214.35	1055.45	1187.89	945.07	1773.15	1313.50	1393.03
Co	0.27	0.31	0.26	0.34	0.21	0.41	0.35	0.39	0.33	0.57	0.50	0.56
Ni	1.04	0.38	0.87	–	0.66	0.10	2.06	0.39	0.16	3.57	0.59	0.44
Sn	–	–	–	–	–	–	–	0.09	0.16	1.23	–	–
Sb	0.30	0.26	0.72	0.25	0.18	0.33	0.26	0.24	0.18	0.31	0.40	0.39

Table 2. Trace metal content in water, μg/l, in October 2006 at Komsomolsk-on-Amur

Element	Left bank, Surface	Left bank, Bottom	300 meters from the left bank, surface	300 meters from the left bank, bottom	500 meters from the left bank, surface	500 meters from the left bank, bottom	700 meters from the left bank, surface	700 meters from the left bank,	900 meters from the left bank, surface	900 meters from the left bank,	Right bank, surface	Right bank, bottom
Cr	0.70	1.44	0.92	0.75	0.77	0.82	1.00	0.95	0.83	1.79	1.86	0.97
Mn	55.23	90.49	72.95	65.45	62.02	67.49	64.72	61.24	46.02	61.45	67.43	43.01
Fe	1226.21	1938.20	1502.05	1589.54	1503.63	1628.12	991.87	958.09	796.83	1179.13	1108.53	865.65
Co	0.36	0.71	0.54	0.46	0.42	0.48	0.50	0.49	0.35	0.54	0.55	0.37
Ni	1.38	2.67	2.00	1.91	1.43	1.27	1.43	1.30	1.33	1.60	1.38	1.89
Cu	1.90	3.06	1.80	1.31	1.99	1.29	1.81	1.29	2.96	9.84	1.39	7.09
Zn	5.23	6.89	6.19	2.42	4.86	2.51	3.29	2.12	4.69	16.70	7.07	11.66
Cd	0.00	0.00	0.01	0.01	0.02	0.01	–	–	0.00	0.01	0.06	0.03
Sn	0.27	2.95	0.29	0.73	0.06	1.33	0.59	0.57	0.33	0.24	0.50	0.28
Sb	0.09	0.09	0.07	0.07	0.07	0.07	0.07	0.07	0.08	0.08	0.08	0.10
Hg	–	–	–	–	–	–	–	–	–	–	0.10	–
Pb	0.70	1.19	0.96	0.84	0.89	0.91	0.81	0.85	0.68	2.48	1.21	1.23

Table 3. Trace metal content in water, μg/l in October at Bogorodskoe

Element	Left bank, Surface	Left bank, Bottom	300 meters from the left bank, surface	300 meters from the left bank, bottom	500 meters from the left bank, surface	500 meters from the left bank, bottom	700 meters from the left bank, surface	700 meters from the left bank, bottom	900 meters from the left bank, surface	900 meters from the left bank, bottom	Right bank, surface	Right bank, bottom
Cr	2.43	1.14	0.77	1.21	0.97	1.19	0.66	0.71	0.95	1.07	1.90	0.86
Mn	44.50	75.38	56.85	83.19	46.05	64.52	38.97	46.61	62.66	70.04	52.74	45.60
Fe	886.63	1323.52	992.16	1371.45	872.29	1192.53	780.77	879.19	1098.44	1200.11	1074.83	925.87
Co	0.29	0.56	0.37	0.58	0.30	0.46	0.26	0.32	0.45	0.52	0.39	0.33
Ni	1.46	1.64	1.29	1.61	1.39	1.65	1.37	0.98	1.34	1.09	2.37	1.31
Cu	2.31	4.23	2.62	3.12	3.28	29.90	31.35	1.96	2.08	2.27	5.20	1.38
Zn	4.32	8.31	8.96	6.45	7.32	30.77	22.19	3.03	3.28	1.92	6.98	1.12
Cd	–	0.01	–	0.00	0.00	–	0.00	0.01	0.00	–	0.00	0.01
Sn	0.52	0.04	0.48	0.13	1.14	0.14	–	–	–	–	2.30	0.27
Sb	0.08	0.08	0.08	0.07	0.07	0.07	0.07	0.31	0.38	0.35	0.08	0.43
Hg	–	–	–	–	–	–	–	–	–	–	–	–
Pb	0.60	0.90	0.63	1.08	0.64	1.60	1.35	0.65	0.90	0.91	0.83	0.62

REFERENCES

1. Butova G.I., Meshchenina L.A., Novorotsky P.V. Climate Change Tendency of the last 110 years in the Lower Amur Basin // Regions of New Developments: Management Strategies. Proceeding of Int. Conf., Khabarovsk, 2004, p. 22-25.
2. Water and Ecology Problems in the Amur River Basin/ Ed. A/N/ Makhinov. Vladivostok, FEB RAS. 2003. 187 P.
3. Makhinov A.N., Chalov R.S., Chernov A.V. Directed Alluvial Accumulation and Lower Amur Riverbed Morphology // Geomorphology. 1994. #4, p. 70-78.
4. Mordovin A.M. Priamurje Water Resources and Their Distribution within the Territory // Zabaikalje Natural Resources and Problems or Natural Resource Use. Proceeding of Int. Conf., Chita. 2001, p. 105-107.
5. Serface Water Resources of the USSR, vol. 18, Far East, bul. 1 Upper and Middle Amur. Hydrometisdat, 1966, 779 P.
6. Chudaeva V.A. Migration of Chemical Elements in Waters of the Far East. Bladivostok: Dalnauka. 392 P.

DYNAMICS OF THE LOWER AMUR WATER CHEMICAL COMPOSITION IN 2006

SHESTERKIN VLADIMIR P.
Institute of Water and Ecology Problems,
Far Eastern Branch of the Russian Academy of Sciences

Chemical composition of water in the Lower Amur is mostly formed due to mixing of the Middle Amur and the Ussuri waters. The Amgun, Tunguska and other Amur tributaries have less influence as their total drainage area makes only 12.1% of the Amur drainage area.

Studies undertaken by the Institute of Water and Ecology Problems, Far Eastern Branch of the Russian Academy of Sciences (IWEP FEB RAS) in 2000-2005 [1,3,4] showed significant changes of hydrological and hydrochemical regime of the Middle Amur water, caused by the construction of dams on the Amur tributaries Sungari, Zeya, Bureya and acceleration of economic activity in the Sungari basin. Such impact on the Amur hydrological regime also continued in 2006. In spring and the beginning of summer an active water resource accumulation in Zeya and Bureya water reservoirs caused low water level in the river in mid-June (Fig.1). Floods formed in the Sungary basin contributed to water level rise in July and August.

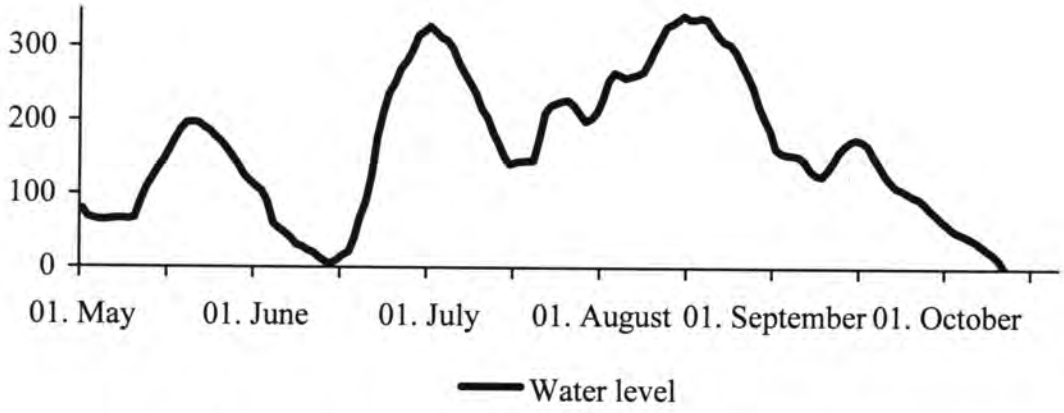

Fig. 1. Water level dynamics (cm) of the Amur near Khabarovsk in 2006

The Russian Hydrometeorological Agency (Roshydromet) conducted monthly monitoring of the Amur water chemical composition from March till October near Telegino village (3km up the City of Khabarovsk) and near Bogorodskoe at three stations equally spread across the river. The Interregional Center for Monitoring Hydroenergy Facilities (Accreditation certificate # ROCC RU 0001.515988) at IWEP FEB RAS carried out water sample analysis. Major ions (Na^+, K^+, Ca^{2+}, Mg^{2+}, SO_4^{2-}, Cl^-) and nutrients (NO_3^-, NO_2^- and NH_4^+, HPO_4^{2-}, Fe, Si) in water were analyzed.

Major Ions. Maximum major ion contents in the Amur water upper Khabarovsk are registered at the very beginning of river freezing due to low water in the Zeya and Bureya in

the pre-winter period. During the freezing period the share of these rivers in the Middle Amur run off gradually increases and thus, major ion contents gradually decrease by the end of March. Such specific features of winter hydrological regime coupled with snow melting water flow into water upper horizons under the river ice cover explain less high concentrations of major ions in the Amur water. That is why in March 2006 these concentrations were 1.3 times lower than in February. Near Bogorodskoe the situation is different. The distance between Khabarovsk and Bogorodskoe (740 km) and slow water current explain higher ion concentrations at Bogorodskoe in March (Fig. 2). Besides, economic activities in Khabarovsk, Amursk and Komsomolsk-on-Amur also contribute to ion concentration increase in the Amur water.

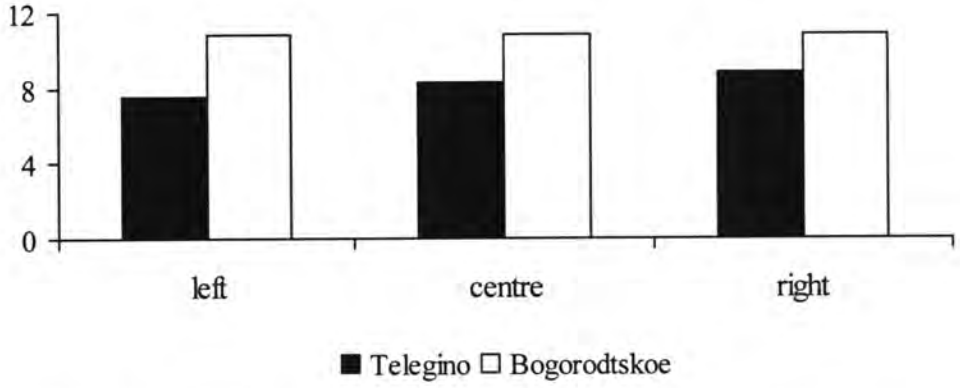

Fig 2. Distribution of calcium ion content (mg/l) across the Amur near Telegino and Bogorodskoe in March 2006.

Distribution of major ions across the river differs at the three stations. Near Bogorodskoe ion content is distributed between the stations more or less equally. Upper Khabarovsk the highest ion content is registered at the right bank of the river. Such difference is explained by the impact of Sungari water with higher ion concentrations compared to Amur water at their juncture [4]. At the beginning of March Na^+ and SO_4^{2-} contents in Sungari water near Tunjang city were 14.5 and 28.5 mg/l respectively and in Amur water near Amurzet village they were 2.1 and 2.9 mg/l respectively. In December 2005 after the accident at the chemical plant in Jilin SO_4^{2-} content in Amur water near Nizhneleninskoe village was much higher (up to 37.3 mg/l).

At the end of freezing period calcium ion prevailed in Amur water among cations (52.6% mg-equivalent) and hydrocarbon ion prevailed among anions 73.3% mg- equivalent). Similar water composition was registered near Bogorodskoe. Na^+, SO_4^{2-} and Cl^- content in water did not exceed 7.5 mg/l, whereas $K^+$and Mg^{2+} content did not exceed 3.0 mg/l.

Snow melting water inflow to the river net in springtime caused the change in major ion content. Decrease of Ca^{2+}, Na^+, SO_4^{2-} and $Cl^-$and increase of Mg^2 and K^+ were registered in Amur water upper Khabarovsk. Significant decrease of Ca^{2+}, Na^+, SO_4^{2-} and Cl^- (e.g. Na^+ 2.4 times) is also registered near Bogorodskoe. Behavior of sulfate ion was an exception as its concentration increased 1.3 times.

More significant changes in water chemical composition are registered during floods. Our studies showed that at this time major ion contents depend much on in which tributary basin the flood is formed [2]. Thus, during the flood in June (Fig.1), formed in the Upper Amur area, major ion contents in the water were the lowest in all the non-freezing period, but during the flood in July and August. Formed in the Sungari basin, it was the highest (Fig. 2). The difference in contents of Na^+, Ca^{2+}, SO_4^{2-} and Cl^- were the highest (1.5-2.0 times).

Near Bogorodskoe the difference in water chemical composition are less evident due to the impact of various river tributaries. Only SO_4^{2-} makes an exception. Its concentration in water in July was 1.65 time higher than in June.

In autumn the contents of Na^+, SO_4^{2-} and Cl^- in the Amur water upper Khabarovsk gradually decreased, while Ca^{2+} and Mg^2 contents were not changed much. Near Bogorodskoe the situation is quite the opposite. Before freezing time major ion contents there reach the highest values, the only exception being Cl^-. These differences seem to be caused by the uneven distribution of chemical components throughout the water mass.

NUTRIENTS

Biogenic substance dynamics differs from the dynamics of major ions. Maximum contents of NH_4^+ and NO_2^- and increased contents of NO_3^- and HPO_4^{2-} were registered in winter low water. Like in previous years [1-2] upper Khabarovsk the highest concentrations were registered at the right bank of the Amur. Near Bogorodskoe there is no much difference in water chemical composition across the river. Dissolved iron and silicon contents did not exceed 0.5 mg/l and 4.5 mg/l. Total nitrogen content at all the station across the river did not exceed 1.09 mg/l.

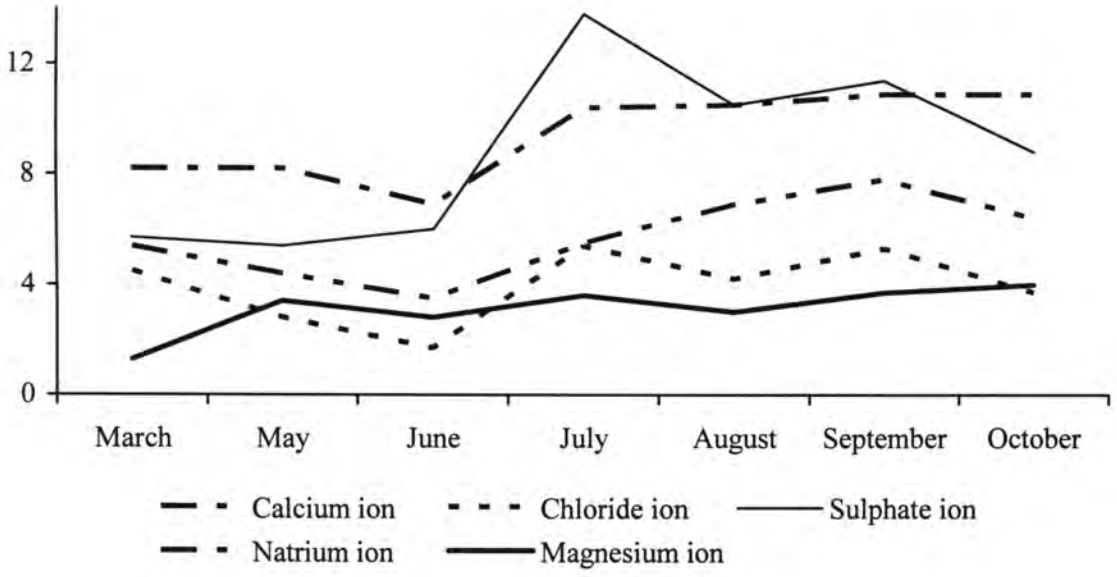

Fig. 3. Dynamics of major ion content (mg/l) in Amur water near Teltgino.

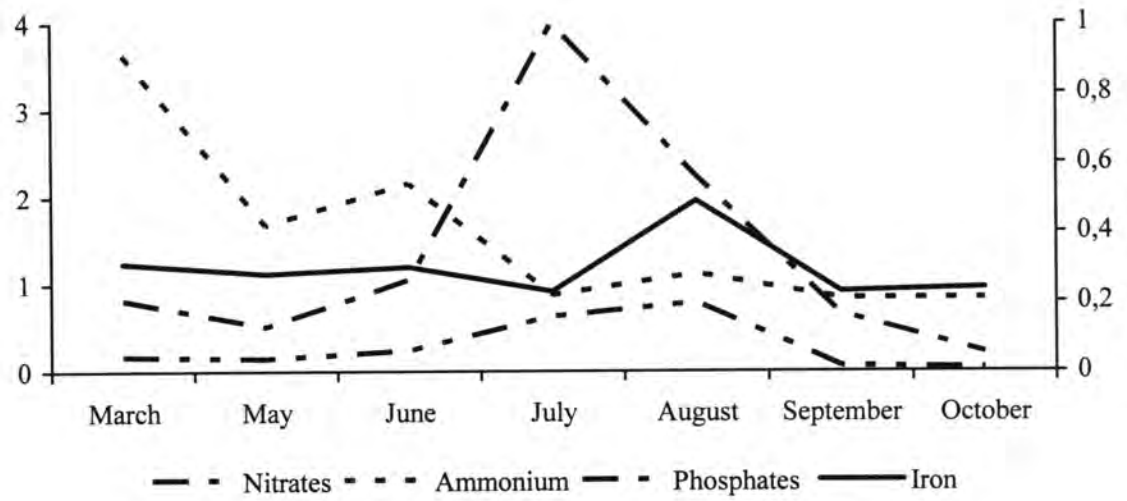

Fig. 4. Dynamics of Nutrients (mg/l) in Amur Water near Telegino.

In spring nitrogen compound contents in water and the difference in their concentrations across the river decreased due to the inflow of snow melting water into the river net. Iron and silicon compounds did not show much concentration changes.

Significant drop of water level in mid-June (up to 23 cm) did not cause much changes in the contents of phosphates and ammonia and nitric nitrogen in river water near Khabarovsk. Nitric nitrogen concentration was the lowest probably due to the growth of plankton. Similar situation was registered near Bogorodskoe, but at the end of June.

Significant changes of nutrient concentrations take place in flood time. The flood tide formed in the Upper Amur caused the increase of phosphates and nitric nitrogen concentrations with their maximums during July and August floods, formed in the Sungary basin. Similar concentrations of these substances were registered in the Amur water in August 1998 after the catastrophic Sungari floods. When the flood reached its peak near Khabarovsk the concentrations of phosphates, total nitrogen, iron and silicon compounds in water were the highest during the non-freezing time. Much difference in nutrient concentration distribution across the river was not observed.

Near Bogorodskoe in summer time NO_3^- and NH_4^+ contents were less compared to those ones near Khabarovsk, while HPO_4^{2-}, Fe and Si contents were of the same level.

In Autumn when flood subsided nutrient contents in water upper Khabarovsk gradually decreased, NO_3^- and HPO_4^{2-}showing a significant drop. Concentrations of these substances and also that of Si at that time were the lowest in the all period of observations. This fact indicates intensive processes in water, such as nitrification and photosynthetic phytoplankton activity.

At that time near Bogorodskoe only total nitrogen content showed significant changes, which can be explained as resulting from floods. That is why, total nitrogen content reached its maximum there by the end of September. Just before river freezing nitrogen compound concentrations significantly decreased. Nutrient concentrations across the Amur are distributed unevenly and their maximal levels are observed at the right bank of the river.

Thus, our studies showed that floods, formed within the Sungari basin had significant impact on dissolved substance content dynamics in the Amur water in 2006 and caused increased concentration levels of Fe and Si compounds, NO_3^- and HPO_4^{2-}.

REFERENCES

1. Shesterkin V.P., Shesterkina N.M. The Sungari Role in Formation of Middle Amur Water hydrochemical Composition in Winter Low Water Level // Biochemical and Hydrochemical Assessment of Terrestrial and Fresh Water Ecosystems. Vol.13. Vladivostok: Dalnauka, 2003.
2. Shesterkin V.P., Shesterkina N.M. Maximal Ion Consentrations in Middle Amur // Biochemical and Hydrochemical Studies of Terrestrial and Fresh Water Ecosystems. Vol. 12. Vladivostok: Dalnauka, 2002, p. 105-116.
3. Shesterkin V.P., Shesterkina N.M. The Impact of Zeya and Bureya Water Reservoirs on Middle Amur Hydrological Regime in Winter // Scientific Base for Ecological Monitoring of Water Reservoirs. Khabarovsk: IWEP FEB RAS, 2005, p. 63-65.
4. Shesterkin V.P., Shesterkina N.M., Forina Yu.A., Ri T.D. Sungari River Hydrochemistry and Amur Water Quality in 2005-2006 Winter Low Water Level // Modern Problems of Regional Development. Khabarovsk: IWEP FEB RAS, 2006, p. 159-162.

HYDROCHEMISTRY OF THE AMUR LIMAN AND THE SAKHALIN BAY

SHESTERKIN VLADIMIR P.
Institute of Water and Ecology Problems,
Far Eastern Branch of the Russian Academy of Sciences

The Amur Liman extends beyond the Amur river mouth and constitutes a strait between Asia and the northern part of the Sakhalin Island. In the south through a narrow Nevelskoy Strait and Tatar Strait it connects the Sea of Japan with the Sakhalin Bay of the Okhotsk Sea. The liman is 185 km long, 40 km wide and 3-4, 5 m deep. Its western shores are heavily raged and mountainous and eastern shores are sandy and low. Maximum width of the Sakhalin Bay is 160 km. The Amur Liman is covered with ice from November till May and the Sakhalin Bay is frozen till June. Daily tides are of 2 meters.

The main stream in the estuary, excluding that part of it which fills large shoals and dry banks, is nearly equally split into three fairways Nevelskoy, Eastern and Southern. The first goes to the north, the second – to the east and the third first goes along the continent shores to the south and then turns to the southeast. They are 3.5 - 22, 1.5 – 15, 3 – 11 meters deep respectively. Shallow areas are covered with vegetation. The Sakhalin fairway in the eastern part of the Liman runs along Sakhalin shores. It is divided into the northern and southern parts, which are split into Eastern and Western ways. The Sakhalin fairway in its northern part is more that 8.5 km deep [2].

Hydrochemical studies were undertaken in the Amur Liman and Sakhalin Bay in the second decade of August 2006. Location of sampling stations is presented in Table 1. Water was sampled from the surface and bottom layers. Water temperature, salinity, pH, oxygen and suspended matter contents were measured in situ with meter TOA DKK WQC-24 (Japan). The Interregional Center for Monitoring Hydroenergy Facilities (Accreditation certificate # ROCC RU 0001.515988) at IWEP FEB RAS carried out water sample analysis. Major ions (Na^+, K^+, Ca^{2+}, Mg^{2+}, SO_4^{2-}, Cl^-), nutrients (NO_3^-, NO_2^-, NH_4^+, HPO_4^{2-}, Si) and trace metals (Al, Mn, Co, Ni, Cu, Fe) were analyzed.

The water in the estuary is well-warmed and little acid (Table). Oxygen content in water exceeds 5.2 mg/l and oxygenation is 62.8%. Our studies in August 1997 near Ozerpakh village revealed higher oxygen content (over 7.8 mg/l) and oxygenation (80%). In the vertical section the highest concentration is observed in bottom layers.

Suspended substances are also distributed in water unevenly. The highest concentrations were observed in bottom layers, and at the deepest station (#2) they reached maximum values (Table). Suspended matter content was 4 times higher at the bottom than at the surface.

In the estuary major ions and biogenic substances are distributed relatively even. Concentrations of major ions are low, and Cl^- is of the same level as atmospheric precipitation in Priamurje. Total content of major ions is less 25 mg/l. In winter low water it increases twice or even more times. Due to low water discharge from Amur marine water impact is quite evi-

dent in the estuary. Thus, in March 1998 Cl^- content in water near Nickolaevsk-on-Amur was 8.3 mg/l and near Ozerpakh village it was 19.1 mg/l.

Nitrate nitrogen prevails among the mineral forms of nitrogen. Nitrate nitrogen content, which is 2-3 times higher compared to that, registered in 1997 is explained by the discharge of big amounts of nitrates from the Sungary River in fool time. Increased concentration of phosphates compared to 2005 can be also explained by the Sungary discharge.

NH_4^+ and NO_2^- concentrations are very low due to the consumption by phytoplankton and vegetation. Same concentrations are typical for this time of year and were also observed in August 1997 and 2005.

Trace metals are spread rather unevenly. Fe and Al concentrations (Table) are the highest. Cu, Ni and Mn contents do not exceed 10 μg/l. Vertical section shows that there are more metals in surface water than in bottom layers bottom.

The Amur Liman is characterized with a complicated current [2]. Irregular daily tides in the Sakhalin Bay and half-day tides in the Sea of Japan coupled with changing discharge of the Amur into the Liman cause very uneven distribution of water chemical composition within the water area and its profile. Mixing of ultra-fresh Amur water and seawater produce lightly salty and weakly alkaline water with oxygen content more than 6 mg/l. In the surface water layers of the liman central part major ion contents are the lowest, and in its most shallow spots there is no much difference in their distribution in vertical section. In very deep spots (station 5) major ion concentrations are 5-6 times lower than in the bottom layers.

Big changes happen to silicon and nitrogen mineral forms. Due to mixing with seawater and plankton consumption their concentrations decrease and especially ammonia nitrogen show significant decrease. Most low nutrient concentrations are registered in bottom layers of deep areas. Compared to silicon and nitrogen mineral forms phosphate concentrations remain increased (Table).

Trace metal concentrations are also changed. Concentrations of some metals increase (Mn, Co, Cu), some do not change (Ni) and some decrease in shallow spots through all water thickness and in deep spots only in the surface layers (Al, Fe.). Such behavior of the studied metals in the Amur Liman has been observed before [3].

In the Sakhalin Bay (stations 7-9) suspended matter content in water and its temperature gradually decrease, and pH value, oxygen concentration and salinity (and thus, major ion contents) increase (Table). Difference in major ion contents in vertical section becomes less with depth increase. Compared to major ions nutrient content is salt water is decreasing and in bottom layers NO_3^- and Si contents drop to detection limits. Ammonia and nitrite nitrogen presence is water is not observed like in the Amur Liman.

With salinity increase Fe, Co, Ni and Cu contents in water also increase. In bottom layers the increase is higher than in the surface layers. That is why the distribution of these metals along the vertical section is uneven (Table). Cu shows the biggest difference in its concentrations between the surface and bottom layers.

Al and Mn behavior is quite different. Al content in water starts to increase at water salinity higher 20 ‰, and Mn content decreases. Bigger decrease of Mn is observed in surface waters compared to the bottom water layers.

Thus, dissolved mater content in the Amur Liman and Sakhalin Bay depends on the Amur water and seawater mixing pattern, and trace metal concentrations also depend on the processes of sedimentation and desorpsion from bottom layers.

REFERENCES

1. Ivanov A.B., Kashin N.P. Main Factors of the Formation of Chemical composition of Atmospheric Precipitation and Snow Cover in Priamurje // Glaciochemical and Cryogenic Hydrochemical Processes. Vladivostok: FEB RAS. 1989, p. 73-87.
2. Solovjev A.I. Amur and Liman Bottom Processes and Waterways. Vladivostok: FEB RAS. 1995, 269 p.
3. Shulkin V.M. Metals in Shallow Water Ecosystems. Vladivostok: Dalnauka. 2004, 279 p.

Table

Chemical composition of Amur Liman and Sakhalin Bay waters

H	T	pH	turbid-ity	S	O_2	Na^+	K^+	Ca^{2+}	Mg^{2+}	Cl^-	SO_4^{2-}
m	°C		g/m^3	‰	mg/l						
St 1 (53.07 lat., 140.48 long,), 10.08.06.											
0.0	23.7	6.79	52.2	0.0	5.29	3.9	1.3	7.2	2.0	2.4	5.3
6.0	23.6	6.54	84.2	0.0	5.58	3.6	1.3	7.2	2.9	2.0	4.4
St 2 (53.03 lat., 140.57 long,), 10.08.06.											
0.0	23.8	7.14	46.8	0.0	5.54	3.6	1.2	7.2	2.4	2.0	6.6
20.0	23.5	6.89	189.4	0.0	-	3.6	1.2	7.2	2.4	1.7	6.1
St 3 (52.54 lat., 141.16 long,), 10.08.06.											
0.0	23.1	6.67	60.9	0.0	5.74	3.7	1.2	6.4	3.4	2.0	3.1
4.4	23.2	6.82	75.8	0.0	5.93	3.7	1.2	7.2	2.9	2.0	4.4
St 4 (52.50 lat., 141.40 long,), 13.08.06.											
0.0	22.0	7.61	28.0	5.4	6.30	1313.0	98.6	80.6	268.1	3200.1	318.0
4.0	21.6	7.69	30.6	6.7	5.56	1326.6	104.2	81.4	263.3	3254.3	460.5
St 5 (53.02 lat., 141.40 long,), 13.08.06.											
0.0	22.6	7.58	108.3	3.3	6.57	831.6	104.2	44.7	129.8	1591.0	208.3
16.6	20.9	7.81	41.8	19.0	6.18	5167.8	285.1	221.2	739.3	9003.6	1381.6
St 6 (53.14 lat., 141.40 long,), 13.08.06.											
0.0	22.0	7.77	23.3	5.6	6.45	1556.8	82.2	65.3	206.6	2513.0	350.9
6.0	22.0	7.71	18.0	6.7	6.45	1669.6	76.8	67.7	212.0	2567.3	350.9
St 7 (53.26 lat., 141.40 long,), 15.08.06.											
0.0	21.4	7.73	7.8	7.6	6.24	2001.6	109.6	87.8	299.0	3615.9	548.2
7.3	9.3	8.00	21.5	-	8.55	3498.2	175.4	137.7	456.1	5966.2	921.0
St 8 (53.38 lat., 141.40 long,), 15.08.06.											
0.0	20.3	7.87	9.4	9.1	6.45	2782.6	131.6	111.6	350.9	5008.0	614.0
9.4	2.1	7.99	2.5	20.9	7.44	6671.9	438.6	319.0	1147	11158.0	2236.8
St 9 (53.50 lat., 141.40 long,), 15.08.06.											
0.0	15.1	8.12	1.9	25.2	8.00	6393.9	394.7	287.7	994.6	14825.2	2105.3
25.2	0.3	7.83	3.7	31.1	14.0	7366.8	460.5	350.9	1205	17971.0	2368.4

Table continued

H	NH_4^+	NO_2^-	NO_3^-	HPO_4^{2-}	Si	Al	Mn	Fe	Co	Ni	Cu
m	mg/l					μg/l					
St 1 (53.07 lat., 140.48 long,), 10.08.06.											
0.0	0.24	<0.005	1.42	0.092	4.9	95.23	5.26	285.65	0.06	1.64	6.10
6.0	0.24	0.005	1.33	0.077	4.9	65.88	5.01	254.07	0.05	1.23	4.42
St 2 (53.03 lat., 140.57 long,), 10.08.06.											
0.0	0.18	0.007	1.46	0.062	4.8	134.48	6.26	331.14	0.05	1.63	3.93
20.0	0.15	<0.005	1.42	0.077	4.9	74.17	5.71	281.05	0.04	1.33	2.89
St 3 (52.54 lat., 141.16 long,), 10.08.06.											
0.0	0.21	<0.005	1.51	0.085	4.9	119.39	5.05	320.94	0.05	0.81	1.60
4.4	0.12	<0.005	0.97	0.081	4.8	80.95	5.45	301.37	0.05	9.67	6.11
St 4 (52.50 lat., 141.40 long,), 13.08.06.											
0.0	<0.005	<0.005	0.58	0.058	4.0	-	16.69	241.14	0.18	1.85	54.14
4.0	0.16	<0.005	0.40	0.069	4.1	5.07	14.76	270.13	0.21	2.22	34.98
St 5 (53.02 lat., 141.40 long,), 13.08.06.											
0.0	<0.005	<0.005	0.58	0.096	4.7	0.35	7.99	176.49	0.10	1.23	11.75
16.6	<0.005	<0.005	0.04	0.054	2.0	1.19	7.76	672.36	0.82	5.03	80.94
St 6 (53.14 lat., 141.40 long,), 13.08.06.											
0.0	<0.005	<0.005	0.71	0.089	4.4	-	9.30	172.65	0.16	1.67	18.44
6.0	<0.005	<0.005	0.75	0.069	4.2	6.19	10.85	194.07	0.16	1.67	27.78
St 7 (53.26 lat., 141.40 long,), 15.08.06.											
0.0	<0.005	<0.005	0.49	0.054	3.9	-	13.09	221.65	0.22	2.02	25.04
7.3	<0.005	<0.005	0.44	0.039	3.3	1.74	12.63	411.92	0.43	3.21	60.04
St 8 (53.38 lat., 141.40 long,), 15.08.06.											
0.0	<0.005	<0.005	0.35	0.042	3.5	-	6.57	356.5	0.36	2.81	42.00
9.4	<0.005	<0.005	0.02	0.046	0.3	2.01	1.76	991.8	0.92	6.12	155.3
St 9 (53.50 lat., 141.40 long,), 15.08.06.											
0.0	<0.005	<0.005	0.40	0.077	0.6	7.71	5.38	550.2	0.62	5.43	55.17
25.2	<0.005	<0.005	0.02	0.023	0.4	5.15	1.00	1318.9	1.20	8.00	200.9

REMOVAL AND FRACTIONATION CHARACTERISTICS OF DISSOLVED IRON IN ESTUARINE MIXING ZONE

TERASHIMA M.[1] AND NAGAO S.[2]

[1] *Research Institute for Humanity and Nature*

[2] *Faculty of Environmental Earth Science, Hokkaido University*

1. INTRODUCTION

The elucidation of fate of iron in estuaries is a key subject for understanding the impact of iron in river water on the bio-productivity in marine environments. In previous studies, more than 90% of the total dissolved iron, defined as the fractions below 400 or 700 nm, has been found to be removed in estuaries via the coagulation induced by an increase in salinity (Sholkovitz, 1976, 1978; Sholkovitz and Copland, 1981). On the other hand, only less than 10% of the dissolved iron remains in the aqueous phase even at salinity of seawater level. Although this fraction may serve as a nutrient for the phytoplankton in marine environments, available information on the chemical form determining the bioavailability is incomplete.

In river water systems, humic substances (HSs), which comprise more than 50% of the dissolved organic carbon (Thurman, 1985), are one of major factors determining the chemical form of iron. For example, the iron in river waters can dissolve as the complexes with HSs (Waite and Morel, 1984; da Silva et al., 1998; Tipping et al., 2002) and the suspended particles such as iron (hydro)oxides protected by HSs (Tipping, 1981). In the estuarine system, such difference in the form may result in the fractionation between the complexes and suspended particles during the mixing with seawater, because the coagulation characters will be significantly different from each other. In general, the colloidal coagulation can preferentially occur in colloids with larger size and higher charge density, obeying the DLVO theory (Hunter, 2001). In previous works, the average hydrodynamic radius of HSs have been evaluated to be below 10 nm (Lead et al., 2000; Ngo Manh et al., 2001; Pranzas et al., 2003; Benedetti et al., 2003), but a few hundred nm for the suspended particles of iron (Nomizu et al., 1988; Baalousha et al., 2006). Thus, these findings suggest that the complexes of iron with HSs could preferentially remain in the aqueous phase in the estuarine condition.

In this work, to clarify the chemical form of iron remaining in the estuary, the removal and fractionation characteristics of iron and HSs in the Bekanbeushi River in Hokkaido were investigated on the basis of the mixing with artificial seawater. The size exclusion chromatography – UV detection (SEC–UV) was applied to monitor the concentration or to identify the removed fraction of HSs (Nagao et al., 2001). The size fractionations of iron and HSs were performed to clarify the form as well as size fractions of remaining iron. Moreover, the size distribution of iron complexes with fulvic acid (FA), which was isolated from the Bekanbeushi River water, was characterized by the size fractionation, and the removal characteristic was elucidated to verify the stability in the estuarine condition.

2. REMOVAL CHARACTERISTICS OF FE AND HS IN BEKANBEUSHI RIVER WATER

Fig.1 shows the concentration of dissolved iron in the river water sample as a function of salinity. The concentration gradually decreased with increasing salinity. At the salinity of seawater level (33.7), approximately 86% of the total dissolved iron was removed, while the remaining 14% remained in the aqueous phase. This result shows that no the dissolved iron in the river water is completely removed in the estuarine condition. On the other hand, only 20% of the absorbance at 280 nm wavelength in the water sample disappeared at the salinity of 33.7. In addition, the degree of disappearance was good agreement with the result of SEC measurements. These indicate that the majority of HSs in the river water sample dissolves stably in the aqueous phase at salinity of seawater level.

Fig. 2 shows the removal kinetic curves of iron and HSs during the mixing with artificial seawater. The kinetic curves were different from each other. The slightly amount of HSs was rapidly removed from the mixture to reach the plateau after 5 min, while the dissolved iron was more slowly removed to reach the plateau after 30 min. This discrepancy means that the dissolved iron and HSs are independently removed during the mixing with the artificial seawater. Thus, these results suggest that the fractionation between the suspended particles of iron and the complexes with HSs can occur in the estuary.

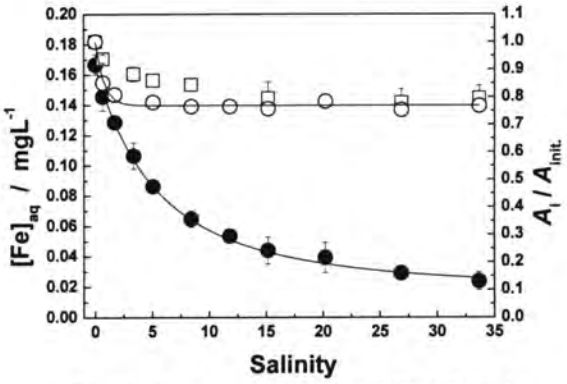

Fig. 1 The concentration of Fe (●) *and residual ratio of HSs* in the *Bekanbeushi River water as a function of salinity. Residual ratio: absorbance at 280 nm* (○), *peak area in SEC* (□).

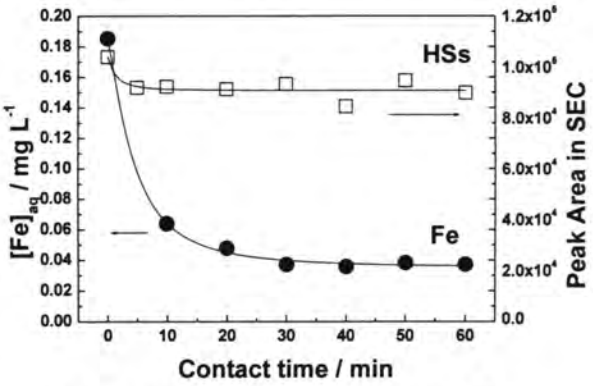

Fig. 2 Removal kinetics of dissolved Fe and HSs in the Bekanbeushi River water.

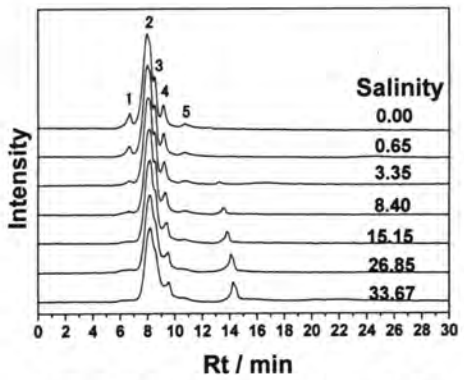

Fig. 3 SEC chromatograms of HSs in the Bekanbeushi River water at each saline conditions.

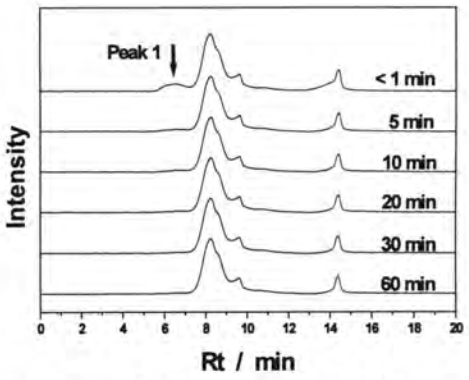

Fig. 4 SEC chromatograms of HSs at a variety of contact time. Salinity: 33.7.

The SEC chromatograms of HSs in the river water sample at each salinity level are shown in Fig. 3. In the river water sample mixed with pure water (i.e. salinity 0.0), the major peaks from 2 to 5 corresponded to that of FA, which was isolated from the river water. The peak 1 was observed in the chromatograms of humic acid (HA) isolated from the river water. The peak 6 was a system peak due to the change of density in the sample solution. Thus, the SEC chromatogram obtained is attributed to the dissolved HSs in the rive water. When the salinity increased, the peak 1 disappeared at the salinity of 3.35. In addition, the peak 1 also disappeared after 5 min, as shown in Fig. 4. Thus, these suggest that one of portion in HA is removed, while the FA remains in the aqueous phase at salinity of seawater level.

As shown in Fig. 2, the fractionation between the complexes with HSs and suspended particles of iron could occur during the mixing with artificial seawater. This fractionation may be explained on the basis of the difference in the size distribution character, as described above. Thus, we examined the size fractionation by using eight types of filters with different pore size (e.i. 5 KDa – 400 nm). Fig. 5 shows the size distributions of iron and HSs in the river water sample. The size distributions were significantly different from each other. Approximately 94% of the dissolved iron was enriched in the size range from 20 to 400 nm, while only 6% of the dissolved iron was distributed below 20 nm. On the other hand, the majority of HSs (i.e. 89%) were enriched in the fractions below 20 nm. In the comparison between the distribution and removal ratios of iron or HSs, the distribution ratios in the range from 20 to 400 nm were approximated to the removal ratios in Fig. 1. In addition, the peak 1 in the difference SEC chromatograms (Fig. 6) was detected in the size fractions from 20 to 400 nm. These results indicate that the iron fractions from 20 to 400 nm are removed from the aqueous phase as a result of the mixing with seawater. As the result followed by this, the distribution ratios of iron and HSs below 20 nm were approximated to the residual ratios of iron and HSs (Fig. 1). Therefore, the dissolved irons below 20 nm are identified as the remaining fractions in the estuarine mixing zone. Also, this result suggests that the fractions distributed below 20 nm are due to the complexes of iron with HSs.

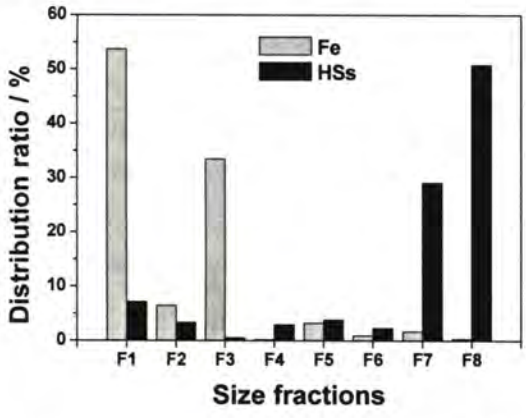

Fig. 5 Size distributions of dissolved Fe and HSs in the Bekanbeushi River water. F1 200 – 400 nm, F2 100 – 200 nm, F3 20 – 100 nm, F4 300KDa – 20 nm, F5 100KDa – 300KDa, F6 30KDa – 100KDa, F7 5KDa – 30KDa, F8 <5KDa.

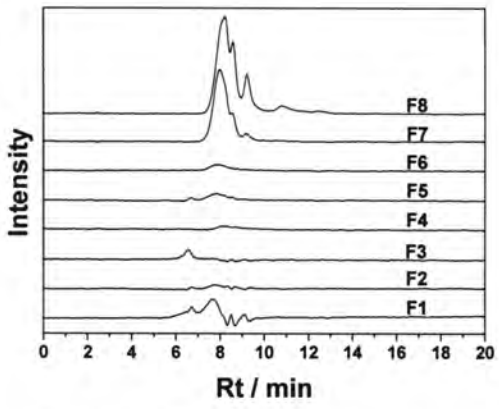

Fig. 6 Difference SEC chromatograms of HSs at each size fraction. F1 200 – 400 nm, F2 100 – 200 nm, F3 20 – 100 nm, F4 300KDa – 20 nm, F5 100KDa – 300KDa, F6 30KDa – 100KDa, F7 5KDa – 30KDa, F8 <5KDa.

3. REMOVAL CHARACTERISTICS OF FE AND HSS IN ARTIFICIAL RIVER WATER

To clarify the size distribution and removal characteristics of iron complex with HSs, the artificial river water was prepared by mixing $FeCl_3$ with FA in the aqueous solution including the major cations in the Bekanbeushi River water (i.e. Ca^{2+}, Mg^{2+}, Na^{+}, K^{+}). Here, FA was chosen as a typical example of aquatic HSs, because the FA comprises the major fraction of HSs in the river water system. Fig. 7 shows the size distributions of iron and FA in the artificial river water. Approximately 82% of the dissolved iron was enriched in the fractions from 20 to 400 nm, while 94% of the total FA was distributed below 20 nm. The size distribution of FA in the absence of iron showed the same pattern as that in the presence of iron (data not shown). Moreover, 95% of the total iron in the absence of FA was enriched in the fractions above 200 nm (data not shown). Furthermore, the distribution ratio of dissolved iron below 20 nm in the presence of FA increased with decrease in pH from 7.2 to 4.0 (data not shown). Thus, these results reveal that the complexes of iron with FA are assigned to the fractions below 20 nm, while the flocks such as iron hydroxide are distributed into the fractions above 20 nm. The residual ratios of iron and FA as a function of salinity are shown in Fig. 8. The dissolved iron was gradually removed by an increase in salinity, while the FA was slightly removed from the aqueous phase. At the salinity of 33.7, the residual ratios were evaluated to be 0.57 for iron and 0.94 for FA, respectively. In the comparison between the residual and distribution ratios of iron or FA, the residual ratios were good agreements with the distribution ratios below 100 nm: $[Fe]_{aq}/[Fe]_{tot.} \approx [Fe]_{<100nm}/[Fe]_{tot.}$, and $[FA]_{aq}/[FA]_{tot.} \approx [FA]_{<100nm}/[FA]_{tot.}$ Based on this result, the iron fractions below 20 nm remain in the aqueous phase at salinity of seawater level. Thus, these results demonstrate that the iron complexes with FA in the river water sample preferentially remain in the aqueous phase after the mixing with seawater.

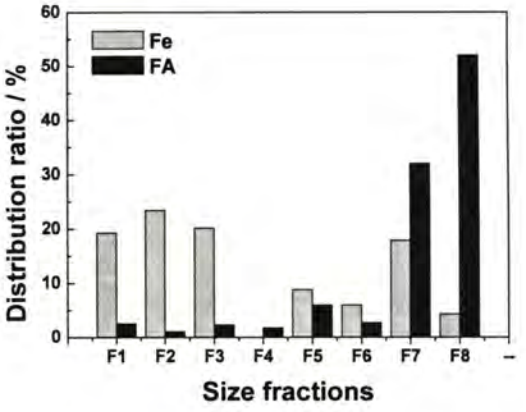

Fig. 7 Size distribution of Fe and FA in the artificial river water. Initial concentrations: 0.1 mg L^{-1} for Fe, 10 mg L^{-1} for FA. pH: 7.2. F1 200 – 400 nm, F2 100 – 200 nm, F3 20 – 100 nm, F4 300KDa – 20 nm, F5 100KDa – 300KDa, F6 30KDa – 100KDa, F7 5KDa – 30KDa, F8 <5KDa.

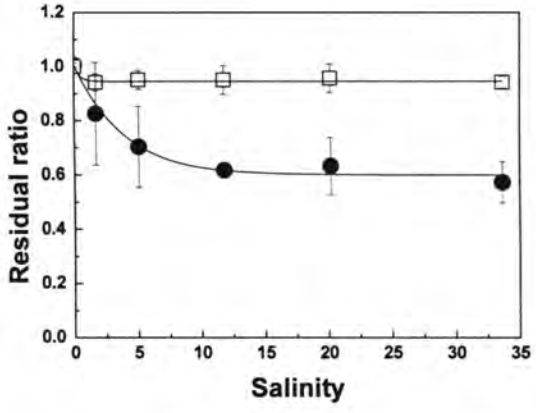

Fig. 8 Residual ratios of Fe (•) and FA (□) as a function of salinity. Initial concentrations: 0.1 mg L^{-1} for Fe, 10 mg L^{-1} for FA.

4. CONCLUSION

The iron fractions distributed below 20 nm in the Bekanbeushi River water sample remained in the aqueous phase at salinity of seawater level. The iron fractions would be due to the complexes with FA. These results demonstrate that the iron complexes with FA in the river water sample preferentially remain in the estuarine mixing zone, but not be removed. Thus, our findings will be useful for understanding the impact of dissolved iron in river waters on the bio-productivity in marine environments.

REFERENCES

Baalousha, M., Kammer, F. V. D., M.-Heino, M., Baborowski, M., Hofmeister, C., Le Coustumer, P., Size-based speciation of natural colloidal particles by flow filed flow fraction, inductively coupled plasma-mass spectroscopy, and transmission electron spectroscopy/X-ray energy dispersive spectroscopy: colloids-trace element interaction. *Environ. Sci. Technol.* **2006**, *40*, 2156 – 2162.

Benedetti, M. F., Ranville, J. F., Allard, T., Bednar, A. J., Menguy, N., The iron status in colloidal matter from the Rio Negro, Brazil. *Colloids Surf. A* **2003**, *217*, 1 – 9.

da Silva, J. C. G. E., Machado, A. A. S. C., and Oliveira, C. J. S., Effect of pH on complexation of Fe(III) with fulvic acids. *Environ. Toxicol. Chem.* **1998**, *17*, 1268 – 1273.

Hunter, R. J., Foundations of Colloid Science, Oxford Univ Pr (Sd), **2001**.

Lead, J., Wilkinson, K. J., Starchev, K., Canonica, S., and Buffle, J., Determination of diffusion coefficients of humic substances by fluorescence correlation spectroscopy: role of solution conditions. *Environ. Sci. Technol.* **2000**, *34*, 1365 – 1369.

Nagao, S., Matsunaga T., Suzuki Y., and Hiraki, K., Convenient method of UV absorbing organic materials in river waters by high-performance gel permeation chromatography. *Chikyukagaku* (Geochemistry) **2001**, *35*, 107 – 120.

Ngo Manh, Th., Geckeis, H., Kim, J. I., Beck, H. P., Application of the flow field flow fractionation (FFFF) to the characterization of aquatic humic colloids: evaluation and optimization of the method. *Colloids Surf. A* **2001**, *181*, 289 – 301.

Nomizu, T., Goto, K., and Mizuike, A., Electron microscopy of nanometer particles in freshwater. *Anal. Chem.* **1988**, *60*, 2653 – 2656.

Pranzas, P. K., Willumeit, R., Gehrke, R., Thieme, J. and Knöchel, A., Characterisation of structure and aggregation processes of aquatic humic substances using small-angle scattering and X-ray microscopy. *Anal. Bioanal. Chem.* **2003**, *376*, 618 – 625.

Sholkovitz, E. R., Flocculation of dissolved organic and inorganic matter during the mixing of river water and seawater. *Geochim. Cosmochim. Acta* **1976**, *40*, 831 – 845.

Sholkovitz, E. R., Boyle, E. A., and Price, N. B., The removal of dissolved humic acids and iron during estuarine mixing. *Earth and Planetary Science Letters* **1978**, *40*, 130 – 136.

Sholkovitz, E. R., and Copland, D., The coagulation, solubility and adsorption properties of Fe, Mn, Cu, Ni, Cd, Co and humic acids in a river water. *Geochim. Cosmochim. Acta* **1981**, *45*, 181 – 189.

Thurman, E. M., *Organic geochemistry of natural waters*, Martinus Nijhoff / Dr W. Junk Publishers, Dordrecht, **1985**, pp. 103 – 110.

Tipping, E., The adsorption of aquatic humic substances by iron oxides. *Geochim. Cosmochim. Acta* **1981**, *45*, 191 – 199.

Tipping, E., Rey-Castro, C., Bryan, S., and Hamilton-Taylor, J., Al(III) and Fe(III) binding by humic substances in freshwaters, and implications for trace metal speciation. *Geochim. Cosmochim. Acta* **2002**, *66*, 3211 – 3224.

Waite, T. D., and Morel, F. M. M., Ligand exchange and fluorescence quenching studies of the fulvic acid – iron interaction, Effects of pH and Light. *Anal. Chim. Acta* **1984**, *162*, 263 – 274.

BIOGEOCHEMICAL PROCESSES OF IRON AND RELATED ELEMENTS IN TERRESTRIAL ECOSYSTEM OF AMUR RIVER

SHIBATA H.[1], YOH M.[2], OHJI B.[2], GUO Y.[2], SHI F.[3], CAI T.[4], XU X.[5], WANG D.[6], YAN B.[6] AND SHAMOV V.V.[7]

[1]Hokkaido University, [2]Tokyo University of Agriculture and Technology, [3]Nankai University, [4]Northeastern Forestry University, [5]Anhui Agricultural University, [6]Northeast Institute of Geography and Agricultural Ecology, CAS, [7]Institute for Water and Ecological Problem, RAS

Terrestrial ecosystem is a one of the important sources of iron to river and ocean ecosystem. Concentration and flux of iron from terrestrial ecosystem to stream and river ecosystem are controlled by the various biogeochemical processes in the watersheds. Many external drivers (including climate, geology, hydrology and so on) and various anthropogenic disturbances (including forest fire, tree harvesting, land use change, agriculture and so on) also strongly influence the spatial and temporal pattern of iron dynamics. The comparative studies based on the monitoring of stream water and soil water in terrestrial watershed with different land-use pattern would be important to understand the natural and anthropogenic fluctuation of iron dynamics in terrestrial ecosystem. Here, we report preliminary results of some biogeochemical investigation in forest, wetland and agricultural ecosystems in terrestrial watershed of Amur River.

Table 1 List of counter-part of collaborative research in each ecosystem of China and Russia.

Ecosystem	Country	Counter-part
Forest	China	Fuchen Shi (Nankai University) Xiaoniu Xu (Anhui Agriculture University)
Forest	Russia	Vladimir Shamov (Institute for Water and Ecological Problem, RAS)
Wetland	Russia	Vladimir Shamov (Institute for Water and Ecological Problem, RAS)
Agriculture Wetland	China	Bai Zhang (Northeast Institute of Geography and Agricultural Ecology, CAS) Chen Xin (Institute of Applied Ecology, CAS)

RAS; Russian Academy of Sciences

CAS; Chinese Academiy of Sciences

I. Characteristics of spatial pattern of iron biogeochemistry in soil and stream water in Chinese forest watershed (written by SHIBATA H., SHI F., CAI T. AND XU X.)

In China, we established two research region for stream chemistry in forest watershed at Liangshui and Daxing'an Mountain and one site for monitoring of river quality in Sungary (Songhua) River near Tongjiang city (Figure 1). In each site, water samples are collected monthly for analysis of concentration of iron and other solutes. In Liangshui and Daxig'an sites, we also collected soil samples to analyze the contents of iron and other elements in soil. In Liangshui site, two sub-catchments named, "Hanyue" are investigated the effect of forest harvesting on iron transport from watershed to stream. The Daxig'an Mountains is located in one of the most damaged area by forest fire in northeastern China.

Concentration of dissolved total iron in Sungary River near Tongjiang city was fluctuated seasonally (Figure 2), and mean values was 0.77 ($\pm$0.41 SD) mg L^{-1} (Figure 3). Shibata (2005) reported that the annual-mean iron concentration of Amur River in 2002 was 0.56 ($\pm$0.17 SD) mg L^{-1}, suggesting the concentration of dissolved total iron in Sungary River is similar level of Amur main channel.

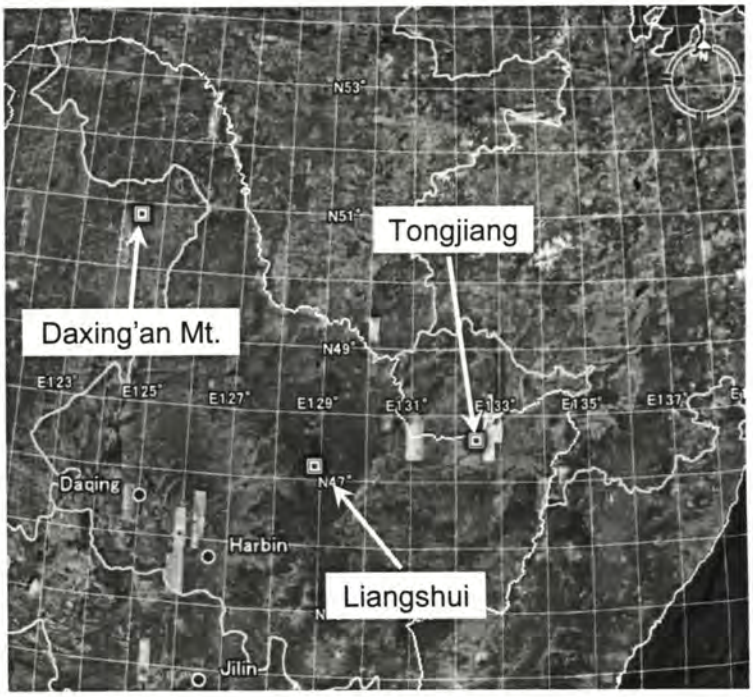

Figure 1. Location of three main research areas for stream chemistry in China

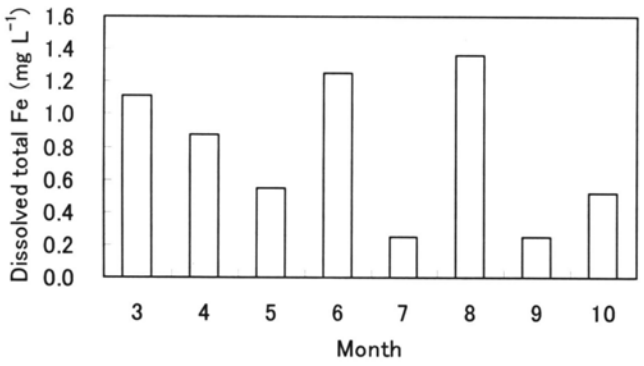

Figure 2. Seasonal fluctuation of dissolved total iron concentration in Sungary river near Tongjiang city in 2006 (unpublished data provided by Shi Fuchen)

Figure 3 shows mean concentration of dissolved total iron in stream water collected in each site from March to October 2006. The mean values at Daxing'an Mountains, Hanyue and Liangshui were relatively lower than that in Sungary River near Tongjiang (Figure 3). We will need to analyze detail comparison in each site to understand the effect of forest fire and tree harvesting on temporal and spatial pattern on iron dynamics in terrestrial watershed (Photo 1).

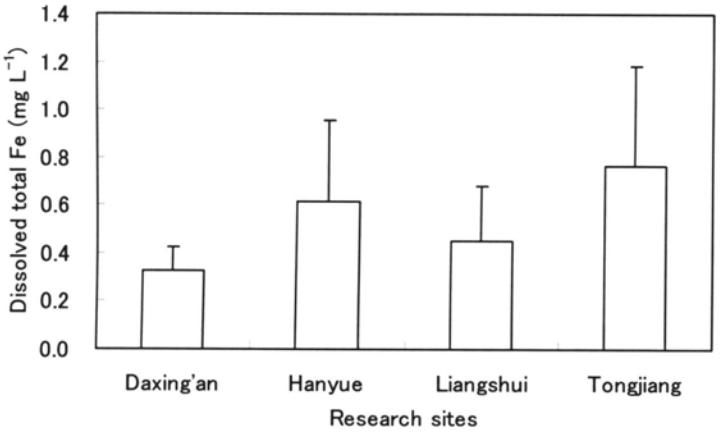

Figure 3. Mean concentration of dissolved total iron in stream water at each research site from March to October 2006 (unpublished data provided by Shi Fuchen). Each bar on box represents standard deviation. Number in each parenthesis means number of sample at each site.

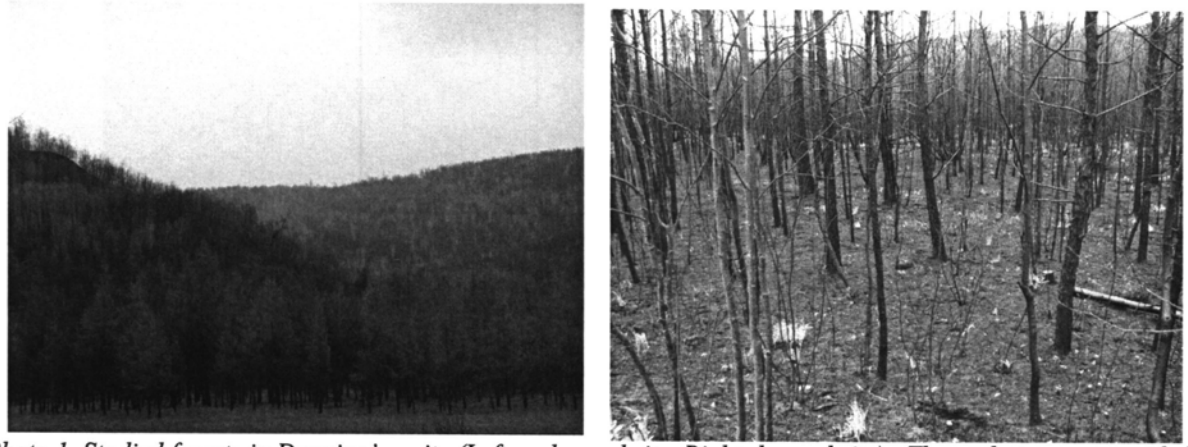

Photo 1. Studied forests in Danxing'an site (Left: unburned site, Right: burned site). These photos are provided by Shi Fuchen.

Analysis of soil chemical property is important to understand the characteristics of actual iron source in ground. We are investigating the contents of iron and related solutes in soil in Lianshui, Hanyue and Daxing'an site (Photo 2). Figure 4 is an example of the preliminary analysis of soil chemical properties in each site. The total nitrogen contents in soil decreased with depth at all sites, and the values at Daxing'an site are relatively lower than those at other two sites, especially at surface soil.

Photo 2. Soil survey at studied forest (provided by Xu Xiaoniu)

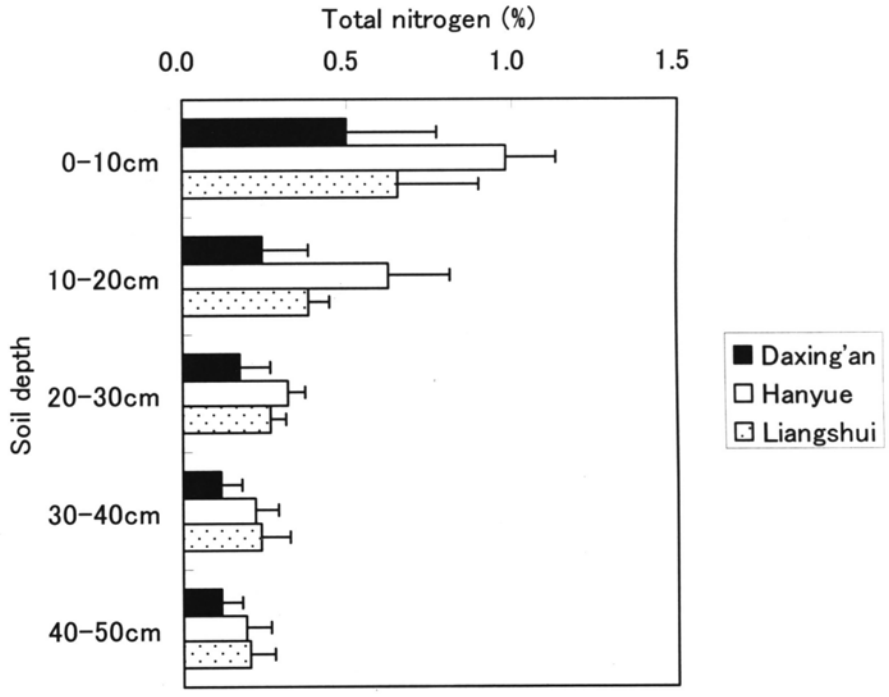

Figure 4. Total nitrogen contents in soil at Daxing'an Mountain, Hanuyue and Liangshui sites (unpublished data provided by Xu Xiaoniu)

II. Spatial distribution of dissolved iron in soil water and stream water in wetland and forest in Russia (written by YOH M., OHJI B. AND SHAMOV V.V.)

1. INTRODUCTION

Dissolved iron is supplied to the Amur river at a concentration of 0.6-0.7 mg/l (Schesterkin, 2004) through iron dissolution processes in its watersheds. The sources of dissolved iron could be related to soil types of Gleysols, Histosols and Podsols (Yoh, 2004). The purpose of our research is to investigate the processes of iron dissolution and transport in natural watersheds in the Amur basin. Spatial distribution of dissolved iron was studied for streams and soil interstitial waters in and around Lake Gassi watershed, which was selected as a model unit that includes typical landscapes of forest, wetland and lake with little human activity.

2. METHODS

1) field survey

The Gassi watershed has an area of about 2400 km^2 and a maximum height of about 950 m. Topography and vegetation of the watershed consist of steep slope (covered by forest) and flat lowland (covered by peatland). The rivers drained from the Gassi watershed flow first into the Gassi lake and then the lake water flows into the Amur river.

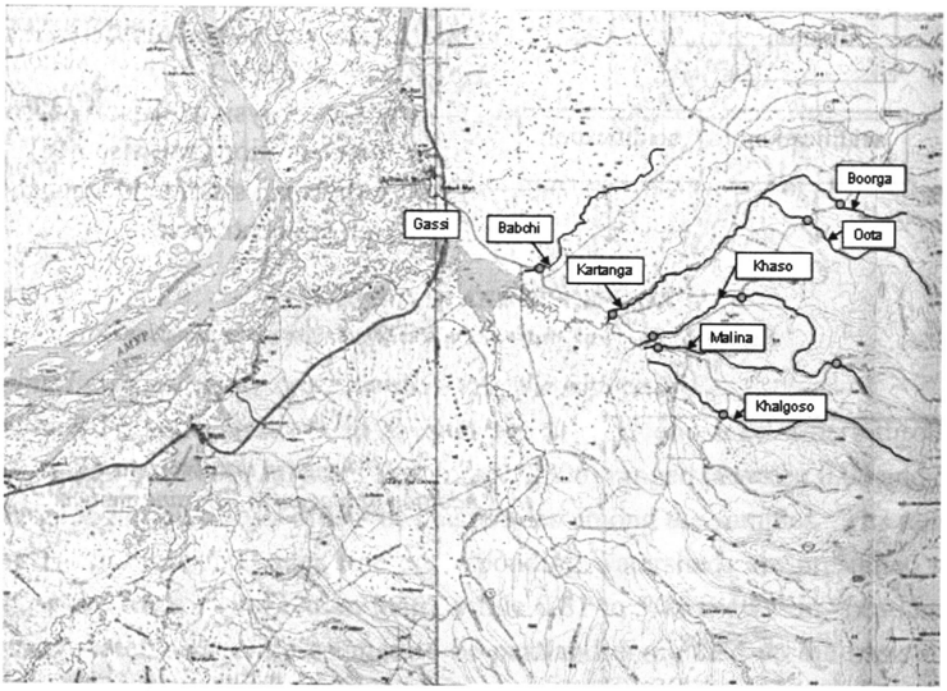

Figure 1 The map of Amur River (left) and Lake Gassi watershed (right) with sampling points. The latitude and longitude of the Gassi lake (center of map) is N49° 03.707' and E136° 31.071'.

Stream water and soil water sampling was conducted preliminarily in October 2005, and in July and September 2006. The location of samplings is shown in Fig. 1 and Tab. 1.

Table 1. The sites of sampling for water and soil water

Site No.	Name of river	Location	Site No.	Name of river	Location
1	Polen	N49° 53.155' E137° 02.528'	11	Babchi	N49° 02.565' E136° 37.374'
2	Nyura	N49° 48.563' E137° 07.632'	12	Kartanga	N49° 00.712' E136° 42.256'
3	Elman	N49° 27.711' E137° 12.337'	13	Khaso (lower)	N48° 59.700' E136° 44.839'
4	Manoma	N49° 26.596' E137° 24.639'	14	Malina	N48° 59.300' E136° 45.195'
5	Anuy	N49° 22.521' E137° 43.215'	15	Khaso (middle)	N49° 01.521' E136° 50.927'
6	Koopturkoo	N49° 17.968' E137° 55.787'	16	Oota	N49° 04.952' E136° 55.231'
7	Gabilli	N49° 15.098' E138° 11.574'	17	Boorga	N49° 05.670' E136° 57.453'
8	Zabyty	N49° 14.069' E138° 13.290'	18	Khalgoso	N48° 56.197' E136° 49.733'
9	Anuy mouth	N49° 18.214' E136° 30.237'	19	Khaso (upper)	N48° 58.598' E136° 56.967'
10	Gassi lake	N49° 03.707' E136° 31.071'			

Water samples were stored in 50 ml polyethylene containers after different treatments in situ as described in Fig. 2. For the acidification for C and D, 0.5 mL of conc. HCl was added to 50 mL of water samples. The pH, electric conductivity (EC), water temperature of stream water and lake water were measured with a pH/EC meter (Horiba, D-20). Duplicate soil water samples were collected from depths of 25 cm and 50 cm below the surface in the vicinity of the water sampling points with a tension lysimeter method.

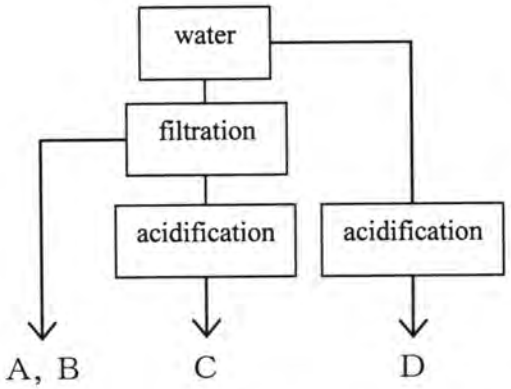

A : for the analysis of major cation, anion, and so on.
B : for the analysis of dissolved organic carbon (DOC)
C : for the analysis of dissolved iron concentration (and also Mn)
D : for the analysis of acid leachable iron concentration

Figure 2. The flow chart of the treatments for water samples.

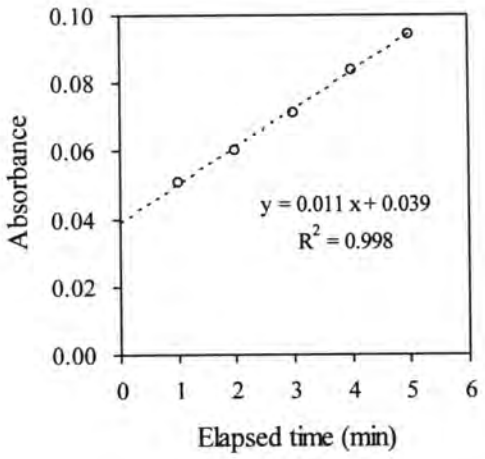

Figure 3. Change in the absorbance after the addition of reagent in ferrozine method.

Free ferrous Fe concentration was measured by a ferrozine method (Stookey, 1970) in situ with a handy colorimeter (Tokyo Kouden, ANA-18A). Eight ml of water sample was

mixed with 2 ml of ferrozine reagent (approximately 8 mM) in a 10 ml volumetric syringe. Because the absorbance increases with time due possibly to an interference by organic-Fe (Ohji et al., in prep), the absorbance at t = 0 was estimated by the interpolation of the curve (Fig. 3).

2) Laboratory analysis

All laboratory analyses of water samples were conducted in IWEP. The analytical items of water chemistry and their methods are listed in Tab. 2.

Table 2 The analytical items of water chemistry and their methods

method	item(s) of measurement	remarks
ICP-MS	dissolved/acid leachable Fe, dissolved Mn, (and Al, Zn, Ni, Co, Cu, Mo)	The internal standard is Xe. The detection limit of Fe is 1 ppb (theoretically, 0.01 ppb). The calibration curves were good.
potassium dichromate method	DOC	Not only DOC but also coexisted reduced matters may be measured. (samples of July, 2006)
TOC analyzer	DOC	(samples of September, 2006)
EDTA titration	Ca^{2+}, Mg^{2+}	
atomic absorption spectrometry	Na^{+}, K^{+}	
molybdenum yellow	Si	
barium chloride spectrophotometry	SO_4^{2-}	
mercury nitrate spectrophotometry	Cl^{-}	

3. RESULTS AND DISCUSSION

(1) The spatial distribution of concentration and the source of Fe

Dissolved Fe concentrations in all samples of river and lake waters throughout three observations (October 2005, July and September, 2006) ranged between 0.04 and 5.70 mg L^{-1}, having a large variation of two orders of magnitudes among the samples. The range was 0.04 to 0.73 mg L^{-1} in "forested" sites (the corresponding watersheds are presumed to be forest-dominated on the basis of vegetation map), while 0.81 to 5.70 mg L^{-1} in "peatland" sites (the corresponding watersheds are presumed to be peatland-dominated on the basis of vegetation map). Thus, we found a clear tendency that peatland area has higher dissolved Fe concentrations (cf. tables in appendix).

Figs. 4 and 5 show the spatial distribution of dissolved Fe concentration as the function of altitude in two observation period. A clear negative correlation exists where Fe concentrations were low at higher altitudes and high at lower altitudes.

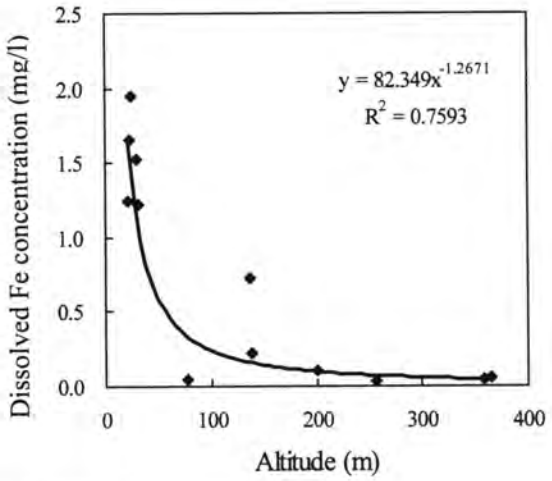

Figure 4
The relationship between dissolved Fe concentration in river water and the altitude (Oct, 2005).

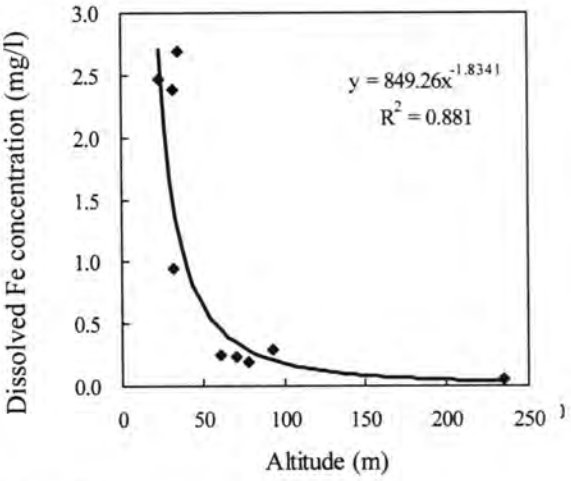

Figure 5
The relationship between dissolved Fe concentration in river water and the altitude (September, 2006).

Fe concentrations in soil water also showed a definite difference among the sites; low level in forest soils and high level in peat soils (Fig. 6). A positive correlation was found between dissolved Fe concentration in soil water and that in river water (Fig 7). It is confirmed from these results that the soil of the latter type of watershed act as the source of dissolved iron in rivers having elevated Fe concentration. Furthermore, we observed that a spray application of 2,2'-bipyridine solution onto peat profile produced a red color. This fact corroborates an occurrence of Fe reduction process to produce ferrous Fe in the soils.

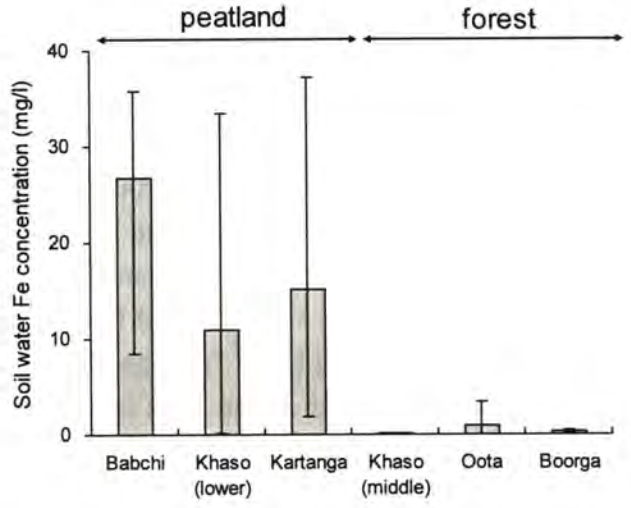

Figure 6
Dissolved Fe concentrations in the soil waters taken from peatland and forest areas. The error bars mean the maximum and minimum levels of Fe concentration.

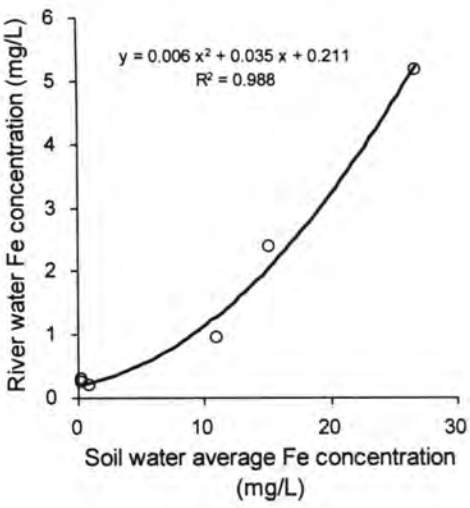

Figure 7
The relationship between dissolved Fe concentrations in soil water and in river waters.

(2) Chemical forms of Fe

Fe in river water is majorly present as an organic form irrespective of its concentration level (Fig. 8). Free ferrous Fe accounted for only a small portion of dissolved Fe with a few exceptional samples.

Fe concentration in river water showed a strong relationship against DOC concentration (Fig. 9) An almost constant ratio of dissolved Fe to DOC concentration suggests the presence of organic-Fe complex with a certain composition (a molar ratio of DOC to Fe of ~51.3) in the river waters of the Gassi basin.

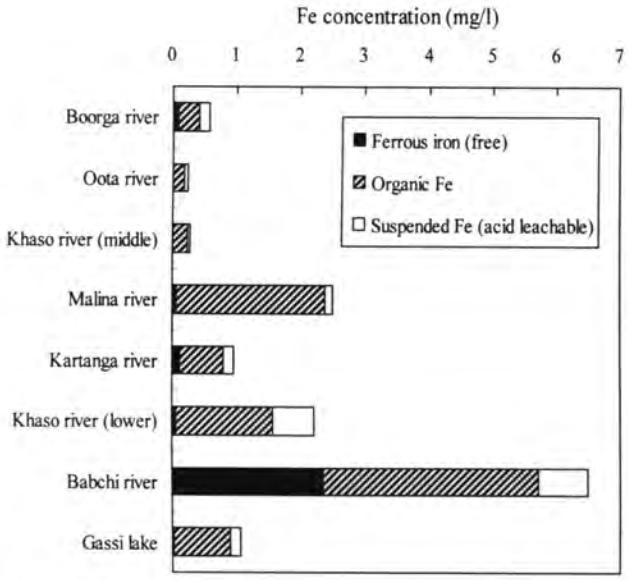

Figure 8
Concentrations of dissolved Fe, free ferrous Fe, and suspended Fe(Jul., 2006). Organic Fe was estimated from the difference between dissolved Fe and free ferrous Fe.

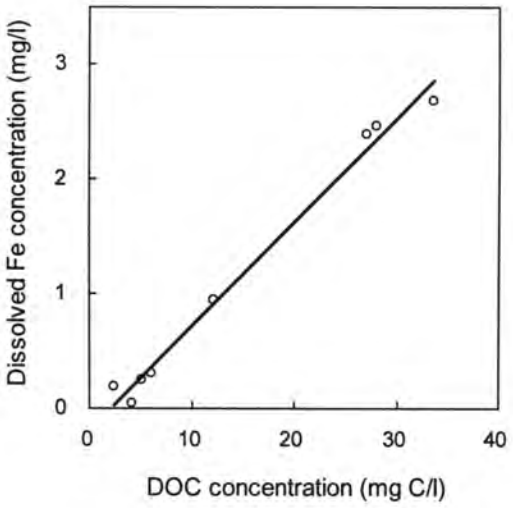

Figure 9
The relationship between DOC and dissolved Fe concentrations in river water. The slope is ~0.0907.

Although dissolved Fe concentration in soil water was positively correlated with that in river water as described above (Fig. 7), the ratio was not unity; Fe concentrations in the river water were ~5 times less than those in soil water. It was sometimes observed that river water from peatland watersheds contained a significant amount of acid leachable Fe (cf. tables in Appendix). It may be likely that dissolved Fe in soil water leads to Fe hydroxides suspended in river water.

(3) Fe in lake water

Dissolved Fe concentration in four river waters collected just upstream of Lake Gassi varied from 0.95 to 5.18 mg L^{-1} (Table 3). The concentration in the lake water, 2.47 mg L^{-1}, was within this range. A "discharge-weighted" average Fe concentration of the rivers was calculated on the basis of relative discharge rates measured on the same period (Fig. 11). The estimated average Fe concentration in river water was 2.61 mg L^{-1}, in a good agreement with the concetration in lake water as above. The result suggests that the Fe concentration in Lake

Gassi, and probably that for the outflowing water to the Amur River as well, may be accounted for by the river waters of this watershed.

Table 3 Dissolved Fe concentrations and discharges of four downstream rivers in September, 2006

Name of rivers	Dissolved Fe concentration (mg/l)	Discharge* (m^3/s)
Khaso	0.95	0.93
Kartanga	2.39	7.17
Malina	2.69	0.06
Babchi	5.18	1.20
Discharge-weighted average Fe concentration: **2.61** (mg/l)		
Observed dissolved Fe concentration of the Gassi lake: **2.47** (mg/l)		

*Discharge data were from Dr. Sharmov.

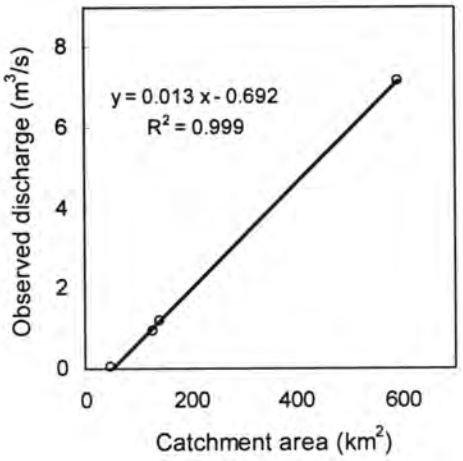

Figure 11
The relationship between observed discharge and catchment area in the Gassi watershed in September, 2006. The slope gives specific discharge of 1.32×10^{-5} (mm s^{-1}). Catchment area was estimated from the map by weighing technique.

(The discharge data were from Dr. Sharmov.)

4. PERSPECTIVE FOR FURTHER RESEARCH

Our field survey in the Gassi basin revealed that peatland (wetland) is important area as the source of dissolved Fe and that dissolved Fe is probably organic-complexed form.

In addition, our results suggested that the concentration of dissolved Fe in river waters might be controlled by DOC concentration. To predict dissolved Fe concentration and Fe flux from a catchment to the Amur river, the estimation of DOC concentration and DOC flux from a catchment is considered to be necessary. To make DOC concentration linked with its catchment characteristics can be an important issue for further research.

III. Dissolved iron concentration in soil water with and without land use change in sanjiang plain, china (written by YOH M., GUO Y., WANG D. AND YAN B.)

1. INTRODUCTION

Sanjiang plain is a vast flat area in the northeast end of China, encircled by Amur River, Songhua River, and Ussuri River. The area is one of the largest wetland in the Amur Basin so that it could be a typical source of iron to this river and the ocean. However, land use change for recent decades has turned that area mostly into agricultural fields, which may lead to significant changes in the biogeochemical cycling and the transport of Fe. The purpose of this subject is to know the Fe behavior in areas with different land use; the concentration and chemical forms of dissolved iron were studied for soil interstitial water in wetland, paddy field and upland field.

2. MATERIALS AND METHODS

Sites and field research

The research sites in Sanjiang plain include three types of landscape (wetland, paddy field, and upland field) of the Sanjiang wetland ecological experimental station (47°35'N, 133°31'E), a wetland near Bielahonghe River (47°31'57.6" N, 133°52'53.2" E), and a wetland in Honghe Sanctuary Natural Researve (47°49'45.8" N, 133°41'38.2" E), in the Heilongjiang province, China. The upland field was planted with soy bean. The average elevation of Sanjiang plain is 56m, and the mean annual precipitation is 600mm and the mean annual temperature is 1.9 °C (Chen et.al., 1996). Water and soil in the wetland are completely frozen in October and begin to melt in late April. The highest and lowest temperatures occur in July and January, respectively.

The soil interstitial water was collected seven times (June, August, September, 2005 and May, July, August, October, 2006) at the Sanjiang wetland ecological experimental station, and four times (May, July, August, and October, 2006) at the Bielahonghe wetland. The soil interstitial water was collected from tree depths (10cm, 50cm, and 60cm) with a tension lysimeter technique, and surface water (0cm) was collected by a plastic bottle directly. The sites for soil water collection had an impermeable formation around a depth of 60cm.

pH, EC and water temperature were measured by a pH meter and an EC meter in situ. Soil Eh was measured by an Eh meter for one depth (10cm) in the sites of wetland, paddy field and upland field of Sanjiang experimental station as above. The Eh probe was installed in May with a replication of 3 or 4.

Chemical analyses

Free ferrous Fe was analyzed colorimetrically by a ferrozine method immediately after soil water collection. Dissolved iron and dissolved manganese were analyzed with an atomic absorption photometer (HITACHI, Ltd.Tokyo Japan. Z-8000) for a sample which was acidified (1mL conc. HCl/100ml) after a filteration with a 0.45μM disposable filter

(ADVANTEC DISMIC-25cs). For the analysis of acid soluble iron, water sample is acidified (4mL conc. HCl/100ml), heated to boil, and then filtered in the same way (APHA 1998). Dissolved organic carbon was analyzed with a TOC analyzer (SHIMADZU TOC-500) for a sample which was filterated and preserved frozen in a glass vial pre-burnt at 550°C.

3. RESULTS AND DISCUSSION

Soil water dissolved iron profiles in the wetland site (station)(a), the Bielahonhe wetland site (b), and the paddy field site (station) (c) are shown in Fig. 1. Considerable seasonal variation in dissolved Fe concentration was observed in these landscapes. As a whole, dissolved Fe concentration level was relatively low in spring (May), but increased with season. The concentration level was largest in summer in the wetland site and in the paddy field site, but in October in the Bielahonhe wetland site; their maxima amounted to 5.0 mg L-1, 3.4 mg L-1, and 17 mg L-1, respectively.

In Fig. 1(d), the concentration levels of dissolved Fe in July are compared among these sites. The profile obtained from Honghe Sanctuary wetland site is also shown in the figure, which is the most preserved wetland area in Sanjiang plain. The result showed that the profile and the dissolved Fe level in the station wetland site was very similar to those in Honghe Sanctuary wetland site. Larger concentration level was observed in the Bielahonhe wetland site on every period (Fig 1 d). In the paddy field (Fig 1c), dissolved Fe levels were consistently somewhat small compared to three natural wetland sites.

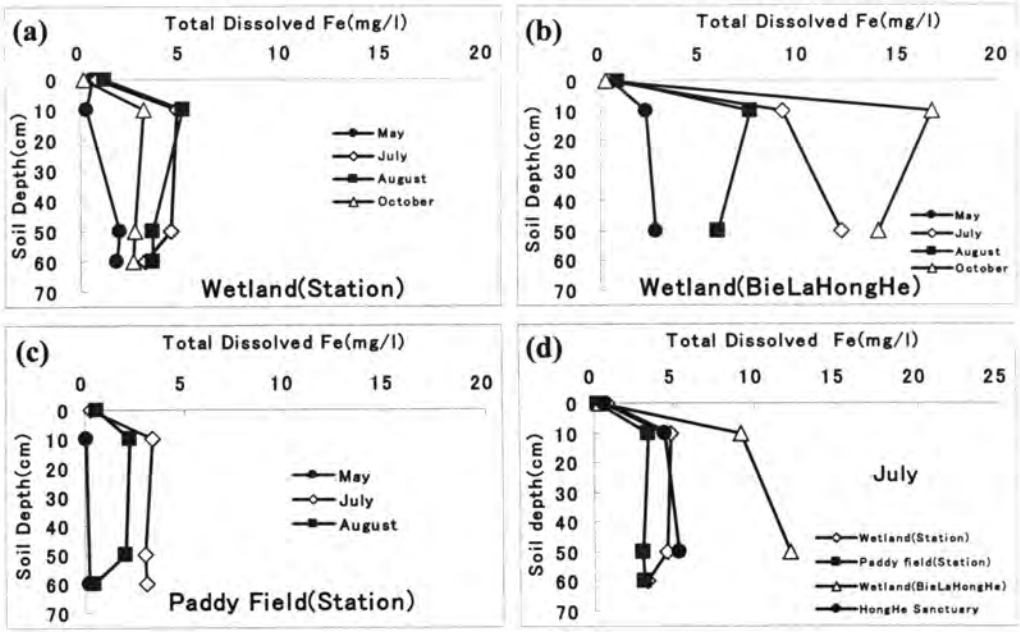

Fig.1 Vertical distribution of total dissolved iron in the wetland and paddy field of sanjiang plain in 2006

It is interesting to note that these profiles of dissolved Fe concentration had a common feature. The concentrations were nearly stable in deeper horizon in all observations. The maximum concentration often occurred at a depth of 10 cm below soil surface. In addition, the surface water (0 cm depth) invariably showed remarkably low concentrations compared with deeper layers. Although the reason for such steep decreases in surface water is unknown, this phenomenon deserves attention in view of the biogeochemical cycling of Fe.

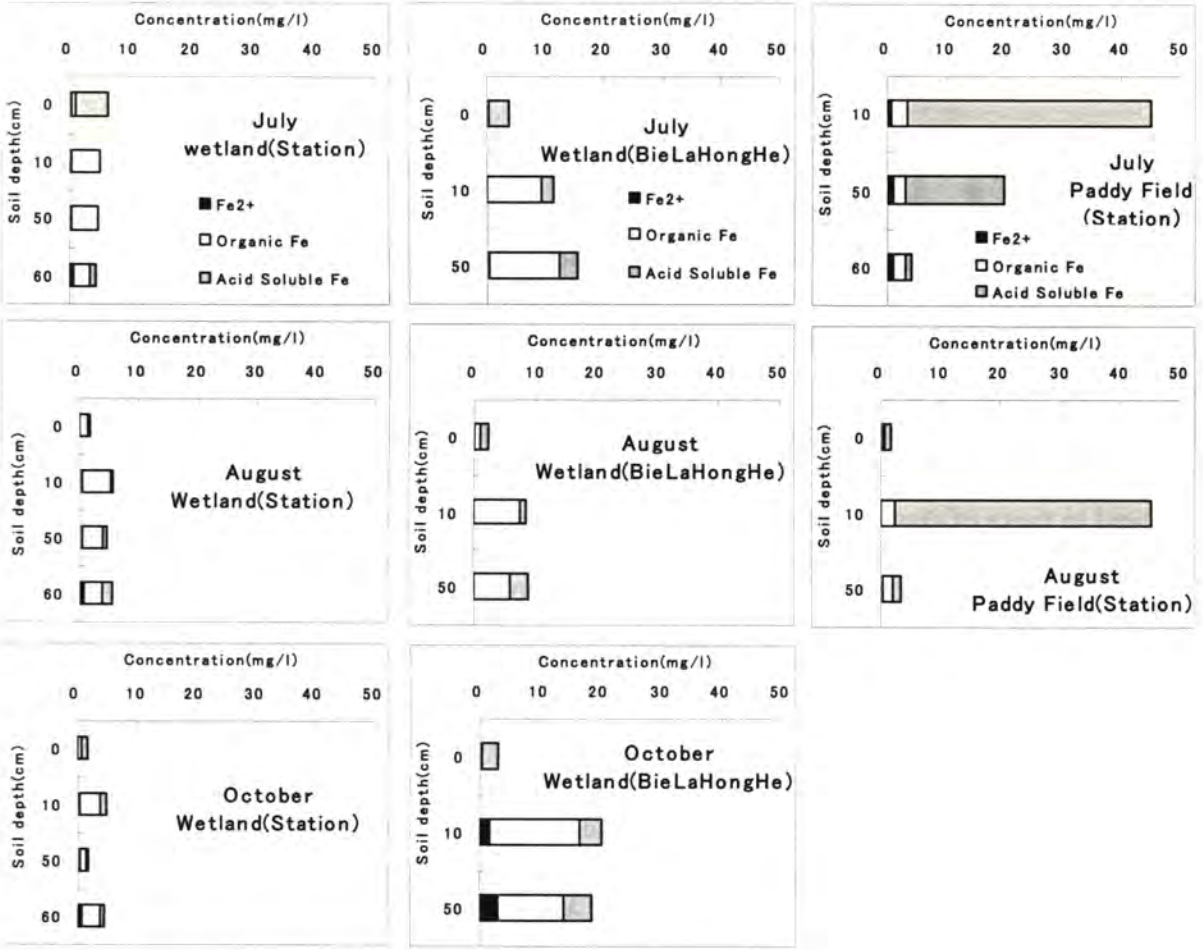

Fig.2
Vertical distribution of different forms of dissolved iron in different seasons for wetland of station, wetland of BieLaHongHe, paddy field of station

The chemical form of Fe in the soil waters of three landscapes on different periods is shown in Fig. 2. Free ferrous Fe generally accounted for 20 % or less of dissolved Fe; i.e., organic iron was the main fraction of dissolved Fe in each site. Relative proportion of organic Fe showed no significant difference between the wetland site and the Bielahonhe wetland site. The soil water in the wetland of Bielahonghe had invariably higher organic Fe concentration than that in the wetland site.

A striking difference found for the paddy field site was that a large amount of Fe was present as acid leachable form, probably Fe hydroxide. Acid leachable Fe was also the major form of Fe in the surface water of two wetland sites, which probably resulted from oxidation

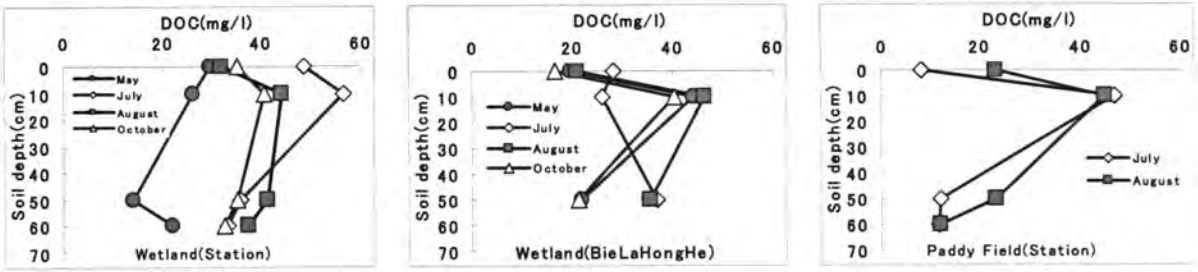

Fig.3
Vertical distribution of dissolved organic carbon in the wetland and paddy field of sanjiang plain in 2006
(a)Wetland of station, (b) Wetland of BieLaHongHe, (c) paddy field of station

of dissolved iron. Precipitaion of Fe by this process partly explains low concentrations of dissolved Fe observed in the surface waters as described above.

The concentration of the dissolved organic carbon often showed a maximum at a 10cm depth and a significant decrease in the surface waters (Fig. 3), analogous to the profiles of dissolved Fe as shown in Fig. 1. Higher concentrations at 10 cm depth may be associated with a peat accumulation observed in that layer in the wetland site. Again, the whole level of DOC concentration were relatively low in spring and tended to increase with season. Although the change of DOC concentration with depth and with season is not completely identical to those of dissolved Fe, a similarity exists in their spatial and temporal changes between these components. There appears no significant difference in DOC concentration level among three landscapes.

Fig. 4 compares the seasonal variation in dissolved Fe concentration in 10 cm and 50 cm depths among wetland, paddy field, and upland field. The data for upland field are hypothetical but realistic as this soil was completely oxic throughout the season. The redox potential in these fields is shown in Fig. 5. Significant amounts of dissolved Fe were detected in warm season for both wetland and paddy field as opposed to upland field. It is obvious that the concentration was constantly higher in both depths in wetland than those in paddy field. Especially, a distinct difference exists for 50 cm depth in late May between both sites, where little dissolved Fe was detected in the soil water of paddy field. Water management is common in paddy field; irrigation in May and drainage in September in this field. This farming practice affected decisively the soil redox condition in paddy field as demonstrated in the Eh value in Fig. 5 (the Eh had positive values in May and October), and consequently the seasonal variation in dissolved Fe concentration in the soil of this site. In addition to the concentration level of dissolved Fe in warm periods, the period itself during which Fe solubilization takes place is suggested to be largely shortened in paddy field, which is also considered as a factor related to the biogeochemical role of this Fe source.

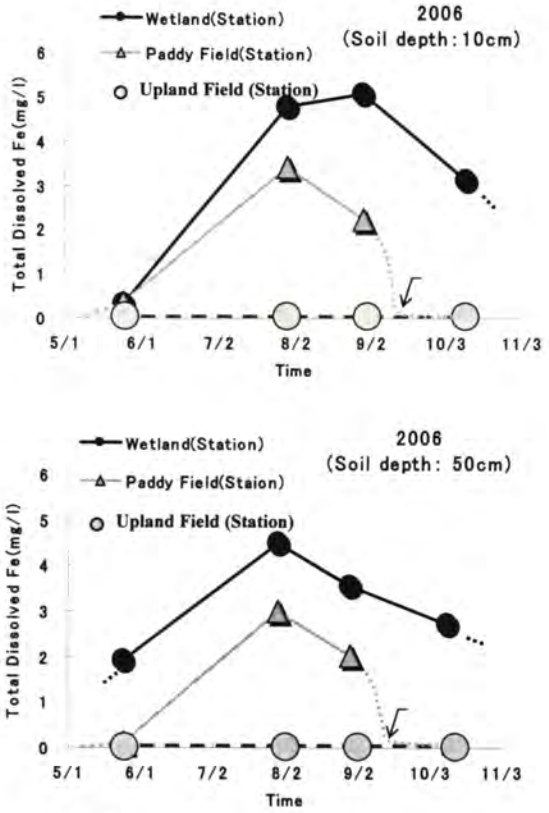

Fig. 6
Seasonal change in dissolved Fe concentration at 10 cm depth (upper) and 50 cm depth (lower) in upland field (●), paddy field (▲) and wetland (●). The arrows denote the period of water drainage management in this paddy field. Dotted lines and the data for upland field are presumptive.

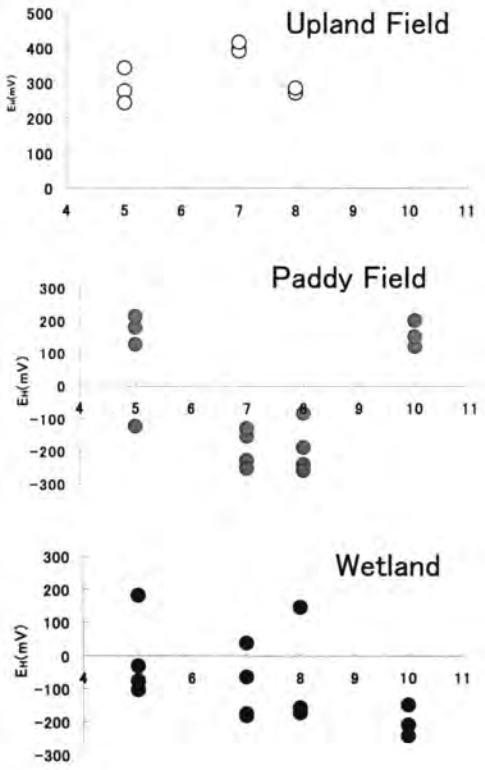

Fig. 5
Seasonal change in Eh at 10cm soil depth in upland field, paddy field and wetland

4. SUMMARY AND FUTURE PERSPECTIVES

The present study has demonstrated a considerable change in both the concentration and the chemical forms of Fe among wetland, paddy field and upland field. It was also found

that dissolved Fe concentration is significantly decreased in surface water compared to deeper soil horizons. This finding is not only interesting in the behavior of Fe but of an important implication in considering the iron transport from land regions to river. The discharge process of soil water in wetland and paddy field and their quantitative importance for the iron transport are unknown yet, being an question on this subject to be investigated next year.

ACKNOWLEDGEMENTS

The authors thank Dr. V. Schesterkin, Dr. V. Kim, Dr. L. Matyushkina and Mr. A. Kuznetsov (IWEP), and T. Ohnishi (RIHN) for their help and discussion during field expedition, and Dr. S. Levshina, Dr. Alexandra (IWEP) and Dr. Danila for their assistance in chemical analysis. We also thank Zhiguo Xu and Yuepeng Pan for their invaluable help in field works, and the stuff of Honghe Sanctuary Natural Researve for allowing us to conduct a research in the wetland.

REFERENCES

American Public Health Association (APHA): 3500.Fe, In, Standard Methods for the Examination of Water and Wastewater (1998)

GangQi Chen. Brief introduction of the Ecological Experimental Station of mire-wetlands in the Sanjiang plain. In, Study in the Wetland of Sanjiang Plain, 1-4. (1996)

Lenore S. Clesceri, Arnold E. (1998) Greenberg and Andrew D. Eaton, Standard Methods For The Examination of water and wastewater, 3: 75-78

Leopold L. B. (1994): A view of the river, Harvard University Press, p.99.

Schesterkin V. P. (2004): Iron content in the middle Amur in winter low water period. Report on Amur-Okhotsk Project, **No.2**, 67-70.

Schlesinger, W.H. (1997) Biogeochemistry, An Analysis of Global Change, 224-260.

Shibata, H. (2005) Processes of iron transport from terrestrial ecosystem to river: Preliminary analysis of spatial and temporal patterns of iron concentrations in Amur River. In 'Report on Amur-Okhotsk Project No. 3: Proceedings of the International Kyoto Symposium 2005', Research Institute for Humanity and Nature, 97-104. Kyoto.

Stookey L. L. (1970): Ferrozine-a new spectrophotometric reagent for iron. Anal. Chem., **42**, 779-781.

Yoh M. (2004): Possible fundamental sources of Dissolved iron in terrestrial environments: their mechanisms, presumed anthropogenic impact, and research needs. Report on Amur-Okhotsk Project, **No.2**, 81-86.

Appendix:

Appendix 1. Results at river and lake sites in October, 2005

Date of sampling	Site No.[1]	Name of river/lake	Dominant landscape of catchment[2]	Fe concentration (mg/l)		pH[5]	EC (μS/cm)	Water temperature (℃)	Altitude[6] (m)
				Dissolved[3]	acid leachable[4]				
10/5	1	Polen river	peatland	1.95	6.12	6.7-7.5	55	4.2	24
10/5	2	Nyura river	peatland	1.24	1.81	7.2	63	6.5	22
10/5	3	Elman river	forest	0.73	0.96	7.1	36	6.1	137
10/5	4	Manoma river	forest	0.23	0.31	7.4	44	7.1	138
10/6	8	Zabyty river	forest	0.05	0.07	6.9-7.3	75	5.1	359
10/6	7	Gabilli river	forest	0.06	0.12	7.0-7.3	58	4.0	365
10/6	6	Koopturkoo river	forest	0.04	0.09	6.7-7.2	25	6.1	257
10/6	5	Anuy river	forest	0.11	0.06	7.3-7.7	44	7.0	200
10/7	9	Anuy river mouth	forest	0.11	0.15	7.2	53	7.2	26
10/7	12	Kartanga river	peatland	1.22	1.37	6.8-7.5	68	6.3	32
10/7	16	Oota river	forest	0.05	0.07	7.2-7.7	52	6.7	78
10/7	11	Babchi river	peatland	1.53	2.18	7.0-7.3	51	7.3	30
10/7	10	Gassi lake	-	1.66	2.84	7.4-7.7	82	10.9	23

[1]The site numbers correspond to those in Table 1.

[2]These are decided by vegetation in map.

[3]Dissolved Fe means the iron fraction that pass through Whatman GF/F filter.

[4]Acid leachable Fe means the iron fraction that pass through Whatman GF/F filter after acidifying samples to ~pH 2: dissolved Fe + acid leachable suspended Fe

[5]Two values at one site means the pH values measured with different two pH meters.

[6]The sea level is zero.

Appendix 2. Results at river and lake sites in July, 2006.

Date of sampling	Site No.[1]	Name of river/lake	Dominant landscape of catchment[2]	Fe concentration (mg/l)		Fe^{2+} (mg/l)	DOC (mgC/l)	EC (μS/cm)	Water temperature (℃)	Altitude[5] (m)
				Dissolved[3]	acid leachable[4]					
7/18	12	Kartanga river	peatland	0.81	0.95	0.12	16.2	33	16.3	32
7/18	13	Khaso river (lower)	peatland	1.57	2.22	0.06	6.9	53	15.0	32
7/18	15	Khaso river (middle)	forest	0.24	0.27	0.00	6.8	47	14.2	61
7/18	16	Oota river	forest	0.17	0.24	0.00	8.3	49	13.5	78
7/19	17	Boorga river	forest	0.42	0.56	0.07	2.3	48	14.7	93
7/19	14	Malina river	peatland	2.38	2.50	0.05	36.7	49	18.4	35
7/19	11	Babchi river	peatland	5.70	6.49	2.34	18.5	62	23.8	30
7/19	10	Gassi lake	-	0.90	1.06	0.01	30.4	47	25.3	23

*pH values were not obtained successfully in this survey.

[1]The site numbers correspond to those in map.

[2]These are decided by vegetation in map.

[3]Dissolved Fe means the iron fraction that pass through GF/F filter.

[4]Acid leachable Fe means the iron fraction that pass through GF/F filter after acidifying samples to ~pH 2: dissolved Fe + acid leachable suspended Fe

[5]The sea level is zero.

Appendix 3. Concentration of chemical components in rivers and lake in July, 2006.

Date of Sampling	Site No.	Name of river/lake	Concentration (mg/l)							
			Ca^{2+}	Mg^{2+}	Na^{+}	K^{+}	Cl^{-}	SO_4^{2-}	Si	Mn
7/18	12	Kartanga river	4.2	2.3	2.51	0.50	1.3	2.78	1.93	0.028
7/18	13	Khaso river (lower)	3.9	2.6	2.53	0.36	0.9	3.23	7.68	0.233
7/18	15	Khaso river (middle)	5.3	2.0	2.34	0.22	- *	3.11	8.06	0.010
7/18	16	Oota river	4.2	2.2	1.89	0.24	0.5	2.43	6.71	0.005
7/19	17	Boorga river	3.3	3.0	2.35	0.41	0.6	3.07	5.82	0.032
7/19	14	Malina river	5.6	4.2	1.91	0.60	1.2	1.45	7.90	0.068
7/19	11	Babchi river	5.6	3.3	1.55	0.37	0.9	5.73	4.69	0.903
7/19	10	Gassi lake	5.6	4.2	1.50	0.66	1.0	6.68	7.30	0.034

Appendix 4. Results at river and lake sites in September, 2006.

Date of sampling	Site No.[1]	Name of river/lake	Dominant landscape of catchment[2]	Fe concentration (mg/l)		Fe^{2+} (mg/l)	DOC (mgC/l)	pH	EC (μS/cm)	Water temperature (℃)	Altitude[5] (m)
				Dissolved[3]	acid leachable[4]						
9/6	12	Kartanga	peatland	2.39	3.22	0.06	27.1	7.05	51	13.8	32
9/6	11	Babchi	peatland	5.18	9.94	0.27	33.6	6.29	57	15.8	30
9/6	16	Oota	forest	0.19	0.35	0.00	2.4	7.15	58	11.8	78
9/6	17	Boorga	forest	0.30	0.54	0.06	6.0	7.13	59	13.4	93
9/7	15	Khaso (middle)	forest	0.25	0.39	0.05	5.1	4.62	55	13.2	61
9/7	19	Khaso (upper)	forest	0.05	0.13	0.01	4.2	5.05	49	10.4	235
9/8	18	Khalgoso	forest	0.24	0.41	0.02	-	6.94	61	15.8	71
9/8	14	Malina	peatland	2.69	3.30	0.01	33.6	6.50	62	15.0	35
9/8	13	Khaso (lower)	peatland	0.95	1.05	0.20	12.2	6.74	56	14.7	32
9/8	10	Gassi lake	-	2.47	3.95	0.04	28.0	7.00	56	20.2	23

[1]The site numbers correspond to those in Table 1.

[2]These are decided by vegetation in map.

[3]Dissolved Fe means the iron fraction that pass through Whatman GF/F filter.

[4]Acid leachable Fe means the iron fraction that pass through Whatman GF/F filter after acidifying samples to ~pH 2: dissolved Fe + acid leachable suspended Fe

[5]The sea level is zero.

Appendix 5. Concentration of chemical components in rivers and lake in September, 2006.

Date of Sampling	Site No.	Name of river/lake	Concentration (mg/l)							
			Ca^{2+}	Mg^{2+}	Na^{+}	K^{+}	Cl^{-}	SO_4^{2-}	Si	Mn
9/6	12	Kartanga river	4.6	3.3	3.05	0.70	0.9	5.38	8.06	0.080
9/6	11	Babchi river	4.6	3.1	3.07	0.83	1.7	4.77	6.34	2.106
9/6	16	Oota river	4.9	3.0	3.04	0.59	0.9	2.02	7.46	0.015
9/6	17	Boorga river	6.4	2.3	4.63	0.54	0.9	3.35	7.46	0.017
9/7	15	Khaso river (middle)	4.6	2.7	2.95	0.66	1.1	2.45	8.96	0.015
9/7	19	Khaso river (upper)	3.8	2.6	4.53	0.98	0.7	2.41	8.96	0.001
9/8	14	Malina river	5.9	4.2	3.76	1.00	1.7	6.49	9.33	0.063
9/8	13	Khaso river (lower)	4.9	3.0	2.85	0.69	1.0	4.69	8.96	0.065
9/8	10	Gassi lake	5.2	2.9	3.44	0.87	1.2	5.33	7.84	0.241

*The sample of the Khalgoso river was not analyzed because of the lack of water.

Appendix 6. Results of Fe concentration in soil water

Date of sampling	Site No.[1]	Name of sites	Dominant landscape of catchment[2]	Fe concentration (mg/l)				Average Fe concentration (mg/l)
				25 cm depth		50 cm depth		
9/6	17	Boorga	forest	-	-	0.10	0.45	0.28
9/6	16	Oota	forest	3.39	0.11	0.02	0.08	0.90
9/7	15	Khaso (middle)	forest	-	-	0.21	-	0.21
9/6	12	Kartanga	peatland	37.2	6.26	1.93	-	15.1
9/8	13	Khaso (lower)	peatland	33.4	9.95	0.13	0.28	10.9
9/6	11	Babchi	peatland	35.8	8.38	35.8	-	26.7
9/8	10	Gassi	-	-	0.07	0.06	0.15	0.09

*The data of DOC concentration in soil water are not obtained yet.

[1]The site numbers correspond to those in Table 1.

[2]These are decided by vegetation in map.

DYNAMIC CHANGES OF SOIL ORGANIC CARBON UNDER DIFFERENT LAND USE TYPE IN SANJIANG PLAIN

CHI G., WANG J., LU C., CHEN X., SHI Y. AND ZHOU L.

Key Laboratory of Terrestrial Ecological Process, Institute of Applied Ecology, Chinese Academy of Sciences

ABSTRACT

The Sanjiang Plain in the northeast part of Heilongjiang Province is one of the largest freshwater marshes in China, which has been experienced intensive cultivation over past 50 years. To understand the dynamic changes of soil organic carbon (SOC) after different durations of cultivation, soil samples down to a depth of 120 cm were collected in layers from the lowland and upland fields having been reclaimed for 5-25 years, with adjacent undisturbed wetland and forestland as the control. The study of the vertical distribution of SOC and its relationship with soil pH showed that the SOC content in undisturbed wetland and cultivated lowland rice fields had a marked decrease from 0-10 cm to 40-60 cm and a less change downward, and a similar variation trend was observed in undisturbed forestland and cultivated soybean fields, only with the difference that the SOC content in 0-10 cm layer was much higher in forestland than in wetland, and lower in soybean fields than in rice fields. For undisturbed wetland, its SOC content in surface layer was decreased by 49.3% and 14.3% after reclaimed for 10 and 25 years, and for undisturbed forestland, 81.9% and 68.3% of its SOC in surface layer were lost after reclaimed for 5 years and 18 years, respectively. The soil pH in surface layer was decreased in the sequences of undisturbed wetland > lowland rice field reclaimed for 25 years > lowland rice field reclaimed for 10 years, and soybean field reclaimed for 5 years > soybean field reclaimed for 18 years > undisturbed forestland. All of these suggested that reclamation made a great loss of SOC in surface layer both in wetland and forestland, and the SOC loss was much greater in forestland than in wetland. The variation of surface soil pH under reclamation could be one of the factors inducing the SOC loss, and a longer period of reclamation combining with rational management could be favorable to the stabilization of SOC.

INTRODUCTION

Soil organic carbon (SOC) is a main factor affecting soil quality and agriculture sustainability. Being a source and sink of plant nutrients, SOC plays an important role in terrestrial C cycle (Freixo et al., 2002).

Land use type has a deep effect on SOC storage, since it affects the amount and quality of litter input, litter decomposition rate, and stabilization of SOC. The SOC loss from irrational land use often leads to some negative impacts on both terrestrial and aquatic ecosystems, and on atmospheric environment (Reeder et al., 1998; Bronson et al., 2004).

The Sanjiang Plain, one of the largest freshwater marshes in China, has been experienced intensive cultivation over past 50 years. About 3.8 Mha of its native marshland has been converted into cultivated land, resulting in a significant change in hydrological properties of the Plain (Liu and Ma, 2000). Many researches were made on the dynamics of methane emission due to this land use change (Ding et al., 2002, 2003, 2004), but the effects of the land conversion on SOC remain largely unknown.

With the cultivated lowland and upland and adjacent undisturbed wetland and forestland as test objects, this paper studied the dynamic changes of SOC under different land use type in Sanjiang Plain.

MATERIALS AND METHODS

1. Study area

The Sanjiang Plain lies in the northeast part of Heilongjiang Province, with a total area of 66,600 km2. This Plain is characterized by smooth terrain, humid climate, and large areas of marsh and forest. Its main soil types are albic soil, meadow soil and bog soil, and its natural vegetations are mainly of marsh vegetation, with woodland meadow scattered on relatively high altitudes. The wetland in Sanjiang Plain is the biggest in area in China (Hao and Wang, 2003).

Sanjiang Plain kept its name of "the Great Northern Wilderness" until the reclamation in mid-1950s. The cultivated land increased from 7.2% in 1949 to 50.0% in 1994, while wetland decreased by 72.2% from 1949 to 1994 and forestland reduced from 30.4%in 1949 to 23.2% in 1983 (Liu and Ma, 2000). Due to the irrational reclamation, regional environmental deterioration, e.g., frequent disasters, regional soil sandification and salinization, soil pollution, water resources decrease, soil fertility decline, and biodiversity worsening, occurred (Marsh Research Department, Changchun Institute of Geography, Academia Sinica, 1983)

2. Sampling sites

The undisturbed wetland and forestland and cultivated lowland and upland in Sanjiang Honghe Farm were selected as test objects, with their sampling sites listed in Table 1.

Table 1. Description of sampling sites

No.	Location	Land use type	Reclamation history
Site 1	47°31.918'N, 133°52.987'E	Wetland	Undisturbed
Site 2	47°31.609'N, 133°53.047'E	Lowland rice field	Reclaimed for 10 years
Site 3	47°32.272'N, 133°30.610'E	Lowland rice field	Reclaimed for 25 years
Site 4	47°32.375'N, 133°30.781'E	Forestland	Undisturbed
Site 5	47°35.299'N, 133°30.172'E	Upland soybean field	Reclaimed for 5 years
Site 6	47°35.405'N, 133°30.012'E	Upland soybean field	Reclaimed for 18 years

3. Soil sampling and analysis

Soil samples were taken from the depths of 0-10 cm, 10-20 cm, 20-40 cm, 40-60 cm, 60-90 cm and 90-120 cm, and duplicates were installed at each sampling site. Soil organic

carbon content was determined by TOC 5000A autoanalyzer, and soil pH was measured in 1:2.5 soil:water suspension by using Elico Digital EC meter. Statistic analyses were made with SPSS 10.0.

RESULTS AND DISCUSSION

1. Soil organic carbon

The SOC content in undisturbed wetland and cultivated lowland rice fields had a marked decrease from 0-10 cm to 40-60 cm and a less change downward (Figure 1a). In 0-10 cm layer, there was a significant difference in SOC content ($P < 0.01$), with the sequence of undisturbed wetland > lowland rice field reclaimed for 25 years > lowland rice field reclaimed for 10 years. Compared with that in undisturbed wetland, the SOC content in 0-10 cm layer in the lowland rice fields having been reclaimed for 10 and 25 years was decreased by 49.3% and 14.3%, respectively.

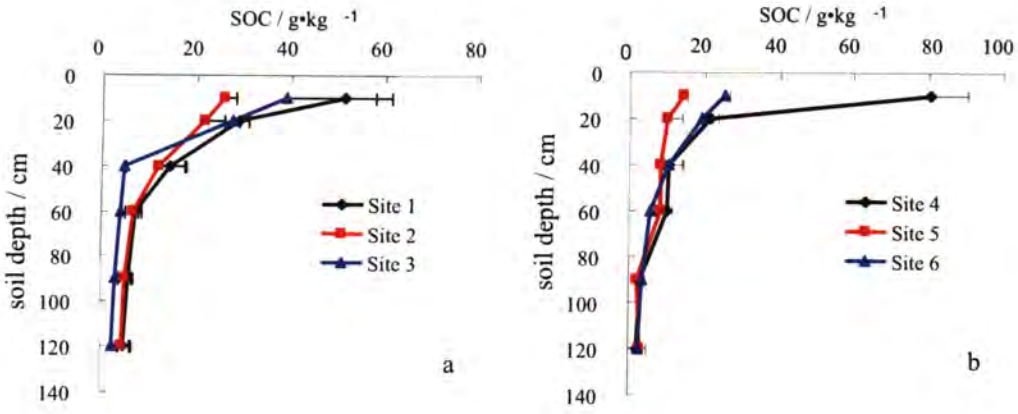

Figure 1. Vertical distribution of SOC under different land use type in Sanjiang Plain.

A similar distribution pattern of SOC was observed in undisturbed forestland and cultivated soybean fields (Figure 1b), only with the difference that the SOC content in 0-10 cm layer was much higher in forestland than in wetland, and lower in soybean fields than in lowland rice fields. Compared with that in undisturbed forestland, the SOC content in 0-10 cm layer in the soybean fields having been reclaimed for 5 and 18 years was decreased by 81.9% and 68.3%, respectively.

The higher storage of SOC in surface layer was closely related with the accumulation of plant materials, while the differences in the dynamics of SOC in this layer should have close relations with the amount and quality of plant residues, as well as the environmental and soil conditions (Dick, 1983; Wander *et al.*, 1998; Needelman *et al.*, 1999).

2. Soil pH

Soil pH decreased with depth in undisturbed wetland, but had a uniform vertical distribution in cultivated lowland rice fields. It was higher throughout the profile in the rice

field with a longer reclamation history than in that with a shorter one. In 0-10 cm layer, there was a significant difference in soil pH, with the sequence of undisturbed wetland > lowland rice field reclaimed for 25 years > lowland rice field reclaimed for 10 years (Figure 2a). On the contrary, the soil pH in undisturbed forestland and the soybean field having been reclaimed for 18 years was increased with depth, and in 0-10 cm layer, soil pH was decreased in the sequence of soybean field reclaimed for 5 years > soybean field reclaimed for 18 years > undisturbed forestland (Figure 2b).

The different distribution patterns of soil pH suggested that reclamation had different effects on soil acidity of wetland and forestland, especially that in surface layer, which should have definite effects on SOC storage. Regression analysis revealed that there was a significant negative correlation between soil pH and SOC in undisturbed forestland and the soybean field having been reclaimed for 18 years, indicating that the higher soil pH after reclamation led to a decreased SOC storage, probably due to the enhanced mineralization of SOC by soil microbes (Motavalli et al., 1995).

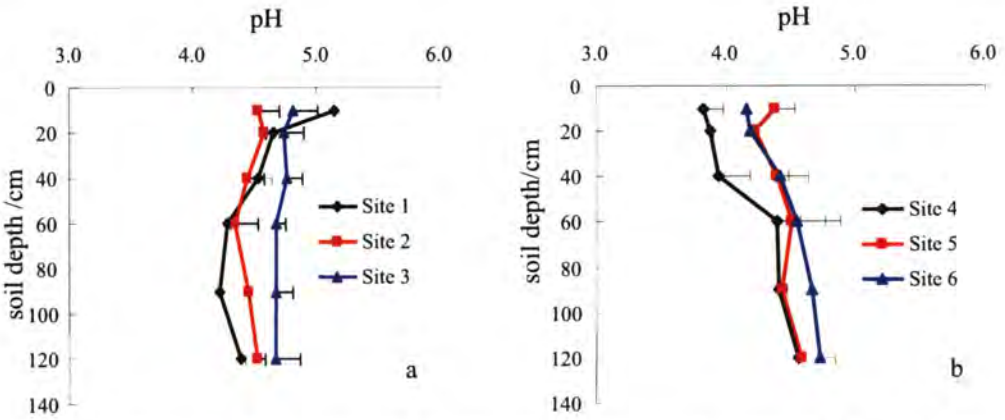

Figure 2. Vertical distribution of soil pH under different land use type in Sanjiang Plain

CONCLUSION

A similar vertical distribution pattern of SOC, i.e., decreased markedly from 0-10 cm to 40-60 cm and less changed downward, was observed in undisturbed wetland and forestland and in their reclaimed fields. The only difference was that the SOC content in 0-10 cm layer was much higher in forestland than in wetland, and lower in soybean fields than in rice fields. Reclamation made a great loss of SOC in surface layer, with a loss rate of 49.3% and 14.3% in wetland after reclaimed for 10 and 25 years, and 81.9% and 68.3% in forestland after reclaimed for 5 years and 18 years, respectively.

Land use type had a significant effect on soil pH. In surface layer, soil pH was decreased in the sequences of undisturbed wetland > lowland rice field reclaimed for 25 years > lowland rice field reclaimed for 10 years, and soybean field reclaimed for 5 years > soybean field reclaimed for 18 years > undisturbed forestland. The variations of surface soil pH under reclamation could be one of the factors inducing the SOC loss.

REFERENCES

Bronson, K., Zobeck, T., Chua, T.T., Acosta-Martinez, V., van Pelt, R.S., Booker, J.D..Carbon and nitrogen pools of southern high plains cropland and grassland soils. Soil Sci. Soc. Am. J. 2004, 68:1695-1704.

Dick, W.A.. Organic carbon, nitrogen, and phosphorus concentrations and pH in soil profiles as affected by tillage intensity. Soil Sci. Sot. Am.J., 1983, 47: 102-107.

Ding, W.X., Cai, Z.C., Tsuruta, H.. Cultivation, nitrogen fertilization and set-aside effects on methane uptake in a drained marsh soil in Northeast China. Glob. Change Biol. 2004, 10:1801-1809.

Ding, W.X., Cai, Z.C., Tsuruta, H., Li, X.P.. Effect of standing water depth on methane emissions from freshwater marshes in northeast China. Atmos. Environ. 2002, 36:5149-5157.

Ding, W.X., Cai, Z.C., Tsuruta, H., Li, X.P.. Key factors affecting spatial variation of methane emissions from freshwater marshes. Chemosphere. 2003, 51:167-173.

Freixo, A.A., Machado, P.L., Santos, H.P., Silva, C.A., Fadigas, F.S. Soil organic carbon and fractions of a Rhodic Ferralsol under the influence of tillage and crop rotation systems in southern Brazil. Soil Tillage Res. 2002, 64:221-230.

Hassink, J., Whitmore, A.P., Kubat, J.. Size and density fractionation of soil organic matter and the physical capacity of soils to protect organic matter. Eur. J. Agron. 1997, 7:189-199.

Hao,Q.J., Wang Qichao，Wang Yuesi et al. The impact of reclamation activities on soil sulfur contents in the Sanjiang Plain. ACTA SCIENTIAE CIRCUMSTANTIAE, Acta Scientiae circumstantiae, 2003, 5(5):614-618.

Liu, Z.G., Ma Xuehui. Effect of reclamation on woil environment in Sanjiang Plain. Pedosphere, 1997, 7(1):73-78.

Marsh Research Department, Changchun Institute of Geography, Academia Sinica. Marsh of Sanjiang Plain(in Chinese). Science Press, Beijing. 1983:208.

Liu, X.T., Ma, X.H. Effect of large-scale reclamation on natural environment and regional environmental protection in the Sanjiang Plain. Scienta Geographic Sinica. in Chinese 2000, 20:14–19.

Needelman, B.A., Wander, M.M., Bollero, FG.A., Boast, C.W., Sims, G.K., Bullock, D.G. Interaction of tillage and soil texture: biologically active soil organic matter in Illinois. Soil Sci. Soc. Am. J. 1999, 63:1326–1334.

Rfmkens, P.F.A.M., van der Pflicht, J., Hassink, J., 1999. Soil organic matter dynamics after the conversion of arable land to pasture. Biol. Fertil. Soils 28:277-284.

Reeder, J.D., Schumman, G.E., Bowman, R.A.. Soil C and N changes on conservation reserve program lands in the Central Great Plains. Soil Tillage Res. 1998, 47:339–349.

Six, J., Callewaert, P., Lenders, S., de Gryze, S., Morris, S.J., Grogorich, E.G., Paul, E.A., Paustian, K.. Measuring and understanding carbon storage in afforested soils by physical fractionation. Soil Sci. Soc. Am. J. 2002, 66:1981– 1987.

Six, J., Paustian, K., Elliott, E.T., Combrink, C.. Soil structure and organic matter: I. Distribution of aggregates-size classes and aggregate-associated carbon. Soil Sci. Soc. Am. J.2000, 37: 509-513.

Shepherd, T.G., Saggar, S., Newman, R.H., Ross, C.W., Dando,J.L. Tillage-induced changes to soil structure and organic carbon fractions in New Zealand soils. Aust. J. Soil Res. 2001, 39: 465-489.

Wander, M.M., Bidart, M.G., Aref, S. Tillage impacts on depth distribution of total and particulate organic matter in three Illinois soils. Soil Sci. Soc. Am. J. 62:1704-1711.

FOREST DEVELOPMENT PROCESS OF KHABAROVSK KRAI AND FULL-FLEDGED REVISION OF FUNDAMENTAL FOREST LAW OF RUSSIAN FEDERATION

KAKIZAWA HIROAKI
Graduate School of Agriculture, Hokkaido University

1. HISTORICAL ANALYSIS OF FOREST DEVELOPMENT IN KHABAROVSK KRAI

Figure 1 shows trend of logging activities of Khabarovsk Krai since1948. Since the late 1960's, the former USSR government put stress on the development of forest resources in the Far Eastern economic region, which resulted in rapid increase of timber production in the region. Khabarovsk Krai, which has been major timber production area in the Far East, also increased its timber production. During 1970's and 1980's timber production in Khabarovsk Krai remained a high level around 140-150 million m2. However, due to economic turmoil after the collapse of former USSR and planned economy, timber harvest dropped drastically, and level of timber harvest in mid-1990's is almost a fourth of 1980's. Although timber harvest has begun to export-led increase since 1998 because of the drop in the Ruble' s value, but still the level of timber harvest is far below 1980's (Kakizawa and Yamane, 2002).

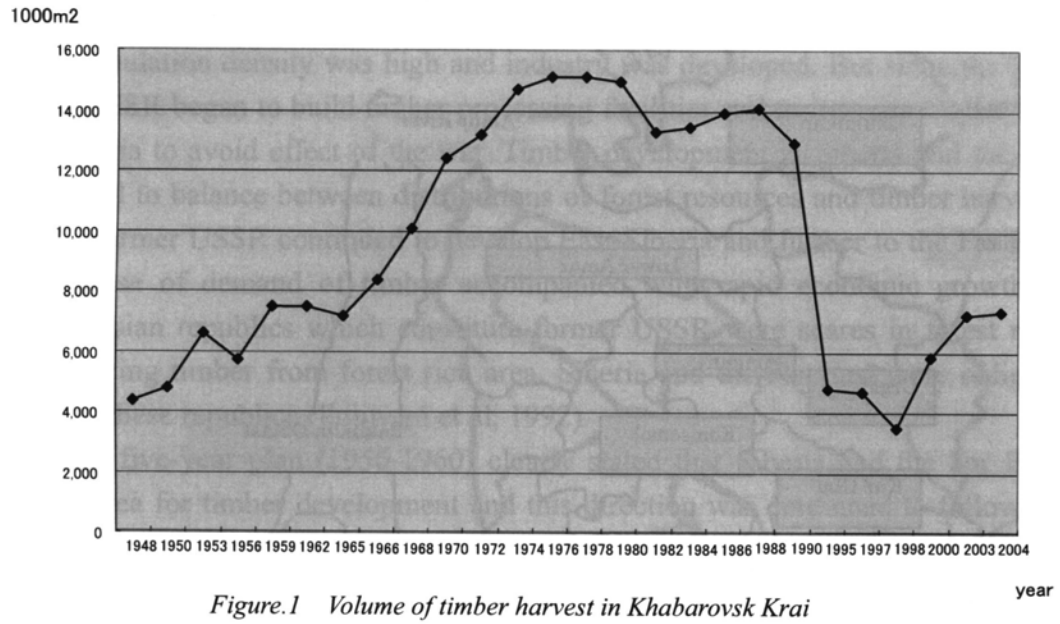

Figure.1 Volume of timber harvest in Khabarovsk Krai

In this paper, forest development in Khabarovsk Krai will be divided into three periods –
Period I; 1950-1960's when timber production began to increase
Period II; 1970-1980's when timber production remained high level
Period III; after 1990's when timber production dropped then recovered oriented by export

Forest development of Period I and II were carried our under planned economy of the former USSR and period III was under transitional economy from planned economy to

capitalist economy.

Basic unit to analyze data on development process was set as forestry region. In Russian federation, basic forest management unit is "leskhoz", but there have been frequent abolish, merge, redivision, and change of boundaries of leskhozes. In contrast, boundary of forestry region has bee unchanged during time period of analysis and considered to be appropriate unit to analyze data. There are 12 forestry regions in Khabarovsk Krai (Fig 2) and trend of timber harvest of each region is shown on Fig 3.

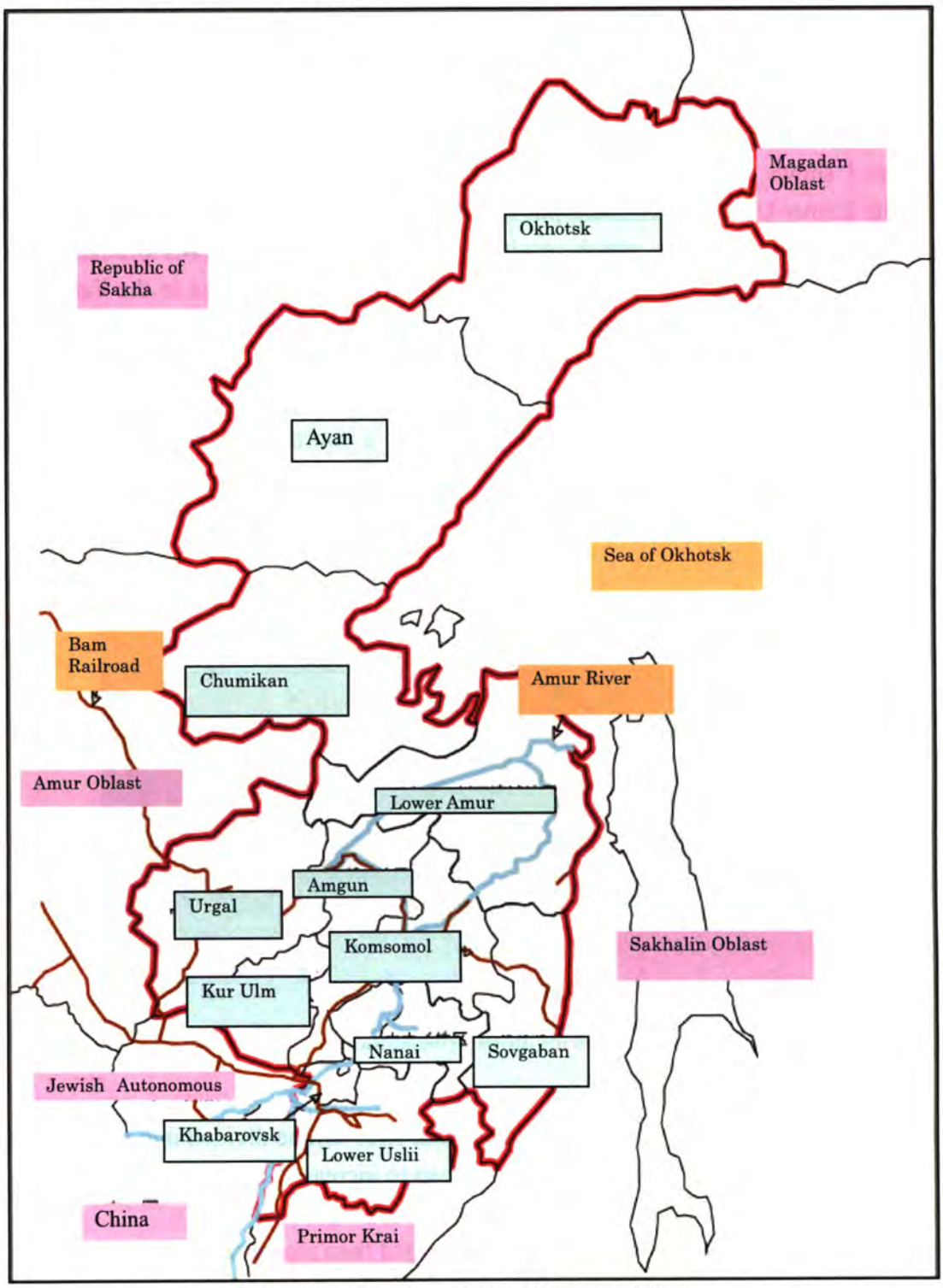

Figure 2. Forestry regions in Khabarovsk Krai

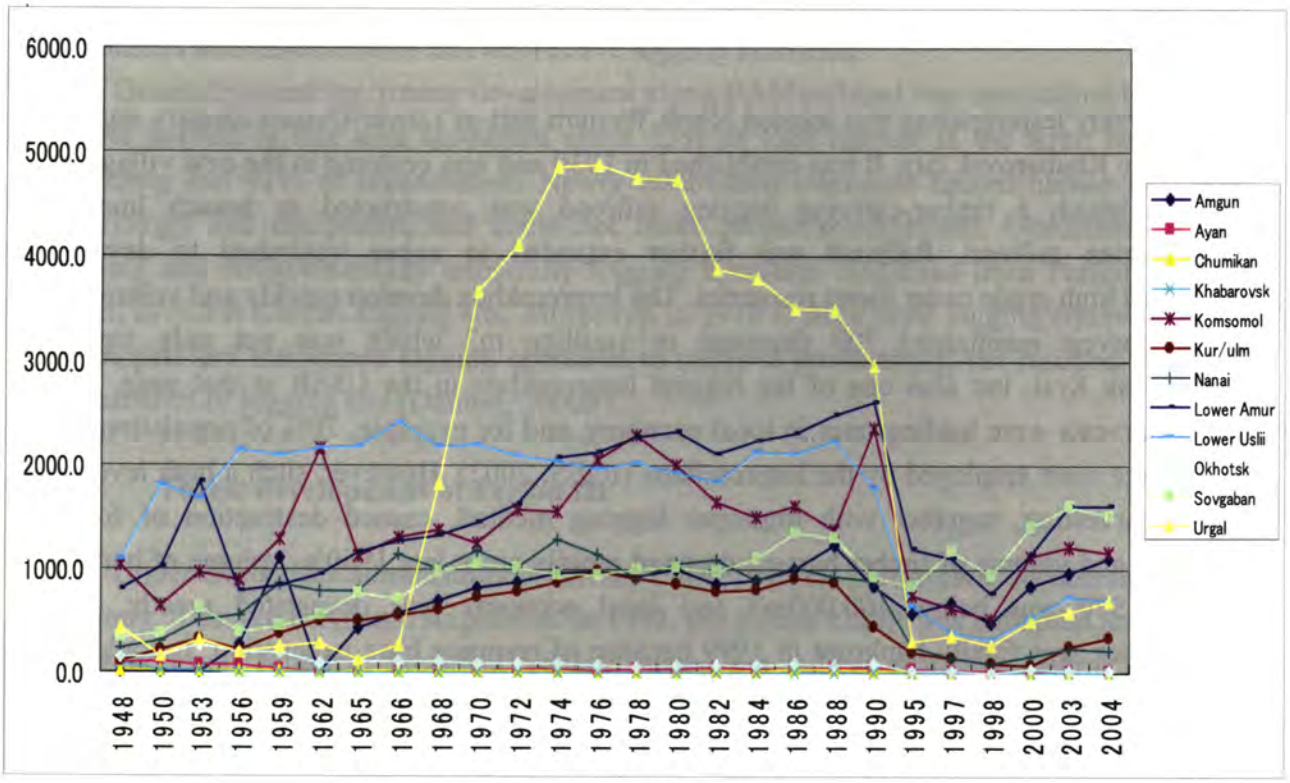

Figure 3. Volume of timber harvest by forestry region

1.1. Forest development of Period I

Originally, forest development of the former USSR had been active in the European part where population density was high and industry was developed. But since the World War II, former USSR began to build timber processing facilities and to increase timber harvest in the East Siberia to avoid effect of the war. Timber development in Siberia and the Far East was also aimed to balance between distributions of forest resources and timber harvest. After the WW II, former USSR continued to develop East Siberia and further to the Far East, to fulfill the increase of demand of timber accompanied with rapid economic growth. Especially, Central Asian republics which constitute former USSR were scares in forest resources and need to bring timber from forest rich area. Siberia and the Far East were obliged to supply timber to these republics (Fujiwara et al, 1992).

Sixth five-year plan (1956-1960) clearly stated that Siberia and the Far East area was priority area for timber development and this direction was continued to following five-year plans. In 1966, Council of ministers of USSR issued decree "On development of timber harvest industry from 1966 to 1970", which mandated further development of timber harvest in Siberia and the Far East, accelerated the development in these region.

In response to these plans, timber harvest was increased during 1950's and 1960's, especially, late 1960's as shown in figure 1. Because infrastructures such as roads and railroad was not well developed in this period, center of timber harvest was Lower-Ussurii, Komsomol, and Lower-Amur forestry regions, which located along the existed Trans Siberian railroad, or Amur and Ussurii River and convenient for log transportation. Especially, Lower Ussurii

forestry region is located close to Khabarovsk city and Tran Siberia railroad, timber harvest was most intense at that time. Following is typical example of timber development in this region.

Oborskiy lespromkhoz was located North Western part of Lower-Ussurii forestry region, adjacent to Khabarovsk city. It was established in 1930 and was centered in the new village of Sita for which a timber-carrying lugging railroad was constructed as branch line of Transsiberian railroad. Railroad was further extended to upper watershed to develop untouched high grade cedar forest resources. The lespromkhoz develop quickly and volume of timber harvest maintained 700 thousand to 1million m2 which was not only top in Khabarovsk Krai, but also one of the biggest lespromkhoz in the USSR at that time. The timber harvests were leading ones in local economy, and for example, 70% of populations of Sita village were employed by the lespromkhoz (IGES, 2002). However, such a high level of timber harvesting, together with improper logging method, caused destruction of forest resources and volume of timber harvest dropped rapidly since late 1960's. Volume of harvest in mid 1970 was below 100,000m3 and local economy was devastated greatly. The lespromkhoz was finally bankrupt in 1999 because of resource base exhaustion. It could be concluded that the way of timber development was unsustainable, and this is not exception but generally observed in the Krai and it continued to the present.

1.2. Forest development of Period II

During 1970's and 1980's, timber harvest in Khabarovsk Krai remained high level of 1.3 – 1.5 million m2. Five-year plan continued to emphasize development of forest resources in the Far East, especially along BAM railroad. Construction of BAM railroad was national project of former USSR and one of major aim was to developed enormous amount of untouched forest resources north of Transsiberian railroad. In 1972, "Long term forest development plan along BAM railroad" was adopted by former USSR as fundamental plan of forest development. Final completion of BAM railroad was 1984, but forest development along the railroad has become active since late 1960's using completed part of the line.

As shown in figure 2, volume of timber harvest of Urgal forestry region located along BAM railroad, increased quite rapidly and reached exerts level in 1970's, and maintained high lever during 1970's and 1980's. This region was originally controlled by Bureinskiy leskhoz, but to prepare to enlarge timber harvest, the leskhoz was divided into Tyrmin and Urgal leskhoz in 1967, and in 1976, Umaltin leskhoz was spin off from Urgal leskhoz and Sogdin leskhoz from Tyrmin leskhoz. Concerning timber industry unit, Urgal lespromkhoz was established in 1951, and Tyrmin and Chegdom lespromkhoz and Urgalles Timber Combinat was established in 1965 (Danilin 2000a). Thus organizational foundation was developed and active timber harvest was carried out. It is noteworthy that development of this area was mainly carried our by North Korean labor forces. Former USSR government signed agreement with North Korean government to lease forest resources and let Korean laborer to log and give 60% of the round wood cut back to the Krai as compensation (Josh, 2004). With this agreement, it made possible to drastically increased volume of timber harvest in these

remote areas, but on the other hand, it was seriously criticized because of quite poor labor conditions and unsustainable and destructive logging activities.

Generally speaking, timber development along BAM railroad was unsustainable. In 1985, timber harvest in this area accounted about 53% of total harvest in the Krai, but 32% of tendering and 41% of regeneration. Newly established leskhozes lucked human resources, technology and equipment, and could not make proper management. Unsustainable high grading and environmentally unfriendly logging operation continued from Period I – even worth in North Korean logging site. Moreover, in 1970's, large scale logging equipments was developed and introduced logging operation to improve productivity, but resulted in serious disturbance of logging site (Danilin, 2000b).

1.3. Forest development of Period III

Under Gorbachev administration, former USSR tried to "perestroika" its economy, but in contrary, it caused economic stagnation. In 1991, the former USSR was collapsed and Russian federation was founded. President Yeltsin carried out radical economic reform to change planned economy to capitalistic economy and it caused serious economic confusion. Together with scale down of domestic market because of the collapse of USSR, timber production felled at a rapid rate, and in middle of 1990's the level was about a fourth of 1980's.

In 1998, financial crisis hit the Russia and timber exports became on the strength of a cheap Ruble (Kakizawa and Yamane, 2002). Since 1998, timber harvest has been increased and it reached 8.2 million m2 in 2005. Destination of timber export in 1990 was mostly to Japan, but China began to increase at a great rate due to increase of timber demand by economic growth and policy to protect natural forest for watershed conservation.

Decrease of timber harvest in early 1990's and increases since 1998 were observed every forestry region, but in Sovgavan, Lower Amur and Amgun forestry region, where good accesses to port to export to Japan, the rate of decrease was relatively low and increases was high. With the increase of timber export to China, timber harvest of Chinese boarder area has also increased relatively high rate.

Currently, forest resources are leased to individual timber company through "arenda" system on the model of Canadian concession system. In this system, forest resources are leased be tender with term of 1-49 years and winning bidder has a right to harvest timber within limit of designated allowable cut. Application for tender are reviewed and selected by forest use committee of Khabarovsk Krai (Kakizawa and Yamane, 2002). The policy of commissions is aggravating of leases in the possession of big users, even creation of holdings (Sheingauz, 2001). These efforts had made increased the average area of lease lots in Khabarovsk Krai from 46.9 thousand ha in 2000 to 50.6 thou. ha in 2005, i.e. by 8%. The total leased accessible wood stock had increased from 574.9 million m^2 in 2000 to 670.4 million m^2 in 2005, i.e. by 16.6%, total AAC of leased lots – from 8.3 to 9.3 million m^2 m, by 12.0%.

The biggest increase had taken place in the leskhozes where there are undeveloped forest tracts: Uktursk – by 114, Gorin – 80, Ulikan – 62, Urgal – 61, Nikolaevs – 32% etc. So, it manifests enlargement of lease lots. At the same time in the leskhozes, where forests

resources are degaraded due to logging activities, the average area of lots had decreased: Avansk – by 82, Nizhnetambov – 55, Kizin – 51, Oborskiy – 42, Komsomolsk – 32, Takhtin – 23% etc.

10 top leasers of 2005 are as floows. Five of them (Arkaim, Badzhalskiy KLPKh-2, Shelekhovsk KLPKh, Ros-DV, and Evoron LPKh) increased their indices, indices of two of them (Sredneamgun LPKh and Vega) remained almost stable, two of them (Rimbunan Hijau and Forest-Starma, which have common owner) had lost a part of leasing, and one of them (Chuin) is a newcomer. Their summary share in the krai's leased area, wood stock and AAC was 33–34% both in 2000 and in 2005. However, they increased their summary area by 22%, wood stock – by 14%, AAC – by 11%, and factual harvest – by 47%. This growth is higher than for all of the leased lots. Thus, enlargement of forest leasers in Khabarovsk Krai are evident for 2000–2005.

The list leasers contained 139 leasers in 2000, 45 of them (32%) did not appear in the list in 2005. At the same time 43 new leasers appeared in the list of 2005 and thus the list contained 137 leasers, 31% of which were new leasers. This means that although big timber companies have developed under current leasing policy, but still many of leasers are unstable and difficult to ensure long-term sustainable forest management.

1.4. Conclusion

In Khabarovsk Krai, active harvest was carried out area along Trans Siberian railroad and big rivers in Period I. Then it moves to the area along BAM railroad in Period II, and to adjacent area to export port and Chinese boarder in Period III. It could be concluded that timber development area was keep moving to pursue forest with good accesses and rich in resources. It should be also emphasized that these development was unsustainable and degraded forest resources were left after logging activities moved to another area.

2. MAJOR REVISION OF FOREST CODE OF RUSSIA

Forest Code of Russia, the fundamental forest law of Russian Federation had been under review for full-fledged revision since 2002. Preparation of new law was first conducted by Ministry of Natural Resources (MNR) and then changed to Ministry of Economic Development and Trade (MEDT). After hot and complicate debate at Duma (Russian house of assembly), finally new Forest Code was moved through Duma, and President Putin singed it on December 8th. It came into effect on January 1st 2007.

2.1. Major content of new Forest Code

1) Ownership of forest.

Ownership of forest has been always the controversial issue in Russia. In 2004, MEDT drafted Forest Code which opened the private ownership of forest. It prescribed that after 15 years of leasing, lease holder could own relevant leased land. However, it brought furious

opposition form public and MEDT had no other choice to withdraw this version of draft. Final version clearly stated that forest fund is under ownership of federal government. However, new code permits small parcel forest lot for privatization. Environmental NGOs are anxious about small parcel of forest will be privatized to build second houses.

Public's distaste for privatization of forest is quite strong and any attempt to introduce privatization of large scale forest land will be failed.

2) Decentralization of forest policy

Forest code of 1997 decentralized forest policy system compared to previous fundamental law, but management of forest and distribution of right to use forest was attributed to federal government. Under Yeltin administration, further decentralized forest policy system and some of local governments introduced their own distribution system of right to use (Kakizawa, 2002). However, Putin administration drastically changed policy direction and forest policy system became centralized one and local governments were forced to abolish their own distribution system (Sheingauz and Kakizawa, 2003).

New Forest Code gives authority of management of forest and distribution of right to use forest to local governments. Federal forest management organization will transferred to local government and forest management will be conducted under direction of local government. Authority to set fundamental direction of forest management is still in the hand of federal government, but new code clearly step forward decentralization of forest policy.

New forest code specified that fundamental unit of forest management is lesnichestvo. Under current forest management system, fundamental management unit is leskhoz and lesnichestvo is local branch of leskhoz. Intension of new forest code is unclear, and this discord of terminology might cause confusion.

3) Distribution system of right of use

Forest Code of 1997 defined the applicant for forest lease tender not only should submit bid price but also proposal for contribution for local economy and society, and their ability logging activities and forest management. However, New Forest Code defined that decision of winner of the tender is only based on bid price. Also, Forest Code of 1997 prohibit sub-lease, but new Forest Code deleted this article. There is concern that company with rich financial resources but no experience on forest management might bulk buying. But Russian government denied this concern because new Forest code introduced anti-monopoly article. Local communities concern that logging company stop contributing to local society.

4) Procedure to conduct logging activities.

Forest Code of 1997 defined that lease holder should negotiate with leskhoz about volume, species, and way of harvest annually, and need to get logging permission ticket from leskhoz. New Forest Code simplified this procedure, and leaseholder is obliged only to make forest use declaration annually based on forest development plan. Environmental NGOs concern that this make difficult to forest management body to control logging activities and to check illegal logging.

New forest Code also defined that lease holder is responsible for forest management of leased forest, but details is not unclear so far.

5) Promotion of process of timber

New Forest Code created new type of forest use – "Forest use for processing wood and other forest resources" - intended to promote process of timber, as timber export of Russia is still log oriented one and development of timber processing industry is high-priority issue. However, new Forest Code did not give any additional measures for the development of timber industry, and thus it is doubtful that this article promotes further investment for processing faculties.

6) New zoning of forest

Traditionally Russian forest was divided into three groups; first group is for forest protection, second group for protection of urban environment and forest deficit area, and third group for forest development. New Forest Code abolished this system and defined that forest will be divided into protection, production and reserved forest.

2.2. Evaluation of forest code

Major characteristics of new Forest Code could be summarized as market oriented and emphasize on promotion of logging activities and processing timber resources. It is partly because the Code was developed by MEDT. It is also pointed out that MEDT lacks knowledge on forest management and current management system, which resulted improper wording and confusion in articles. Member of Duma and official of MNR also admit that there are defectiveness on new Forest Code as administration hastened Duma to pass it. However it has also advantage that procedures for auction was clearly defined and anti-monopoly articles was introduced.

It is very difficult to forecast the influence of new Forest Code on forest management at this time. There are bunch of very real problems to carry out this new Forest Code. Firstly, federal budget for 2007 does not include any expenses to carry out the Code, and MNR and local government will face financial problems. Secondly, to carry out this code fully, 56 normative documents should be developed and 24 decrees and 32orders should be revised. 12 laws are contradicting with this code. In this sense, it takes time to carry out this code and also unclear how actually the code will implement. There has been frequent policy change and reorganization, so the organization engaged in forest policy and management was exhausted and weakened. It could not expect that the new Forest Code bring bright future for forest management in Russia at least the near future.

REFERENCES

Danilin, A. (2000a) History of forest management of Khabarovsk Krai, Khabarovsk Publishing service (In Russian)

Danilin, A. (2000b) Forestry, Khabarovsk Publishing service (In Russian)

Fujiwara, K. Kakizawa, H. and Ishii, Y. (1992) Trends of Forest Management and Forest Industries in the former USSR Far East, Research Bulletin of Hokkaido University Forest 49(2)

IGES (2002) Russia Country Report 2001, IGES

Josh N. (2004) Russian Far East, A Reference Guide for Conservation and Development, Daniel & Daniel

Kakizawa, H. (2002) Development of Institutional Framework of Russian Forest Sector--Focusing on Federal-Local Relationship, Journal Forest Economics 48(1)

Kakizawa, H. and Yamane, M. eds. (2003) Russian forest and forestry, J-Fic.

Sheingauz, A. (2001) Forest Sector of Khabarovsk Krai' principle orientation of development

Sheingauz, A. and Kakizawa, H. (2003). The development of forest policy in the Russian Federation—With a focus on Khabarovsk Krai. In *People and forest—policy and local reality in Southwest Asia, the Russian Far East, and Japan*, Inoue, M., and Isozaki, H., eds., Kluwer Academic Publishers

OVERVIEW OF FOREST DEGRADATION AND CONSERVATION EFFORTS IN THE AMUR BASIN IN THE TWENTIETH CENTURY, WITH A FOCUS ON HEILONGJIANG PROVINCE, CHINA

YAMANE MASANOBU
Kanagawa Prefecture Natural Environment Conservation Center

1. INTRODUCTION

Forests are a key element of the landscape in the Amur Basin and play a very important role in maintaining the watershed's ecosystem and material flows, from the Amur River's upper tributaries in China to the Okhotsk Sea in the Russian Federation. Since the beginning of the twentieth century, however, the forests in the basin have been destroyed or seriously degraded, mainly due to farmland development, forestry development, and forest fires.

Various reports have been published on the state of the forests, forestry activities, and the causes of forest fires on Russia's side of the basin (i.e., Kakizawa 2004; Sheingauz and Kakizawa 2003; Kakizawa and Yamane 2003; Kakizawa et al. 2005). For this project, studies of areas such as forest policy and the timber trade were conducted with the aim of clarifying the direct and indirect impacts of human activities on the forests in the basin, with a focus on the northeastern province of Heilongjiang in China.

As for forestry activities on China's side of the basin, a detailed study of Heilongjiang Province (Dai 2000) was based on various earlier studies (e.g., Ikebe 1933; Ogino 1965; Tao 1987). Information in reports on forest fires and conservation efforts in the area is fragmentary, however, and thus compiling a multifaceted review is helpful in examining the causes of forest loss and to aid discussion of a forward-looking agenda.

In order to examine the impact of human activities on the forests of Heilongjiang, this article reviews the following three subjects, based on key documents and other available information:

1. Changes in forest resources in China in the latter half of the twentieth century, highlighting the relative position of Heilongjiang Province
2. The state of forestry development and forest fires in Heilongjiang as major proximate causes of forest loss on China's side of the Amur Basin
3. An outline of important recent forest conservation policies

2. CHANGES IN FOREST RESOURCES IN THE LATTER HALF OF THE TWENTIETH CENTURY

In 1950, forests covered only 8.3 percent of the total land area of China. This is because China's forests had been devastated due to decades of war and incursion by the Russian Empire and Japan at the end of the nineteenth century.

The general coverage of forest area has increased considerably since then, compared with

the state of forests at the time of founding of the People's Republic of China in 1949, although this fluctuated a little during the 1970s to 1970s. China's forested area in 1993-1998 was 158.941 million hectares (ha), accounting for 16.6 percent of its total land area. Among them, the forested area is 133.704 million ha, increased by 9.051 million ha compared with the area in 1984-1988, when China's third regular forest resource survey was conducted.

At the establishment of the People's Republic of China, forested land was unevenly distributed, but the regions of the northeast (Heilongjiang, Jilin, and Liaoning provinces) and southeast (Yunnan and Sichuan provinces) held more than 70 percent of China's total forest area.

Based on the national forest resource inventory (1993–1998), forested land in China covered 16.8 percent of the country, although its distribution was still not uniform. At the time, three northeastern provinces (Heilongjiang, Jilin, and Inner Mongolia) and ten southern provinces (Zhejiang, Anhui, Fujian, Jiangxi, Hubei, Hunan, Guangdong, Guangxi, Hainan, and Guizhou), contained more than 30 percent of China's remaining forests. Two western provinces—Sichuan and Yunnan—held nearly 20 percent of the total. Thus the growing stock is concentrated in these three regions.

Heilongjiang's forests were left almost untouched until the middle of the nineteenth century. Since that century's end, however, forestry development in the area progressed significantly, and, consequently, forest coverage of the province's total land area had decreased to 37.6 percent by the middle of the twentieth century. Even so, the forests of Heilongjiang were still important, because they represented more than 20 percent of China's total forested area and were still a significant resource for timber production.

Thus, intensive timber production continued during the latter half of the twentieth century, and the forested area

Table 1.Forested area and forest coverage in China and Heilongjiang Province in the latter half of the twentieth century

Index/year		China	Heilongjiang	Heilongjiang's share (%)
Total land area		960,272	45,461	4.7
Forested area (1,000 ha)	1950	79,703	17,100	21.5
	1973-76	121,860	25,200	20.7
	1977-81	115,277	15,294	13.3
	1984-88	124,653	15,615	12.5
	1988-93	133,704	16,162	12.1
	1994-98	158,941	17,603	11.1
Forest coverage (%)	1950	8.3	37.6	
	1973-76	12.7	34.9	
	1977-81	12.0	33.6	
	1984-88	13.0	34.4	
	1988-93	13.9	35.6	
	1994-98	16.8	38.7	

Sources: State of Current Forest Resources in China 1949-1993, Ministry of Forestry, 1996-1998.

Table 2. Several indices of forest resource degradation in Heilongjiang's state forests during the latter half of the twentieth century

Year	1962	1986
Share of coniferous forests' stand volume (m^3)	68.6	18.5
Mean timber volume (m^3)	1.2	0.5
Mean stand DBH* (cm)	32.3	13.3
Mean stand volume of natural forest (m^3)	199	111
Mean stand volume of mature forest (m^3)	226	157
Mean stand age (years)	220	100

Source: Dai (2000) *Diameter at breast height.

decreased to 15.3 million ha by 1977-81 as a result (Table 1). Forest coverage also decreased to four points.

The forests recovered gradually after the 1980s, and in 1994-98 forest coverage exceeded that in the 1950s, but the degradation of forest resources, including notable loss of mature forests and the resultant smaller sizes of timber being harvested, continued until the end of the twentieth century (Table 2).

To summarize, severe forest loss occurred in Heilongjiang during the twentieth century, and it can be assumed that the changes in forest cover had considerable effects on the watershed ecosystem and material flows in the Amur Basin.

3. FORESTRY DEVELOPMENT IN HEILONGJIANG PROVINCE[1]

3.1. Before the establishment of the People's Republic of China

At the end of the nineteenth century the construction of the Chinese Eastern Railway, which started at Chita and went through Manzhouli, Haribin, and Suifunhe to Vladivostok, was a catalyst of forestry development in Heilongjiang (Figure 1).

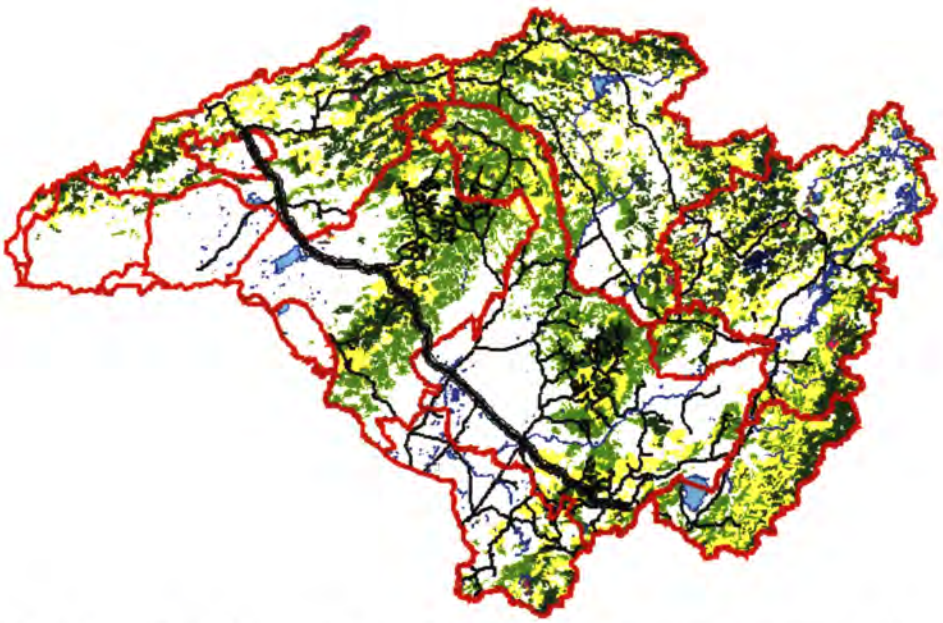

Figure 1. Map of Heilongjiang Province. Current administrative boundaries (red lines), forest distribution (green-colored areas), and the railway network in the Amur Basin (black lines). The route of the Chinese Eastern Railway is the bold black line.

Until the 1850s, close to the end of the Qing Dynasty, the government had employed a strict conservation policy to protect the forests in the northeast region of the territory, and the forests were still in their natural state. After the dynasty's end, however, the Russian Empire undertook construction of the Chinese Eastern Railway, and then logging was begun to produce a huge amount of wooden ties for rail lines and fuel wood for the train locomotives.

[1] This section is based on an article written by Dai (2000)

As a result, any land within 70 kilometers of the Chinese Eastern Railway line was deforested by Russian Empire outfits and China–Imperial Japan joint ventures until around 1930. From 1931 to 1945 the still-untouched forests in the Amur Basin in northeast Heilongjiang, such as those in the Lesser Khingan Range and the Songhua River basin, were developed into the hinterlands when Manchuria, established by Imperial Japan, constructed a logging railroad connecting up with the Chinese Eastern Railway line. An estimated 1.17 billion cubic meters (m^3) of timber was extracted during this period, indicating that forestry activities became more intense than ever. Consequently, the forested area in the province decreased from 27.8 million ha in the 1930s to 17.1 million ha in 1945, and the volume of standing stock saw a large decrease from 3.6 billion m^3 to 2.4 billion m^3.

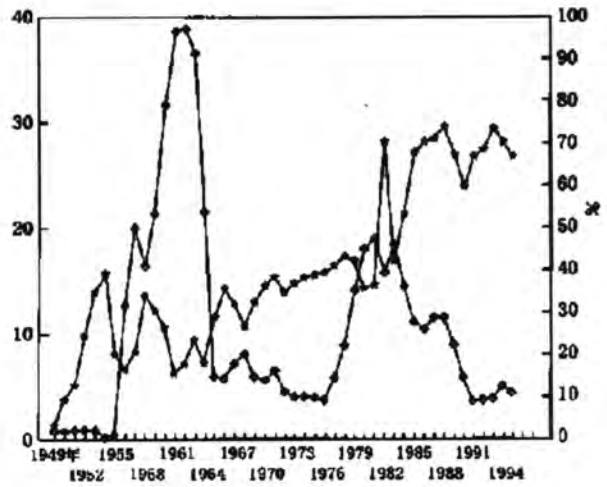

Figure 2. Change in logging area (☆=million ha) and the rate of clear-cutting (◇=percent.) in Heilongjiang state forests. Source: Dai 2000.

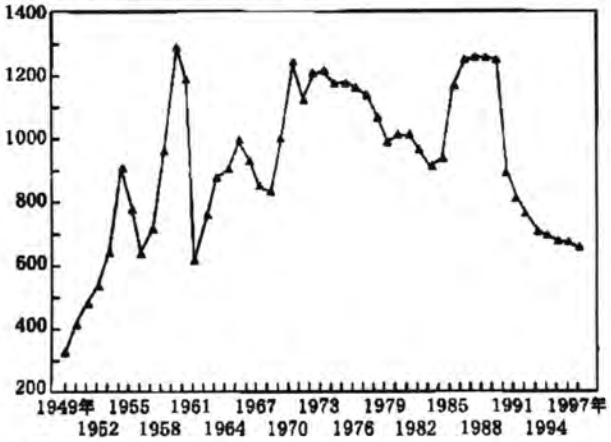

Figure 3. Change of logging volume (million m^3) in Heilongjiang state forests. Source: Dai 2000.

3.2. From establishment of the People's Republic of China to the middle of the 1970s

After Communist Party leader Mao Tse-Tung (Mao Zedong) founded the People's Republic of China, the forests on China's side of the Amur Basin were designated as state forest. Forestry development then progressed more intensely under the control of the central government. Initially, from 1945 to 1952, the area produced a massive amount of timber to support the liberation war and post-war reconstruction. Timber production during the time was estimated at 21 million m^3 totally, half of the total timber production of the whole country (Figure 2). Heilongjiang's local government decided to develop infrastructure with the aim of strengthening forestry development, resulting in various extensive projects, such as railway recovery, new railway construction for logging, relocation of sawmills, and extension of logging rail lines from resource-depleted areas to the resource frontier. As a result, forestry development expanded again into pristine areas.

When the new China entered a strong phase of economic development after 1953, the country succeeded in establishing a centralized economic planning system modeled after the system in the former Soviet Union. The state forest in Heilongjiang was allocated an annual

planned timber production volume by the central government, and thus forest management leaned further towards unsustainable methods to achieve the imposed production target.

Since Heilongjiang Province contained the most abundant natural resources, such as coal, timber, and reclaimable barren lands, in addition to having suitable infrastructure for resource development and industrialization, the province was assigned to be a major natural resource-driven industry area. As for the state forests in the province, the "northeast state forest regional development master plan" was established, and more intensive forestry development was started based on the plan.

Because of this situation, a very high target of timber production was set for the province, and unsustainable forestry activities accelerated rapidly as a result. Some areas began to employ intensive selective-cutting in timber production, and the rate of clear-cutting by logging operations also increased significantly. Consequently, the speed of forest loss in the province accelerated further (Figure 3).

This forest management style based on over-harvesting continued until 1962, when the Great Leap Forward[2] ended. After that, the government tried to modify forest management policy to be more sustainable. Unfortunately, this attempt did not last long. The Great Proletarian Cultural Revolution started in 1966, which eliminated the state's forest management system, and unsustainable practices recommenced.

The annual mean timber production volume in Heilongjiang's state forest during this period was more than 20 million m^3, and more than 50 percent of the area logged was being clear-cut and not replanted. As a result, forest loss in the province worsened.

3.3. From the latter half of the 1970s to 1998

The Great Cultural Revolution in China ended in 1976, and then the country rapidly evolved into a commodity-based economy under planned socialism. In the background of such policy change, the state decided to switch its forest management policy from being destructive to being more sustainable under the forest law of the country, which was established in 1979 and finally entered into force in 1984. Unfortunately, over-exploitation continued due to the unabated pressure on the forests in Heilongjiang to achieve high production goals, and forest loss in the area continued. Annual mean resource depletion reached 38 million m^3, which was twice the annual growing stock in the area.

After 1992, when China's transition to a market economy accelerated, a decrease in timber production due to forest resource depletion in the area became a serious issue, and consequently deficits in income from state forests became more acute. The cumulative deficit of state forests reached 1 billion yuan, and half of all state forests stayed in the red for more than two consecutive years until 1995.

The cumulative impacts of forestry development on the land led to devastating floods downstream of logged areas after the 1980s. Large-scale floods continue to occur frequently

[2]An economic and social plan used from 1958 to early 1962 which aimed to use China's vast population to rapidly transform mainland China from a primarily agrarian economy dominated by peasant farmers into a modern, industrialized communist society (Source: Wikipedia, http://en.wikipedia.org/).

and the damage they cause has become more extensive. A catastrophic flood in 1998 in the watersheds of the Songhua, Yellow, and Yantze rivers, which killed 3,000 and affected 240 million people, is still fresh in the people's memory. Finally, the Natural Forest Protection Project was launched in 1998, leading to significant cuts in timber production from state forests. Structural over-exploitation of natural forests in the area,, which had continued throughout the twentieth century, finally ended.

4. FOREST FIRES AND THEIR CAUSES IN CHINA AND HEILONGJIANG IN THE LATTER HALF OF THE TWENTIETH CENTURY

4.1. Dynamics

China is one of the countries in the world with a large number of forest fires occurring annually. According to forest distribution figures, the characteristics of climate in China and forest fire statistics collected for nearly 50 years, it can be concluded that most forest fires occur in the northeast (the provinces of Heilongjiang, Jilin, and Inner Mongolia), where the main tree species are larch and Korean pine, and in the southwest (Yunnan, Sichuan and east Xizang provinces), where the main species are Yunnan pine (*Pinus yunnanensis*) and Simao pine (*Pinus kesiya var. langbianensis*).

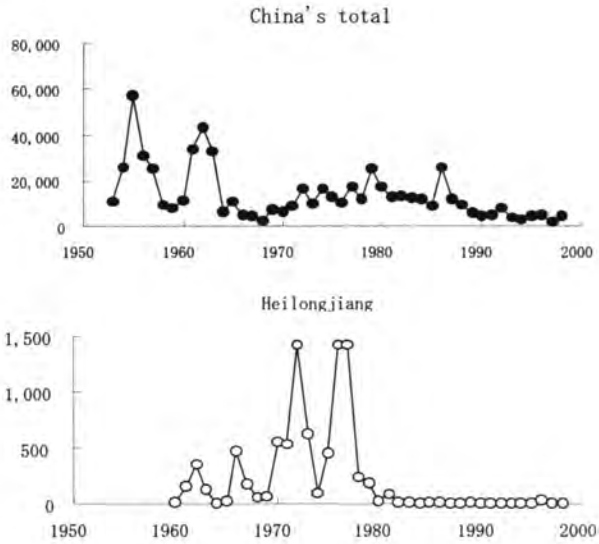

Figure 4. Change in the number of forest fires in all parts of the country and Heilongjiang from 1950 to 1998. Sources: National Forestry Statistical Materials, Ministry of Forestry for 1985–1997 data; China Forestry Statistical Yearbook 1998, State Forestry Administration for 1998 data.

In the 40 years between 1950 and 1990, around 620,000 fires were recorded (Figure 4), burning 36 million ha of forest (Figure 5). Most fires were observed in state forests in the three northeastern provinces, and frequent fires have accelerated the degradation of forest resources, mainly in natural forests.

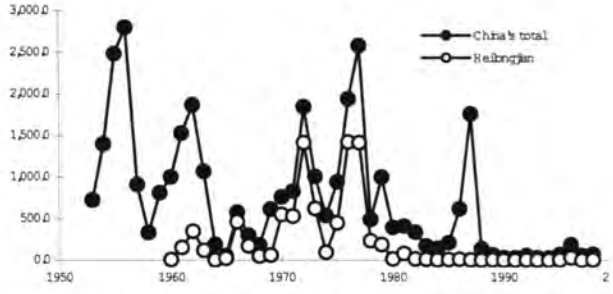

Figure 5. Change in the affected forest area in 1,000 ha of forest fires in all parts of the country and in Heilongjiang from 1950 to 1998. Source: Same as figure 4.

Forest fires occurred most frequently until the middle of the 1960s. More than 20,000 fires per year were recorded in seven of the years between 1950 and 1965.

The number of forest fires then decreased slightly until 1968, but during the 1970s it

increased again, with more than 10,000 fires recorded per year. In the 1990s the number of fires dropped significantly to 5,000, due to the strengthening of fire control and diminished forestry activities.

Changes in the frequency of forest fires in Heilongjiang vary slightly compared to the rest of China. Forest fires in the province occurred most frequently in the 1970s, with the number being from 500 to 1,500 per year, but the number dropped dramatically thereafter.

The sizes of affected forest areas follow similar trends to the number of forest fires. Until the middle of the 1960s, during years with many recorded forest fires, more than 1 million ha were affected annually in Heilongjiang, indicating that forest fires, along with forestry development, were a major proximate cause of forest loss here.

From 1970 to 1990, four years suffered extremely large fires, which affected a forest area of more than 1 million ha, and thus forest fires remained a major proximate cause of forest loss in the country. The forest areas affected in the whole country from the middle of the 1960s to 1978 showed closely similar dynamics as in Heilongjiang ($r = 0.95$), and the share of Heilongjiang exceeded 50 percent for most years during this period. Thus the facts indicate that forest fires in China during the period were predominantly in Heilongjiang.

After catastrophic forest fires occurred in the northeast region in 1987, the central government strengthened the fire control system. The frequency of fires and area damaged by forest fires decreased dramatically in the 1990s. The cumulative damage of fire on forest resources over the years, however, is serious and cannot be ignored.

4.2. Causes

Although the causes of forest fires vary, there are only two main categories of cause: human or natural (Table 3). Relatively few forest fires have natural origins, mainly lightning. Forest fires caused by lightning are relatively more common in unexploited forested areas in the northeast. Depending or origins, forest fires caused by humans are classified as "production" fires, "non-production" fires, and fires due to negligence.

Table 3. Causes of forest fires in China from 1989 to 1990 and from 1996 to 1998

Causes	1989-90	1996-98
Production origin (%)	49.3	38.2
Non-production origin (%) (mainly negligence origin)	48.3	53.6
Lightning	0.5	0.8
Others (%)	1.9	1.1
Total number of forest fires (%)	11,901	11868

Source: Research on China's Natural Disaster Deduction Countermeasures - Volume 2, China Science and Technology Publishing House, 1998

Burning for cultivation and fires caused by machinery fall under the production fire origin classification. Burning for cultivation is the main cause of forest fires in the southwest, where many local ethnic groups use traditional slash-and-burn cultivation in agriculture. This tradition is changing as cultivation methods change, but it is still used to some extent, and can cause forest fires very easily. Train locomotives running along railways are the main cause of forest fires in the northeast, and farm tractors moving along roads may cause sparks or flames,

sometimes leading to large forest fires.

In the northeast, most forest fires are of non-production origin, livelihood origin, or accidental origin. Smoking in the forest, using fire for heating or cooking, burning paper for devotional purposes in tombs, etc., are customary uses of fire in day-to-day life as people follow their cultural traditions. It is likely that most forest fires in Heilongjiang are closely related to human activities, since both the number and area of forest fires increased in sync with the over-exploitation of forest resources.

5. RECENT EFFORTS IN FOREST CONSERVATION

5.1. Afforestation

Since the founding of the People's Republic of China in 1949, vast areas of forests on steep slopes have been converted to cultivated land or pasture. Cultivated land with a slope of more than 25 degrees was estimated at over 6 million ha in the 1990s. Conversion of steep forestlands has caused a decrease of wood production for home consumption (such as for fuel or construction) and serious topsoil erosion.

On the other hand, the central government promoted various afforestation projects since the end of the 1970s and developed a large area of man-made forests (Figure 3). As a result, a substantial increase of forest area and total growing stock can be seen in forest resource statistics. These resources have not yet matured, however, because of the brief history of afforestation.

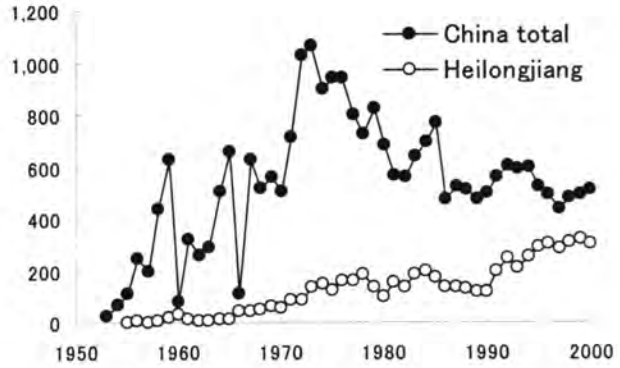

Figure 6. Change of afforestation area in China and Heilongjiang from 1949 to 2000. Sources: National Forestry Statistical Materials, Ministry of Forestry, 1985–1997; China Forestry Statistical Yearbook 1998–2000

Although forests in Heilongjiang have been degraded since the end of the nineteenth century due to intensive forestry development and frequent forest fires, afforestation was encouraged only after the 1990s. The area of afforestation was very small until 1970. Even in the 1980s, when several national afforestation projects were launched, the average area of afforestation was only around 100,000 ha per year, still a low level compared to the total forested area of the province. Eventually, in the 1990s, afforestation was intensified. Consequently, the province had many young man-made forests and few mature ones at the end of the twentieth century.

5.2. Natural Forest Protection Project

The most recent key national forest policy for forest conservation is the Natural Forest Protection Project (NFPP). It was announced in 1997 and launched in 1998 in order to

accelerate the improvement of the ecological environment in degraded natural forests and, at the same time, to realize biodiversity conservation and sustainable development for social and economic welfare. According to the master plan, this project focuses on natural forests in 17 provinces or autonomous regions, including the state forests in Heilongjiang Province.

The Chinese government has implemented the NFPP with great enthusiasm by means of such measures as concentrated investments, full-scale implementation jointly mandated by central and local governments, and rapid structural reforms of the forest sector, with mainly governmental and central control of implementation. The project was divided into a first phase (1998–2000) and a second phase (2001–2010).

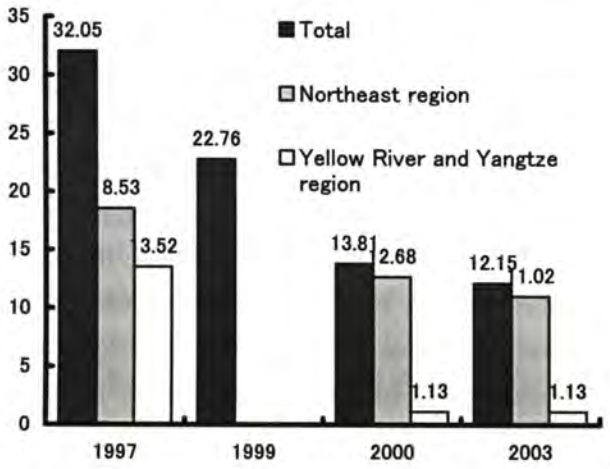

Figure 7. Change of timber production due to the NFPP (million m^3)

Remarkable progress has been made since 1998 in natural forest protection through intensive implementation of the NFPP group of newly launched forest policies. Between 1998 and 2000 the central government invested 2.68 billion yuan (US$322 million) in the project (Chinawood 2001, February). In 2000, in addition to 1.3 billion yuan ($156 million) spent on natural forest protection, the government allocated a subsidy of 420 million yuan ($50.4 million) for the conversion of farmland into forest and pasture, and a subsidy of 92 million yuan ($11 million) for dealing with desertification.

So far, 4.64 million ha in the forest zones and 790,000 ha in other areas have been afforested. Additionally, 516,000 ha of natural forest areas were allocated for regeneration with supplementary silvicultural work (Yamane 2002).

State forest restructuring has also been promoted at a rapid pace. A reshuffling of personnel affected 190,000 workers. Moreover, the numbers of retired employees and layoffs in 1998 reached 110,000 and 90,000, respectively. In fiscal 1999, 280,000 positions were reshuffled, in addition to 320,000 retirements and 150,000 layoffs. In this way the project has steadily progressed by a top-down approach. On the other hand, the drastic changes in natural forest management and reforms of state forest policies have caused various negative economic and social impacts at the local level.

Domestic timber production has continued shrinking due in part to the implementation of the NFPP (Figure 7). In 1999, the nation's planned timber production was registered at 53.27 million m^3, a drop of 8.9 percent from the year before. The year 2000 saw domestic planned timber production shrink to 46.73 million m^3, a reduction of 6.54 million m^3 from 1999. The drop in log production in protected zones was dramatic, falling 62.1 percent from 32.05 million m^3 in 1997 to 12.15 million m^3 in 2003. In northeast state forests, it dropped to 11.02 million m^3 in 2003 from 18.53 million m^3 in 1997. The largest reduction was in state forests in Heilongjiang.

The strict implementation of the NFPP has brought various impacts not only on regional communities and industry but also on the national economy, including the timber trade and industry.

The most notable impact was a rapid increase of log imports from Russia (e.g., Yamane 2001; Yamane and Lu 2001; Zhu 2002). With the very strong demand for timber from natural forests in the country, the timber shortage caused by implementation of the NFPP has been compensated for by importing timber, especially from Russia. Russian logs have dominated China's timber trade for a number of reasons (Yamane 2001). First, Russian logs were higher in quality and larger in diameter compared with Chinese timber, and in terms of potential uses they compare well to alternatives coming from China's northeast region, such as Mongolian pine, Korean pine, and larch. Second, Russian timber was cheap or moderate in price due to low labor costs in Russia and because of low transportation costs brought about by the volume of border trade. Third, imported Russian timber can readily replace the dwindling supplies from China's natural forests in the northeastern and northwestern regions, where harvesting has decreased or even stopped altogether as a result of logging bans imposed under the NFPP.

As shown in Figure 5, log imports from Russia jumped from 1997 to 1998 and since then have increased continuously. In 2001 China passed Japan to become the top timber importer from Russia. The total log import volume reached around 20 million m^3 in 2005. The number is almost equal to the domestic production cut caused by the NFPP, and it means that imported Russian logs have become a substitute of timber from natural forests in China.

Russian logs exported to China are harvested in eastern Siberia and the Russian Far East. The Russian side of the Amur Basin inevitably became a major source of timber, because untouched forests still existed even at the end of the twentieth century. This means that the NFPP, which is aimed at conservation of degraded forests in China, will likely cause the rapid loss of Russian forests.

6. CONCLUSION

As this paper has outlined, rapid forest loss occurred on China's side of the Amur Basin during the twentieth century due to the intensive impacts of human activities, such as human-caused forest fires and forestry development for timber production. Forest conservation efforts, with a focus on afforestation, were implemented in the second half of the twentieth century. Unfortunately, forest loss did not stop because forests in the area were considered to be an unlimited source of timber for the country. Eventually, the forest resources were depleted, leading to a serious drop in production and to a rise in environmental devastation such as large-scale floods, which reached unprecedented levels. Thus, a radical forest conservation policy, named the Natural Forest Protection Project, which includes logging bans or restrictions, was launched in 1998. Forests on China's side of the Amur Basin have subsequently benefited from the conservation efforts in China. Unfortunately, due to the growing demand for timber in China, a sudden drop of domestic timber supply brought a steep increase in timber imports from Russia, and this has accelerated forest loss on Russia's

side of the Amur Basin. Moving forward, timely action is needed to rectify this unsustainable situation. A shift toward policies that promote basin-wide forest planning and conservation through China–Russia bilateral cooperation are major challenges in the twenty-first century.

REFERENCES

Dai, Y. (2000). *National forest management and community in China, its development and process*, pp281. Nihon Ringyo Chousakai, Tokyo. (In Japanese. The title is a tentative translation by the author.)

Ikebe, Y. (1933). *Man Mo Ringyo no Kinkyo (Recent history of forestry in Manchu country)*. 149pp, Dai Nippon Sanrin Kai, Tokyo. (In Japanese. The title is a tentative translation by the author.)

Kakizawa, H. (2004). Dynamics of forest resources in Russia and related changes in forest management and policies—Focusing on the Khabaro v sk Region. Report on Amur-Okhotsk Project No.3.

Kakizawa, H., and Yamane, M., eds. (2003). Russian forest and forestry, J-Fic, 238pp.

Kakizawa, H., Sakashita, A., and Park, H. (2005). Underlying causes of land use change and degradation of natural resources in the Amur Basin. Report on Amur-Okhotsk Project No.3.

Ogino, T. (1965). *Chosen, Mashu, Taiwan Ringyou Hattatsu Shiron (History of forestry development in Korea and Taipei.* 587pp. Rinya Kosai Kai, Tokyo. (In Japanese. The title is a tentative translation by the author.)

Sheingauz, A., and Kakizawa, H. (2003). The development of forest policy in the Russian Federation—With a focus on Khabarovsk Krai. In *People and forest—policy and local reality in Southwest Asia, the Russian Far East, and Japan*, Inoue, M., and Isozaki, H., eds., Kluwer Academic Publishers, 187–200.

State Forestry Administration (SFA), PR China. *China national forest resource statistics 1973-2000*. China Forestry Publishing House, Beijing, P. R. China.

Tao, Y. (1987). History of forestry development in the Northeast Region. Jilin Academy of Social Sciences. (In Chinese. The title is a tentative translation by the author.)

Yamane, M. (2001). China's recent forest-related policies. Overview and background from the perspective of economic growth and forest conservation. Policy Trend Report 2001, 1-12. IGES Forest Conservation Project.

Yamane, M. (2002). China's recent forest-related policies: Overview and background from the perspective of economic growth and forest conservation. Policy Trend Report 2002, 1-14, IGES Forest Conservation Project.

Yamane, M., and Lu, W. (2001). Analytical overview of recent Russia-China timber trade. *International Review for Environmental Strategies* 2(2), 335-347.

Zhu, G. (2002). China wood market, the status of Russia timber in China importing market and suggestions. 16-37, in the proceeding titled "Sino-Russian Wood Trade & Investment Conference," November 17-18, 2002, Beijing, China.

Appendix 1. Log production in China and its northeast provinces from 1985 to 1998 (m^3)

Year	China total	Heilongjiang Province	Share (%)	Inner-Mongolia	Share (%)	Jilin Province	Share (%)	Total share of the three provinces
1985	53,135,500	14,938,500	28.1	4,096,900	7.7	5,367,300	10.1	45.9
1986	54,186,900	16,025,700	29.6	4,845,200	8.9	5,682,400	10.5	49.0
1987	53,861,200	15,971,900	29.7	5,211,800	9.7	5,735,800	10.6	50.0
1988	51,937,200	16,555,700	31.9	5,318,500	10.2	5,362,200	10.3	52.4
1989	50,370,600	16,679,900	33.1	4,939,000	9.8	5,614,800	11.1	54.1
1990	51,085,300	13,603,800	26.6	4,933,500	9.7	5,436,000	10.6	46.9
1991	52,892,800	12,263,800	23.2	4,562,300	8.6	5,091,300	9.6	41.4
1992	56,268,900	11,756,800	20.9	4,706,400	8.4	4,721,300	8.4	37.6
1993	58,603,900	11,476,900	19.6	4,808,500	8.2	4,923,300	8.4	36.2
1994	60,133,900	11,635,300	19.3	4,722,600	7.9	5,222,500	8.7	35.9
1995	62,469,900	11,632,600	18.6	5,104,000	8.2	5,504,400	8.8	35.6
1996	60,730,900	11,926,600	19.6	5,101,400	8.4	5,411,200	8.9	36.9
1997	59,354,400	11,247,400	18.9	4,987,600	8.4	5,296,600	8.9	36.3
1998	55,557,400	10,520,600	18.9	4,720,800	8.5	4,912,700	8.8	36.3

Sources: National Forestry Statistical Materials, Ministry of Forestry, 1985-1997
Note; log imports (million m^3, bar) and share (%, line) of total imports

DEVELOPMENT OF WATER FACILITIES, FARM LAND AND LAND USE CHANGE IN SANJIANG PLAIN

SAKASHITA A. AND PARK H.
Department of Agricultural Economics, Graduate School of Agriculture, Hokkaido University

1. RESEARCH ACTIVITIES OF 2006

1) Schedule of field research

August 30 – September 6

Jilin University and North Eastern Asian research center: We gathered of socio-economic information of north western area, especially about agriculture developmental history of San Jiang Plain. We also discussed with Professor Yi Bao Zhong regarding relationship between the location of Manchuria exploitation team and current state farms.

September 7 – October 11

The General Bureau Bao Quan Ling Division of State Farm of Heilongjiang province, Xin-Hua Farm , Production Group 17: Preliminary preparation for the questionnaires research of 64 farms and information- recording research of 12 farms (time period: March 1, 2007 – February 28, 2008)

2) Details of research activities

(1) Targeted farm

The initial plan of the research area was Farm 291 of Hong Xing Long Division. However, due to internal problem of that farm, the research area was changed to be Bao Quan Ling Division Xin-Hua Farm. We focused our research to Xin-Hua Farm, Production Group 17. Farm area of this group is 552.6ha (100% rice paddy). In terms of the number of farms to be researched, questionnaire research has changed from 100 to 64 farms; and information-recording research has decreased from 30 to 12 farms.

(2) Brief overview of research area

Historically, the development of rice paddy up to 1968 was continuation of rice paddy introduced by 'Japan Man Meng Exploitation Team'. Then, the area was converted to dry field until 1992 due to the lack of knowledge in cultivating rice paddy under Great Proletarian Cultural Revolution. Since1994, the area become rapidly back to rice paddy.

Xin-Hua Farm, Production Group 17 consisted from 64 farms, and an average area of one household was 8.6 ha in 2006. Total income per farm from the rice paddy was142, 489 Yuan (about 2,020,000 Yen), and income per farm from growing rice paddy was 66,114Yuan (about 940,000 Yen).

(3) Outline of questionnaire survey

Purpose of questionnaire survey is to understand the situation and problems of individual operation of rice paddy farm. All of 64 farm household of Xin-Hua Farm, Production Group 17 (farms) was surveyed (Table 1)

Followings are content of questionnaire survey.

1. Family structure
2. Issues concerning contract farming at state farm; career before operating the farm, distribution of land and machinery from state farm after contract, changes of area of farming after contract, location map of current farm land, pump drainage channel (handwritten)
3. Current state of farm operation; production and sales of major agricultural produce, machineries and facilities, revenue and expenditure, future plan.

Table1 Number of farmers in Production Group 17

No. of farmers	Area of land	Age	Family size	No. of farmers	Area of land	Age	Family size	No. of farmers	Area of land	Age	Family size
1	10.45	40	4	23	6	28	3	45	18.3	32	5
2	9.1	45	4	24	11.6	50	4	46	7	52	4
3	4.95	30	5	25	5.4	30	4	47	7.95	32	4
4	10	42	3	26	3.8	45	3	48	7.9	56	5
5	5.5	45	3	27	3	35	3	49	13.65	46	5
6	5	44	3	28	5.5	51	2	50	10.8	37	5
7	7	52	5	29	4.1	33	3	51	3	41	4
8	3.85	46	3	30	10.1	42	5	52	4.7	37	3
9	7.15	46	5	31	8.25	48	5	53	4.7	42	3
10	9.1	47	3	32	9	38	3	54	4.7	37	3
11	9.05	37	3	33	9	26	3	55	12.1	41	3
12	8.5	48	4	34	8.95	38	2	56	5.6	41	3
13	11.7	37	6	35	13.85	24	4	57	5.8	42	3
14	6.4	51	3	36	9.2	31	3	58-1	10	33	3
15	6.95	35	3	37	8.5	47	4	58-2	7.4	29	3
16	5	40	3	38	15	33	3	59	8	29	3
17	9.9	26	3	39	14.3	41	4	60	9.7	39	3
18	13	53	6	40	16.55	35	3	61	10.9	43	4
19	4	35	3	41	17.4	41	3	62	8	41	3
20	7	45	3	42	9	26	5	63	9.5	50	3
21	12	40	3	43	6.4	57	5	64	6.55	51	5
22	5.25	56	3	44	10.6	50	4	subtotal	176.25	52	3
subtotal	170.85			subtotal	205.5			total	552.6		

Source: Submitted by Production Group 17.

NB: 58-1/2are brothers, and so were counted as a single farm, though have sine begun working independently.

(4) Outline of record keeping research

Purpose of research; check the stability of rice paddy management and water usage.

Content of research; Ask 12 farmers to keep record their farming operations. Farmers were selected to cover various scale of management.

Research period; from March 1, 2007 to February 28, 2008

2. TENTATIVE RESULT OF QUESTIONNAIRE SURVEY

The questionnaires were still under analysis, but Tables 2 – 5 gave typical three example of household. Followings are brief overview of these farms.

(1) Production of rice paddy, changes of technologies (Table 2)

In terms of work force, there is not so much difference among sample families. No.1 and No.2 are managed by two relatively young people, 32 and 31 years old, and 26 and 24 years old respectively, and No.3 is managed by a couple (44 and 41 years old) and their eldest son (19 years old). In terms of employment, No.1 has two employees for year-round and one seasonal employee; No. 2 has one employee, while No. 3 has no employee. This result showed that large scale farmers fulfill deficit of labor force by employees.

For raising seedlings, all the farmers owned greenhouse and managed individually. The seeds are provided by Seed Company every year. Seedlings are grown on mat, so it requires large amount of work force for seeding. Large and medium farmers employed worker for these operations.

No.1 and No. 2 carried out plowing and rotary operation by their own plowing machinery and tractor. As No. 3 does not own these machineries, ask contractor to do these operation. Water pumping for irrigation was done from April 10.

Rice planting is carried out by planting machinery, which was introduced in 1990s (No.1 has two and No.2 has one). Generally, the planting team is consists of one operator, four auxiliary worker, and two supplemental planters with a total of 7 people.

In terms of pest control, aerial spraying was tested in 1988 and has been applied since 1996 (rice blast fluid pesticide and fluid fertilizer).Usually, two times of aerial spraying in a year, at the end of July and middle of August. However, 2006, cost for spraying dramatically increased (80 Yuan/ha to 130 Yuan/ha), and most of the farmers refused to do it. So pest control in 2006 was applied by individual farm carrying the mist by each farm using portable spray.

Until 2-3 years ago, paddy was harvested and tied by hand. Currently, combine is commonly used for harvest operation. No.1 and No. 2 owned combine with width of 2.5 m, but No.3 borrowed combine from his relatives.

Production Group 17 irrigating paddy field using wells. All the farms own their own well. Until 4-5 years ago, average size of well was 20cm diameter with depth of 20m. However, recently, large and medium size farmers have begun to use wells with depth of 30m, to make do and mend wells. No.1 has three 20m wells; No.2 has two 30m wells; and No.3 has one 20m well.

As mentioned earlier, large and medium scale farmers have started using combine, tractor, and rice planting machinery, but small scale farm less than 5 ha has not own such machinery. It is also pointed out farming operation of large and medium scale farmers was made possible by employed workers. However, recently, work force has begun to moves urban area and it made difficult for large and medium scale farmers to have sufficient labor force.

Table 2. Summary of farm management (XinHua Farm, Production Group 17, three subjects)

No. of Farmers		No.1(No.17-45)	No.2(No.17-42)	No.3(No.17-6)
Name (Age)		Wang zhao guo(32)	Li zhi wei(26)	zhao yan(44)
Paddy area		18.3ha	9ha	5ha
Family size		m32,f31,m9	m26,f24,f2	m44,f41,m19
Farm working family members		m32,f31	m26,f24	m44,f41,m19
power tiller	HP	12hp(used)	12hp(used)	
	Date of introduction	1989	1994	
	price	2,600Yuan	6,500Yuan	
tractor	HP	25hp(used)、40hp	30hp	
	Date of introduction	1998, 2004	2004	
	price	13,000Yuan、53,000Yuan	31,400Yuan	
raising seedling facility	size	180 ㎡×2、120 ㎡×13	135 ㎡×7	204 ㎡×2、144 ㎡×2
rice transplanter	HP	6Lines(used)、8Lines	6Lines	
	Date of introduction	1992, 2000	1996	
	price	3,000Yuan,11,500Yuan	9,800Yuan	
harvester	size	combine harvester(2.5m)	combine harvester (2.5m)	
	Date of introduction	2005	2006	
	price	54,000Yuan	63,000Yuan	
wells		20cm×20m×3、20cm×30m×1	20cm×30m×2	20cm×20m×1
employ		full time 2(12,000Yuan)、part time2	full time 1 (6,000Yuan)	

Source:Primary interview (Sep.2006).

(2) Economic situation of farmers (Table 3)

Production Group 17 of Xin-Hua Farm introduced Kong Yu163 (breed in Hokkaido breed variety) in 2004, but harvest in 2005 was quite poor. So, the most of farmers stopped using Kong Yu163and began to use breed variety called 'Ken Jian' which was breed in agricultural experimental station of General Bureau of State Farm. No. 1 grew 10 ha of Ken Jian No.6 and 8.3 ha of Ken Jian No.10、 and. No.2 grew Ken Jian No.6. No 3 continued to grow Kong Yu163 as harvest of previous year was not so bad.

In this section, we will examine the economic situation of the farmers. As mentioned before, harvest in 2005 was poor, so we will examine the situation in 2004.

Table3 Summary of statement of income and expenditure (XinHua Farm, Production Group 17, three subject, 2004)

No.of farmers	No.1(No.17-45)	No.2(No.17-42)	No.3(No.17-6)
Name(Age)	Wang zhao guo(32)	Li zhi wei(26)	zhao yan(44)
Paddy area	18.3ha	9ha	5ha
type of rice seed in the year 2004	KongYu163 13.3ha	KongYu163 9ha	KongYu163 5ha
type of rice seed in the year 2005	KongYu163 18.3ha	KongYu163 9ha	KongYu163 5ha
type of rice seed in the year 2006	KenJian6 10ha, KenJian10 8.3ha	KenJian6 9ha	KongYu163 5ha
unit crop	8.5t	8.0t	7.5t
rice quota per hectare	4.5t	4.5t	4.5t
gross yield of rice	113t	72t	37.5t
rice quota(Liangyou Co.)	59.9t、1.50yuan/kg	40.5t	22.5t
XinMian Co.	53.1t、1.75yuan/kg	31.5t	15t
gross income(yuan)	192,100	115,200	56,210
cost(yuan)	89,995	62,200	33,380
management cost	74,795	52,100	23,040
production material	20,570	17,850	6,790
labor cost	9,800	4,500	0
land rent (2,250yuan per hectare)	29,925	20,250	11,250
etc.	14,500	9,500	5,000
family expenses(yuan)	15,200	10,100	10,340
surplus(yuan)	102,105	53,000	22,830

Sources: Primary interview, additional information submitted by production group 17(Sep.2006).

No.1 farmed 13.3 ha and harvest was 113t (8.5 t/ha) in 2004. There was rice quota system, which obliged farmers to provide 4.5 t/ha to food company in lower price, and total amount of was 60 t in total. The rest was sold to Xin Mian Company. Total income was 192,100 Yuan, and cost was 74,795 Yuan. The labor cost was 13% of the total cost. Farmers have to pay rent, and it cost 2,250 Yuan /ha, the total was 29,925 Yuan (16 %). Profit was more than 100,000 Yuan, excluding domestic expenses. Using this profit No1 enlarge farm land for 5 ha.

No.2 farmed 9 ha, and harvest was 72 t (8 t /ha). The rice quota was 40.5 t in total and sale to Xin Mian Company was 31.5 t. The total income was 115,200 Yuan, and operating cost was 52,100 Yuan, including rent of 20,250 Yuan (18%). Domestic expenses were 10,100 Yuan and the balance of 53,000 Yuan was profit.

No. 3 farmed 5 ha and harvest was 37.5 t (7.5 t/ha). Rice quota was 22.5 t and the rest of the 15 t was sold to Xin Mian Company. The total income was 56,210 Yuan and cost was 23,040 Yuan, including the land rent of 11,250 Yuan (20%). Domestic expenses were almost same with No2- 10,340 Yuan, and the profit was 23,000 Yuan.

Currently, the price of rice is 1.60 Yuan per kg and even the small scale farmer, managing less than 5 ha, could get profit though tiny amount. However, it could also be pointed out that the ratio of quota and land rent was high, and especially land rent has been increased. These factors would become burden for farmers (Tables 4 and 5).

Table4 Changes in procurement of rice quota (Yuan per kilogram, ton per hectare, ton, Yuan)

year	unit price	quantity of procurement		total procurement price
		unit area	total procurement	
2000	1.16	4.5(2.5)	39,510	45,831.6
2001	1.14	4.5(2.5)	43,382	49,455.5
2002	1.03	4.5(exemption)	35,000	36,050.0
2003	1.03	4.5(3.0)	26,314	27,103.4
2004	1.52	4.5(4.0)	27,930	42,453.6
2005	1.54	4.5(exemption)	28,890	44,490.6
2006		2.5		

Sources: Primary interview(Sep.2006), additional information submitted by production group 17.
NB: The number in the () is from primary interview.

Table5 Changes in land rent (Yuan per hectare)

year	field	paddy
2000	1,570	1,890
2001	1,750	2,250
2002	1,750	2,250
2003	1,570	1,850
2004	1,850	2,250
2005	1,850	2,250
2006	1,850	2,890

Source: Submitted by Production Group 17.

(3) Problem of rice paddy management of Production Group 17

1) Potential deficit of water for irrigation

The lack of water for irrigation is serious potential issue. Farmers began to use 30m depth well sinking that is deeper than 20m depth in 4 or 5 years ago.

2) Out migration of labor force.

Farmers has been depended their farm operation on workers who live around farm village. However they began to move urban areas to seek high salary.

3) Increase of land rent

The charge of land rent cost is increasing remarkably. It was 1,890 Yuan/ha in 2000, but 2,890 Yuan/ha as 1.5 times in 2006.

3. RESEARCH PLAN OF 2007

1) Make further analysis on the questionnaire survey in 2006, and write a paper on operational problem of rice paddy farms in Plain, San Jiang China (tentative title)
2) Intermediate check of book keeping on August 2007. Collect account book, and conduct supplement research on March 2008.

EVALUATION OF LAND-COVER CHANGE IN AMUR BASIN USING NDVI DERIVED FROM NOAA/AVHRR PAL DATASET

HARUYAMA S.[1], MASUDA Y.[1], KONDOH A.[2], MUROOKA M.[3] AND YAMAGATA K.[4]

[1]*The University of Tokyo, Graduate School of Frontier Science,*

[2]*Center for Environmental Remote Sensing, Chiba University,*

[3]*Hokkaido Abashiri Fisheries Experiment Station,* [4]*Jyoetu University of Education*

ABSTRACT

The authors analyzed recent land-cover change in the Amur River basin using a technique proposed by Kondoh (2004) for the analysis of satellite data (NOAA/AVHRR PAL dataset). The aim was to obtain an objective evaluation of how agricultural activity is affecting the natural environment of this area. Four parameters, ΣNDVI, NDVImax, NDVIstd, and TRJ were adopted to reflect surface conditions, and their linear trends from 1982 to 2000 were examined. Signs of land-cover change were apparent in the five areas chosen for further study. In particular, in Heilongjiang Province land-cover change through agricultural activity was detectable by this analysis.

Key word: The Amur River Basin, NDVI,NOAA,Land cover change

1. BACKGROUND OF STUDY

The Amur River is an international river with a total length of 4350 km and a huge drainage area of 2,051,500 km^2. Its upstream region is in Mongolia, which has a steppe climate (Köppen's Bs world climate zone). Its midstream and downstream regions flow through China and the vicinity of the Russian border, which lies in the cool-temperate zone with low winter rainfall (Dw zone).

Recently, environmental changes originating in the land-cover change have been occurring in the Amur River basin. For instance, the wetland habitat of the crane has been shrinking because of land development, increased sedimentation of rivers through the development of arable land, increased chemical loading of rivers through the expansion of agricultural activity, and air pollution due to forest fires.

In particular, the agriculture has been developed by Chinese government and the cultivated area has been increased in these 20 years in Heilongjiang Province[1]), and the area has changed into an important food production region[2]).

In contrast, the Russian territory through which the river passes has been in a state of economic depression since the collapse of the old Soviet federation. Therefore, the regional differences in land-cover change in the Amur River basin are great. An objective evaluation

of the factors influencing anthropogenic land-cover change in the basin is needed [3]). The only research data that we have on land-use and land-cover change in the area is the results of statistical material analyses of individual regions[4]). There has been no research on the entire Amur River basin; nor has there been any research on secular variations in land cover.

We therefore performed satellite remote-sensing research on the secular variations in land cover over the entire Amur River basin. By using the NDVI (Normalized Difference Vegetation Index), we aimed to pinpoint regions that are experiencing marked land-cover changes and to explain the trends in these changes.

2. OUTLINE OF STUDY AREA

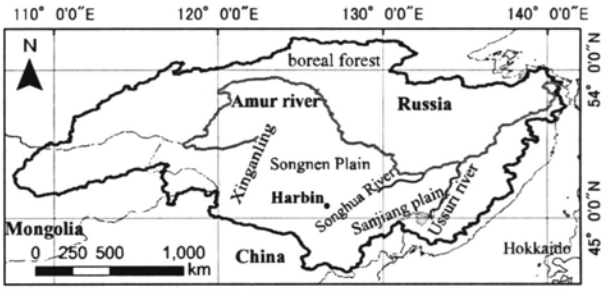

Figure 1. Amur River basin

The Amur River basin is located at lat 41.42°–55.56°N and long 107.32°–141.70°E. The direction of the flow of the Amur River changes as the river courses from midstream to downstream to the east. The river is joined by the Ussuri River which flows from south to north around Khabarovsk, and by the Songhua River which flows from southwest to northeast around Sanjiang Plain (Figure 1). Structural geographical changes are seen in the Amur River basin as the river flows from west to east. The mountainous district more than 1000 m above sea level (asl) extends to the west, and plains where the altitude is below 100 m spread out around Sanjiang plain (Figure 2).

Peat wetlands are distributed in the floodplains and on the plains of the valley bottoms in the hilly country south of the Amur River. Agricultural activity is active in the eastern Amur River basin. However, the climate is very cold: in the city of Harbin the annual mean temperature is 4.6 °C, and the temperature in January is –20 °C [5]). The monthly mean temperature in July is 25 °C, and rainfall is concentrated in summer. Only one crop is planted each year in the Amur River basin[6]).

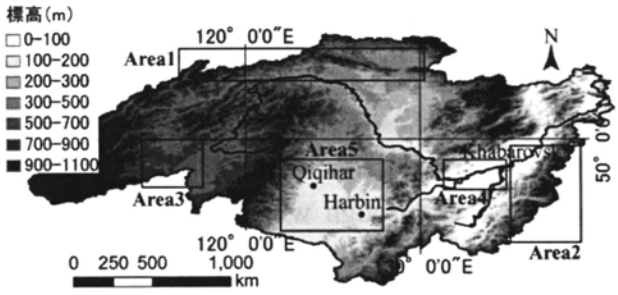

Figure 2. Elevation map of Amur river basin

3. DATA USED

3.1. NOAA/AVHRR PAL Dataset (PAL data)

Pathfinder AVHRR(Advanced Very High Resolution Radiometer) Land (PAL) data offered by the DAAC (Data Active Archive Center) of NASA/GSFC (National Aeronautics and Space Administration / Goddard Space Flight Center) was used to analyze land-cover changes in the Amur basin. The PAL dataset was collected by the AVHRR sensor installed on the NOAA (National Oceanic and Atmospheric Administration) weather satellite; Ch (channel). 1 (visible light), Ch. 2 (near-infrared rays), Ch. 4, Ch. 5 (heat infrared rays), and NDVI data are included. PAL data from July 1981 are available and can be analyzed from 1982 to 2000 to use the whole year data. Moreover, because PAL data are collected globally, the entire Amur River basin could be analyzed: this is why this dataset was the most suitable for the study.

The PAL data are composites collected every 10 days, and include data divided the year into 36 seasons. The spatial resolution is converted from 8km into 0.1° (about 10 km) of both latitude and longitude with the tool that the homepage offered (http://daac.gsfc.nasa.gov).

The NDVI relates to the density and active growth of green plants, and it can be calculated from differences in the spectral reflection of chlorophyll in the visible light and near-infrared ranges[7]). NDVI is widely used for the observation and evaluation of vegetation, and it is assumed to be related to vegetation parameters such as land cover[8]), leaf area index (LAI) [9]), and biomass[10]). In PAL data, NDVI is calculated by the following formula.

$$NDVI = (Ch.\ 2 - Ch.\ 1) / (Ch.\ 2 + Ch.\ 1)$$

3.2. Statistical materials used in the agricultural and field investigation

The amount of land in Heilongjiang Province transformed for irrigation between 1980 and 2000 was determined from the Heilongjiang Province statistical yearbook (2001). Moreover, the area sown to the main commercial crops between 1978 and 2000 and the patterns of transition of production were determined from the statistical material[11]). In September 2005 we performed a field investigation in which we used GPS and digital cameras to observe and record the land cover in the Sanjiang plain, the Songnen Plain and around Khabarovsk Krai.

4. METHOD OF STUDY: ANALYSIS OF SECULAR VARIATION FROM 1982 TO 2000

We used the technique proposed in 2004 by Kondoh to analyze the global-scale vegetation and land-cover changes from 1982 to 2000 from the PAL data [12]) and to thus clarify the land-cover changes over the entire Amur River basin. Coordinates were given to the image by geometric collection. The following four parameters were used for the analysis: sum of NDVI (ΣNDVI) during the year; maximum NDVI ($NDVI_{max}$), standard deviation ($NDVI_{std}$) of ΣNDVI; and the trajectory on the Ts (surface temperature)–NDVI scatter chart (TRJ) [13]). The flow chart in Figure 3 was used for PAL data analysis.

$NDVI_{max}$ is used as an index related to the production of commercial crops, because it shows the growth situation of plants in every year. ΣNDVI is an index that corresponds to the biomass each year. $NDVI_{std}$ is used as an index that shows the disturbance of vegetation, because it shows the level of biomass increase and decrease every year. For instance, both ΣNDVI and $NDVI_{std}$ change throughout the year in regions where floods and forest fire occur frequently and in regions where a big difference in the growth of vegetation by the timing of snow melting in each year.

The TRJ is an index that shows the direction of the land cover change (For instance, the value of TRJ shows positive when there is a tendency to the land cover change from the forest to the bare ground). TRJ is obtained from the scatter chart of Ts and NDVI. NDVI is shown on the horizontal axis and Ts on the vertical axis. Land-cover change can be calculated by applying a straight line to the tracks for every year, and analyzing the change in inclination of the straight line over 19 years. The inclination of the TRJ grows when the land cover changes from meadow to bare ground and the inclination of the TRJ declines when the land cover changes into forest.

As a threshold between vegetated and non-vegetated, the commonly used value of NDVI = 0.1 was applied[12]). Pixels whose NDVI is lower than 0.1 are judged as non-vegetated regions and excluded from the calculation. Moreover, the validity of the PAL data analysis results was verified by above-mentioned statistical material analysis and the regional field investigation; thus the areas in which the influence of artificial land alteration was greatest were determined.

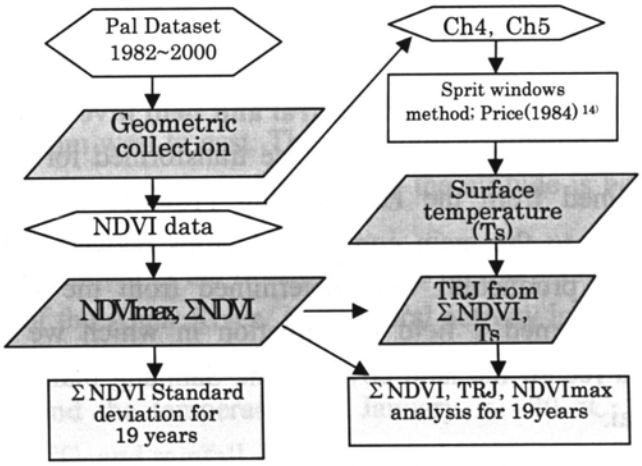

Figure 3 Flow chart of PAL data analysis

5. RESULTS AND CONSIDERATION

5.1. Analysis of secular variation in land cover from 1982 to 2000

The NDVI value falls below the threshold in winter because the Amur River basin is covered with snow. Therefore, the secular variation in each parameter represents the NDVI changes from early spring to autumn. Figures 4 to 7 show the changes in each NDVI index in the Amur River basin over the 19-year period (1982–2000). From among these results we selected and interpreted five regions in which the changes in each parameter were clear.

5.1.1. Area 1

Area 1 is located between lat 52.75°–54.85°N and long 116.75°–130.35°E and is covered by extensive coniferous forest. Figure 5 shows that the value of ΣNDVI increased over this area. The area of ΣNDVI = 0.05 or more extended both east and west and was distributed in a low mountainous district 500 to 800 m asl. $NDVI_{std}$ was also high (1.5 or more) (Figure 6) in the area where ΣNDVI is high. No remarkable change in $NDVI_{max}$ (Figure 4) or TRJ (Figure 7) was seen across the region.

In 1997 Myneni found increased vegetation activity and discussed the relationship of this activity to global warming in northern Eurasia, Alaska, and the Canadian northwest (lat 45°00–70°00N) during the period 1982–1990 [7]). Moreover, the temperature rose by 4 °C in winter in these three regions during 1961–1990 [15]). Therefore, this temperature change appears to have been reflected in an increase in ΣNDVI in that the vegetation growth period was extended: the snow melted in early spring because the temperature rose early in winter. Moreover, the value of $NDVI_{std}$ increased because the difference in ΣNDVI within each year was large; Area 1 can thus be interpreted as a region influenced readily by both yearly changes in meteorological conditions and global climate change.

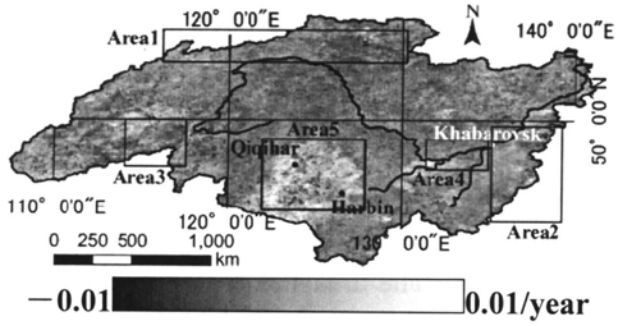

Figure 4. **$NDVI_{max}$** *(secular variation 1982–2000)*

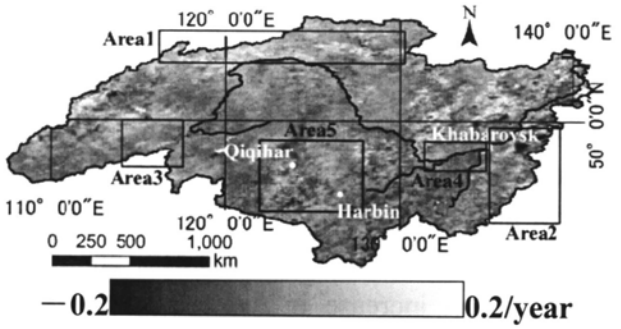

Figure 5. **ΣNDVI** *(secular variation 1982–2000)*

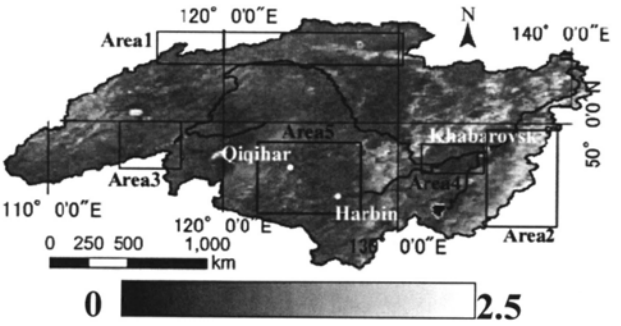

Figure 6. **$NDVI_{std}$** *(secular variation 1982–2000)*

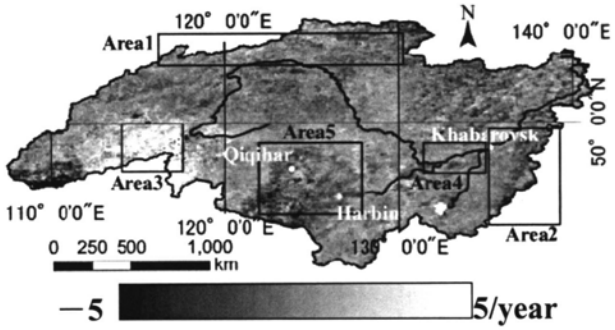

Figure 7. **TRJ** *(secular variation 1982–2000)*

5.1.2. Area 2

Area 2 is located at lat 43.65°–50.15°N and long 134.65°–140.75°E. In this region coniferous forests extend from 500–1300 m asl. An area where $NDVI_{std}$ was greater than 1.5 (Figure 6) and ΣNDVI was 0.05 (Figure 5) was distributed from southwest to northeast along the basin's boundary. No marked change was seen in $NDVI_{max}$ or TRJ (Figures 4, 7). However, an area of ΣNDVI = –0.21 (decreased biomass) extended from Khabarovsk to about 250 km eastward. Large-scale forest fires occurred in Khabarovsk Territory in 1976, 1998–1999, and 2001, and the Far Eastern taiga covering 25,000 km^2 received damage in 1998 [16]). We consider that this decrease in ΣNDVI in Area 2, and thus the decrease in biomass, resulted from the frequent forest fires.

5.1.3. Area 3

Area 3 is located at lat 47.00°–50.00°N, long 114.50°–118.00°. In this region the plateaus and hills extend to 550–900 m asl. The area has a steppe climate, and the main region is covered by meadow vegetation. The whole area had TRJ = 3 (Figure 7), but ΣNDVI, $NDVI_{max}$, and $NDVI_{std}$ (Figures 4, 5, 6) showed no marked changes.

Therefore, the increase in TRJ must be derived from an increase in Ts. Generally, with meadow vegetation such as that in Area 3, there is a period of bare ground between snow melting and foliation. Consideration of ΣNDVI, $NDVI_{max}$, $NDVI_{std}$, and the vegetation of Area 3 leads to the interpretation that the period of bare ground increased over the 19 years, and the Ts rose because snow melt occurred increasingly early; as a result, the TRJ increased.

Moreover, when supplementing for the NDVI index, an increase in the bare ground period is not simply related to an increase in the biomass in the meadow vegetation of Mongolia. Because it receives a complex influence according to the temperature, precipitation and soil water content[17]). Kondoh et al. (2002) divided the vegetation zone in the world into the vegetation zone of the water dependence and the energy dependence[18]), Area 3 is located in the transition belt of both. When the influence of the climate change and the man activity expected in the 21st century is foreseen, the boundary of the ecology zone is thought to be the weakest region. Therefore, it is scheduled that it keeps monitoring in the future and a detailed research is done about an increase of TRJ in this area.

5.1.4. Area 4

Area 4 is located at lat 46.55°–47.85°N, long 129.55°–134.05°E. This region is known as

the Sanjiang Plain, and here the floodplain is distributed to about 50–70 m asl. North and south part of the Songhua River, the $NDVI_{max}$ = 0.008 (Figure 4) and the TRJ was about –3.0 (Figure 7). In particular, the changes in these parameters on the floodplain between the Songhua River and the Amur River are plain. When biomass increases and the conditions for vegetation growth improve, transpiration becomes active and Ts decreases. Moreover, the heat budget at ground level is changed by water transmission via irrigation and Ts decreases [12]). TRJ decreased by these factors. Therefore, the secular variation in each parameter in Area 4 can be interpreted as showing land-cover change through the development of agricultural activity.

From viewpoint of biological diversity, the wetlands in this plain are important natural environment. Further research is requested about what influence the reclamation of the wetland gives natural environment especially, in this area.

5.1.5. Area 5

Area 5 is located at lat 44.75°–48.75°N and long 121.85°–128.05°E and is called the Songnen Plain. An increase in $NDVI_{max}$ (Figure 4) was clear on the floodplain and on the hills, which are at an altitude of about 130–280 m. The $NDVI_{max}$ was 0.005 in the hill zone to the north of the city of Harbin. The hill zone to the west or southwest of the city of Quiqihar had a larger $NDVI_{max}$ (0.006). ΣNDVI and TRJ (Figures 5, 7) also showed obvious changes in the floodplain and hill zones: TRJ was below –1 and ΣNDVI equaled 0.1.

In Area 5, an area that extends for 200 km north of the city of Harbin and has seen a marked expansion in the area under rice cultivation since the 1980s [4], the ΣNDVI was 0.08 and the $NDVI_{max}$ was 0.005 (Figures 4, 5). The trends in each parameter were similar to those in Area 4 and can be interpreted as indicative of land-cover change in response to the development of agricultural activity. ΣNDVI increased in the low mountainous districts (especially those higher than 200 m asl), suggesting that increases in afforestation, as well as in agricultural activity, increased the ΣNDVI[4]).

5.2. Verification of validity of PAL data analysis

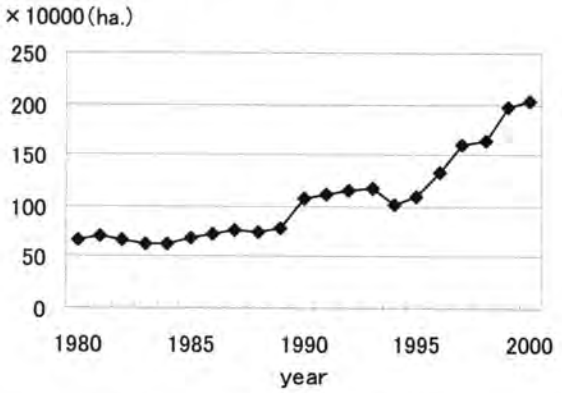

Figure 8. Transition of area under irrigation in Heilongjiang Province

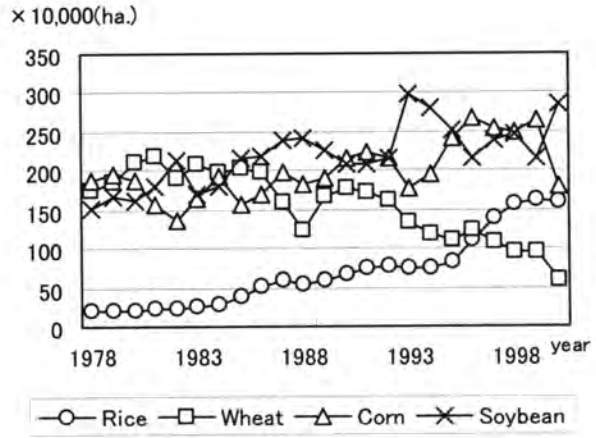

Figure 9. Transition of area sown to commercial crops in Heilongjiang Province

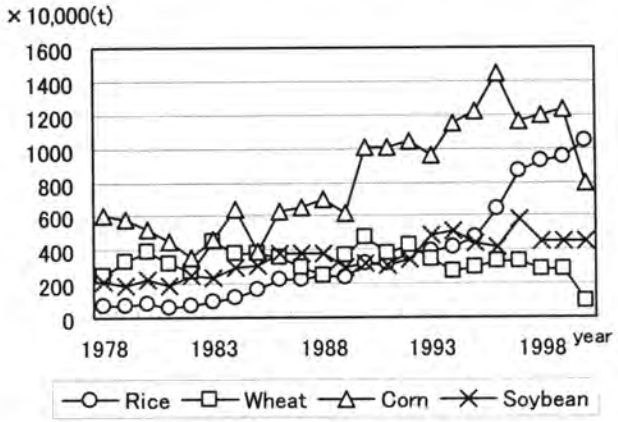

Figure 10. Transition in production of commercial crops in Heilongjiang Province

The validity of PAL data analysis was verified by analyzing agricultural statistics from Heilongjiang Province. Statistics for Areas 4 and 5 were used, because we considered that the influence of artificial land alteration was the greatest in these two areas out of the whole Amur River basin. These regions are important food production regions of Heilongjiang Province.

The area of Heilongjiang Province under irrigation expanded rapidly by 300% or more (from 670,500 to 2,032,000 ha) in the 21 years from 1980 through 2000 (Figure 8). The area sown to commercial crops and the production of rice increased greatly in the 23 years from 1978 through 2000 (750%—214,100 to 1,606,000 ha—in the case of planted area and 1460%—715,000 to 10,422,000 t—in the case of rice harvest (Figures 9, 10).

Moreover, the increase of corn production is remarkable in the first half of the 90's. And in the rice farming, both area and production increase as a rapid increase of the irrigation area since the latter half of the 90's.

In our September 2005 field investigation, we confirmed that floodplains were being used for rice fields, hillside terraces for soybean fields, and hills for cornfields. Only parts of the wetlands remained. Therefore, in Area4 and 5, the irrigation maintenance is done to the upland farming (Wheat, corn and soybean) at the beginning of the 1990's, and the irrigation area has increased. As a result, it is thought that production increased around corn fields. On

the other hand, an increase in the irrigation area in the latter half of the 1990's is thought to be rice field development by the wetland reclamation because of the increase of rice production and sown area in this period.

The land cover change by the development of an agricultural activity was shown by analyzing PAL dataset in these regions. It is thought that this analysis caught the change in an agricultural form like the above-mentioned.

6. SUMMARY

We demonstrated the trends in land-cover change in the Amur Basin from 1982 to 2000 spatially by using four indices calculated from the NDVI. Moreover, we were able to explain the land-cover change in five selected areas by combining and interpreting these indices. Land-cover change in the Amur River basin is especially remarkable in the grain production region of Heilongjiang Province in China.

To validate the results of the PAL data analysis, we performed a statistical material analysis and field investigation for Areas 4 (Sanjiang Plain) and 5 (Songnen Plain). We confirmed that the secular variation in each parameter in these regions was associated with arable land development for irrigation and with land-cover changes from rice farming development.

Thus, the transformation of the region from past to present was clarified by this land-cover change study. This research should be helpful in planning the future development and administration of the basin. By using data on land-cover change and elevation it should also be possible to approximate the changes in volumes of materials transported into the river.

ACKNOWLEDGMENT

This research is part of a project on "Human Activities in Northeastern Asia and Their Impact on the Biological Productivity in North Pacific Ocean", by the Research Institute for Humanity and Nature (RIHN).

REFERENCES

1.Ganzey S.S., 2005. Transboundary Geo-Systems in the South of the Russian Far East and in Northeast China. Vladivostok, Dalnauka.(in English)

2.Motoki Y., 2001, Agricultural land use change of north east China—view of role of rice production. LU/GEC (LandUse for Global Environmental Conservation) Project Report VII, CGER-REPORT, CGER-1048-2001, pp.83–98, (in Japanese)

3.Shiraiwa T., 2005, The Amur Okhotsk Project. Report on Amur-Okhotsk Project, No. 3, December 2005, Research Institute for Humanity and Nature, pp.1–2(in English)

4.Himiyama Y., 2001, Land use change in northeast China—GIS database and evaluation for sustainable development. LU/GEC LandUse for Global Environmental Conservation) Project Report VII, CGER-REPORT, CGER-1048-2001, pp.83–98, (in Japanese)
5.China Map publishers,2004,Atlas of China. China Map Publishers, Beijing, China, [in Chinese]
6.Lin M., Hasegawa K.,2005, The problems on the Large-Scale management of rice production in Heilongjiang Province—A case study on G-Village in Fujin city—. Bulletin of Department of Agriculture, Mie University, 32, pp.61–78,(in Japanese)
7.Myneni R. B., Keeling C. D., Tucker C. J., Asrar G., Nemani R. R.,1997, Increased plant growth in the northern high latitudes from 1981 to 1991. Nature 386, pp.698–702(in English)
8.Sannier C. A. D., Taylor J. C., du Plessis W., Campbell K.,1998, Real-time vegetation monitoring with NOAA/ AVHRR in southern Africa for wildlife management and food security assessment. International Journal of Remote Sensing, 19(4), pp.621–639(in English)
9.Spanner M. A., Pierce L. L., Running S. W., Peterson D.L.,1990, Seasonal AVHRR data of temperature coniferous forests: relationship with leaf area index. Remote Sensing of Environment 33, pp.97–112(in English)
10.Box E. O., Holben B. N., Kalb, V.,1989, Accuracy of the AVHRR vegetation index as a predictor of biomass, primary productivity and net CO2 flux. Vegetatio 80, pp.71–89.(in English)
11.China Statistics Publishers,2001, Statistics of Heilongjiang Province. China Statistics Publishers, Beijing, China (in Chinese)
12.Akihiko K. (2004): Analysis of vegetation and land cover change using global remote sensing. Japan Society of Hydrology and Water Resources, 17(5), 459–467, (in Japanese)
13.Nemani R., Running S.,1997, Land cover characterization using multitemporal red, near-IR and thermal-IR data from NOAA/AVHRR. Ecological Applications 7(1), pp.79–90.(in English)
14.Price C. J.,1984, Land surface temperature measurement from the split window channels of the NOAA 7 Advanced Very High resolution radiometer. Journal of Geophysical Research 89, pp.7231–7237.(in English)
15.Chapman W. L., Walsh J. E.,1993, Recent variations of sea ice and air temperatures in high latitudes. Bulletin of the American Meteorological Society 74, pp.33–47.(in English)
16.Makhinova A. ,2003, Smoke from forest fires and innocent hostages to experiments with nature, Siberian Agreement Interregional Association, A quarterly political information and analytical illustrated magazine, No.2 (12), pp.47–52.(in Russian)
17.Kondoh A., Kaihotsu A., Hitata T. and Dorgorsuren,2005, Interannual Variation of Phenology and Biomass in Mongolian Herbaceous Vegetation, Journal of Arid Land Studies, 14(4) , pp.209-218, [in Japanese]
18.Kondoh A., Tateishi K., Runtunuwuand P.,2002,Relating Vegetation Activity to Climatic Variation and Atmospheric CO2 Content, Japan Society of Hydrology and Water Resources, 15(2) , pp.128-13, [in Japanese]

THE BASIC FEATURES OF LAND-USE IN AMUR RIVER WATERSHED

GANZEY S.S.[1], YERMOSHIN V.V.[1], MISHINA N.V.[1] AND SHIRAIWA T.[2]

[1] *Pacific Institute of Geography FEB RAS, Vladivostok, Russia*

[2] *Research Institute for Humanity and Nature, Kyoto, Japan*

INTRODUCTION

Research of interactions «land-ocean» draws more attention of experts of various scientific fields. It is explained by a variety of diverse links between them and by complexity of studying them. At that it is abundantly clear that the changes of natural environment occurring on the continent influence the sea systems. Changes in the last ones, in turn, affect stability of in-land systems.

The Sea of Okhotsk is one of the main fishing areas in the Far East of Russia. This sea plays an essential role in economies of Japan, Republic of Korea and other countries. The studies in last years [1] revealed that phytoplankton development in Northern Pacific is restrained by a low degree of utilization of nitrates, phosphates and silicates dissolved in sea water because of low contents of dissolved iron in waters. In result the efficiency of phytoplankton is decreasing that brings to reduction of main fishing resources stocks. Since, due to considerable entry of dissolved iron with waters of Amur River, the Sea of Okhotsk does not belong to the similar water bodies, but significant changes in land tenure within its watershed result in reduction of this element entry. It can cause a decreasing of phytoplankton efficiency and it can have serious economic consequences. The major factors of formation of dissolved iron is a presence of great volume of organic stuff and anaerobic conditions. Therefore, the role of forest and wetland ecosystems, which recently are undergone with significant transformations by row of reasons in Amur River watershed is great in regulation of volumes of its entry.

This circumstance served as a basis for initiation of the international research Amur-Okhotsk Project financed by Japanese government. The main purpose of the project is to develop a plan of sustainable land-use in Amur River watershed for conservation of present efficiency of the Sea of Okhotsk's ecosystem.

It is necessary to note that active surveys of the areas within the watershed of Amur River have been begun already in the end of the XIX - beginning of the XX century, and it is associated with names of so well-known travelers and scientists - naturalists like Venjukov M.I., Maak R.K., Maksimovich K.I., Przhevalsky N.M., Obruchev V.A. and others. Besides that, the Chinese part of Amur River watershed permanently attracted attention of Russian researchers. D.N.Anuchina's works [2, 3] were ones of the first, which in a complex considered natural features, population and an economy of Manchuria.

A huge role in studying the natural environment of the Far East of Russia and Manchuria was played by Komarov V.L. [4] which ideas about zoning of 4 natural areas and 4 florae areas of the same name (Manchurian, Daurian, Okhotsk and Siberian) have been

widely recognized and commented in floristic, botanic and geographical, and landscape aspects [5].

A great volume of research works of both scientific, and scientific and applied character, has been fulfilled by Amur Expedition, organized in the beginning of the last century [6-8] to study an opportunity of economic development of Amuro-Ussuriiskii krai, further resettlement of peasants, development of trade and industry.

During the post-war time the works devoted to the economic and geographical characteristic of Manchuria have been published [9, 10].

An essential contribution to accumulation of extensive material about differentiation of natural environment in Amur River watershed has been made by the Russian-Chinese Joint Amur Expedition under the Council on Industrial Forces Organization of the USSR Academy of Science, and by Heilongjiang Expedition of the Chinese People's Republic, carried out the surveys in the second half of the 50s of the last century [11]. The results of these surveys became the basis for fulfilling a whole series of thematic works, in which natural environment of Amur River watershed was considered not only within the separate countries, but also as an integral geographical formation, which parts are interconnected closely. Among these works it is necessary to mention about soil and geographical zoning of Amur River by Liverovskii Yu.A. and Rubtsova L.P. [12]; a vegetation map of Amur River watershed [5, 13]; Nikolskaya V.V.'s work devoted to studies of morpho-structures of Amur River watershed [14]; and a number of others. It is necessary to point out also to works of Murzaeva E.M. [15], Efremov Yu.K. [16] of the same period, devoted to the characteristic of nature and economy of Northeast China.

Modern interest to the studies of trans-boundary watershed of Amur River is proved by publication of works devoted to the trans-boundary diagnostic analysis of Ussuri River [17] and of Khanka Lake [18], to researches of issues of its economic development [19, 20], water and environmental problems [21], land resources assessment [22], trends of economic interaction between the Russian Far East of Russia and Northeastern China [23]. The common feature of the works in last years is that the analysis of situation within the watershed is made as a rule by large units of administrative and territorial division (ATD) situated on its territory. Use of such data is associated with that the information about separate parts of Amur River watershed is often incomplete, diverse, and dissimilar in details, methods of data collection and processing.

Since the unified data on land structure for the surveyed territory are also absent, the map of "Modern Land-Use Zoning Map of the Amur River Basin" has been made in the scale 1 : 2,500,000 (Fig. 1).

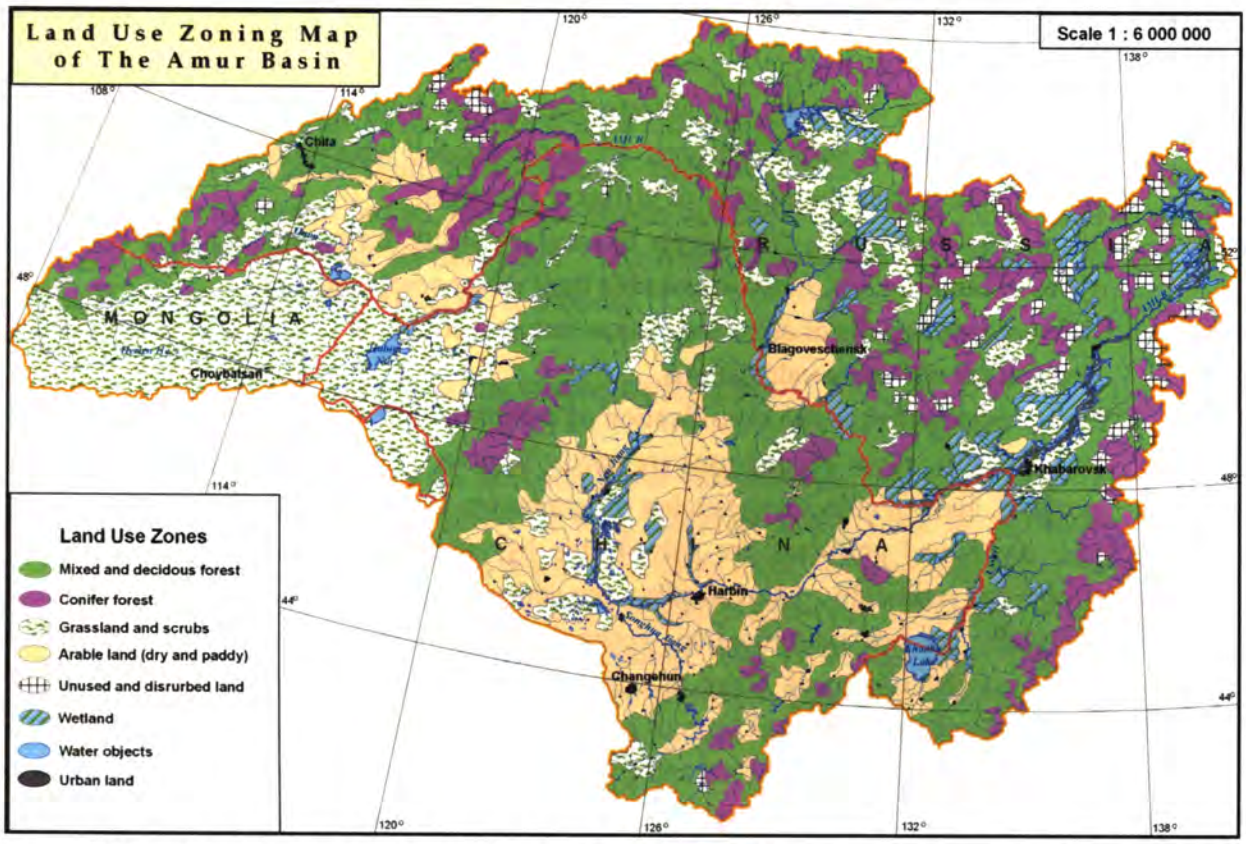

Figure.1 Modern Land-Use Zoning Map of the Amur River Basin. By figures are numerated: 1 - deciduous and mixed forests and sparse forests; 2 - coniferous forests; 3 - meadows, steppes, bushes; 4 - agricultural lands; 5 - disturbed and unused lands; 6 - large settlements; 7 - water bodies; 8 - boggy and humidified lands; 9 - state boundaries; 10 - border of the watershed.

MATERIALS AND METHODS

A set of satellite images of Landsat-7 (USA) in 2000-2001 was the initial basic information for compilation of the layer "Modern Land-Use In Amur River Watershed". The composite compilations of the average resolution from 30 m and more mainly have been used in the work. The satellite images of Landsat TM with resolution 15-30 m have been used to specify some most disputable territories. Decoding was made in GIS ArcView 3.3 software using a special extension Image Analysis to form shape files and the subsequent their converting to

Arc/Info coverings. Besides direct interactive expert decoding of satellite images, the following sources have been used as reference and correcting information converted to electronic raster and then to vector format: 1. A map of vegetation of Amur River watershed in the scale 1:2,500,000 edited by Sochava V.B. [13]; 2. A map of vegetation of Mongolian National Republic in the scale 1:3,000,000 (1990); 3. A map of vegetation of China from the Vegetation Atlas of China in the scale 1:1,000,000 [25]; 4. Raster topographical maps in the scale 1:500,000.

Specific and at the same time most typical feature of the projects fulfilled on trans-boundary territories consists in discrepancy of initial data on the territories of different countries [26, 27]. It resulted in a set of problems of geo-information exchange, geo-

information flows and forming of uniform geo-information space. We highlight here only those which have a direct attitude to the theme of the present survey.

1. Along the state boundary, all information layers, both common geographic and thematic ones to a variable degree, are not coincided with each other practically if they are taken from the sources of different countries.
2. Distinctions in contents of concepts of similar objects, for example, nature reserves, types of land-use, etc. make impossible their direct combined use.
3. Different assessments of anthropogenous factors, ecological standards and restrictions demand for special re-calculations.
4. Various approaches to the classification of complex objects (roads, settlements, types of vegetation, types of land-use) are used. Various substantial concepts, principles, grounds, and not coinciding number of gradations can be used in classifications [27].

All the mentioned problems are solved step by step, first of all conceptually, then technologically and practically. Conceptually - the general bases of classifications are defined and agreed usually towards simplification. Technologically - the principles and sequence of overlapping of information layers along the state boundaries are determined on the basis of invariant geographical structures and lines of geographical space like watercourses, roads, etc. Practically - the united layers are unified and formed, the topology of objects is compiled, and the layers are correlated among themselves forming horizontal and vertical structures of geo-information space.

The same problems were solved in drawing up of a map of modern land-use in Amur River watershed. First of all, it was necessary to make a uniform classification of types of land-use since the classifications accepted and used in Chinese People's Republic, Russia and Mongolia differ essentially. Since the approaches to mapping land-use in Mongolia and in Russia are similar, we give more details to the Chinese classification.

In Chinese People's Republic the unified "through" state classification of lands embracing various levels of analysis, from the small-scaled level up to middle and large scaled level, is accepted. In total, three classes differing in detail of description of typological characteristics of lands are used. The categories of lands of the first class reflect their most general properties allowing to allocate, for example, 'cultivated lands", 'forest lands', "meadows", 'water bodies', 'industrial lands', 'unused lands', and to generate from them a legend at drawing up of maps in the scale 1:2,500,000 and smaller. The maps made in the scale 1: 1,000,000 use more fractional typological characteristics. For example, the type 'cultivated lands' is subdivided into the subtypes 'paddy fields' and 'dry agricultural lands' (arable lands). The forest lands and meadows are subdivided into subtypes depending on density of wood stands or on density of a grassy cover. Thus, the territories with density of wood stands over 30 % belong to the forest lands, the territories with density of stands from 10 to 30 % belong to sparse forests, etc.

From our point of view, use of the state classification of lands accepted in the Chinese People's Republic for charactering modern land-use in Amur River watershed, narrows a volume of helpful information on character of economic activities in its limits though it essentially simplifies its mapping. In our country more complex and detailed typification of

land-use (land tenure) has been accepted and realized in statistics. However, it practically was not applied to mapping of large territories because of its ambiguity.

The classification of forest lands has been corrected. In addition to the density of wood stands their typological characteristics have been introduced. The coniferous, mixed, deciduous forests, sparse forests, and other forests have been defined in forest lands in result (Fig. 1). For details please see the paper "The basic geographical information for GIS of Amur River basin" (Yermoshin et al., this book).

DISCUSSION OF RESULTS

We determined the total area of Amur River watershed as 2.05 million km^2. There is a little difference from the data given in other sources. Distinctions in estimation of the watershed area are associated with inclusion or without inclusion of several closed watersheds in the southern areas of East Mongolia and in the southwestern part of Autonomous Region of Inner Mongolia of the Chinese People's Republic into its composition. The area of the watershed changes at that from 1.8 up to 2.09 million km2. According to our data, the Russian part of the watershed takes 49.3 % of the watershed territory or 1.01 million km2, the Chinese part - 42.2 % (0.86 million km2), the Mongolian part - 8.5 % (0.18 million km^2).

The natural and climatic conditions in Amur River watershed considerably change in both latitudinal and meridional directions. Several vegetation zones like mountainous tundra, taiga, a zone of mixed broadleaved forests, a forest-steppe zone, steppe, semi-desert are defined there. Climatic conditions change from arid ones to superfluous damp ones. All that determines a natural variety of land resources of the watershed which have been subject to active economic development for last 125 years [19].

At present forest areas occupy over a half (54.3 %) of the watershed territory. Over 30 % of this area is occupied by mixed and coniferous woods situated mainly in the Russian territory. It is necessary to note that majority of fire-sites, loggings and sparse forest are also located in the Russian territory that reflects adverse trends in forest management, developed on our territory in the 1990s of the last century. Deciduous forests occupying about 15 % of all forest lands, dominate in the Chinese part of the watershed.

The agricultural lands occupying nearly 20 % of its territory are the second type of lands by the area in the watershed. The lion's share of cultivated lands including irrigated, is located in the Chinese part of the watershed. Prompt reduction of wetlands is one of the consequences of its active agricultural development. According to the Chinese researchers [28] a share of wetlands on Sanjiang Plain for the period from 1950 to 2000 reduced 52.5 %, from 32.4 thousand km^2 up to 9.2 thousand km^2, at the same time the share of agricultural lands has increased from 10.2 % up to 55.1 %. At that, most part of wetlands is located still on the Russian territory.

Table 1. The types of land-use developed in the watershed area.

Type of land-use	Area, km^2	Russia, %	Mongolia, %	PRC, %
Coniferous forests	277.6	77.1	3.0	19.9
Mixed forests	347.3	66.5	1.8	31.7
Deciduous forests	316.2	37.4	1.0	61.6
Sparse forests	145.4	73.1	3.2	23.7
Fire-sites	27.1	97.1	1.8	1.1
Other forest lands	5.4	Not determined	41.1	58.9
Meadows	257.2	9.5	54.7	35.8
Bushes	121.7	67.7	4.7	27.6
Reclaimed lands	26.0	9.1	Not determined	90.9
Not reclaimed agricultural lands	347.5	23.3	0.7	76.0
Lakes	10.6	48.9	7.7	43.5
Water reservoirs	2.5	81.9	Not determined	18.1
Wetlands	140.0	68.1	0.1	31.8
Settlements	2.7	37.2	Population less 100 thousand people	62.8
Not used lands	0.7	93.0	Not determined	7.0
Waste lands	0.2	83.6	Not determined	16.4
By-golets bushes with mountainous tundra	13.3	96.1	1.0	2.9
Loggings	8.7	77.7	Not determined	22.3

Meadows and bushes totally make about 20 % of the area of Amur River watershed also.

The Russian part of the watershed partly or completely covers the territories of 6 administrative units in the south of the Far East, the Chinese part - three units, and Mongolian - four units (Table 2).

The territorial distribution of types of modern land-use reflects both natural and climatic conditions of the territory, and also national features of nature management, historical and modern trends in development of economy of the countries. Figure 2 shows modern land-use in Amur River watershed in the context of administrative units.

The main tracts of coniferous forests on the Russian territory are in Khabarovskii Krai, Amurskaya and Chitinskaya oblasts - 73.4; 68.7 and 48.3 thousand km2 correspondingly. The mixed forests are dominating type of vegetation, their main share is concentrated in the same administrative units. Deciduous woods prevail in Amurskaya Oblast, Khabarovskii Krai and in Chitinskaya Oblast. Amurskaya Oblast also takes leading position in the area of sparse

forests (39.9 thousand km2) and in the area of meadows and bushes vegetation (36.2 thousand км2).

Wetlands are widespread in Khabarovskii Krai and in Amurskaya Oblast, 48.6 and 28.2 thousand km2 correspondingly. The area of wetlands in Primorskii Krai is much less, 6.8 thousand km2.

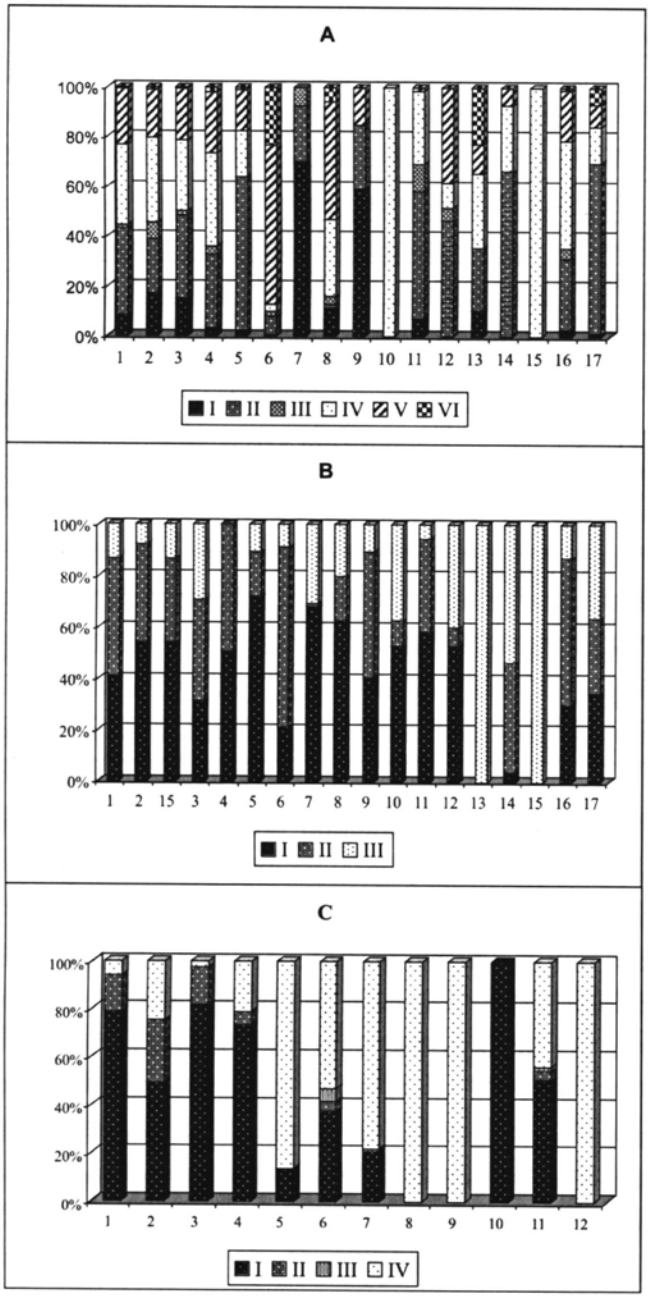

Figure.2 Structure of land-use in Amur River watershed according to the administrative units.

A - Russian portion of the watershed: I - Primorskii Krai; II - Khabarovskii Krai; III - Evreiskaya Autonomous Oblast; IV – Amurskaya Oblast; V – Chitinskaya Oblast; VI – Aginskii Buryatskii Autonomous Okrug.

B - Chinese part of the watershed: I - Heilongjiang Province ; II - Inner Mongolia Autonomous Region ; III - Jilin Province.

C - Mongolian part of the watershed: I - Hentei Aimak; II - Tuva Aimak; III - Sukhebator Aimak; IV - Dornod Aimak.

Types of land-use. Forests: 1 - coniferous; 2 - deciduous; 3 - mixed; 4 - sparse forests; 5 - fire-sites; 6 - meadows; 7 - reclaimed lands; 8 - not reclaimed agricultural lands; 9 - lakes; 10 - water reservoirs; 11 - wetlands; 12 - residential territories; 13 - unused lands; 14 – by-golets bushes with high-mountainous tundra; 15 - waste grounds; 16 - bushes; 17 - timber cuttings; 18 - other forest lands.

Table 2 Units of administrative-territorial division in China, Russia and Mongolia, situated in Amur River watershed.

Administrative unit	Area, thousand km^2	Area in the watershed, thousand km^2	Watershed share of the administrative unit, %
People Republic of China			
Heilongjiang Province	454.0	442.7	97.5
Inner Mongolia Autonomous Region	1183.0	296.7	25.1
Jilin Province	187.0	125.5	67.1
Russia			
Primorskii Krai	165.9	101.0	60.9
Khabarovskii Krai	788.6	313.7	39.8
Evreiskaya Autonomous Oblast	36.0	36.0	100
Amurskaya Oblast	363.7	315.3	86.7
Chitinskaya Oblast	412.5	224.5	54.4
Aginskii Buryatskii Okrug	19.0	19.0	100.0
Mongolia			
Aimak Hentei	80.3	73.0	91.0
Aimak Tuve	74.0	9.5	12.9
Aimak Sukhebator	82.3	7.54	9.1
Aimak Dornod	123.6	85.1	68.9

The main tracts of lands used in agricultural production are situated in Chitinskaya Oblast, 38.2 thousand km^2 and in Amurskaya Oblast, 25.1 thousand km^2. Irrigated lands prevail in Primorski Krai that is associated with rice growing in several frontier areas.

The forests most subjected to fires are in Khabarovskii Krai. There are observed 16.1 thousand km^2 of burned down or dead forests that makes 61.5 % of the area of similar lands on the Russian territory. Their share in Amurskaya and Chitinskaya oblasts is also great, 18.4 % and 16.6 % correspondingly.

Most active loggings are in Khabarovskii Krai and in Amurskaya Oblast. At that, the share of the logging area in Khabarovskii Krai exceeds over 2 times the same average share in other regions of the Russian part of Amur River watershed.

On the Chinese territory the coniferous forests occupy the largest area within the Great Khingan Ridge in Inner Mongolia Autonomous Region, 25.3 thousand km^2. The area of coniferous forests in Heilongjiang Province, 22.5 thousand km^2 slightly cede to them. Mixed forests prevail in Heilongjiang Province, 59.7 thousand km^2 that makes 54.2 % of the area of these forests on the Chinese territory. The share of mixed forests in Inner Mongolia Autonomous Region and in Jilin Province is less, 32.5 % and 13.3 % correspondingly. The Heilongjiang Province also has the largest areas of deciduous forests, 105.2 thousand km^2. Sparse forests and bushes are most widespread in Inner Mongolia Autonomous Region that is

caused both by natural and climatic features of the territory, especially in its southern portion, and by industrial loggings of timber within the Great Khingan Ridge till 1998. Decoding of satellite images allowed us to reveal the other feature of modern state of forests on the Chinese territory. There is observed the considerable divergence between the data of the Atlas of vegetation of Chinese People's Republic [25] and the decoded data. For example, the northern portion of the Great Khingan Ridge is shown in the Atlas of vegetation as a zone of practically continuous distribution of coniferous forests. However, the decoded data show that at present the deciduous forests dominate there, and the coniferous and mixed forests are typical in the central and southern portions of the Great Khingan Ridge.

A high share of timber cuttings in Jilin Province, 36.3 % of the logging area in the Chinese part of the watershed appeared to be unexpected also. It is necessary to note that the center of timber cuttings in the Chinese People's Republic has moved to the artificial forests, partly created for these purposes. Besides that, it is necessary to take into account that the used data can not reflect the present situation in full because the objects of the area less 50 km^2 have not been displayed on final map, in practice forest tracts of the smaller areas are frequently cut down.

The main areas of agricultural lands, reclaimed lands, wetlands which shares are 63.1 %, 67.8 % and 58.3 % of the area of similar categories of lands in the Chinese part of Amur River watershed, are situated in Heilongjiang Province. It is interesting to compare the data on irrigated lands, received in result of decoding satellite images, and the official statistical data. A large portion of irrigated lands in Heilongjiang Province is used for rice growing. The statistical data show [29] that in Heilongjiang Province in 2001 paddy fields occupied 1598 thousand hectares, the decoded data practically completely coincide with these figures, or 1600.9 thousand hectares.

In the Mongolian portion of Amur River watershed the forested territories are situated in Hentei, Tuva and Dornod aimaks. At that, most part of coniferous, mixed and deciduous forests locate in Hentei Aimak, 79.1 %, 82.1 % and 49.3 % of the area of these forests of the whole Mongolian territory correspondingly. There are also 73.5 % of sparse forests, and nearly 51 % of bushes of this portion of the watershed.

Dornod Aimak is also characterized with a wide spectrum of land-use. Deciduous forests dominate among forested lands, which share makes 24.7 % of these forests in the Mongolian portion of the watershed. The share of coniferous and mixed forests is much less, 5.6 % and 2.3 % correspondingly. Sparse forests and bushes are widely distributed, 21 % and 43.5 %. Approximately a half of meadows of the Mongolian portion of the watershed is concentrated in this aimak. There are also 86.5 % of its agricultural lands.

Despite of small area of Tuva Aimak in Amur River watershed (5 %), over 15 % of coniferous and mixed forests, 26 % of deciduous forests, and 8 % of meadows and bushes of the Mongolian portion of Amur River watershed is distributed there.

CONCLUSION

The map "Modern land-use in Amur River watershed" in the scale 1:2,500,000, compiled by results of decoded satellite images Landsat TM, has allowed us for the first time from unified positions and in uniform scale to assess a character, structure, national features of land-use on the territories of Mongolia, Chinese People's Republic and Russia, included in Amur River watershed. Chinese portion of the watershed is the most economically developed one.

Comparison of the compiled map with thematic maps from the Atlas of vegetation of China [25], and with the map of vegetation of Amur River watershed [13] shows essential simplification of structure of forests towards a prevalence of invaluable woods. Especially it concerns to the northern portion of the Great Khingan Ridge, Less Khingan (both in Russian, and in Chinese portions), northern portion of Sikhote-Alin Ridge, and Chitinskaya Oblast. These changes resulted from active policy of industrial timber cutting existed on the Chinese territory of the watershed up to the end of the 1990s last century, proceeding timber cuttings on the Russian territory, and also forest fires, annually arising, especially on the Russian territory. 78 % of the cut forests in Amur River watershed and 97 % of the burned forests are on the Russian territory.

A significant expansion of the area of agricultural lands that occurred in the Chinese People's Republic in the 1990s and in 2000-2001 has been observed. These changes at first concern Sanjiang Plain, and eastern foothills of the Great Khingan. In many cases it is associated with reduction of the area of wetlands and forests. Most part of wetlands is still concentrated in the Russian portion of the watershed (in Amurskaya Oblast, Evreiskaya Autonomous Oblast and Khabarovskii Krai).

These essential distinctions in modern land-use on the territory of countries belonging to Amur River watershed stipulate an existence and development of sharp transboundary environmental problems. Among them are impoverishment of biodiversity, disturbance of migration ways of wild animals and their forage reserve, fragmentation and partly destruction of habitats, increased fire danger, high risk of flooding, contamination of surface waters, water and atmospheric transfer of polluting substances.

The compiled electronic map is, in first, an information basis for carrying out of the further analysis of system of land-use in Amur River watershed, and, in second, as an electronic layer it is a component of forming geo-information space of the whole Amur River watershed.

Development of the unified policy of ecologically balanced land-use agreed between the countries is necessary for improvement of ecological situation in the watershed.

Researches has been carried out at financial support of the Research Institute for Humanity and Nature, Kyoto, Japan, and due to the grant of the Far Eastern - Siberian Branch of the Russian Academy of Science No 06-II-CO-09-036, and the grant of the Far Eastern Branch of the Russian Academy of Science No 06-III-A-09-393.

REFERENCES

1. Tsuba F. and 25 others. A mesoscale iron enrichment in the Western Subarctic Pacific induces a large centric diatom bloom // Science, 2003, v. 300, No. 5621. P. 958-961.
2. Anuchin D.N. East Manchuria // Physical geography. Vol. III-IV, 1896. P. 149-157.
3. Anuchin D.N. Manchuria // Physical geography. Vol. I-II, 1897. P. 101-127.
4. Komarov V.L. Manchurian expedition of 1896 // Proceedings of Imperial Russian Geographic Society, Vol. XXXIV, Issue II, 1898. P. 117-184.
5. Sochava V.B. Botanic and geographical parities in Amur River watershed // Amur taiga (complex botanical surveys), Leningrad, Nauka, 1969. P. 5-15.
6. Lands of Amur Railway region. Works of the Amur Expedition. Issue III. Compiled by Kryukov I.F., agriculturist of Migration Board. St. Peterburg, 1911, 400 pages.
7. Korotkii M.F. Sketch on vegetation of Zeisko-Bureinskii district of Amurskaya Oblast // Works of the Amur Expedition, Issue 16, Vol. 3. St., Peterburg, 1912.
8. Mitinskii A.N. Materials about the status and needs of trade and industry in the Far East // Works of the Amur Expedition. Issue VIII. St. Peterburg, 1911, 284 pages.
9. Anuchin V.A. Geographical sketches on Manchuria. Moscow, OGIZ-GeographGIZ, 1948, 300 pages.
10. Glushakov P.I. Manchuria. Economic and geographical description. Moscow, OGIZ, 1948, 263 pages.
11. Nikolskaya V.V., Chichagov V.P. About joint researches of the Chinese and Soviet geographers in Amur River watershed // Proceedings of the USSR Academy of Science, Geographical Serie, 1957, No. 2, P. 166-168.
12. Liverovskii Yu.A., Rubtsova L.P. Soil and geographic zoning of Pri-Amurye // Issues of natural zoning of the Soviet Far East in connection with district lay-out. Moscow, Publishing House of the Moscow State University, 1962, P. 149-170.
13. Vegetation Map Of Amur River Watershed // Ed. by academician Sochava V.B. The USSR Academy of Science, 1969. Scale 1:2,500,000.
14. Nikolskaya V.V. Morfostructure of Amur River watershed. Moscow, Nauka, 1972, 295 pages.
15. Murzaev E.M. Northeast China. Physiacla and geographical description. Moscow, Institute of Geography of the USSR Academy of Science, 1955, 252 pages.
16. Efremov Yu.K. Northeast of foreign Asia // Foreign Asia. Physical geography. Moscow, 1956, P. 378-425.
17. Program of sustainable land-use and rational distribution of lands in Ussuri /river watershed and adjacent territories (Northeast China and the Russian Far East). Birlington. 1996, 98 pages.
18. Kachur A.N., Jin X., Baklanov P.Ya., Ganzei S.S. et al. Diagnostic analysis of the Lake Khanka Basin (People's Pepublic of China and Russian Federation). UNEP/CRAES/PGI FEBRAS. Nairobi. 2001, 136 pages.
19. Baklanov P.Ya., Ganzei S.S. Main stages and tendencies in development of land-use in Amur River watershed // Geography and natural resources, 2004, No. 4, P. 19-28.

20. Ganzei S.S., Mishina N.V. Land-use and Land-cover Changes in the Amur River Basin (South of the Russian Far East and North-East China) // Land-use and Land-cover Changes in the Separate Regions of the World. IGU - LUCC Atlas, 2005. Vol. 3-4. P. 49-62.
21. Water and ecological problems of Amur River watershed. Institute of water and ecological problems, FEBRAS, Vladivostok, 2003, pages 187.
22. Karakin V.P., Sheingauz A.S. Land resources of Amur River watershed // Bulletin of the Far Eastern Branch of the Russian Academy of Sciences, 2004, No. 4, P. 23-37.
23. Tattsenko K.V. Tendencies of economic interaction between the Far East of Russia and Northeast China. Vladivostok, DalNauka, 2006, 216 pages.
24. The Mongolian People's Republic. The National Atlas. Ulan Bator - Moscow. 1990.
25. The Vegetation Atlas of China. 1:1,000,000. Chinese Academy of Science. Science Press, Beijing, China, 2001.
26. Ganzei S.S. Trans-boundary geosystems of the south of the Far East of Russia and Northeast of China. Vladivostok, DalNauka, 2004, 231 pages.
27. Yermoshin V.V. Features of formation of geo-information space for nature conservation projects on transboundary territories // Proceedings of the XII Workshop of geographers of Siberia and the Far East, October 5-7, 2004, Vladivostok, Pacific Institute of Geography, FEBRAS, 2004, P. 155-157.
28. Liu H., Zhang Sh., Li Z., Lu X., Yang Q. Impact on wetlands of large-scale land-use changes by agriculture development: the Small Sanjiang plain, China // Ambio, v. 33, No. 6. P. 306-310.
29. Heilongjiang Statistic Yearbook, China Statistics Press, 2001. 440 p.

CREATION OF GIS FOR AMUR RIVER BASIN: THE BASIC GEOGRAPHICAL INFORMATION

YERMOSHIN V.V., GANZEY S.S., MURZIN A.V., MISHINA N.V. AND KUDRYAVTZEVA E. P.

Pacific Institute of Geography FEB RAS, Vladivostok, Russia

INTRODUCTION

According to the technical task of the contract between the Pacific Geographical Institute, FEBRAS and Research Institute for Humanity and Nature Inter-University Research Institute Corporation National Institutes for Humanities (Kyoto, Japan) the following works have been fulfilled:

1. Compiled electronic (digital) base common geographic coverages, including:
- Relief in horizontal lines every 300 meters.
- Hydrological network: main channels, tributaries, lakes, water reservoirs, channels.
- Settlements divided into: states capitals; centers of krais (oblasts), provinces; cities over 1 million, from 1million to 500 thousand, from 500 thousand to 100 thousand of residents.
- Road network: railways, motor roads: highway, other covered roads.
- Borders: state, administrative of krais (oblasts), provinces.
2. Made an electronic 3D-model of relief - DEM (using data of Shuttle Radar Topographic Mission (SRTM) with step of 15 arcsecond).
3. Created a map (electronic coverage) "Modern land-use in Amur River basin" on the basis of decoded satellite images of LANDSAT–TM 2000-2001 with resolution on the spot 50-100 meters.
4. Compiled an electronic coverage "Geological Structure"
5. Compiled an electronic coverage "Vegetation of Amur River basin"

RESULTS

Thus, all the works on geo-informational provisioning for the project have been fulfilled in two blocks, 1 – base general geographic one, and 2 – base thematic one. All the electronic coverages have been made on Arc/INFO, ArcView platforms in the detailed scale 1:2,500,000 of common projection of the following parameters:

projection albers
datum puk
units meters
spheroid krassovsky
52 0 0 /* 1st standard parallel

64 0 0 /* 2st standard parallel
135 0 0 /* central meridian

1. THE COMMON GEOGRAPHICAL COVERAGES

The common digital geographical coverages were created:

1. Relief in horizontal lines: 100, 200, 300, 400, 500, 600, 800, 1000, 1500, 2000, 2500 meters.
2. Hydrological network: main rives and channels, tributaries, lakes, reservoirs, channels.
3. Settlements: states capitals; centers of krais (oblasts), provinces; cities with population more 1 million, from 1million to 500 thousand, from 500 thousand to 100 thousand, from 10 thousand to 100 thousand.
4. Road network: railways, motor roads: highway, other hard covered roads.
5. Borders: state, administrative of krais (oblasts), provinces, aimaks.
6. Digital 3D model of relief was built using data of the Shuttle Radar Topographic Mission (SRTM) with step of 8 arcsecond (250m). Shuttle radar topographic mission (SRTM) – Radar topographic survey by the US Government. Accuracy – 90 meters, in height - 20 meters. URL ftp://e0srp01u.ecs.nasa.gov/srtm/version1/. Date of source data: February 2000.

Vector maps Vmap0 in scale 1:1'000'000 for the whole territory of Russia and China distributed by the USA National Geospatial Agency (NGA) were initial data for the main coverages. These data are available for downloading through special web-site (http://geoengine.nima.mil/geospatial/SW_TOOLS/NIMAMUSE/webinter/rast_roam.html)

Relief in horizontal lines and points of fixed height above sea level was made from digital model of relief (DEM). The data for all common geographical coverages have been corrected according to the base topographic maps in scale of 1: 1,000,000, published in 1975-1989. The data for settlements and roads have been corrected according to "The National Economic Atlas of China", published in 1994.

2. THE COMMON THEMATIC COVERAGES

1. Map (electronic coverage) "Modern land-use in Amu River basin" (Fig. 1)

Mainly composite montages of average resolution of 30 m and over were used directly in the work. The resolution 30 m is rather redundant for receiving a final result in scale

1:2,500,000, therefore the resolution changed up to 50-100 m was applied for various territories. The images with resolution 15-30 m were used to specify some most disputable territories. Decoding was made in ArcView 3.3 by means of special extension Image Analysis to form shape files subsequently converted into the Arc/Info coverages. In addition to direct interactive expert decoding of satellite images to get reference and correcting information, the following sources like (1) The vegetation map of Amur River basin 1:2,500,000 edited by academician Sochava V.B. (1968), (2) The vegetation map of

Mongolian People's Republic 1:3,000,000(1990), (3) The Vegetation Atlas of China 1:1,000,000 (2001) converted into the electronic raster form were used.

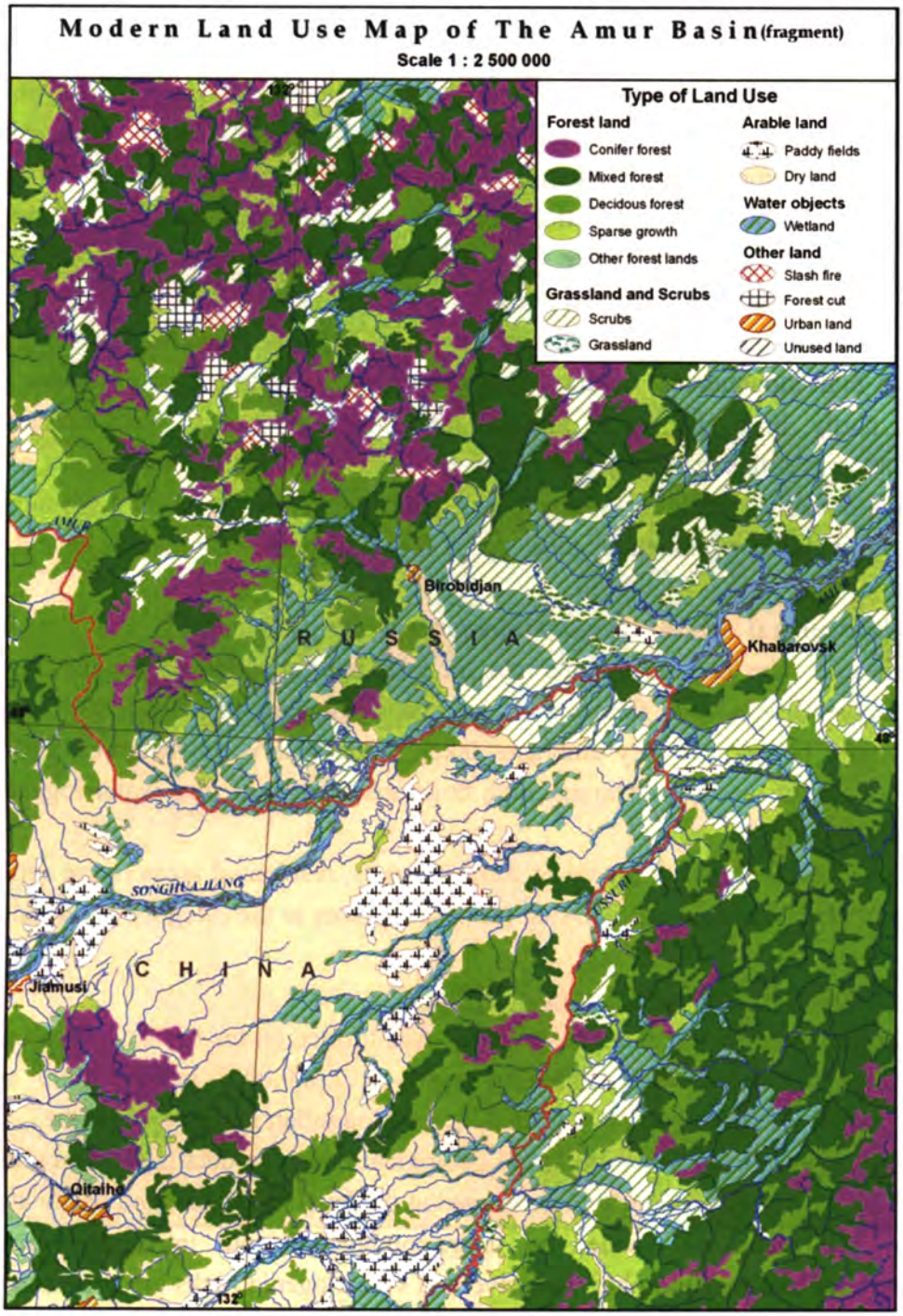

Figure.1

As a result of processing accessible primary sources, first of all, materials of remote sensing, the following categories of modern land-use have been revealed within the territory of the whole of Amur River watershed: forest lands, meadows and bushes, agricultural lands, water bodies, and other lands. These categories, in turn, are divided into types of modern land-use as object (information cell) of mapping. Since the scale of mapping is small enough, and a level of generalization is high, the types concept includes various kinds of land-use and

of natural state of lands. At that, a genesis of each type of lands is not considered; they can be formed through very different way.

The 'coniferous forests' type includes fur, abies, Korean pine, pine, larch forests and their versions. The 'mixed forest' type includes all transitive versions from coniferous to deciduous forests at their approximately equal ratio. The 'deciduous forests' type includes broadleaved and small-leaved forests and their versions. The 'sparse forests' type includes rare forests of various composition, alternation of woods with bushes with density of stands less than 30 %. At that, as already mentioned above, the genesis of this type of lands is not considered; they can be formed after fires, loggings, etc. The 'other forests' type includes forest plantations, including, industrial ones.

The category 'meadows and bushes' embraces types - meadows, bushes, by-golets bushes with high-mountainous tundras. The 'bushes' type includes bush, meadow and bush lands, and partly, bush and sparse forested lands at prevalence of bush vegetation. The 'meadows' type is rather variable, and at the given stage of studies it includes any grassy vegetation - actually meadows, steppes, etc. The 'golets bushes with high-mountainous tundras' type includes mountainous pine, dwarf forms of high-mountainous bushes, tundras, goletses.

The 'agricultural lands' category embraces types - reclaimed and not reclaimed agricultural lands. The 'reclaimed lands type includes mainly paddy fields, and the type 'not reclaimed lands' - arable lands, fallow lands, haymaking sites, pastures.

The 'water bodies' category embraces lakes, water reservoirs, swamps. The 'wetland' type includes various kinds of swamps: high bogs, mari, etc., and also water-logged flooded meadows and marches.

Fire-sites and loggings at places of former forests, residential areas (large settlements), industrial and unused lands (quarries, slag-heaps, etc.) enter to the category 'other lands'.

2. Electronic coverage "Geological structure" (Fig. 2)

Electronic coverage "Geological structure» was formed on the basis of "Geological map of Pri-Amurye and adjacent territories by scale 1: 2,500,000" printed 1999 and "The Geological map by scale 1: 3,000,000 from Atlas of Mongolian People's Republic", 1990.

The coverage reflects a distribution of geological bodies in details corresponding to the scale 1:2,500,000. Every geological body is aged at the level of system, and partly at the level of section. The rocks are divided by their composition into intrusive, volcanogenic, sedimentary ones and metamorphic. Intrusive and volcanogenic rocks are presented in more details. Thus, granites are divided into granitoids, diorites, gabbroids, ultrabasites, alkaline and partially more detailed, e.g. granitoids include: granites, granodiorites, monzogranites, granosyenites. Volcanogenic rocks by composition are divided into sour, middle, basic, alkaline, mixed. Tectonic fractures are divided into mantle, lithospheric, crusty, which, in turn, are divided into covered and not covered by sedimentary strata.

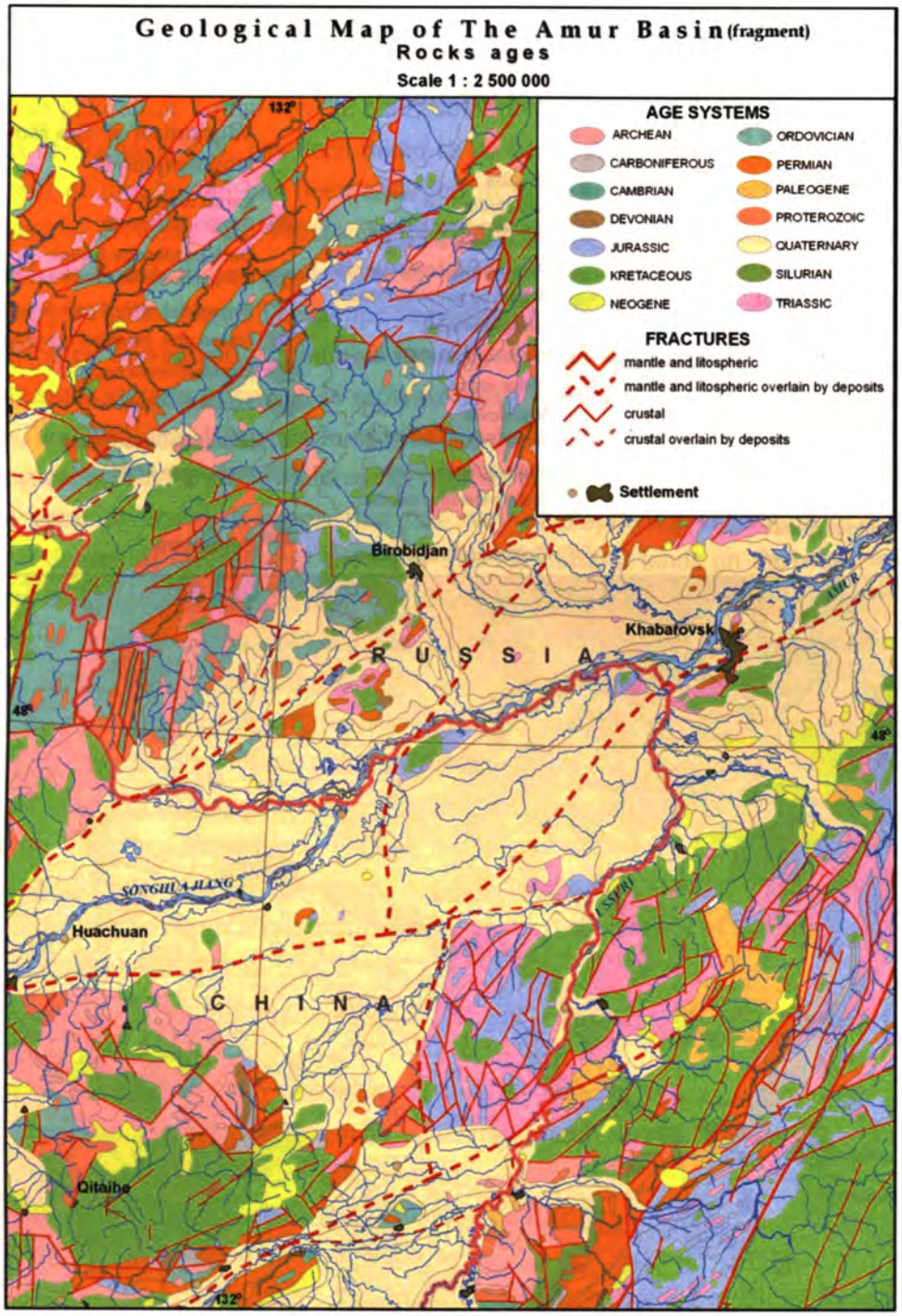

Figure.2

3. Electronic coverage "Vegetation of Amur river basin" (Fig. 3)

Goal of the work is to compile a map of vegetation of Amur River basin on the basis of unified description.

Used sources: 1. The vegetation map of Amur River basin 1: 2,500,000 edited by academician Sochava V.B. (1968). 2. The vegetation map of Mongolian People's Republic 1: 3,000,000 (1990). 3. The Vegetation Atlas of China 1: 1,000,000(2001). The legends (descriptions) to these maps had been made on the basis of different approaches.

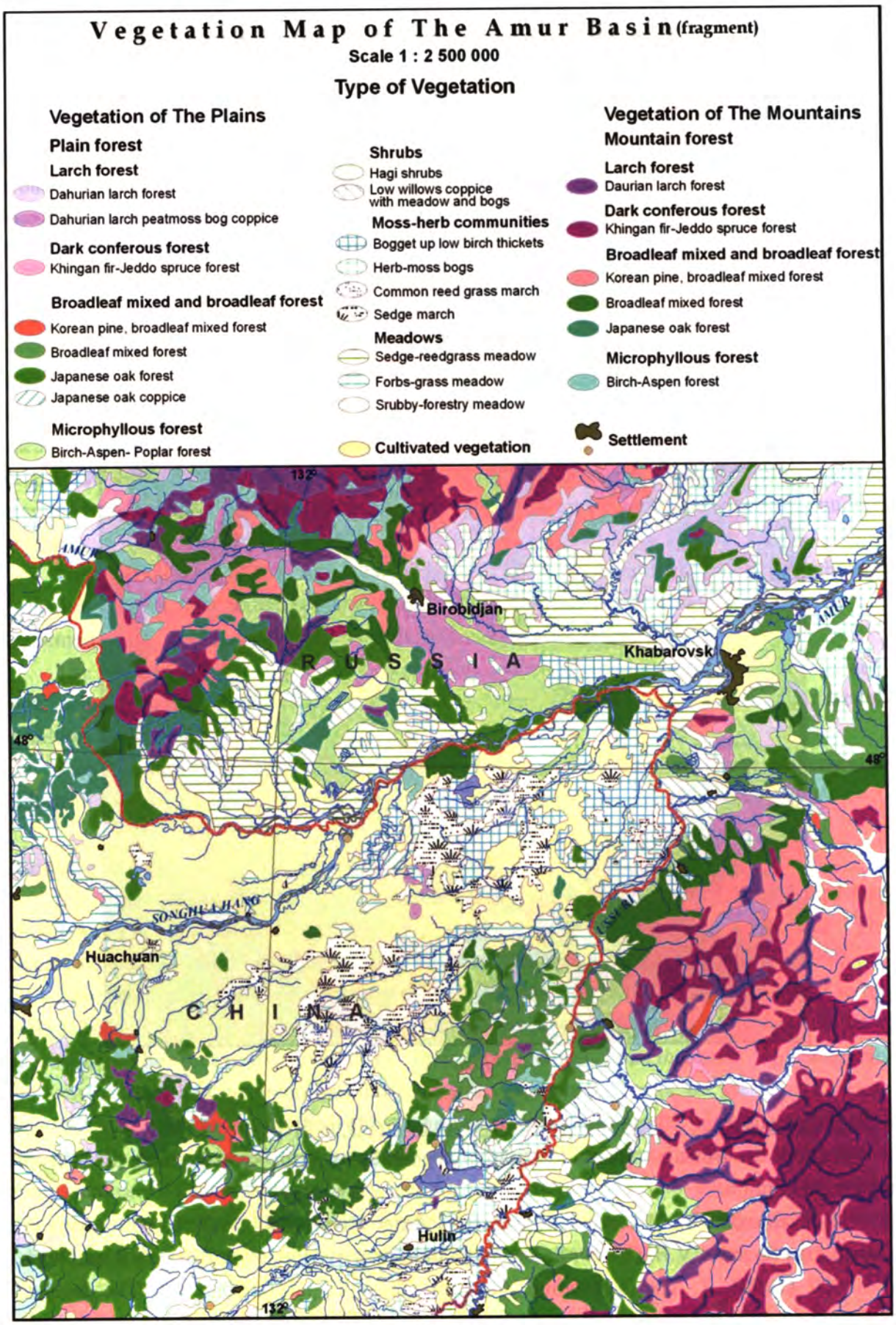
Vegetation Map of The Amur Basin (fragment)
Scale 1 : 2 500 000
Type of Vegetation
Vegetation of The Plains
Plain forest
Larch forest
Dahurian larch forest
Dahurian larch peatmoss bog coppice
Dark conferous forest
Khingan fir-Jeddo spruce forest
Broadleaf mixed and broadleaf forest
Korean pine, broadleaf mixed forest
Broadleaf mixed forest
Japanese oak forest
Japanese oak coppice
Microphyllous forest
Birch-Aspen- Poplar forest
Shrubs
Hagi shrubs
Low willows coppice with meadow and bogs
Moss-herb communities
Bogget up low birch thickets
Herb-moss bogs
Common reed grass march
Sedge march
Meadows
Sedge-reedgrass meadow
Forbs-grass meadow
Srubby-forestry meadow
Cultivated vegetation
Vegetation of The Mountains
Mountain forest
Larch forest
Daurian larch forest
Dark conferous forest
Khingan fir-Jeddo spruce forest
Broadleaf mixed and broadleaf forest
Korean pine, broadleaf mixed forest
Broadleaf mixed forest
Japanese oak forest
Microphyllous forest
Birch-Aspen forest
Settlement
132°
48°
Birobidjan
Khabarovsk
RUSSIA
SONGHUA JIANG
Huachuan
CHINA
Hulin

Figure.3

Fulfillment of the set task required a uniform legend which would reflect the basic geographical rules of vegetation distribution within the Amur River basin. Besides that, it was necessary to generalize a map for the Chinese part of the basin. The legend developed under leadership of Sochava V.B. has been taken as its basis. A group of associations as the main mapped unit of this legend has been enlarged to the level of a formation to unify the data. Besides that, a dividing into vegetation of plains (zonal division) and mountain territories (height and zonal distribution of vegetation) has been made in the course of generalization for the Chinese part of the basin. The steppe vegetation has been divided into two types according to the attributes of vegetation namely: meadow steppes and sod-cereal steppes. It is quite admissible since steppes remained in separate small islands among tracts of mastered lands on the plains, and sod-cereal steppes locate mainly on heights over 500 meters above sea level. The ecological and dynamic rows have been allocated for river valleys which vegetative cover differs in great diversity. It seems that this way of displaying vegetation of river valleys increases a degree of clearness of the map. The agricultural lands on the whole territory are shown by one sign. In the territory of Mongolia entering into the Amur River basin, agriculture is not developed at all, and pastures occupy very small area. This way of displaying agricultural lands seems to allow someone to see a degree of territories' mastering.

The compiled map of vegetation shows a variety of modern vegetative communities and rules of their distribution. Their distribution reflects zonal (in plains) and height-zonal (in mountains) changes of vegetative cover on this great territory which is complex by combination of natural conditions. Totally, the legend includes 69 types describing the basic formations of forests, meadows, steppes, bogs, shrub thickets and agricultural lands on plains and mountains of the Amur River basin. There are two short parts of vegetation classification (legend) as examples below:

Vegetation on the low lands, plains and low plateau

Larch forests

Dahurian larch (*Larix dahurica=L. gmelinii*) forests

Common pine (*Pinus silvestris*) - Dahurian larch forests

Japanese oak - Dahurian larch forests

Birch (*Betula platyphylla*)- Dahurian larch forests

Dahurian larch peatmoss bog coppice

Korean Dahurian larch (*Larix olgensis*) forests, including artificial forests

Korean Dahurian larch peatmoss bog coppice

Dark coniferous forests

Common pine (*Pinus silvestris*) forests, including artificial forests

Khingan fir- Jeddo spruce (*Picea jezoensis, Abies nephrolepis*, locally with *Picea obovata*

Khingan fir- Jeddo spruce with Koyama spruce (*Picea koraiensis*) forests

Mountain vegetation

Mountain forests

Larch forests

Dahurian larch forests
Common pine (*Pinus silvestris*) - Dahurian larch forests
Japanese oak - Dahurian larch forests
Birch (*Betula platyphylla*)- Dahurian larch forests
Korean Dahurian larch forests, including artificial forests
Korean Dahurian larch sphagnum bog coppice
Siberian larch forests

All the information coverages having common borders and/or direct relations sequentially and conceptually are conformed to each other in much the same way in complex and atlas cartography making the through spatial rows. Practically every row has at least one spatial intersection with others. Thus, most coverages have common invariants directly or implicitly.

Sequence of the coordination of digital layers for Amur basin GIS

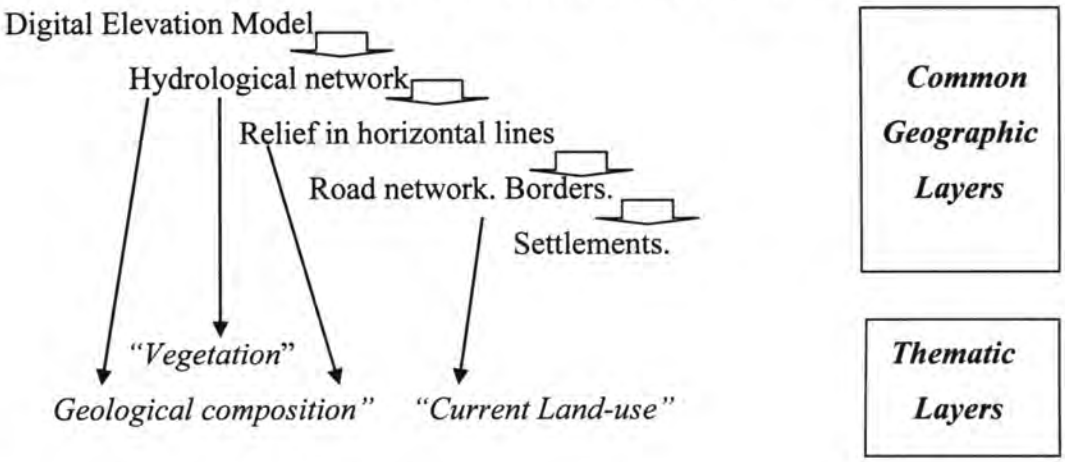

CONCLUSION

The cartographical assessments of various components received in the course of fulfilling the project enable to reveal the main features of differentiation and disturbance of the natural environment in Amur River watershed, and to define the areas playing a key role in changing of dissolved iron coming into the Sea of Okhotsk watershed. At present, the work on compiling an electronic coverage and relevant database and soil map comes to an end.

From our point of view, continuation of the works on creation of GIS for Amur River watershed demands more detailed assessments on middle and probably on large-scaled level of several key areas: watersheds of the rivers being inflows of Amur River, subjected to considerable anthropogenous impact and transformation (for example, Anyui River watershed, lower reaches of Zeya River).

It is supposed to continue also works on drawing up an electronic coverage (and then a map) of landscape composition of Amur River watershed. It will allow us to assess the natural

situation fully, on the one hand, and, on the other hand, to carry out more correct planning of nature conservation and nature management actions within the watershed.

REFERENCES

Geological map of Pri-Amurye and adjacent territories" // Ed. by Krasny L.I., Peng Yunbiao, VSEGEI, Harbin, St.-Petersburg, Blaboveschensk, 1996-1999.

The Geological Map of Pri-Amurye and Adjacent Territories. Scale 1:2,500,000. An explanatory note. Ed. Krasny L.I. et al. VSEGEI Publishing House. St.-Peterburg-Blagoveschensk-Harbin, 1999, 135 pages.

The Mongolian People's Republic. The National Atlas. Ulan Bator - Moscow. 1990.

The Vegetation Atlas of China. 1:1,000,000. Chinese Academy of Science. Science Press, Beijing, China, 2001.

Vegetation Map of Amur River Watershed // Ed. by academician Sochava V.B. The USSR Academy of Science, 1969. Scale 1:2,500,000.

ANALYSIS OF LAND COVER ON THE SANJIANG PLAIN, CHINA, USING JERS-1/SAR DATA

MUROOKA M. [1], HARUYAMA S. [2], MASUDA Y.[2],
YAMAGATA K. [3] AND KONDOH A.[4]

[1]*Hokkaido Abashiri Fisheries Experiment Station,*
[2]*University of Tokyo, Graduate School of Frontier Science,*
[3]*Division of Social Studies, Joetsu University of Education,*
[4]*Center for Environmental Remote Sensing, Chiba University*

1. INTRODUCTION

The Sanjiang Plain is in the middle region of the Amur River basin of China. There are much wetland on this plain. Agricultural development by the Chinese government over the past 20 years has resulted in a considerable increase in the area under cultivation (Ganzey, 2005, Singh *et al.*, 2001). Changes to land cover in the Amur River basin as a result of the decreasing area of wetland influence the biomass of the Sea of Okhotsk, into which the Amur River flows (Shiraiwa, 2005). Consequently, an objective assessment of the human impact on the natural environment of this region is needed.

Remote sensing is a good candidate to understand the changes in land cover over time because the Sanjiang Plain is wide and flat. SAR (synthetic aperture radar) can provide high-resolution data under all weather conditions. The JERS-1/SAR program was active in the 1990s, when land cover on the Sanjiang Plain changed dramatically. The JERS-1/SAR program used the long microwave band (L-band) to which vegetation is transparent, thus allowing direct observation of the soil.

Dobson *et al.* (1995) showed that JERS-1/SAR could distinguish urban areas, forests, and grass fields. Hess *et al.* (2003) used JERS-1/SAR data from different seasons to calculate the area of seasonal inundation in the Amazon Basin. Ishizuka (2006) developed a technique to use SAR data to calculate the area of cropped paddy fields. Haruyama *et al.*(2006) produced a landform map of the Mekong delta by using JERS-1/SAR data.

We used JERS-1/SAR data here to calculate the change in area of the wetlands and to determine the types of landform on which the land cover had changed. Furthermore, we used Chinese government statistical data (Chinese Statistics Publisher, 1992-1996) to verify the land cover changes that we calculated from the satellite data.

2. STUDY AREA

The Sanjiang Plain is in eastern Heilongjiang Province, where it lies between the courses of the Songhua, Amur, and Ussuri rivers. The plain is neighboring to Russia by the Amur and Ussuri rivers (Figure 1). There was an area which was unaffected by human activity, called

Figure 1. Sanjiang Plain and rivers. (The gray area shows the "triangular area" unaffected by human activity. Black circle shows the location of Hong Hua Natural Reservation Area..)

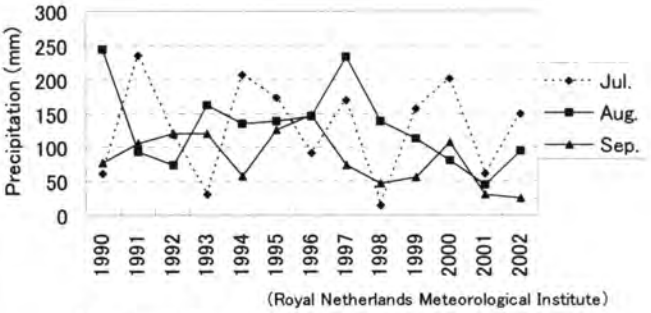

Figure. 2. Precipitation of July, August, and September from 1990 to 2002 at the Observation Station in Khabarovsk.

"triangular area" located the opposite side of Khabarovsk. Rainfall occurs mainly from July to September on the Sanjiang Plain. The KNMI (Royal Netherlands Meteorological Institute) station at Khabarovsk (Figure 1) is the nearest observation point to the study area. Rainfall data for July to September from 1990 to 2002 are shown in Figure 2.

Liu *et al.* (2005) studied the relationship between human activities and the natural environment in northeastern China and suggested that river water levels in this area tend to rise rapidly because unregulated cultivation of wetlands has reduced the size of flood-control basins. Runoff from reclaimed and cultivated areas causes both soil erosion and riverbed deposition of soil. In 1998, these effects contributed to the most serious flood ever recorded in Heilongjiang Province.

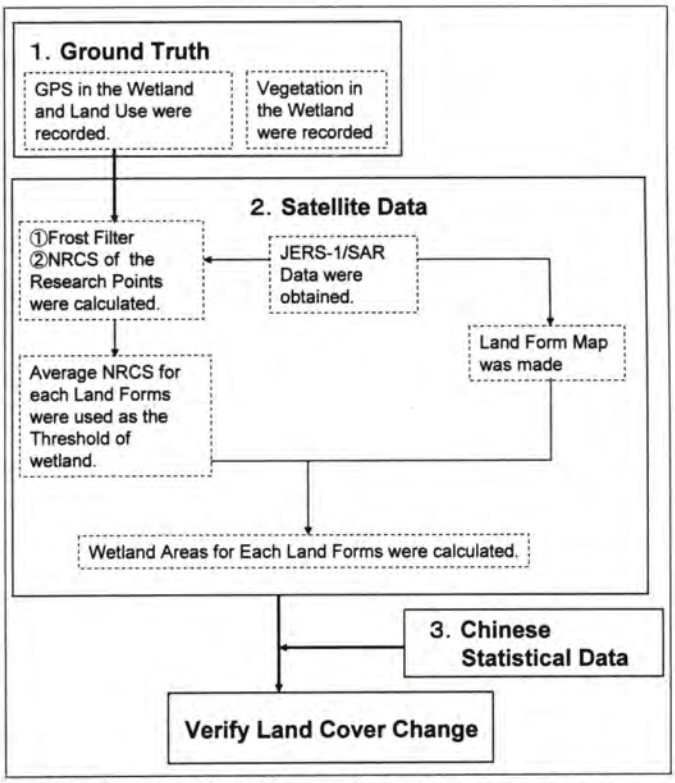

Figure 3. Flowchart of land cover change assessment by JERS-1/SAR.

The Sanjiang Plain is an important source of food for China. For example, in Jamus Prefecture, which is the main area of Sanjiang Plain, the cultivated area was 607000 ha, the soybean area was 36%, the rice area was 24%, the corn area was 17% in 2000 (Ganzey, 2005) However, environmental problems such as flooding and soil erosion have affected production in recent years. The Heilongjiang Province

government halted the cultivation of wetlands by a "wetland reservation enhancement declaration" in December 1998.

3. METHODS

Figure 3 shows a flowchart of the method employed.

3.1 Field research (ground truthing)

Ground truthing was carried out in the wetland of the Sanjiang Plain in September, because at that time field production is most differing seemingly and the paddy fields are dry. Thus wetlands and paddy fields could easily be distinguished by using the NRCS (normalized radar cross-section) from the JERS-1/SAR data. NRCS was used to make the SAR digital recordings independently of the equipment used. The algorithm used was:

$$\text{NRCS [dB]} = 10log_{10}(I^2) + CF$$

where I is the digital SAR value and CF is the conservation coefficient (Japan Photogrammetory Associates, 1998).

In the field study, positional information in the wetland area was recorded by a GPS (GARMIN eTrex Venture). Land use and vegetation on land neighboring the wetland were also recorded. The heights of slightly elevated areas were measured with a hand level (Nobel K50-1560).

3.2 Satellite data process

For comparison with the results of the September field study, two sets of seven sheets of JERS-1/SAR data were obtained, one set recorded in September 1992 and the other in September 1996. The dimensions of one sheet of JERS-1/SAR data are 6400 × 6000 pixels, and 1 pixel represents 12.5 × 12.5 m.

Landform map was constructed from the 1996 SAR data, based on observed textures and NRCS. SRTM (Shuttle Radar Topography Mission) data recorded by NASA in 2000 were also used to check the altitude.

A geometric correction based on the geodetic projection WGS84 was applied by using the nearest neighbor method. A Frost Filter which was proposed in 1982 by Frost *et al.* was applied to remove speckle noise, which was characteristic of the SAR data.

The GPS data were plotted on the corrected SAR data and NRCS values on the pixel where the ground truthing conducted were calculated.

The average NRCS values for each landform in the wetlands were used as threshold levels to determine the wetland area. The areas within Russia and along the northern Songhua River, and islands were ignored. The wetland areas of each landform on the Sanjiang Plain were then calculated.

3.3 Chinese statistical data

By using Chinese statistical data (Chinese Statistics Publisher, 1992–1996), the change in area cultivated per farmer from 1990 to 1996, the rural population change from 1989 to 1999, and the main areas of farm production from 1992 to 1996 were determined.

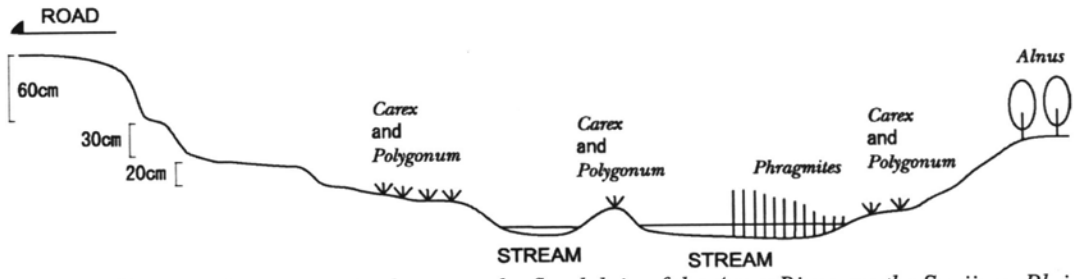

Figure 4. Cross-section of a wetland area on the floodplain of the Amur River, on the Sanjiang Plain.

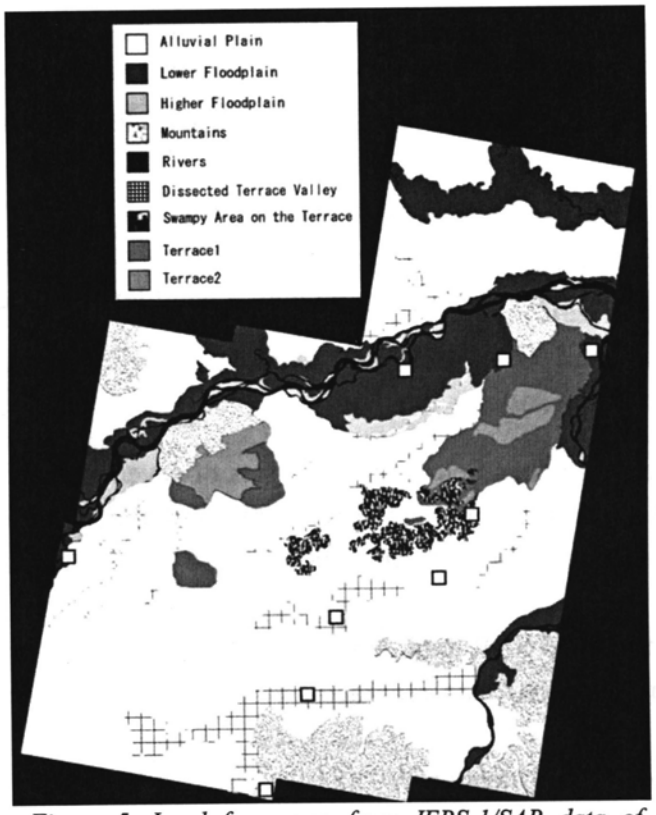

Figure 5. Land form map from JERS-1/SAR data of September 1996. Squares show the wetland areas where field investigations were carried out in this study.

4. RESULTS

4.1 Field investigation (ground truthing)

Field investigation of a wetland on the floodplain of the Amur River (Figure 4) revealed that the vegetation cover was mainly species of *Carex*, *Polygonum*, *Phragmites*, and *Alnus*. Land other than wetlands was cultivated for paddy fields, soybean, and corn.

4.2 Satellite data

For construction of the landform map (Figure 5), landforms were classified on the following basis. *River*: areas covered with water, including the Amur, Songhua, and Ussuri rivers and their tributaries. *Mountains*: areas of deep water table; lineations marking the valley borders were clearly identifiable on satellite images. *Floodplain*: areas around rivers where traces of water flow were clearly evident. Areas of shallow water table were defined as lower floodplains. Where a shallow water table was not evident, the area was defined as a higher floodplain. Natural levees were included in the higher floodplain classification. *Swampy area on the terrace*: scattered areas of deeper water table within dry area. *Dissected terrace valley*: areas of shallow water table, but without surface water. *Alluvial plain*: all areas not categorized above. Two terraces were observed on the alluvial plain.

The ranges of NRCS values for selected landforms were compared (Figure 6). The average NRCS value was lowest for dissected terrace valleys and highest for mountains. The widest range of NRCS values was calculated for the lower floodplain. The NRCS values showed multiple peaks in their distributions, for areas of alluvial plain and swampy areas on the terraces.

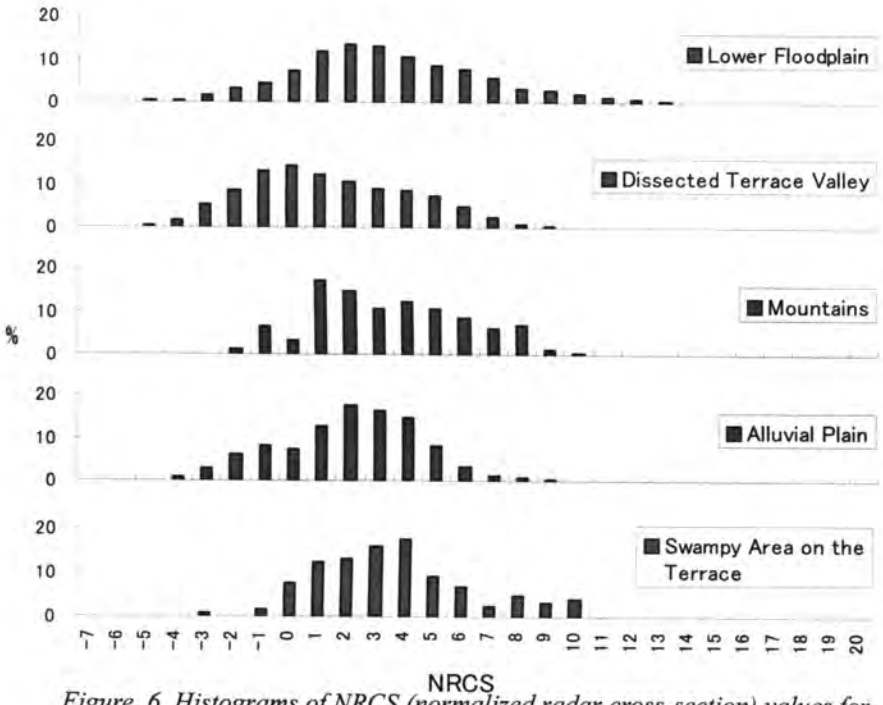

Figure. 6. Histograms of NRCS (normalized radar cross-section) values for selected wetland landforms.

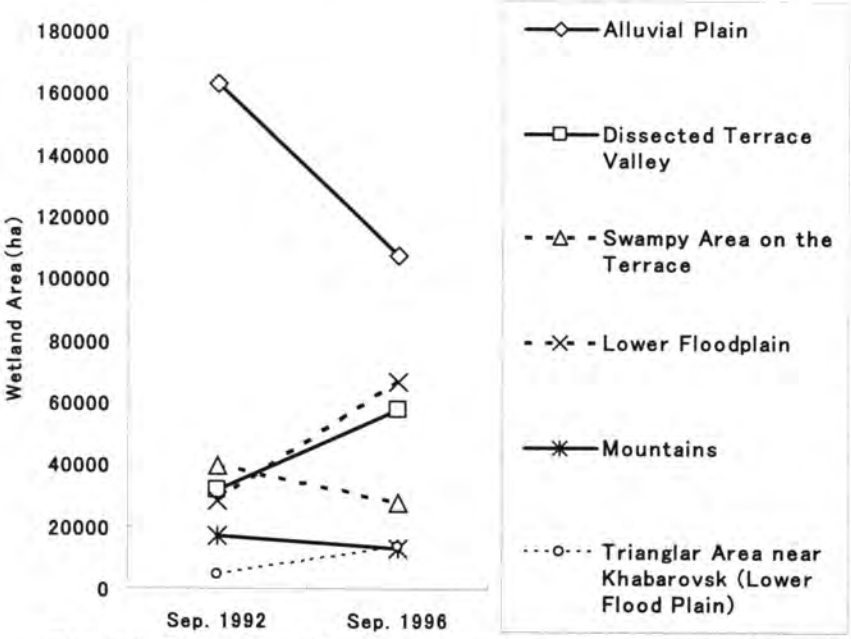

Figure 7. Comparison of areas occupied by each landform in 1992 and 1996, as calculated from JERS-1/SAR data. The "triangular area" near Khabarovsk was an area unaffected by human activity.

The average NRCS values for each landform in the wetlands were used to define the wetland threshold. These threshold NRCS values were applied to SAR images of 1992 and 1996. A comparison of the areas of each wetland landform in 1992 and 1996 (Figure 7) revealed that between 1992 and 1996 the wetland areas on the lower floodplain increased by a factor of 2.4; on dissected terrace valley they increased by a factor of 1.8; on the alluvial plain and swampy areas on the terraces they decreased by 34% and 30%, respectively; and on the mountains they decreased by 22%. The triangular area of lower floodplain land near Khabarovsk (Figure 1), which was unaffected by human activity, tripled in area.

4.3 Chinese statistical data

From 1990 to 1996 in Heilongjiang Province, the area of land cultivated per farmer increased by 10% and that of non-cultivated land decreased by 25% (Table 1). The population of farmers slightly decreased from 1994 to 1996, and the agricultural labor force increased slightly, from 5 382 000 in 1990 to 5 835 000 in 1996 (Figure 8). From 1992 to 1996, the area cultivated for paddy fields increased by 7%, for wheat fields decreased by 30%, for corn fields increased by 11%, for soybean fields increased by 20%, and the total cultivated area increased by 2% (Table 2).

Table 1. Areas (ha) of croplands, neglected lands, mining, and aquaculture per farmer in Heilongjiang Province in 1990 and 1996.

Category	1990	1996
Crop lands	1.119	1.236
Negrected lands	0.083	0.062
Mining area	0.005	0.005
Aquaculture	-	0.003

(Chinese Statistical Data)

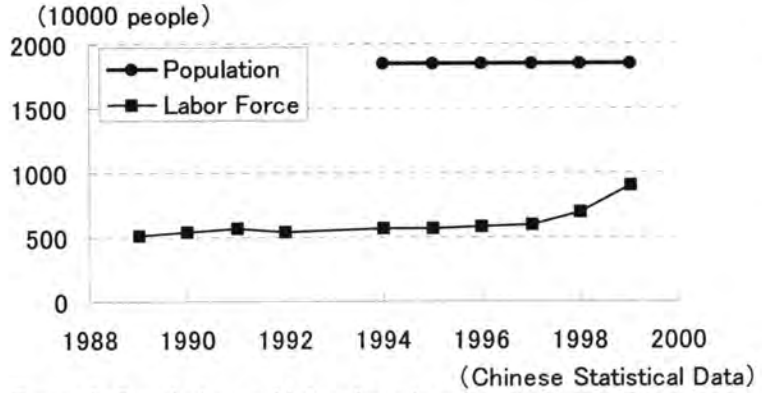

Figure 8. Population and labor force in an agricultural village in Heilongjiang Province.

Table 2. Total cultivated area and areas of main crops in Heilongjiang Province (1000 ha). There was no data of crop area in Chinese Statistical Data in 1995.

	1992	1993	1994	1995	1996
Total Seeding Area	**8479.4**	**8647.2**	**8670.0**	-	**8647.4**
Rice	778.4	735.5	747.1	-	835.1
Wheat	1614.6	1336.5	1198.5	-	1116.3
Corn	2165.9	1776.8	1964.2	-	2411.2
Soya	2160.2	3071.8	2940.9	-	2589.0

(Chinese Statistical Data)

5. DISCUSSION

The area of wetland in the triangular area of lower floodplain near Khabarovsk tripled from 1992 to 1996 (Figure 7). This can be attributed to high precipitation from July to September 1996 (Figure 2). However, from 1992 to 1996 the area of wetland decreased on the alluvial plain and in swampy areas on the terraces, but increased in dissected terrace valley. This suggests that cultivation of the wetlands on the alluvial plain and in old swampy areas decreased their capacity to hold rainwater and resulted in flow of rainwater into the old river courses (Figure 7).

The population of farmers slightly decreased from 1994 to 1996 (Table 1), but much crop lands were increased and much neglected lands were decreased per farmer (Figure. 8).

The total cultivated area increased from 1992 to 1996 (Table 2). The greatest increase in total area under cultivation on the Sanjiang Plain within Heilongjiang Province occurred from 1985 to 1995 (Singh and Himiyama, 2001), which suggests that this was the period when much of the wetlands of the plain were cultivated for paddy, corn, and soybean fields.

Depth to the water table in the Hong Hua Natural Reservation Area have been getting lower since the 1980s (Sanjiang Plain Wetland and Ecology Observation Station, unpublished data). Unregulated cultivation of wetlands has increased the frequency of flooding and the severity of soil erosion and salt accumulation, resulting in damage to the cultivated land. Continued flooding has the potential to make farming impossible on the lower floodplain. The extensive farmlands of the Sanjiang Plain are economically important; however, for them to remain sustainable, the wetlands must be preserved to provide a flood-control basin.

This study used quantitative analysis of satellite data over a large area to clarify the changes in land cover on the Sanjiang Plain from 1992 to 1996, and should thus contribute to planning for sustainable land use in the region.

ACKNOWLEDGEMENT

Many thanks to Yasuhiro KUWAHARA for FORTRAN programming work of SAR processing and GPS data plotting performed at the Abashiri Fisheries Experiment Station.

REFERENCES

Ganzey, S.S., 2005, Transboundary geo-systems in the south of the Russian Far East and in northeast China. Vladivostok Dalnauka. Vladivostok.

Singh, R.B., Fox J. and Himiyama, Y., 2001, Relationship between agricultural land use change and socioeconomic factors in north-east China in recent decades. *Land Use and Cover Change*, 239–245.

Shiraiwa, T., 2005, The Amur Okhotsk Project. *Report on Amur-Okhotsk Project,* No. 3. 1–2.

Japan Photogrammetry Associates, 1998, *Synthetic Aperture Radar Image Handbook* (Asakura Books, Tokyo) (In Japanese).

Dobson, M.C., Ulaby, F.T. and Pierce, L.E., 1995, Land-cover classification and estimation of terrain attributes using synthetic aperture radar. *Remote Sensing of Environment*, **51**, 199–214.

Hess, L.L., John, M.M., Evlyn, M. L. M. N., Claudio, C. F. B., Mary, G. (2003): Dual-season mapping of wetland inundation and vegetation for the central Amazon basin. *Remote Sensing of Environment*, 87, 404-428.

Ishizuka, N. (2006): Using synthetic aperture radar (SAR) for measuring the area of paddy fields. Noukankenpou, 24, 95-151. (In Japanese)

Haruyama, S., Shida, K. (2006): Assessment of flood risk by JERS-1/SAR in Mekong Delta. *Geoscience Journal*, 115(1), 72-86. (In Japanese)

Royal Netherlands Meteorological Institute (KNMI : Royal Netherlands Meteorological Institute): http://www.knmi.nl/ (data by observation point: http://climexp.knmi.nl/allstations.cgi?someone@somewhere+precipitation+12), 21/Aug/2006.

Liu, Y., Wang, D., Gao, J., Deng, W. (2005): Land use/cover changes, the environment and water resources in northeast China. *Environmental Management*, 36(5), 691-701.

Frost, V.S., Stiles, J.A., Shanmugan, J.A., and Holtzman, J.C. (1982): A model for radar images and its application to adaptive digital filtering of multiplicative noise. *IEEE Trans, Pattern Analysis and Machine Intelligence*, 4(2), 157-166.

Curtis, J.R., Randy, N. (2003): The Wetlands of China—an Overview. *Wetland Wire*, 6(2), 1-8.

Chinese Statistics Publisher (1992–1996): *Chinese Annual Statistical Books, 1992–1996.* Chinese Statistics Publisher, Beijing. (In Chinese)

GEOMORPHOLOGICAL RESEARCH IN SANJIAN PLAIN 2006

YAMAGATA K.[1], HARUYAMA S.[2], MASUDA Y.[2] AND MUROOKA M.[3]

[1]*Joetsu University of Education,*

[2]*Graduate School of Frontier Science, University of Tokyo,*

[3]*Hokkaido Abashiri Fisheries Experiment Station*

1. INTRODUCTION

The dissolved iron in watersheds is supplied from soil and bedrock whose chemical and physical properties influence the dissolution rate of iron and vary with regional environmental factors. Geomorphological condition is one of the important factors affecting the properties of soils and sediments, and the spatial distribution of soil and related environmental characteristics are vital for understanding the sources of iron. The processes of soil and sediment formation control their characteristics, and the spatial distribution of the characteristics of soils and deposits can be inferred by uncovering the process by which each geomorphological unit is formed. Thus, we began by analyzing the topography of the Amur River basin, and because fluvial deposits record recent environmental changes in the watershed, including the impact of human activities, we sought to reconstruct the historical environmental changes in the Amur River basin using the floodplain sediment, which provided information on past environmental variations in the catchment.

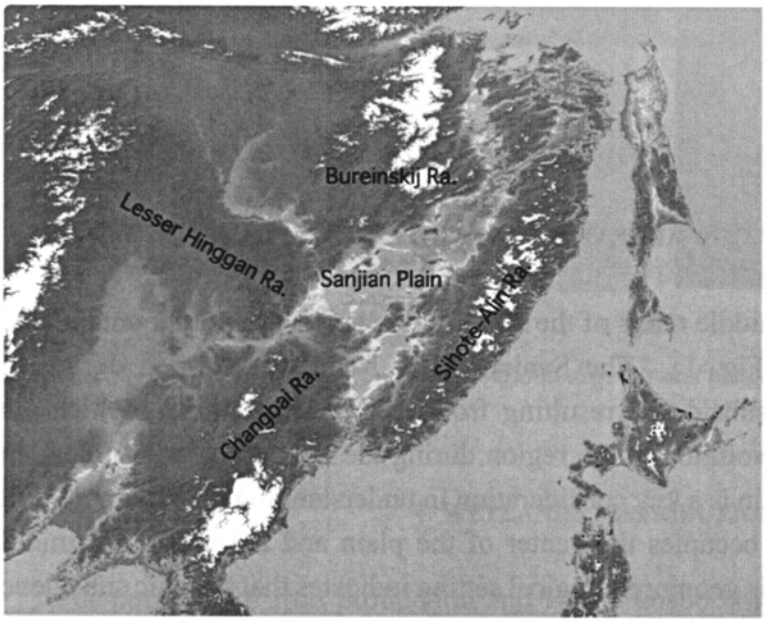

Figure 1. Topography of the middle and lower reaches of the Amur River.

2. METHODS

In 2006, we focused on the Sanjian Plain in Northeast China. We analyzed its topography and wetlands with remote sensing, and developed a preliminary geomorphological classification map of the Sanjian Plain. Geomorphological land classification mapping is basis of research directed toward classifying land cover change and investigating fluvial processes. The map classifications are then compared and verified with actual ground observations in the field.

The field survey was conducted during 19–29 September 2006 in the Sanjian Plain with the cooperation of the Northeast Institute of Geography and Agricultural Ecology, Chinese Academy of Sciences. We investigated soil and sediment profiles in each topographic unit throughout the Sanjian Plain unit and collected continuous, 2–3-m sample profiles from outcrops or sediment cores using hand boring equipment and a geoslicer (Photo 1).

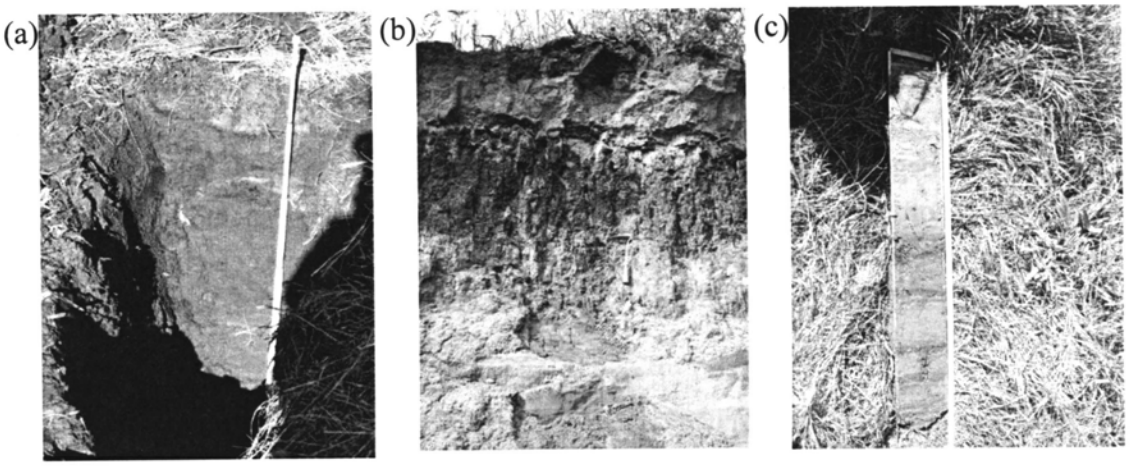

Photo 1. Soil and sediment profiles of a pit (a) and an outcrop (b). (c) Geoslicer.

3. GEOMORPHOLOGICAL FEATURES OF THE SANJIAN PLAIN

The Sanjian Plain is in the middle reach of the Amur River and is an intermountain basin formed by tectonic movement (Fig. 1). The Sanjian Plain basin was formed during the Quaternary period by intensive subsidence resulting from tectonic movements, which also influenced the geomorphologic evolution of the region during the Holocene epoch. Thus, the geomorphology of the alluvial plain is a key consideration in understanding the region's fluvial processes. A large swampy area occupies the center of the plain and the upper and middle terraces surrounding the plain. This geomorphological setting indicates that tectonic subsidence has been continuous since the early Quaternary.

Although the alluvial surface in the basin is extremely flat, several levels of fluvial terraces were identified. The geomorphology of the Sanjian Plain is classified into nine categories: mountain and hill, upper terrace, middle terrace, lower terrace, terrace-incised valley, residual river course, natural levee, floodplain, and the present river floor. Each terrace could be further

subdivided into several levels. The lower terrace occupies a large area of the Sanjian Plain basin and the present meandering river shallowly dissects the surface.

Peat sediments occur on each surface (Fig. 2). The peat layer on the middle terrace is covered by eolian loess and is completely decomposed (Figs. 2–6). The terrace is additionally composed of thick gravel deposits. Thus, the middle terrace is assumed to have been formed during the last glacial period.

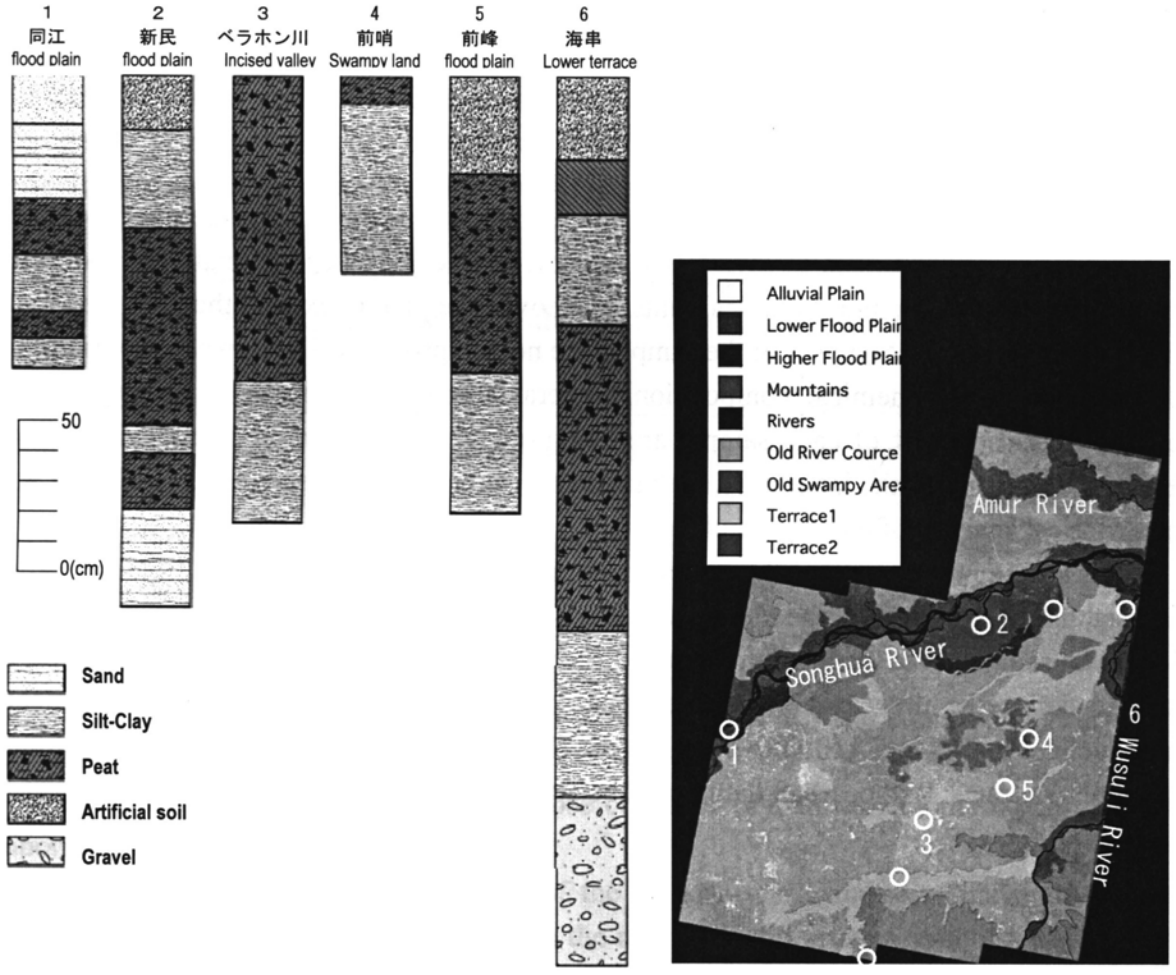

Fig. 2. Columnar sections of fluvial and wetland deposits and the geomorphologic classification map of the Sanjian Plain.

4. WETLANDS DISTRIBUTION

For purposes of iron production and river transportation, swamps and wetlands are the topographical units of greatest interest. As a large area of the Sanjian Plain is occupied by wetlands, the plain is important for the production and transport of iron to the main Amur River. However, the wetlands area in the Sanjian Plain has been decreasing rapidly in recent years because of farmland encroachment.

The wetlands are located on terraces covered by clay sediments and on the floodplains and

incised valley floor. Peat sediments occur in most of the wetlands, and the thickness of the peat deposits varies with the topography. Most of the peat deposits forming at present on the floodplains along Heillonjian, Songhua, and Wusuli rivers are less than several tens of centimeters thick. In contrast, thick peat deposits are found on the incised valley floor.

Recent coarsening of fluvial deposits occur at many localities on the floodplain along the Heillonjian, Songhua, and Wusuli rivers, where peat and silt–clay layers are covered by sandy deposits (Figs. 2-1 and 2-2). This is thought to be caused by farmland exploitation in the hilly terrain and indicates that the interruption of peat formation and the decay of wetland pose continuing problems.

5. FUTURE STUDY

We require additional verification on the ground to complete the geomorphological classification map, and need to investigate the soil profiles and depositional composition of currently undefined geomorphological units. Moreover, we plan to expand the map area in the downstream direction. Analyses of the samples are now in progress. The downcore variation in physical properties, chemical composition, mineral composition, magnetic properties, and micro-charcoal content of each sample are being analyzed to ascertain paleoenvironmental changes. The result of the laboratory analyses of the sediment samples will be combined with the historical analysis of the maps and data.

It is also important to trace the sediment sources in studying variations in these properties. To establish the source of the floodplain deposits, we will compare the properties of the floodplain sediments of the Sanjian Plain and each branch of the Amur River. Furthermore, we need to define the time axis for the sediment profiles. We plan to use the environmental radionuclides 137Cs and 210Pb to establish the chronology and to estimate average sediment accumulation rates. Radiocarbon dating will be applied as needed.

SOME ASPECTS OF FOREIGN TRADE RELATIONS OF THE AMUR-OKHOTSK REGION'S COUNTRIES

MISHINA NATALIAV.
Pacific Institute of Geography, Far Eastern Branch, Russian Academy of Sciences

Present-day transformation of natural environment of the Amur River basin is mostly determined by economic activity of human being. Intensity, the level and trends of land utilization in China and Russia arise from natural land conditions as well as from wide range of economic, social and political reasons. Some driving forces of land-use changes emerge and operate primary inside one country while other have international character like foreign trade. It has been known that the rise of resources demand in one country may result in their more intensive utilization and have negative environmental consequences in other. From that point of view land-use situation, capacity and restrictions of resources use in the Amur-Okhotsk region are strongly connected with the international trade among China, Russia and Japan.

Wood, marine and agricultural products are of the most importance in studying resources' and primary products' flows between principal countries of the Amur-Okhotsk region. Certainly the research of resources flows on the regional level of the Russian Far East and the Northeast part of China where the largest part of the Amur River basin is located are the most interesting and important. However for the analysis of the situation in separate regions it is necessary to understand the main features and tendencies of the whole country. That is why principal stages of that study are as follows.

1. Comparative analysis of the main indices, geographical and commodity structure of foreign trade of China, Russia and Japan.

2. Studying of the mutual trade of those countries (dynamics, commodity structure of import and export, principal partners).

3. Investigation of the participation of the Russian and Chinese administrative unites located within the Amur River watershed in the resources and primary products trade among China, Russia and Japan.

4. Analysis of interaction between the resources trade and land-use changes on the regional level of the Amur River Basin.

The basic source of data for resources and primary products exchange is national foreign trade statistics. The most part of data needed to carry out the first and second stages of the investigation was gathered in Japan during the author's work in Research Institute for Humanity and Nature (Kyoto) as an invited research fellow in April – October 2006. Some results of data analyzes for the period 1995-2004 are presented in this paper.

Comparison of few principal indicators of Russia, China and Japan (Table 1) represents significant contrast of the Amur-Okhotsk region. Average population density of Japan almost in 2,5 times exceeds a similar parameter of China and more than in 40 times the Russian one. GDP and GDP per capita of Japan exceed the Russian indicators almost in 15 and 17 times respectively whereas the difference between indicators of Russia and China is not so large.

Table 1. Some major country's indicators, 2004 [2, 7-8]

Indicator	Japan	Russia	China[1]
Total area, thous. km^2	387	17075	9597
Population, thous. persons	127687	144200	1299880
Population density, persons / km^2	342.4	8.4	135.4
GDP, millions of US $	4945121	329746.9	1653090.6
GDP per capita, US $ / person	38728	2287	1271

1- Excluding Taiwan, Hong Kong and Macao

The basic parameters of foreign trade of the Amur-Okhotsk region's countries also essentially differ (Fig. 1). In period from 1997 to 2001 Japan had rather significant fluctuations of export-import volumes and in 2001-2004 the stable expansion of the foreign trade turnover is observed. In China rapid growth of trade parameters took place since 1998. By 2004 foreign trade turnover of China has exceeded that of Japan. The balance of foreign trade in all examined countries was positive during 1995-2004.

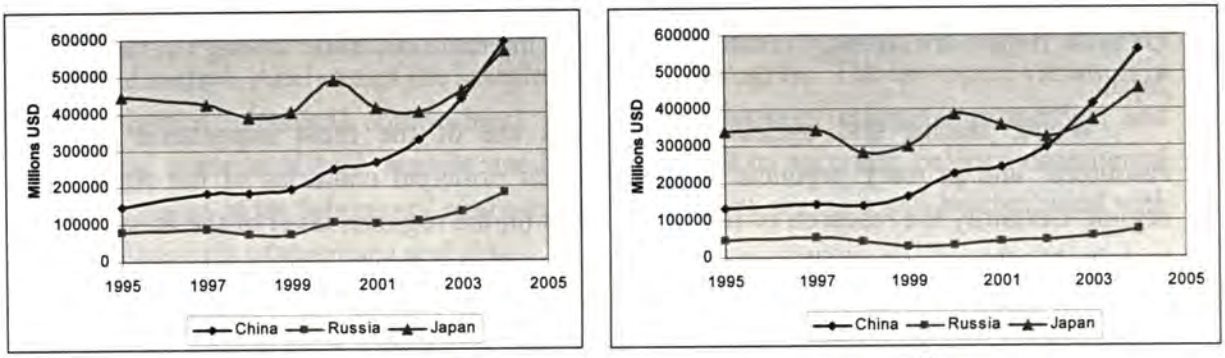

Fig. 1. Dynamic of export (A) and import (B) value of Amur-Okhotsk countries [1-2, 6-9]

More detailed analysis of data for 2000-2004 (Table 2) allows us to draw a conclusion that Japan had the most stable foreign trade activity during this period. Trade of balance of Japan increased in 9.5 % and turnover in 17 %. In the period under consideration the greatest growth of balance has taken place in Russia (more than on 50 %) in spite of the fact that expansion of import volumes was higher than export's rise. The trade of China was the most dynamical, it's foreign trade turnover has increased in 2.4 times. As well as in two other countries Chinese rates of import's growth were higher than export's parameters.

Table 2. The principal foreign trade indices, billions of US$ [2, 7-8]

Indices	Japan		China		Russia[1]	
	2000	2004	2000	2004	2000	2004
Total value	873.5	1022.1	474.3	1154.5	137	257.3
Export	487.3	566.4	249.2	593.3	103.1	181.7
Import	386.2	455.7	225.1	561.2	33.9	75.6
Foreign trade turnover	+101.1	+110.7	+24.1	+32.1	+69.2	+106.1

[1] Custom statistics

The commodity structure of export and import of the considered countries is also not equal. For the Russian export the high share of mineral products is characteristic. Mineral fuel, oil and materials of their processing form the most part of that group of goods. Its share in

exports of Russia increased from 42% up to 64 % from 1995 to 2005 [8-9]. The commodity structure of the Japanese export is defined by significant share of the machinery and transport equipment (66 % of exported production in 2004) [7]. The estimation of export structure of China is difficult because of a big part of industrial output unshared on categories of customs statistics. Nevertheless it is possible to note that in 2004 the greatest part of export was composed by goods of light and textile industry, rubber products, nonmetals and metallurgical production (27 %). Nonfood raw material had also significant specific weight in China exports (16 %) [1-2].

As a whole according to the United Nations international trade data (Table 3) the share of manufactured products in the Russian export was about 52 % in 2002. If to take into account that a number of industrial goods such as nonmetallic minerals, the basic metals and a significant part of wood are not deeply processed, then the share of raw materials in export can be increased approximately up to 60 %. China and Japan are defined by a significant part of the manufactured goods in their exports (95% and more 99 % respectively).

Table 3 Exports by industrial origin in 2002, % of total value [5]

Descriptions	China	Japan	Russia
Total exports	100	100	100
Agriculture	2.6	0.3	3.2
Mining quarry	2.2	0.1	44.6
Manufacturing	95.2	99.6	52.2
- Food, beverages, tobacco	2.8	0.4	0.7
- Textiles	23.1	1.6	0.7
- Wood and products	0.9	0.0	1.3
- Paper and products	0.7	0.7	1.8
- Chemicals	9.6	11.1	16.6
- Non metal minerals	1.7	1.0	0.3
- Basic metals	2.5	4.9	13.0
- Metal manufactures	48.0	74.6	8.2
-Other manufactures	6.0	5.4	9.7

The commodity structure of import of Russia is characterized by high specific weight of the machinery and transport equipment increased from 40 % in 2003 up to 44 % in 2005, and a significant share of agricultural raw materials and foodstuffs (28 % and 18 % in 1995 and 2005 respectively) [8-9]. The structure of Japanese import, as well as export, is various and roughly well balanced by ratio of different commodity groups. Each of such commodities as general and electronic machinery, foodstuffs, and manufactured goods make up approximately 10-15 % of imported production. The fuel's import has the more significant volumes only (20 % of import 2004) [7]. In China in 2004 the commodity-leader on volume of import was the group of the goods including light industry products, the nonmetallic and metallurgical goods, rubber (22 %). The share of the goods of the chemical industry has made up 20 %, nonfood raw material had almost the same specific weight (increase in 9 % since 1995) [1-2]. Thus, raw materials made up about 25 % of import of Russia in 2003 (foodstuffs, agricultural raw material, wood, etc.). In Japan and China such goods composed about 30 % of imports.

The analysis of a geographical structure of foreign trade of the examined countries has shown that today China and Japan are the major foreign trade partners for each other (Table 4). These countries also play a significant role in export and import of Russia whereas latter is not included in number of "top five" partners of China and Japan.

Table 4 Five principal foreign trade partners of Amur-Okhotsk region's countries, % of export (import) total value [2, 7-8]

Foreign trade	China, 2004	Japan, 2004	Russia, 2005
Export	USA (21%) Hong Kong (17%) **Japan (12.4%)** Republic of Korea (4.7%) Germany (4.0%)	USA (22.4%) **China (13.1%)** Republic of Korea (7.8%) Germany (3.3%) Singapore (3.2%)	Netherlands (10.2%) Germany (8.2%) Italy (7.9%) **China (5.4%)** Turkey (4.5%)
Import	**Japan (16.8%)** Taiwan (11.5%) Republic of Korea (11.1%) USA (7.9%) Germany (5.4%)	**China (20.7%)** USA (13.7%) Republic of Korea (4.8%) Australia (4.3%) Indonesia (4.1%)	Germany (13.5%) **China (7.4%)** **Japan (5.9%)** USA (4.6%) Italy (4.6%)

While carrying the comparative analysis of foreign trade of the Amur-Okhotsk countries, conformity of export volume of one country, for example of Japan to Russia, to import volume of Russia from Japan, and on the contrary was assumed. However, comparison of the foreign trade data from official statistical sources of Russia, China and Japan has shown their essential divergence. So in 2004 the Chinese parameters describing export and import of China to Russia exceed the Russian data on import and export to China on 20 % (Table 5). Volumes of import of China from Japan exceed the Japanese data of export to China approximately on 30 % whereas the Chinese data on export to Japan less than value of the import published by the Japanese statistical service also almost on 30 %. Distinction of export volumes of Russia to Japan and value of import of the Japanese side reaches 40 %. Difference of the Russian import from Japan and the Japanese export is not so great (26 %).

Table 5 Mutual foreign trade of the main countries of Amur-Okhotsk region in 2004 according to the state statistical sources, mln USD [2, 7-8]

		Export		
		Russia	China	Japan
Import	Russia	---	9098 / 7576	3120.4 / 3941
	China	10105 / 12127.4	---	74018.5 / 94326.7
	Japan	3404 / 5713	73509 / 9443562	---

Divergence of foreign trade volumes is so considerable that last years data on negative or positive character of Japan-China and Japan-Russia (Table 6) trade balance do not coincide too. According to the Chinese data in 2002 and 2004 imports from Japan exceeded export to

Japan, whereas the Japanese statistical data shows essential dominance of imports volume from China above value of export to China.

Difference of those data caused most likely by methods of import and export calculation in each of the countries. It is forced us to examine mutual foreign trade of the Amur-Okhotsk countries separately from positions of Russia, China and Japan. In accordance with data of table 6 the volume of the foreign trade operations of Russia is essentially less than that of China and Japan. Since 2002 the leading position by volumes of trade between the countries of the region is occupied by China.

Table 6 Dynamics of Foreign Trade, mln USD [1-2, 6-9]

Countries		Exports				Imports			
		1995	2000	2002	2004	1995	2000	2002	2004
China	Japan	28462.7	41654.3	48433.8	73509	29004.7	41509.7	53466	94326.7
	Russia	1664.7	2233.3	3521.7	9098.1	3798.4	5769.9	8406.7	12127.4
Japan	China	22172.0	30886.8	38307.7	74018.5	36354.8	56047.2	59446.2	94435.2
	Russia	1161	575.5	907.7	3120.4	4784	4660.4	3153.8	5713
Russia	Japan	3174	2764	1803	3404	763	572	980	3941
	China	3371	5248	6837	10105	865	949	2401	4746

In spite of the bigger volumes of Chinese trade with Japan in 1995-2004, the trade of China and Russia developed more actively. Import volumes from Russia to China exceeded volumes of export, but exports to Russia from China extended more rapidly - it increased in 5 times for 9 years. In Chinese trade with Japan growth of import volumes was higher. It also corresponds to Japanese statistical data specifying more intensive expansion of export deliveries in trade with China (more than in 3 times for 9 years). As a result China's share in export and import of Japan increased in 8 and 10 % respectively.

In Table 7 the commodity structure of Japan export to China and Russia is presented. It shows that more than 50 % of all Japanese export to China was made by machinery and transport equipment both in 1995 and 2004. Specific weight of raw materials in total amount of imported goods to China has changed insignificantly (by 1.1 %), however its value has increased in 5 times. Therefore the share of China in the total Japanese export of raw materials has changed from 9 up to 35 % (basically synthetic rubber, steel and scrap iron).

Table 7 Value and structure of Japan exports by principal commodity to Russia and China [7, 12]

Commodities	China				Russia			
	mln USD		% of total value		mln USD		% of total value	
	1995	2004	1995	2004	1995	2004	1995	2004
Foodstuffs	93.0	295.2	0.4	0.4	5.7	25.9	0.5	0.8
Raw materials & mineral fuels	525.0	2649.3	2.4	3.5	22.4	10.9	1.9	0.3
Chemicals	2040.0	9180.1	9.3	12.4	29.3	36.4	2.5	1.2
General machinery	6066.0	17076.5	27.7	23.1	439.5	398.8	37.6	12.8
Electric machinery	4806.0	19440.6	21.9	26.3	310.5	320.2	26.5	10.3
Transport equipment	941.0	4197.8	4.3	5.7	97.0	1967.8	8.3	63.0
Other	7460.1	21181.1	34	28.6	265.7	362.9	22.7	4.4
Total	21931.0	74020.7	100	100	1170.1	3122.9	100	100

The Japanese export to Russia during 1995-2004 increased the values of all commodity groups except for raw material and mineral fuel, but the significant gain was observed only in categories of foodstuffs and transport equipment. The growth of transport's share in export from Japan was huge from 8 up to 63 %. As a whole both in 1995 and 2004 the most part of the Japanese export to Russia was made by machinery and transport equipment, 84 and 86 % respectively. Their share in the all-Russian import of the given category of goods in 2004 has reached almost 13 % [4]. It is necessary to note that the structure of the Japanese export to Russia, estimated with the Japanese data basically coincides with the structure of import from Japan made by the Russian materials (Table 9).

Thus, Japan for China and Russia was and remains the supplier of the manufactured goods. According to JETRO (Japan External Trade Organization) in 1985-2000 their share in export to China made up 95-98 %. In the Japanese export to the USSR and then to Russia the specific weight of industrial production gradually increased from 90 up to 98 %, and its significant part was composed by products of machinery and transport equipment (also made growth with 40 up to 70 %) [10-13]. Comparison of the commodities of the Japanese industrial goods taken out to China and Russia shows that the structure of export to China is more balanced on shares of separate commodities whereas in export to Russia one category of the goods dominates.

Manufactured goods (including in field "other" at Table 8), machinery and transport equipment were the basic kind of products imported from China to Japan in 2004. Besides it Japan traditionally exports from China a plenty of foodstuffs (15 % of the total Japanese import of foodstuffs, 20 % of fish and 60 % of vegetables in 2004). Among raw goods the principal are wood, agricultural and textile raw materials. Totally Japan imported about 5 % of all primary goods from China and 3.2 % from Russia.

Table 8. Value and structure of Japan imports from Russia and China by principal commodity [7, 12]

Commodities	China				Russia			
	mln USD		% of total value		mln USD		% of total value	
	1995	2004	1995	2004	1995	2004	1995	2004
Foodstuffs	4704.1	7413.2	13.1	7.9	1353.1	1094.8	28.4	19.2
Raw materials	1354.6	1550.7	3.8	1.6	837.1	932.7	16.9	16.3
Mineral fuels	2097.1	3252.4	5.8	3.4	347.1	1469.3	7.3	25.7
Chemicals	1332.7	3048.6	3.7	3.2	53.7	74.8	1.8	1.3
Machinery & transport	5161.7	34026.0	14.4	36.0	5.1	7.3	0.1	0.1
Other	21271.9	45144.0	59.2	47.8	2166	2136.9	45.5	37.4
Total	35922.3	94434.8	100	100	4763.3	5715.8	100	100

As for import of Japan from Russia in 2004 the manufactured goods were leading by value and share commodity (36 %). The most part of that category of goods was composed by metal products. On JETRO data in 2000 Russia played a significant role in the Japanese import of lead and zirconium ores [13], and in 2005 about 33 % of all the Russian export to Japan fell at aluminium and its products [4]. Foodstuffs also have significant specific weight in import from Russia, 98 % of which consisted of fresh, chilled or frozen fish and seafood. 9/10 of raw materials imported by Japan from Russia are wood (mainly a round wood). For

the last 10 years an active growth of mineral fuel and oil imports is also observed. It is necessary to note that according to the data of the Japanese statistics the balance of trade with Russia was negative in 2004, and from the Russian data follows that trade with Japan was also negative (Table 6). Nevertheless the commodity structure of Japanese import from Russia compiled on the basis of the Japanese data practically has no divergences with structure of the Russian export to Japan Ttables 8, 10).

As whole modern structural changes of the Japanese import from China and Russia are the continuation of the processes that has started in the middle 1980s. Data of Table 9 confirm that during the last 20 years the shares of foodstuffs, raw material and fuel imported by Japan from China systematically reduced, and the share of manufactured goods actively increases. The specific weight of equipment and transport in the Chinese import at the beginning of the 1990s was only 3 %, thus the share of the given category has increased in more than 30 % for 15 years.

Table 9 Generalized structure of Japan import, % of total value [10-13]

Commodities	1985	1990	1995	2000
	China			
Foodstuffs	14.4	16.1	13.1	10.7
Raw materials & mineral fuels	58.6	33.2	9.6	6.6
Manufactured goods	24.7	50.2	76.9	82.7
Other	2.3	0.5	0.4	0.8
Total	100	100	100	100
	Russia			
Foodstuffs	7.1	9.6	28.4	28.6
Raw materials & mineral fuels	56.8	38.4	24.9	20.1
Manufactured goods	24.7	44.0	43.5	51.2
Other	11.3	8	3.2	1.6
Total	100	100	100	100

In import from the USSR and Russia till 2000 the share of raw material and the mineral resources also reduced. But that process was accompanied by growth of specific weight of fish and seafood, and different sorts of metal products made up and makes up 80-90 % of the manufactured goods of import. Besides that after 2000 significant growth of mineral fuel imported from Russia is observed (from 48.7 up to 139.5 billion US dollars in 2005), that essentially changes the commodity structure of foreign trade with Russia.

From the Russian position the volume of its export-import transactions with China extends more intensively than with Japan though the values of the foreign trade turnover with these countries are comparable, and import from these countries increases higher rates than volumes of export (Table 6). In structure of the Russian export to China (Table 10), as well as in trade with Japan the raw material and superficial processing production have significant shares. In the value of the goods taken out from Russia in 2004 mineral products (actually fuel and energy goods) had the greatest share. It is necessary to note that in 2000 the value and share of oil and fuel in export was in 8 times less than in 2004 [3-4].

Table 10 Value and structure of Russia foreign trade by principal commodity to China and Japan in 2004 [4]

Commodities	China				Japan			
	Export		Import		Export		Import	
	Mln USD	%	Mln USD	%	Mln USD	%	Mln USD	%
Foodstuff and agricultural raw	112.6	1.1	440.5	9.3	93.5	2.7	10.8	0.3
Mineral products	3085.8	30.5	87.2	1.8	914.8	26.9	10.2	0.3
Chemicals, rubber	1268.3	12.6	366.4	7.7	47.2	1.4	153.8	3.9
Wood, pulp and paper	1408.8	13.9	88.5	1.9	660.2	19.4	7.4	0.2
Textile materials and products, footwear	8.3	0.1	744.7	15.7	1.1	0.0	2.1	0.1
Metals and metal products	1620.3	16.0	276.3	5.8	1425.3	41.9	276.5	7.0
Machinery & transport equipment	1030.2	10.2	2012.6	42.4	17.1	0.5	3388.6	86.0
Other	1570.7	15.5	730.0	15.4	244.5	7.2	91.4	2.3
Total	10105.1	100	4746.2	100	3403.9	100	3940.9	100

Metals, basically black (about 80 %), and their products take the second place in export volumes. The share of that group of goods in structure of the Russian export to China was reduced to 12 % since 2000. The share of timber taken out in 2004 was kept at the level of 2000 due to almost a double increase of its value (from 763.7 million up to 1.4 billion USD). The share of foodstuffs in the Russian export to China was low, and more than 60% of that production made fish and seafood. Such industrial goods as machines, equipment and vehicles, and the goods of the chemical industry formed about 20 % of the exports.

In the import of the Chinese production to Russia in 2004 the greatest share belongs to products of machinery and transport equipment (Table 10). The share of that commodity rose in 30 % since 2000, and its value has grown in 18 times [3-4]. Stable position in structure of the import from China is occupied by textile production and footwear (from 149 up to 745 million USD in 2000-2004). The foodstuff has the greatest specific weight out of the goods which we considered as resource. Its value has increased in 3 times for the 4-years period, but the share in total amount of the imported goods was reduced almost by 7 %. In 2004 meat and meat products, vegetables, fruit and nuts, and their products which formed 60 % of foodstuff's value became basic objects of deliveries from China. In total 4 % of foodstuffs [4] were imported from China to Russia. As a whole import from China, as well as from Japan, differs by a high share of an industrial output significant part of which is made by the consumer goods.

On that transitional stage of the research we can make a few main conclusions. The analysis of foreign trade among the Amur-Okhotsk countries has shown that it has the basic tendencies inherent to trade of Russia, China and Japan. Among the given countries Russia has the least values of foreign trade, and in mutual trading contacts it takes the last place. In deliveries from Russia as a whole a share of a fuel and energy component increases, the share of metals and their products reduced, export of wood kept at some rather stable level. Those trends find reflection in the Russian-Chinese and Russian-Japanese trading contacts. In China increase in a share of the manufactured goods and expand of the import of raw material and

fuel is typical. And that situation is also represented in the Chinese trade with Russia and Japan.

For last 5-10 years China and Japan became for each other the leaders by the value of export-import operations, mainly due to escalating of trade by manufactured goods. Significant participation of those countries in the foreign trade turnover of Russia has the same reason while Russia remains for them mostly the supplier of raw material and not deeply processed production. But the Russian participation in maintenance of the raw-material base of Japan and China is essentially lower than a share of the given countries in import of the industrial goods by Russia.

Further investigation of foreign trade relations of Amur-Okhotsk countries in a greater degree will be looked to the trade of selected resources. The scale and level of the study will be mainly depended on details of accessible statistics.

In conclusion I would like to express my acknowledgement to Prof. Shiraiwa for the idea of resources flows study, as well as for the possibility of interesting work at the Amur-Okhotsk project and RIHN.

REFERENCES

1. Chinese Statistical Yearbook, 2000. Beijing: China Statistics Press, 2000. 864 p.
2. Chinese Statistical Yearbook, 2005. Beijing: China Statistics Press, 2005. 915 p.
3. Customs statistics of foreign trade of Russian Federation, 2001: Moscow: Federal custom service, 2002. 507 c.
4. Customs statistics of foreign trade of Russian Federation, 2005. Moscow: Federal custom service, 2006. 751 p.
5. International Trade Statistics Yearbook. Vol. I. New York: UN Department of Economic and Social Affairs Statistics Division, 2004. 693 p.
6. Japan Statistical Yearbook, 2002. Tokyo: Statistical Research and Training Institute and Statistics Bureau of the Ministry of Internal Affairs and Communications, 2002. 921 p.
7. Japan Statistical Yearbook, 2006. Tokyo: Statistical Research and Training Institute and Statistics Bureau of the Ministry of Internal Affairs and Communications, 2006. 893 p.
8. Russia in figures. Federal state statistical service – http://www.gks.ru, 2006.
9. Russian statistical yearbook, 2004. Moscow: Russian statistical committee, 2004. 725 p.
10. White paper on International trade Japan. Tokyo: JETRO (Japan External Trade Organization), 1986. 426 p.
11. White paper on International trade Japan. Tokyo: JETRO (Japan External Trade Organization), 1991. 427 p.
12. White paper on International trade Japan. Tokyo: JETRO (Japan External Trade Organization), 1996. 398 p.
13. White paper on International trade Japan. Tokyo: JETRO (Japan External Trade Organization), 2001. 371 p.

PRELIMINARY REPORT ON CHEMICAL ANALYSIS OF AEROSOLS COLLECTED AT OKTYABR'SKY, KAMCHATKA, RUSSIA

MATOBA S.[1], MINAMI H.[2], NARITA Y.[3] AND UEMATSU M.[3]

1 Institute of Low Temperature Science, Hokkaido University

2 Hokkaido Tokai University

3 Ocean Research Institute, the University of Tokyo

INTRODUCTION

Mineral dust containing iron from the Asian continent is transported eastward over the North Pacific, especially spring (Uematsu et al., 1983). The air-borne iron is considered to be the only one source of input in the central part of the northern North Pacific. In fact, it was found that a near doubling of biomass production was observed in the mixed layer in the North Pacific over a 2-week period after the passage of a cloud of Gobi desert dust (Bishop et al., 2002). The Amur-Okhotsk Project propose that main source of dissolved iron in the Sea of Okhotsk associated with marine product is the Amur River. However, the contribution of the air-borne iron to the marine product in the Sea of Okhotsk cannot be negligible. Therefore, we have to precisely evaluate the contribution of air-borne iron deposited on the Sea of Okhotsk. In order to estimate flux of air-borne iron transported from the Asian continent to the Sea of Okhotsk, We carried out aerosol sampling at Oktyabr'sky, Kamchatka, Russia from Octorber 2005. Here we report the preliminary data of aerosol sampling and chemical analysis.

AEROSOL SAMPLING

Oktyabr'sky, where aerosol sampling was conducted, is in the southwestern part of the Kamchatka Peninsula (Fig1). It is in a middle of sandspit which faces the Sea of Okhotsk on the west side, and the Bolshaya River and wet land on the east side. An aerosol sampler system (ACS-21: Kimoto Electric Co., LTD.) was installed in a small house facing the Sea of Okhotsk in the middle of Oktyabr'sky in October 2005. The sampler was established on the 2nd floor of the house, and connected a polyvinyl chloride pipe which was penetrated through a roof of the house. Ambient air was inhaled through the pipe by the aerosol sampler (Fig 2). The sampler system has a computer to record data of sampling condition (flow rate, running time and so on) and meteorological condition which is monitored by an aerovane and a thermometer installed on the roof of the house during sampling. The sampler also has a control unit to confine the meteorological condition when the sampler runs. There were two chimneys of factory or power station in Oktyabr'sky, and we could see them on the roof of the house. To prevent from contaminating emission from their chimneys, aerosol was sampled only when wind direction was within 170-340° and wind speed was more than $1.0 m \cdot s^{-1}$ (Fig. 3).

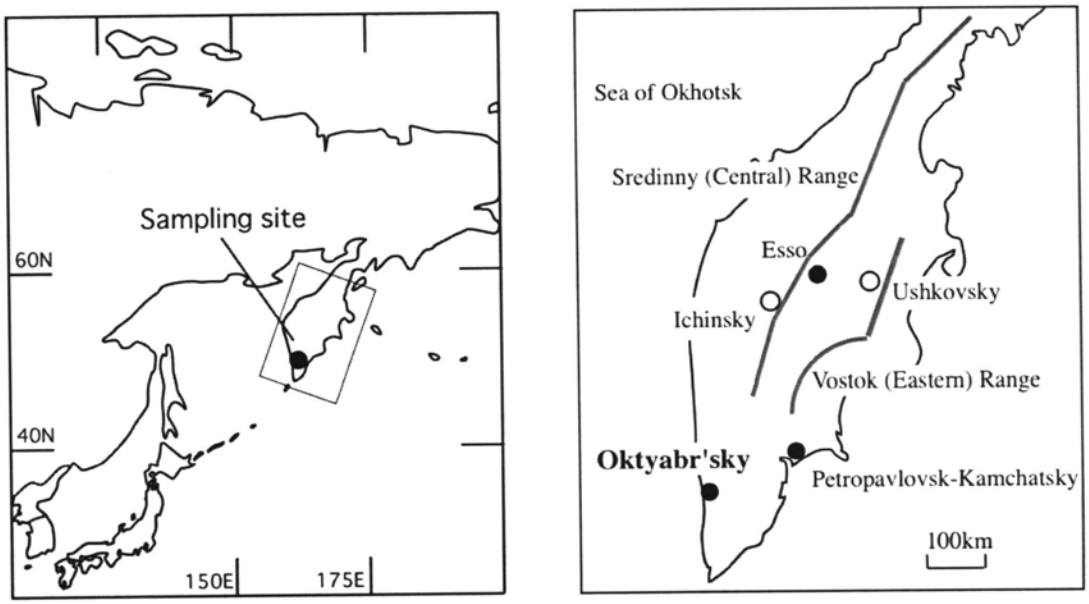

Fig 1. Location of Oktyabr'sky

Aerosol was aerodynamically classified into coarse particle (>2.5μm) and fine particle (<2.5μm) by an impactor attached onto the filter unit, and was collected on Teflon filters (PF040, 90mm diameter: Toyo Roshi Kaisha, Ltd). Coarse particle and fine particle were concentrically collected on the central part and outer part of the filters, respectively. The filter was settled in a plastic cassette case. The cassette case was automatically changed once every one week. The filters was refrigerate after sampling.

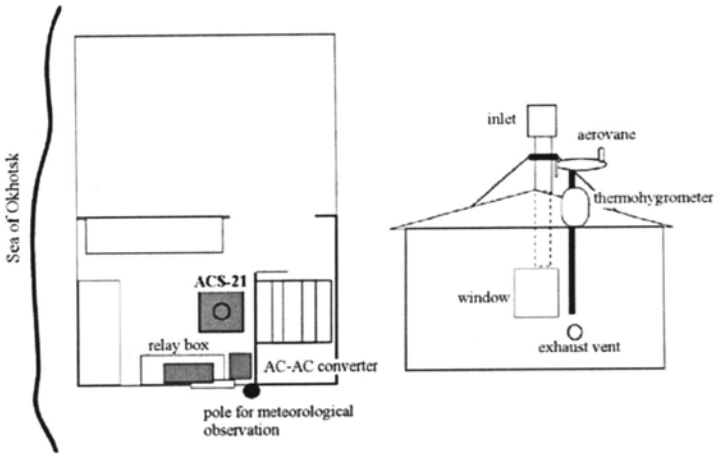

Fig 2. Scematic view of the aerosol sampler

The aerosol sampling was conducted from 19 October 2005 to 15 May 2006. During the sampling period, electric power failure sometimes occurred, and the plastic cassettes were not exchanged in scheduled date. The aerosol sampler was damaged by

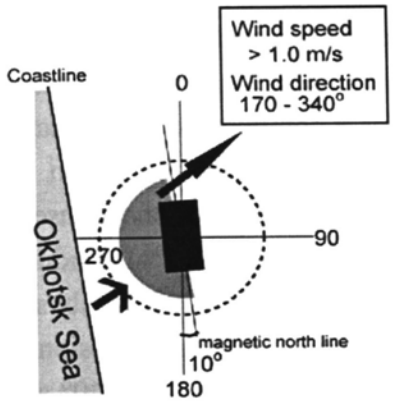

Fig 3. Confine of wind direction to operate aerosol sampling

300V of electrical current when electrical surging occurred at Oktyabr'sky on 15 May. The sampler has not been repaired yet, though we tried to repair it at several times.

The aerosol sampling was managed by ROSHYDROMET (Russian Federal Service For Hydrometeorology and Environmental Monitoring).

CHEMICAL ANALYSIS

The filters were divided into several fragments for chemical analysis of water-soluble substances and of total amount of chemical substances. Water-soluble components in the aerosol were extracted by 10 min ultrasonication with ultrapure water. The concentration of chemical component (Na^+, NH_4^+, K^+, Mg^{2+}, Ca^{2+}, Cl^-, NO_3^-, and SO_4^{2-}) was determined by an ion chromatography. To facilitate the measurement of the total component, the samples were digested in mixed acid (HNO_3, HF, and $HClO_4$) by a microwave device. The concentration of chemical elements (Al, Fe, Ca, Mg, Mn, Na, Ti, Zn, Sr, Cr, and Ba) was determined by an inductively coupled plasma atomic emission spectrometry. All chemical analysis was done in Hokkaido Tokai University.

RESULT

On water-soluble anion species, dominant species was Cl^- from sea-salt. Mass content of Cl^- was 57-90 %, 43-89 %, and 66-87 % in coarse particle, fine particle, and total of them, respectively. Secondary species was SO_4^{2-}. Mass content of SO_4^{2-} was 7-42 %, 11-52 %, and 12-32%, in coarse particle, fine particle, and total of them, respectively. Mass content of NO_3^- was less than 5 % in whole samples. On water-soluble cation species, dominant species was Na^+ from sea-salt and secondary and tertiary was Mg^{2+} and Ca^{2+} mainly from terrestrial source. Mass content of Na^+ was 80-100 %, 55-100 %, and 78-100 % in coarse particle, fine particle, and total of them, respectively. Mass content of terrestrial elements (Mg^{2+} and Ca^{2+}) was 0-20 %. 0-22 %, and 0-20 % in coarse particle, fine particle, and total of them, respectively. Remarkable differences of chemical composition of water-soluble species between coarse and fine particle were not observed.

On acid-digested elements, dominant element was Na. The mean concentration of Na was 1.1 $\mu g \cdot m^{-3}$ and 2.7 $\mu g \cdot m^{-3}$ in coarse and fine particle, respectively. The mean mass content of Na was 79%, 85%, and 82 % in coarse and fine particle, and total of them, respectively. The mean concentration of Fe was 0.024 $\mu g \cdot m^{-3}$ and 0.025 $\mu g \cdot m^{-3}$ in coarse and fine particle, respectively. The mean mass content of Fe was 1.7 %, 0.8 %, and 1.1 % in coarse and fine particle, and total of them, respectively. Remarkable differences of chemical compositions of acid decomposed element between coarse and fine particle were not observed. Concentrations of all elements but Zn and Cr show high correlation ($r > 0.8$) with Al. Therefore, it estimates that these elements are terrestrial dust, and Zn and Cr are from anthropogenic emission.

Fig.4 shows the variations of concentrations of some chemical species in aerosols at Oktyabr'sky. Concentrations of sea-salt (Na^+, Cl^-) in winter (December, January, and

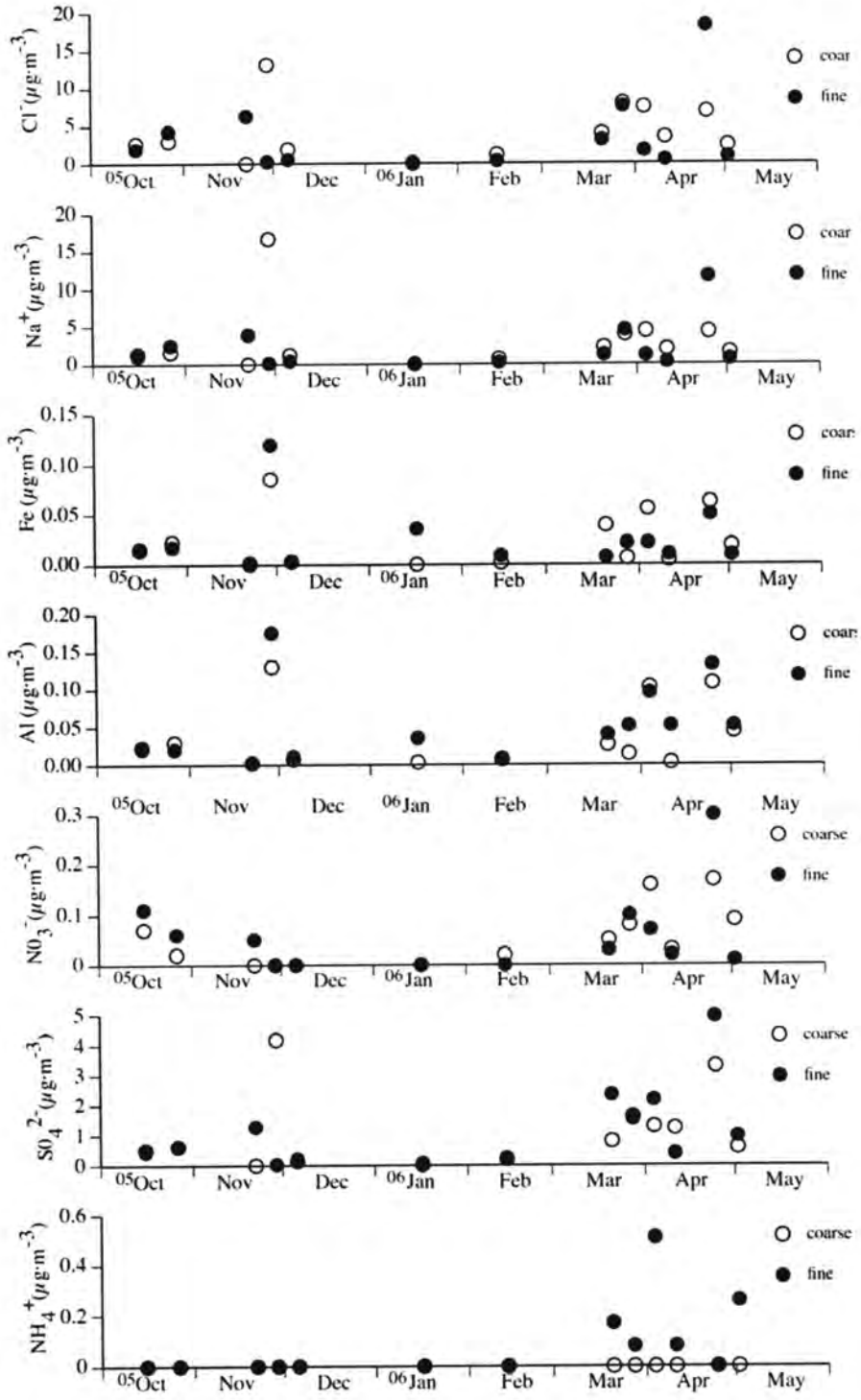

Fig 4. Concentrations of chemical species in aerosols at Oktyabr'sky

February) were lower than in the other months. Because the surface of the Sea of Okhotsk along Oktyabr'sky was open in winter, low concentration of sea-salt in aerosol in winter was not caused by freezing of sea-surface. Frequency of westerly wind in winter was less than 10 % while frequencies of westerly wind in October, and that in March, and April were more

than 50 % and 25%, respectively. Therefore, the variation of sea salt concentration is reflected in the variation of meteorological condition at Oktyabr'sky.

Concentrations of terrestrial dust (Fe and Al) were rather high from March to May, and showed sporadic peaks at the end of November and in April. Moreover, Fe showed a peak in March. Coarse/fine ratio of the concentration of Fe increased at the sporadic peaks in March and April. On the other hand, coarse/fine ratio of the concentration of Al did not show any significant trends, however in general coarse particle concludes 90 % of total Al at Japan when Asian dust is transported (Narita et al., 2005). We estimate that the sporadic peaks of Al and Fe result from Asian dust event, and the concentration of Al and Fe at other period is background level, in spite of uncertainness of Al behaviors.

On anthropogenic species, SO_4^{2-} and NO_3^- showed the different behaviors. Concentrations of NO_3^- increased in both of coarse and fine particles in autumn and spring. Concentration of SO_4^{2-} increased only in fine particles in spring. These behaviors seem to be reflected in emission source of them. The increasing in the concentration of NH_4^+ in fine particles in spring could be reflected in forest fire occurring in Siberia.

ESTIMATION OF IRON FLUX FROM ASIAN CONTINENT TO THE SEA OF OKHOTSK

In order to evaluate the contribution of air-borne Fe to marine product at the Sea of Okhotsk, it is needed to estimate Fe flux to the Sea of Okhotsk. Fig. 5 shows the variation of Fe in aerosol at Oktyabr'sky and Sapporo, Hokkaido, Japan from October 2005 to May 2006. Aerosol at Sapporo was collected at the rooftop of Hokkaido Tokai University, and was analyzed as that from Oktyabr'sky was done (Minami unpublished data). Two peaks of Fe in Sapporo were observed on 10-17 April and on 24 April to 1 May. According to the Lidar observation of National Institute for Environmental Studies, dust concentration increased on 11 April and on 25 April at Sapporo. (http://www-lidar.nies.go.jp/). Around the same time, Fe concentration at Oktyabr'sky increased on 5-12 April and on 26 April to 3 May. Therefore, we assume that these peaks of Fe result from Asian dust events, and after observing at Sapporo on 11 and 25 April, Asian dust was transported to Oktyabr'sky around 12 and 26 April, respectively.

Tsunogai et al. (1985) revealed the exponential relationship between atmospheric concentration of Asian dust and the transport distance from Asian continental coast. Mori et al. (2002) also showed the exponential relationship between atmospheric concentrations of crustal elements and the

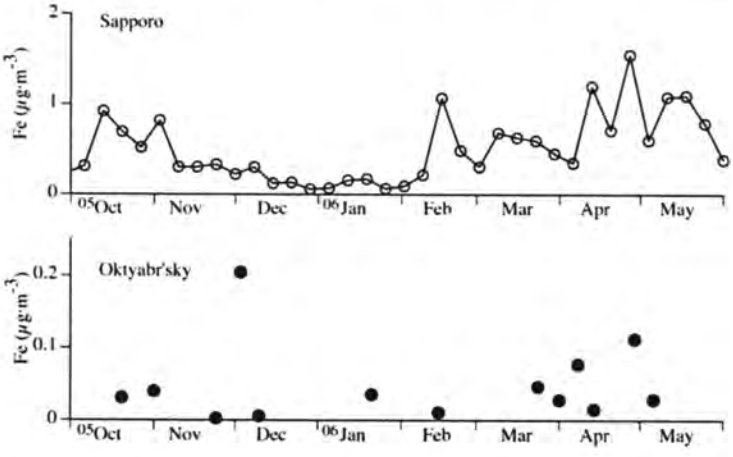

Fig 5. Fe concentration in aerosol at Sapporo and Oktyabr'sky

distance from the source region of Asian dust. Both of these estimations show that the atmospheric concentration of dust or crustal element at certain location exponentially decreases with the transport distance. Therefore, we use the following formula to estimate the concentration of Fe at certain point over the Sea of Okhotsk (C):

$$C = a \exp (b X)$$

where X is the distance from Sapporo, a is the concentration of Fe at Sapporo, and b is constant. Table 1 shows the concentration of Fe at Sapporo and Oktyabr'sky, constant b, and the distance at which concentrations diminish by half (half-concentration distance) at the event on 11 and 25 April. Because the half-concentration distances are equal to the value (330 km for Fe) reported by Mori et al. (2002) and the value (490 km for dust) by Tsunogai et al. (1985), it is possible to estimate the approximate concentration of Fe in relation to the distance from Sapporo.

Uematsu et al. (2003) calculated the total deposition velocity of dust of 0.5 cm· s^{-1} at Sapporo based on the annual deposition flux and the annual mean atmospheric dust concentration. We adopt this value of total deposition velocity, and assume that the high concentration of Asian dust continues for half a day according to the Lidar observation described as above, we estimate the Fe flux over the Sea of Okhotsk (Fig. 6).

For the next step, we are going to investigate the solubility and related behaviors of Fe in seawater in order to estimate how much air-borne Fe can be used for marine production.

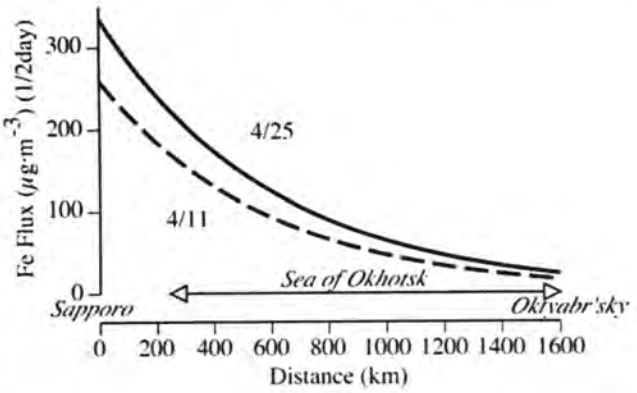

Fig 6. Estimation of Fe flux during half day of Asian dust event observed on 11 and 25 April at Sapporo

ACKNOWLEDGEMENTS

We are grateful to RUSHYDROMET for their management of the aerosol sampling. We are also grateful to the Red Cross at Kamchatka for their kind support of installing of the sampler. We thank Sergei Stephanovich at Okytabr'sky who actually cared the sampling system. We thank Nataria Homich for her kind support and interpretation.

REFERENCES

Bishop, J. K., Davis, R. E. and Sherman, J. T. (2002): Robotic observation of dust storm enhancement of carbon biomass in the North Pacific. Science, 298, 817-821.

Mori, I., Nishikawa, M., Quan, H. and Morita, M. (2002): Estimation of the concentration and chemical composition of kosa aerosol at their origin. Atmos. Environ. 36, 4569-4575.

Narita, Y., Ui, T. and Uematsu, M. (2005): Atmospheric transport of crustal and anthropogenic elements in aerosols from the Asian continent to the western North Pacific during the spring, 2001. Chikyukagaku, 39, 1-15. (In Japanese with English abstract and figure captions).

Tsunogai, S., Suzuki, T., Kurata, T. and Uematsu, M. (1985): Seasonal and areal variation of continental aerosol in the Surface air over the western north pacific region. J. Oceanogr. Society of Jpn., 41, 427-434.

Uematsu, M., Duce, R., Prospero, J., Chen, L., Merrill, J. and McDonald, R. (1983): The transport of mineral aerosol from Asia over the North Pacific Ocean, Journal of Geophysical Research, 88, 5343-5352.

Uematsu, M., Wang, Z. and Uno, I. (2003): Atmospheric input of mineral dust to the western North Pacific region based on direct measurements and a regional chemical transport model. Gophys. Res. Lett., 30(6), 1342, doi:10.1029/2002GL016645.

ICE CORE DRILLING AT MOUNT ICHINSKY, KAMCHATKA, RUSSIA

MATOBA SUMITO[1] AND ICHINSKY GLACIOLOGICAL EXPEDITION MEMBERS[2]

[1] *Institute of Low Temperature Science, Hokkaido University*

[2] *A full list of authors appears at the end of this paper*

INTRODUCTION

Mineral dust containing iron from the Asian continent is transported eastward over the North Pacific, especially spring (Uematsu et al., 1983). The air-borne iron is considered to be the only one source of input in the central part of the northern North Pacific. In fact, it was found that a near doubling of biomass production was observed in the mixed layer in the North Pacific over a 2-week period after the passage of a cloud of Gobi desert dust (Bishop et al., 2002). It is, therefore, necessary to estimate the contribution of atmospheric transport of iron to the biomass production in the Sea of Okhotsk and the northern North Pacific.

Ice-core obtained from the North Pacific region is a suitable proxy to estimate total depositions of mineral dust over the North Pacific. We identified several peaks of iron associated with Asian dust event in the ice-core obtained from Mount Logan, Canada. We estimate the annual average of total deposition of iron was 10mg/m^2·yr (Matoba and Shiraiwa, 2006). On the Asian side of the North Pacific, Shiraiwa and co-workers obtained an ice core from Mount Ushkovsky in 1998 (Shiraiwa et al., 1999), but they could not extract meaningful information on chemical substances from that ice core, because Ushkovsky volcano is near several active volcanoes and thus includes a huge amount of chemical substances emitted from those volcanoes. Therefore, we mounted an expedition to obtain an ice core from the caldera glacier on Mount Ichinsky, which is located far from any active volcanoes (Matoba et al, 2007).

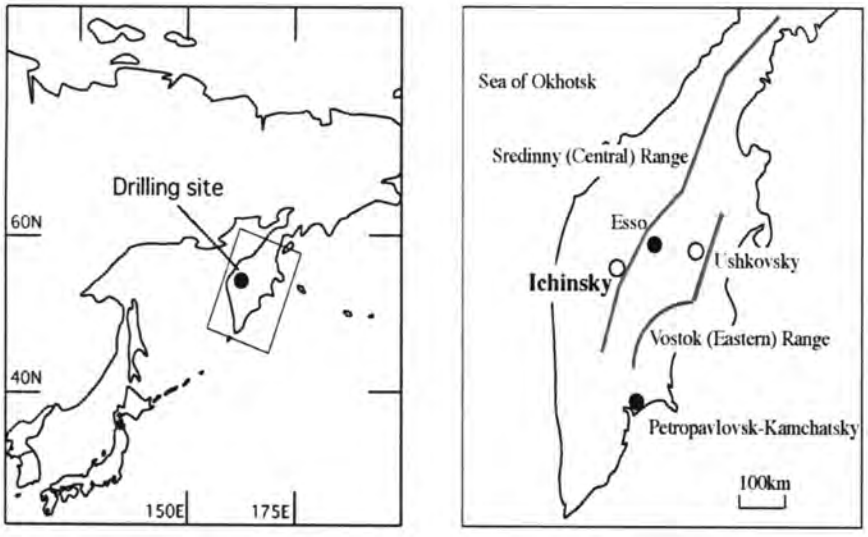

Fig 1. Location of Mount Ichinsky

THE DRILLING SITE

Mount Ichinsky (55°46'N, 157°55'E; summit elevation, 3607 m) is in the central part of the Kamchatka Peninsula, Russia (Figs. 1). It is a stratovolcano and the highest mountain in the Sredinny (central) Range of Kamchatka. On its summit is a caldera measuring 3 km x 5 km. The caldera is covered with an ice cap that is approximately 500 m in diameter. Mount Ichinsky erupted several times in the Holocene. The age of the earliest volcanic deposit overlying a Late Pleistocene moraine is estimated as about 10000–15000 years, and the most recent eruption occurred within the last 1800 years and at least several hundred years ago (Volynets et al., 1991). Glaciers flow from the caldera down both the steep northeast slope and the gentle southwest slope.

PARTICIPANTS

This project was launched as an international collaborative program between the Institute of Volcanology and Seismology, Russian Academy of Science, Russia (IVS-RAS), and the Research Institute for Humanity and Nature (RIHN) and the Institute of Low Temperature Science, Hokkaido University (ILTS-HU), Japan.

Initially, we planned to carry out the expedition in June, 2006. On this expedition, we were going to carry out snow surveys at several altitude along climbin route as well as ice core drilling. We expected that the snow surveys revealed the relationship between climate condition around the ground level and characteristics of snow at high altitude. The snow survey was going to carry out with a support of Mountain Activity Support, Hokkaido (MASH). The participants in the expedition were as follows;

Dr. Sumito Matoba (ILTS-HU), leader of expecition and glaciologist
Mr. Kazuo Higuchi (MASH), leader of field activity and mountain guide
Dr. Sergei V. Ushakov (IVS-RAS), chief of logistics and volcanologist
Mr. Kunio Shimbori (ILTS-HU), chief driller and engineering
Dr. Takayuki Shiraiwa (RIHN), leader of snow survey expedition and glaciologist
Mr. Alexander A. Ovsiannikov (IVS-RAS), logistics and volcanologist
Mr. Alexander G. Manevich (IVS-RAS), logistics and geophysicist
Mrs. Tatyana M. Zideleeva (IVS-RAS), cook and glaciologist
Mr. Takeshi Toida (Grad. Sch. Environ. Sci. -HU), driller and glaciologist
Mr. Tatsuru Sato (Grad. Sch. Environ. Sci. -HU), snow survey and gloaciologist
Mr. Hirotaka Sasaki (Grad. Sch. Environ. Sci. -HU), ice-core processor and glaciologist
Dr. Yaroslav D. Muravyev (IVS-RAS), ground support and volcanologist/glaciologist.

However, we were forced to change our plans because of customs troubles and bad weather at Mount Ichinsky described as below.

Secondary, we planned the expedition in August, 2006. On this expedtition, we had to concentrate ice-core drilling because we did not have enough time, participants and budget. The participants in the project were as follows;

Dr. Sumito Matoba (ILTS-HU), leader and glaciologist

Dr. Sergei V. Ushakov (IVS-RAS), chief of logistics and volcanologist
Mr. Kunio Shimbori (ILTS-HU), chief driller
Mr. Tetsuhide Yamasaki (Geotech Inc. Ltd.), driller
Mr. Alexander A. Ovsiannikov (IVS-RAS), logistics and volcanologist
Mr. Alexander G. Manevich (IVS-RAS), logistics and geophysicist
Mrs. Tatyana M. Zideleeva (IVS-RAS), cook and glaciologist
Mr. Stanislav Kutuzov (Inst. Geography-RAS), drilling assistant and glaciologist
Mr. Hirotaka Sasaki (Grad. Sch. Environ. Sci. -HU), ice-core processor and glaciologist
Dr. Yaroslav D. Muravyev (IVS-RAS), ground support and volcanologist/glaciologist.

Table 1. Dates of field studies and logistics

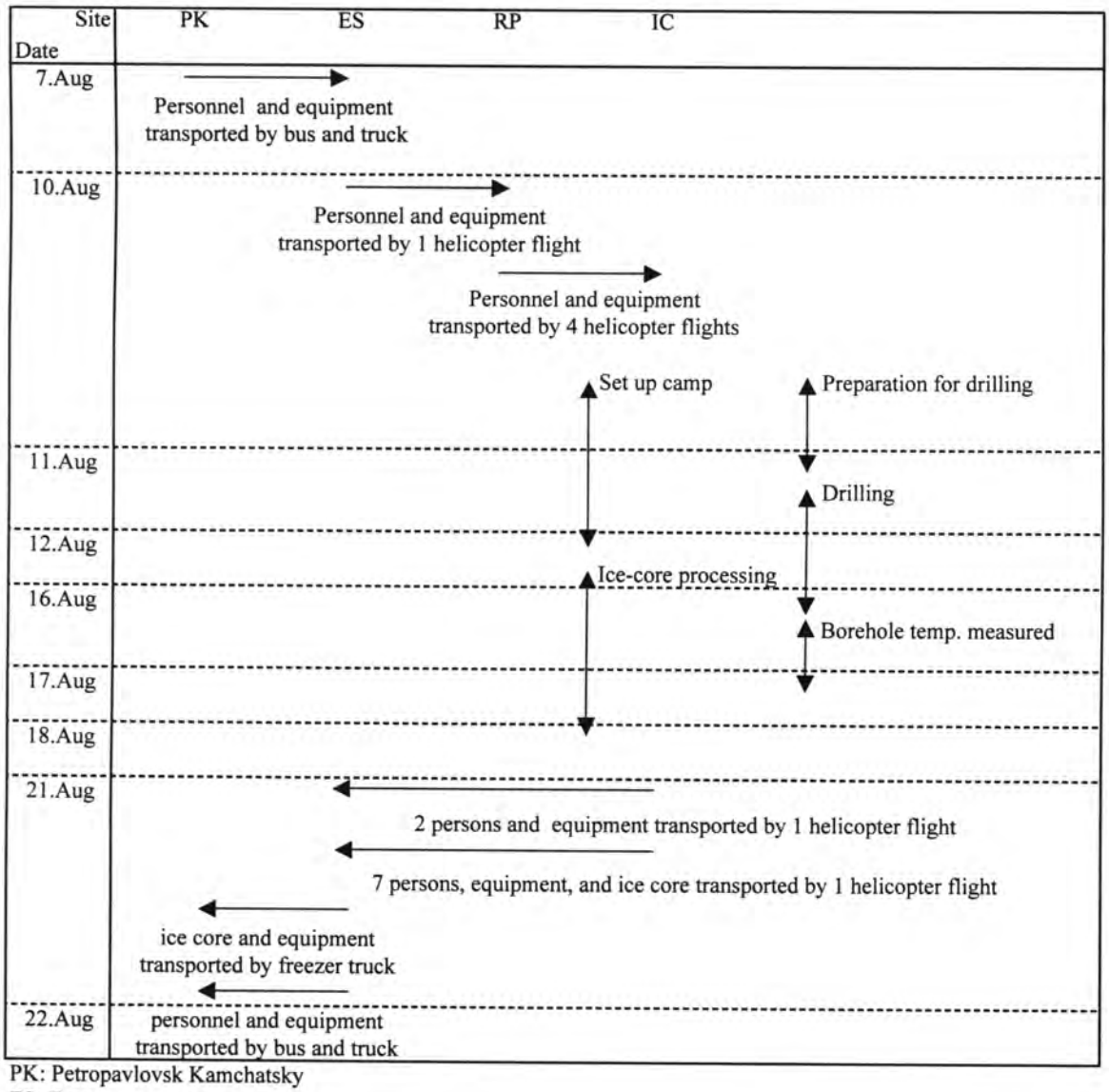

PK: Petropavlovsk Kamchatsky
ES: Esso
RP: Relay point
IC: Ichinsky

ITINERARY

Equipment was shipped from ILTS-HU on 1 April, and arrived at the Vostochnu port around 10 April. In Vostochnu it took 1 month to process preliminary entry. The equipment finally arrived at Petropavlovsk-Kamchatsky on 26 May. In Petropavlovsk-Kamchatsky, it took 2 weeks to make clearance of the equipment, and the equipment finally arrived at IVS-RAS on 12 June. As described above, initially we planned to carry out the expedition in June 2006, but we were forced to change our plans.

We traveled from Petropavlovsk-Kamchatsky, where the IVS-RAS is located, to Esso, the helicopter site closest to Mount Ichinsky, carrying 1500 kg of equipment by truck, and the members of the expedition by bus.

We flew personnel and equipment from Esso to the summit of the caldera via a relay point at the northern foot of Mount Ichinsky in an MI8 helicopter on 10 August, 2006. One flight was required from Esso to the relay point, and four flights from the relay point to the caldera summit, to transport nine people and the equipment.

After establishing our camp, we started ice-core drilling in the afternoon of 11 August and finished in the afternoon of 16 August. We measured the temperature in the borehole from the night of 16 August until the morning of 17 August. In tandem with the ice-core drilling, from 12 to 17 August, we also measured the density of the ice core, observed its stratigraphy, and collected samples for chemical analysis from half samples of the ice-core samples from surface to 47.22 m depth.

All personnel and equipment, and the 115-m-long ice core, were flown to Esso by the same helicopter on 21 August, which required two flights from the summit to Esso. The first flight did not stop at the relay point because the helicopter had mechanical trouble and had to return Esso as soon as possible for repairs. The ice core was stored in a freezer truck at Esso and transported to Petropavlovsk-Kamchatsky on 21 August. The itinerary is summarized in Table 1.

CAMP SITE

Our camp (Fig. 2) included a drilling tent, kitchen tent, sleeping tents, and an ice-core processing trench. We chose a flat area for the drilling site, where we believed that the strain of ice was simple, and where the thickness of glacier was the largest. The GPS position of the drilling site was 55°40'38.3"N, 157°43'28.2"E, 3595 m a.s.l. To prevent the collapse of the tents by strong winds, we dug down 50 cm below the snow surface before erecting the tents, and we constructed 1-m-high snow walls on the windward side of all tents. We also dug a trench (4 m x 2 m, 2 m deep), which we covered with plywood and vinyl sheets. In this trench, we made a 3-m-long worktable and a 1-m-long light table with snow, installed a band saw (Ryowa model BSW-200), and carried out ice-core processing.

There was heavy rain with strong winds from the night of 11 August to the morning of 13 August; as a result, the guy ropes of the drilling tent were pulled out of the snow surface,

and the drilling tent was almost blown away on the morning of 13 August. We repaired the drilling tent in the afternoon of 13 August and were able to restart drilling in the afternoon of 14 August. From 18 to 19 August, another very heavy storm tore the kitchen tent and two sleeping tents, so four expedition members lived in the ice-core trench from 19 to 21 August.

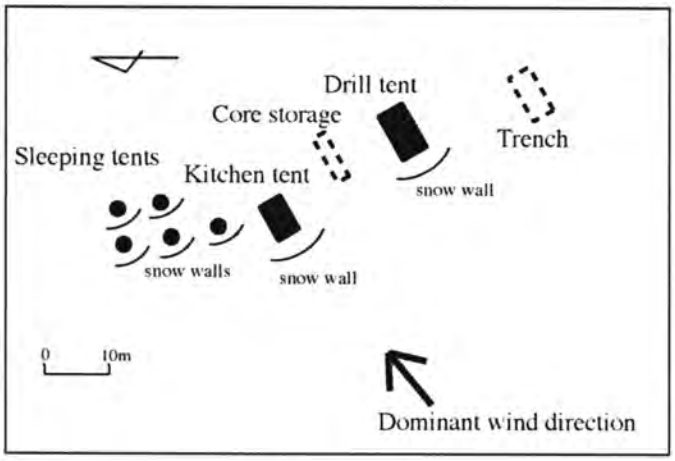

Fig 2. Campsite map

After the rainfall on 11 August, some crevasses appeared up near the drilling and kitchen tents. We connected the kitchen tent, drilling tent, and the ice-core processing trench with a life rope so that we could walk safely between them, even during whiteout conditions.

ICE-CORE DRILLING

We used an electromechanical ice-core drilling system developed by Geotech Co. Ltd., Nagoya, Japan. The system was also used for an expedition to Mount Belukha, Altai Mountains, Central Asia, in 2003 (Takeuchi et al., 2004). Specificatons of the drill system are shown in Table 2.

Table 2 Specification of an electro-machanical drill

Drill	
Diameter (inner/outer)	98/125mm
Drill/barrel length	2130/1350mm
Drill moter	DC 100V, 350W, 4000rpm, 8.5kg cm
Type of anti-torque	Leaf spring type
Winch	
Size	L860 x W 390 x H450
Hoisting speed	84-59m min-1
Winch motor	DC 100V, 750W
Torque	0.84N m
Mast	Fixed type, alumium pipe
Cable	Armored cable of 4.7mm diameter

We used a generator (YAMAHA model EF 2300) with a four-cycle, single-cylinder gasoline engine for the drilling operation. The fuel was 96-octane gasoline, which we bought in Petropavlovsk-Kamchatsky. For high-elevation use, we replaced the fuel spray nozzle in the carburetor with one with a smaller hole. To prevent the air intake from closing up because of a frozen air filter in the cold conditions, we removed the air filter made of sponge from the

air filter unit. To prevent the carburetor from freezing, we attached a metal plate from the exhaust muffler to the carburetor, to conduct heat to the carburetor.

After installing the drilling system in the drilling tent on 11 August, we started the ice-core drilling in the afternoon of 11 August. On 13 August, heavy rain and strong wind tore the drilling tent and wet the control box of the drilling system. We needed 1 day to repair the drilling tent and control box, and then we restarted drilling on 14 August. On 16 August, we recognized that the drill was slipping on a hard layer, could not advance any more, and tips of rock were collected in the drill barrel, so we made the judgment that the drill had reached bedrock. The length of the wire was 114.99 m, and the number of drilling runs completed was 236.

The temperature in the drilling tent was more than 0 °C, and this warmth caused various problems during the drilling operation. Ice chips melted on the drill easily during the preparation in the drilling tent, and the melted ice refroze onto the inside and outside of the barrel or the head mount of the drill in the borehole, where surrounding borehole temperature was below 0 °C. The frozen chips in the barrel scratched and broke the ice core during the drilling operation. When we pulled the ice core out of the barrel, the frozen chips acted as prongs and obstructed smooth displacement of the ice core from the barrel. When the melted chips froze on the shoes, that is, the parts of the drill head that control the cutting pitches of the drill, we felt with our fingers through the wire that the drill's cutters slipped on the bottom of the borehole, and the drill did not advance.

To prevent such problems, we shortened the amount of working time between when the drill was brought up above the snow surface and when it was returned to the borehole. Four or five people participated in the drilling operation, which involved taking down the drill, pulling the barrel out of the jacket, removing the ice core from the barrel, blowing the ice chips out of the barrel and jacket with an air compressor, replacing the barrel in the jacket, putting the drill back up, and inserting the drill into the borehole. To remove the ice core from the barrel after pulling the barrel out of the jacket, we inclined the barrel and tapped it with a plastic hammer to dislodge ice chips from the inside of the barrel. After a rather large amount of ice chips had dropped, the ice core was free to slide in the barrel and could be easily removed. According to Zagorodnov et al. (2002), an effective way to avoid jams caused by ice chips is to brush and lubricate with antifreeze the barrel and the inside surface of the jacket. However, we did not use liquid antifreeze because it could contaminate the ice core. We also did not brush the barrel, because it warmed up during brushing. Instead of brushing, we blew the ice chips out of the barrel and jacket with an air compressor. We completed these procedures within 2 min for each run, and inserted the drill back into the borehole before the ice chips in the barrel and jacket melted.

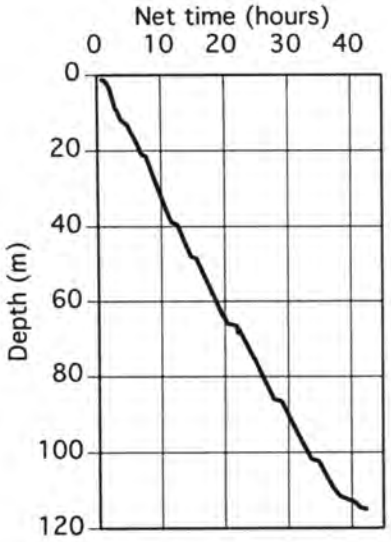

Fig.3 Cumulative drilling time (h) versus depth (m)

It took a total of 42.5 h to drill down to 114.99 m (Fig. 3). The production rate was 2.71 meters per hour. An ice core 90–93 mm in diameter and approximately 0.5 m long was consistently recovered from each drilling run. No brittle ice was found in the whole depth, although brittle ice usually appears below a depth of 100 to 150 m in mountain glaciers or small ice caps (Takahashi, 1996; Koci, 2002). No thick volcanic ash layer, which had been trouble for drilling at Mount Ushkovsky (Shiraiwa et al., 1999), damaged the cutters of the drill. The drilling operation is summarized in Table 3.

Table 3 Drilling operation

Run No	Depth (m)		rake angle of cutter(degree)	shoe	number of catchers
1	0.00		40	5P[1]	3
101	48.38				2
157	75.93		45	no[2]	
222	110.86		40	5P	
229	112.95			no	
232	114.02		40[3]	5P	
235	114.99	bedrock			
236	114.99				

[1] Shoe of 5mm pitch (5mm per one rotation)
[2] Operation without shoe
[3] Dolphin mount system (Takahashi, 2005)

BOREHOLE TEMPERATURE

The temperature of the borehole wall was measured after the ice-core drilling was completed, from the evening of 16 August to the morning of 17 August. The wall temperature was measured with a thermistor sensor (Techno-seven model BYE-64), which was kept in direct contact with the wall of the borehole by leaf springs (Kameda et al., 1993). The resistance of the sensor (12 Kohm at 0 °C) was measured by a digital multimeter with resolution of 10 ohm. Because of the large difference in the resistance between the sensor and the cable, the cable resistance was considered to be negligible.

The sensor was inserted into the borehole and stopped for measurement at the bottom (113.65 m), and at 105, 100, 80, 60, 40, 30, 20, 15, 10, 7, 5, and 2 m below the surface. The sensor was stationary during all wall-temperature measurements. Readings of the digital multimeter were made at 1, 10, 30, and 60 min after placement at each depth. The temperature decreased with time because the frictional heat generated by movement was dissipated until the equilibrium temperature was reached. We estimated the equilibrium temperature from the equilibrium curve that we obtained from our measurements.

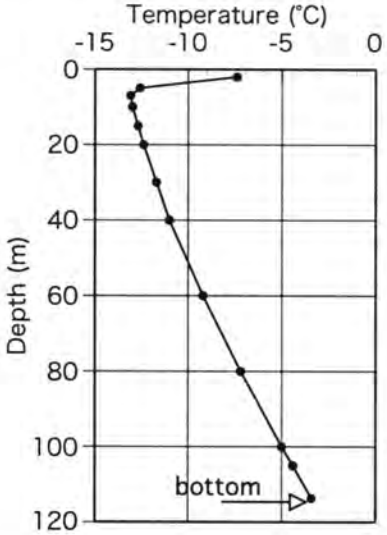

Fig4. Temperature profile of the borehole wall

The temperature at 10 m depth was –13.0 °C, and the temperature at the bottom of the borehole was –3.4 °C (Fig. 4). From 10 m to the bottom, the temperature increased linearly with depth as shown in Ushkovsky glacier (Shiraiwa et al., 1999).

ICE-CORE PROCESSING AND ICE-CORE PROPERTIES

We processed the ice-core samples from the surface to 47.22 m depth as follows. We recorded the stratigraphy of the ice core on chart sheets at real scale using a light table and measured the bulk density of the core. We then cut the ice-core samples in half vertically with a band saw. Half samples of the ice-core samples were packed into polyethylene bags and packed into insulated boxes and transported to Esso. The other halves of the ice-core samples were cut at 50- to 70-mm intervals, and each subsample was placed in a new polyethylene bag in the ice-processing trench after the surface of ice sample was removed with a band saw. The subsamples were then melted in a water bath, or at ambient temperature, and decanted into pre-cleaned polyethylene bottles either on site, or later in a laboratory at IVS-RAS. The total number of subsamples was 894.

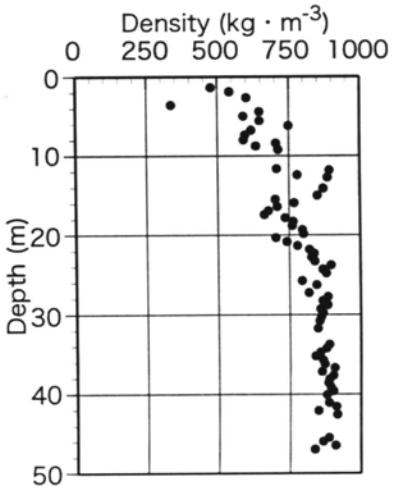

Fig.5 Bulk density profile of the ice core from the surface to 50 m depth

Bulk densities from the surface to 50 m depth (Fig. 5) were calculated from the diameter, weight, and length of each ice-core segment obtained in a single drilling run. If part of a sample was lost, we excluded it from the measurement. Several calculated density values were too high because of the low precision of the scales and so on. Therefore, we multiplied all the densities by 0.965 as a correction value to adjust the highest density value to that of pure ice. The pore close-off depth was at approximately 25 m, which is shallow in comparison with that of the Ushkovsky glacier (55 m) (Shiraiwa et al., 1999).

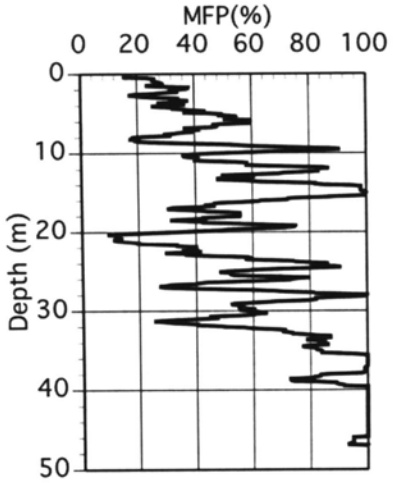

Fig.6 Profile of the melt-feature percentage (MFP) in the ice core. MFP indicates the proportion of ice layers in 1-m-long sections

We also recorded the profile of the melt-feature percentage (MFP, Fig. 6), which is the thickness of frozen ice layers in a 1-m-long section of ice core. MFP is generally used as an indicator of summer temperature at a site where ice layers are formed only by melting occurring at the snow surface (Koerner, 1977). However, the ice layers observed in the ice core at Mount Ichinsky were not only formed by surface melting. As described above, heavy rainfalls

occurred during the expedition. We observed on the snow wall of the trench that rain infiltrated into the accumulated snow, pooled at the boundary of snow layers, and formed ice layers without disturbing the snow layers between the surface and pooled layer of rainwater. After a heavy storm on 18 August, we observed rapid growth of a thick frost layer on the glacier surface on 19–20 August, when the air temperature was below 0 °C and a large amount of mist from the Sea of Okhotsk was carried over the site by a strong wind. The interior of the frost was composed only of ice, which formed on 20 August, and its surface was covered with frost or snow flake, which were attached on the morning of 21 August. The thickness of the frost was 0.1–0.4 m, so the contribution of the frost to the surface mass balance and MFP analysis was not negligible. We expect that the mechanisms of formation of these various kinds of ice layers will be revealed by detailed stratigraphic observations and chemical analyses of the ice core, allowing information on climate variations on the glacier and related environmental variations in Kamchatka to be extracted.

ACKNOWLEDGEMENTS

We are grateful to Akiyoshi Takahashi of Geotech Co. Ltd. for technical support and comments for the drilling operation. We are grateful to Dmitry Isaev of the Institute of Volcanology and Seismology for his substantial contribution regarding customs procedures.

REFERENCE

Bishop, J. K., Davis, R. E. and Sherman, J. T. (2002): Robotic observation of dust storm enhancement of carbon biomass in the North Pacific, Science, 298, 817-821

Kameda, T., Narita, H., Shoji, H., Nishio, F., Fujii, Y. and Watanabe, O. (1993): Melt features in ice cores from Site J., southern Greenland: some implications for summer climate since AD1550. Ann. Glaciol., 21, 51-58.

Koci, B. (2002): A review of high-altitude drilling. Mem. Natl. Inst. Polar Res. Spec. Issue, 56, 1-4.

Koerner, R. M. (1977): Devon Island ice cap: core stratigraphy and paleoclimate. Science, 196, 15-18.

Matoba, S. and Shiraiwa, T. (2005): Kosa records in an ice core from Mt. Logan, Yukon, Canada. Report on Amur-Okhotsk Project No.3, Shiraiwa T. (Eds), Amur-Okhotsk Project, Kyoto, pp. 105-110.

Matoba, S., Ushakov, S. V., Shimbori, K., Sasaki, H., Yamasaki, T., Ovshannikov, A. A., Manevich, A. G., Zhideleeva, T. M., Kutuzov, S., Muravyev, Y. D. and Shiraiwa, T. (2007): The glaciological expedition to Mount Ichinsky, Kamchatka, Russia. Bulletin of Glaciological Research, in press.

Shiraiwa, T., Nishio, F., Kameda, T., Takahashi, A., Toyama, Y., Muravyev, Y. D. and Obsyannikov, A. (1999): Ice core drilling at Ushkovsky ice cap, Kamchatka, Russia. Seppyo, 61(1), 25-40 (In Japanese with English abstract and figure captions).

Takahashi, A. (1996): Development of a new shallow ice core drill. Seppyo, 58(1), 29-37 (In Japanese).

Takahashi, A. (2005): Development of an ice core drilling usable for warm ice. Seppyo, 67(3), 245-250 (In Japanese).

Takeuchi, N., Takahashi, A., Uetake, J., Yamazaki, T., Aizen, V. B., Joswiak, D., Surazakov, A. and Nikitin, S. (2004): A report on ice core drilling on the western plateau of Mt. Belukha in the Russian Altai Mountains in 2003. Polar Meteorol. Glaciol., 18, 121-133.

Uematsu, M., Duce, R., Prospero, J., Chen, L., Merrill, J. and McDonald, R. (1983): The transport of mineral aerosol from Asia over the North Pacific Ocean, Journal of Geophysical Research, 88, 5343-5352.

Volynets, O. N., Patoka, M. G., Melekestsev, I. V. and Zubin, M. I. (1991): Ichinsky volcano. In Active volcanoes of Kamchatka, 1, Fedotov, S.A. and Masurenkov, Yu.P. (Eds) Nauka Publishers, Moscow, pp. 280-294 [in Russian and English]

Zagorodnov, V. S., Thompson, L. G., Mosley-Thompson, E. and Kelley, J. J. (2002): Performance of intermediate depth portable ice core drilling system on polar and temperate glaciers. Mem. Natl. Inst. Polar Res., Spec. Issue, 56, 67-81.

ICHINSKY GLACIOLOGICAL EXPEDITION MEMBERS;
MATOBA S.[1], USHAKOV S. V.[2], HIGUCHI K.[3], SHIMBORI K.[1],
OVSHANNIKOV A. A.[2], MANEVICH A. G.[3], ZIDELEEVA T. M.[3], TOIDA T.[4],
SATO T.[4], SASAKI H.[4], KUTUZOV S.[5], MURAVYEV Y. D.[3] AND SHIRAIWA T.[6]

Affiliations for authors:
1 Institute of Low Temperature Science, Hokkaido University
2 Institute of Volcanology and Seismology, Russian Academy of Science
3 Mountain Activity Support Hokkaido
4 Graduate School of Environmental Science, Hokkaido University
5 Institute of Geography, Russian Academy of Science
6 Research Institute for Humanity and Nature

RUNOFF PROPERTIES OF THE AMUR RIVER AND THE CONSTRUCTION OF THE HYDROLOGICAL MODEL INCORPORATING DISSOLVED IRON TRANSPORT

ONISHI TAKEO
Research Institute for Humanity and Nature

INTRODUCTION

The Amur River is one of the largest trans-boundary river which runs through the boundary between China and Russia. The catchment area of the river is 2,050,057km^2 which is the nineth largest river in the world and the total length of the river is 4,350km. Thus, huge amount of fresh water is supplied by the Amur river to the Sea of Okhotsk (Ducklow et al., 2003). The Sea of Okhotsk is one of the most biologically productive regions in the world, and it supports high fisheries production. Recent studies show that dissolved iron plays an important role to maintain the biological productivity of the Sea of Okhotsk, and we suppose that one of the possible sources of dissoloved iron is fresh water from the Amur river. Iron is an essential nutrient not only for the biological productivity of the Sea of Okhotsk but also for most biota. However, it is not well understood that how dissolved iron is produced and transported through the terrestial ecosystem. One of the our goals in the project is to clarify the mechanism of producing dissoloved iron in the terresial ecosystem and to construct a hydrological model which incorporate the mechanism of dissolved iron production. In this report, I discuss some hydrological properties of the amur river basin, and figure out the basic structure of the hydrolgoical model incorporating dissolved iron production.

1. GEOGRAPHICAL PROPERTIES OF THE AMUR RIVER BASIN

The catchment area of the Amur river is 2,050,057km^2, and the total length of the river is 4,350km which is the seventh longest river in the world. As shown in Figure1, average elevation and maximum elevation of basin are 545m and 2,641m respectively. More than 50 percent of the land are located under the elevation of 500m. Main tributaries of the basin are Songhua (Chinese part),Argun, Zeya,Silka, Ussuri. Each basin area is 53,5232km^2, 29,8361km^2, 23,3311km^2, 20,2924km^2, 19,5101km^2. In addition, average river bed slope

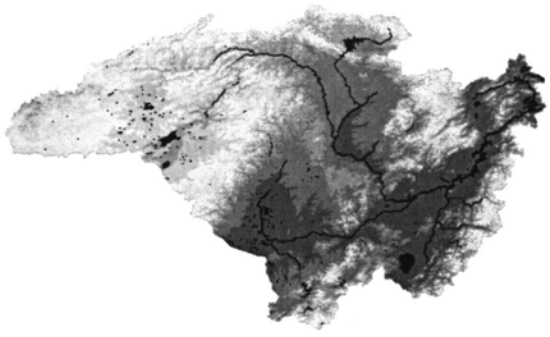

Figure1. Outline of the Amur River Basin

from the river mouth to Khabarovsk calculated from DEM data which was construced by SRTM (Shuttle Radar Tomography Mission) is about 1/25,000. Compared to the other large continental river, it is cleared that the Amur river basin is very flat.

Figure 2 shows the landuse composition ratio of the basin. Most dominant land use is forest which consists of mixed forest, deciduous forest, and coniferous forest. Next, dry land occupies major part of the landuse. Most part of the dryland locates in the Songhua river basin. Wetland consists about 7 % of the total basin area. And most part of it locates along the main course of the Amur river. From on-site investigation through this year and last year, Forest and wetland have a possibility of producing dissolved iron. Figure 3 is a plot of iron concentraton of main tributaries against the forest and wetland mixed with forest. It shows that dissolved iron concentration from forest is slightly lower than that from wetland mixed with forest.

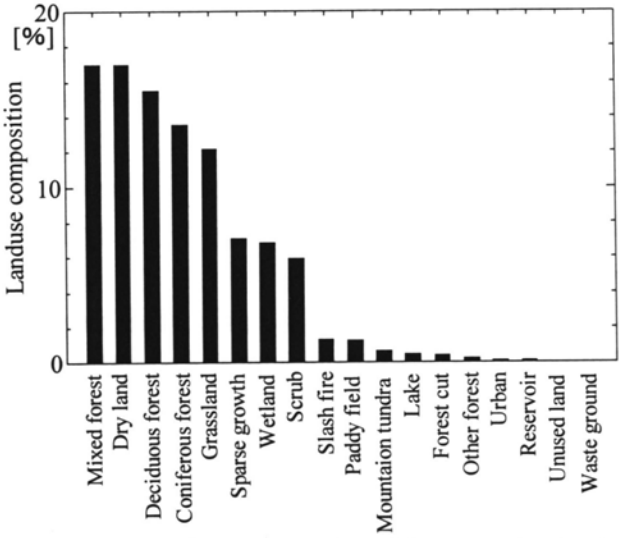

Figure 2. Landuse composition of the amur river basin

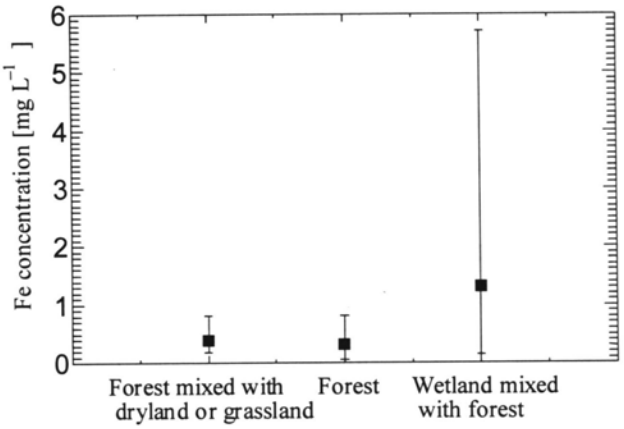

Figure 3. Fe concentration range plotted against landuse pattern of catchment area

From the view point of constructing the hydrological model, if we can find some relation between topographical property of catchments and iron concentration of the river water, we can incorporate such relationship into hydrological model (Shibata et al., 2004). Thus, here, we investigate the relationships between topographic index and annual mean dissolved iron concentration of the main tributaries which were measured in 2002 and Gassi Lake catchment. Topographic index is defined as follows (Beven and Kirkby, 1979).

$$a / \tan \beta \qquad (1)$$

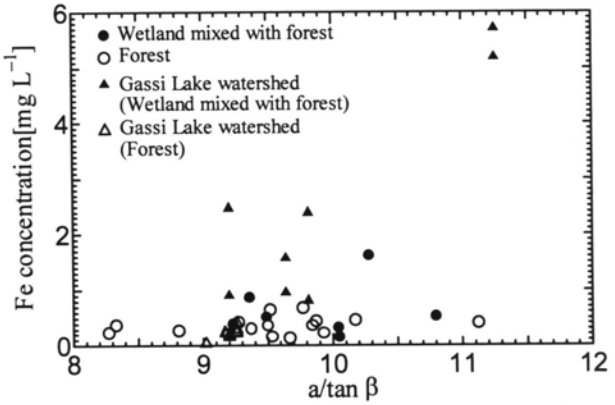

Figure 4. Fe concentration plotted against mean a/tanb of each catchment

Here, a: catchment area per unit contour length[L^2], β:most gradient slope of the each grid[-].

Figure 4 is a plot of annual mean dissolved iron concentration of the main tributaries against the mean topographic indicies of a catchment area of the point where dissolved iron concentration was measured. It can not to be found distinct relationship between topographic indicies and iron concentration of each tributaries. One main reason is supposed to be that hydraulic conductivity and soil types of each catchment is also important effect on the productivity of the dissolved iron. However, it can be said that productivity of dissoloved iron from forest is constantly below 1.0mg L^{-1} in spite of the values of $a/\tan\beta$. On the other hand, catchments which include wetland have a tendency to produce higher dissoloved iron concentration than forest in general.

2. DISCHARGE DATA AND WATER BUDGET

One of goals of our project is to assess the impact of human activities on the productivity of dissolved iron. Within the Amur river basin, many wetland in China have converted to the dry land and paddy fields especially in the past 20 years. Another possible impact of human activity was the construction of dam mainly for electricity in the upper part of the Zeya river in 1978. Thus, to evaluate impacts of these activities on the hydrological properties and dissolved iron productivity, relatively long term meteorological data is needed.

Figure 5 shows the annual precipitation, evapo-transpiration, discharge at the Bogorodskoye and calculated discharge by substituting evapo-transpiration amount from precipitation amount during the period from 1948 to 2002. Annual precipitation and evapo-transpiration amount of the basin is constructed from the National Centers for Environmental Prediction (NCEP) / National Centers for Atmospheric Research (NCAR) Reanalysis1 data sets (http://www.cdc.noaa.gov/cdc/data.ncep.reanalysis.html). Annual discharge data is from

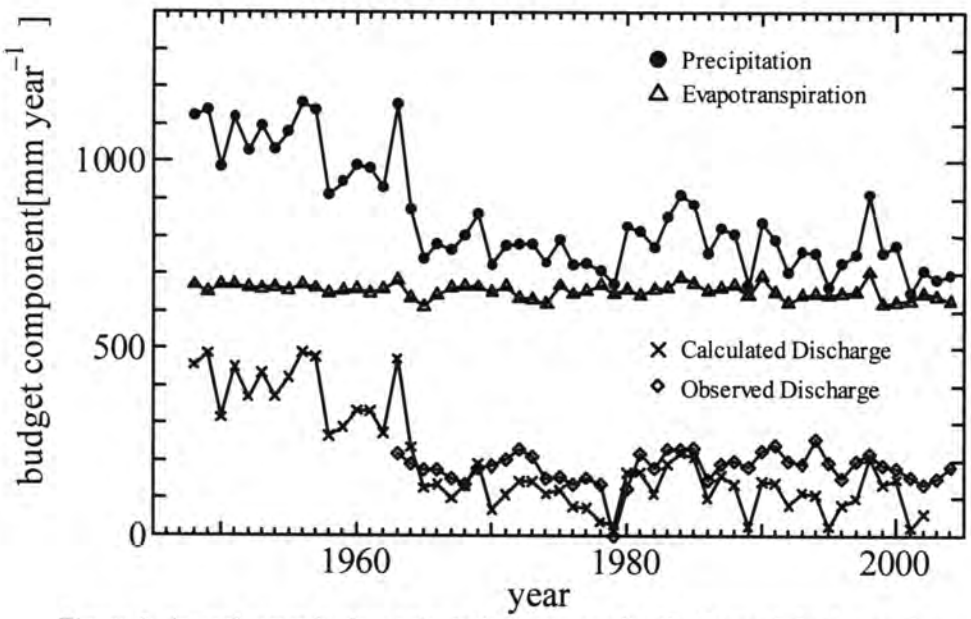

Figure 5. Annual water budget calculation compared with observed discharge data

Global Runoff Data Center (GRDC, http://grdc.bafg.de/servlet/is/987/). Annual trend of calculated discharge is roughly corresponding to the observed discharge. However, there is non-negligible discrepancy between measured discharge data and calculated discharge amount especially during the period from year 1990 to 2000. When we use these data as an input to the hydrological model, some modification to the precipitation and evapo-transpiration should be done.

For the purpose of detecting the evidence of impact of human activities on river discharges, I attempted to detect the drastic change of discharge regime. To do this, select any year within the annual discharge data set of interest, and the data set are split into two data sets: one is before the selected year and the other is after the selected year. And the significance of difference between two annual discharge data sets using Student's t-statistics (Oki, 1999, Press et al., 1993) was evaluated. The t-statistics for the difference of variance of two data sets (here, we define one data set as $x_i(i=1,N_x)$, and the other data set as $y_i(i=N_y)$) is defined as follows.

$$t = \frac{\bar{x} - \bar{y}}{\left[\sigma(x)^2 / N_x - \sigma(y)^2 / N_y\right]^{1/2}} \tag{2}$$

Here, $\bar{x}$:mean of x_i, $\bar{y}$:mean of y_i, $\sigma(x)$:variance of x_i, and $\sigma(y)$: variance of y_i.

Figure 6 shows the significance of the t-statistic for the observed discharge at the Khabarovsk. Significance level is drastically decrease around early 1960's, but it does not go down below the level 0.01. Although it is difficult to identify the reasons, there might some important changes occured during early 1960's. If an assumption that there was no significant antholopogenic impact in the Russian part during early 1960's is correct, there is a possibility that some anthlopogenic impact has occured along the Songhua river. At least, the impact of dam construction on the discharge regime of middle and lower part of the Amur river is not

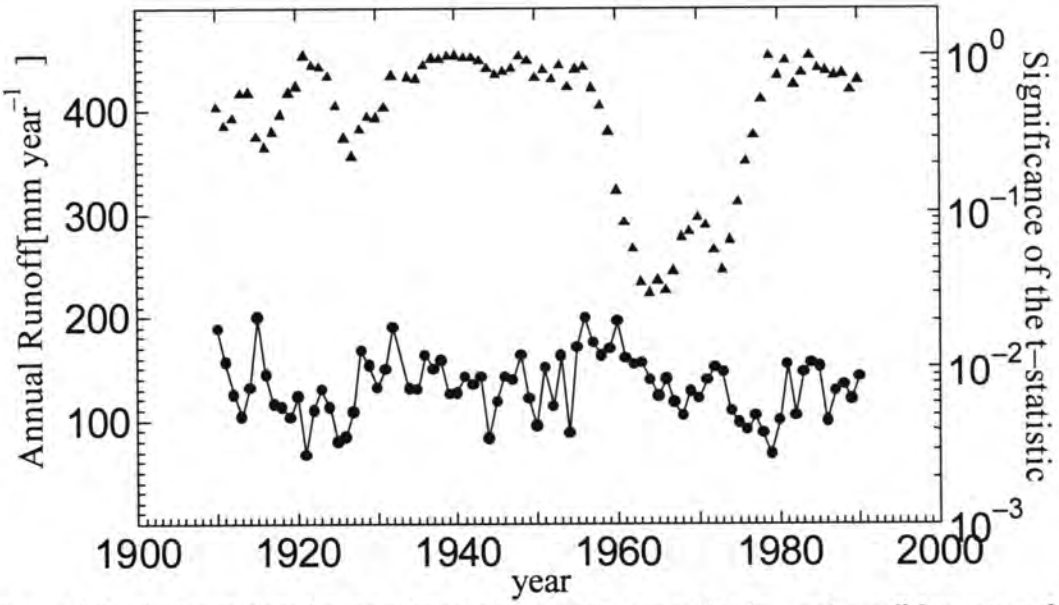

Figure 6. Student's t-statistic for the differecne between the two splitted annual runoff data sets at the Khabarovsk observation station

detected. However we can not reject a possibility of the dam impact on the discharge regime and dissloved iron productivity along the Zeya river basin, because Khabarovsk is about 1,000km downstream of the confluent point of the Zeya river and the Amur river. Thus, we should examine whether significant discharge change has occured along the Zeya river after the construction of dam.

3. CONSTRUCTION OF HYDROLOGICAL MODEL INCORPORATING DISSOLVED IRON TRANSPORT

As shown in Figure 7, hydrological model which incorporates the dissolved iron production consists of two steps according to the scale difference. First, using GETFLOWS (Tosaka et al. 2000) which is one of the distributed-physically based models, we construct a model which can simulate discharge regime and dissolved iron concentration simultaneously in the relatively small scale basin. Free ferrous iron is produced through continuous redox processes in soils. Though, redox processes are complex biogeochemical process, for N types of chemical species, N convection-dispersion system equations can be formulated in general. However, if we can identify N types of chemical species related to the free ferrous iron and dissolved iron production, we can not identify all parameters. Thus, in our model, we only consider the exchange between dissolved iron and iron absorbed to the solid phase in soils. Through the optimization process, we identify parameters which can describe dissolved iron production from each landuse such as wetland, forest, paddy fields, and dryland. This step is now under progress. Based on parameters for each landuse which are identified by the first step, hydrological model for the whole catchment scale is going to be constructed.

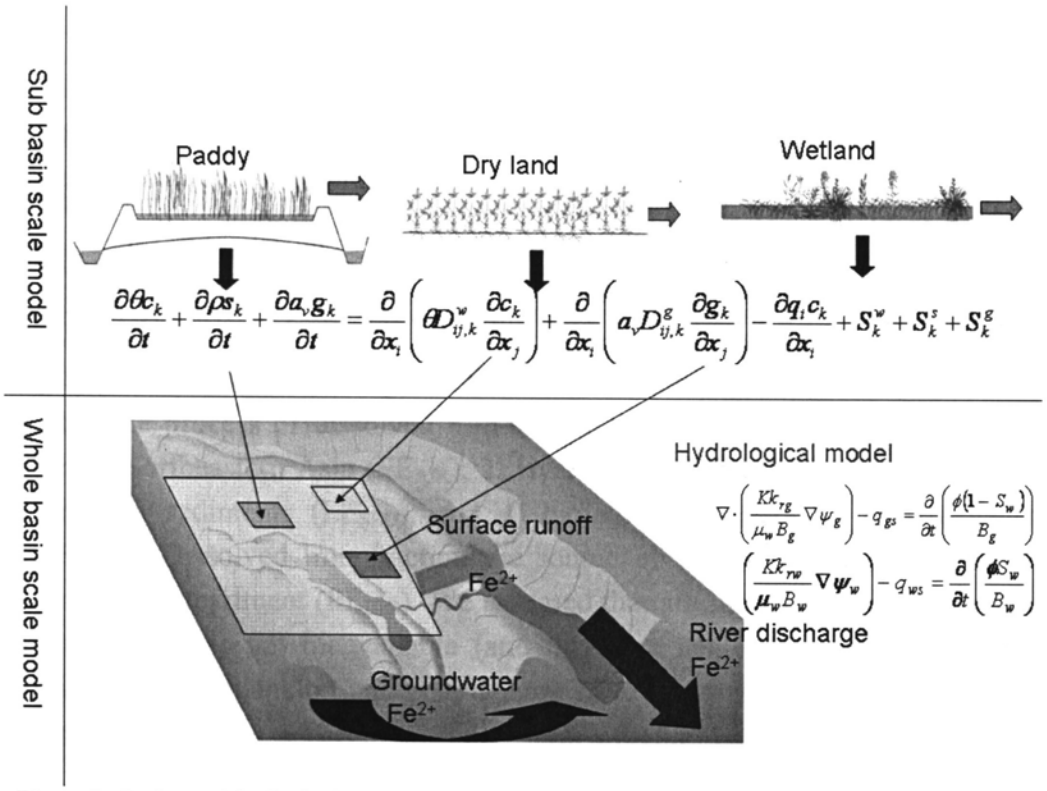

Figure7. Outline of the hydrological model which incorporate the mechanisim of dissolved iron production

4. SUMMARY

In this report, first, relationships between dissolved iron concentration of main tributaries of the Amur river basin and topographic indices of a catchment area of each tributaries are examined. There was no clear relationship between dissolved iron concentration and topographic index. It is supposed that other factors such as soil types or hydraulic conductivity are dominant to control dissolved iron concentration. Second, a possibility of impact of human activities on runoff regimes of the Amur river is examined using Student's t-statistics. The construction of the Zeya dam has no distinct impact on the discharge regime of the middle and lower reach of the Amur River. Third, outline of the hydrological model which incorporates dissolved iron transport mechanism is explained.

REFERENCE

Beven, K.J., Kirkby, M.J. (1979): A Physically-based variable contributing model of basin hydrology, Hydrolgical Science Bulletin, **24(1)**, pp.43-69

Ducklow, H.W., Oliver, J.L. and Smith Jr. W.O. (2003): The role of iron as a limiting nutrient for marine plankton processes, 'Interaction of the major biogeochemical cycles (Melillo, J.M., Field, C.B. and Moldan, B. Eds,)', Island Press, pp.295-310, Washington.

Oki T., and Mushiake K. (1999): Construction of the global river discharge dataset and the analysis of annual river discharge fluctuation characteristics, *Journal of Hydroscience and Hydraulic Engineering*, **43**, pp.151-156 (In Japanese)

Press, W.H., S.A. Teukolsky, W.T. Vetterling and B.P. Fannery (1993): Numerical recipes in C (Japanese version), pp.452-457

Shibata H., Konohira E., Satoh F. and Sasa K. (2004): Export of dissolved iron and the related solutes from terrestrial to stream ecosystems in northern part of Hokkaido, northern Japan, In, 'Report on Amur-Okhotsk Project: Proceedings of the Kyoto workshop 2004', Research Institute for Humanity and Nature, pp.87-92, Kyoto.

Tosaka H., Itoh,K., and Furuno T. (2000): Fully coupled formulation of surface flow with 2-phase subsurface flow for hydrological simulation, Hydrol. Process, **14**, pp.449-464

A LOWER TROPHIC ECOSYSTEM MODEL INCLUDING IRON EFFECT IN THE OKHOTSK SEA

OKUNISHI T.[1] AND KISHI M. J.[2]

[1] *Graduate School of Engineering, Hokkaido University*

[2] *Graduate School of Fisheries Sciences, Hokkaido University*

ABSTRACT

We applied a three dimensional ecosystem - physical coupled model including iron effect to the Okhotsk Sea. In order to clarify the sources of iron, four dissolved iron compartments, based on the sources of supply, were added to Kawamiya et al. (1995)'s model (KKYS) to create our ecosystem model (KKYS-Fe). We hypothesized that four processes supply iron to sea water: atmospheric loadings from Northeastern Asia, input from the Amur River, dissolution from sediments and regeneration by zooplankton and bacteria. We simulated 1year, from 1 January, 2001 to 31 December, 2001, using both KKYS-Fe and KKYS. KKYS could not reproduce the surface nitrate distribution after the spring bloom, whereas KKYS-Fe agreed well with observations in the northwestern Pacific because it includes iron limitation of phytoplankton growth. During spring bloom, the main source of iron at the sea surface is from the atmosphere. The contribution of riverine iron to total iron utilized for primary production is small in the Okhotsk Sea. Atmospheric deposition, iron flux from sediment and regeneration of iron in the water column play an important role in maintenance of high primary production in the Okhotsk Sea.

MODEL DESCRIPTION

Material flows in our ecosystem model are shown in Fig. 1. This model is based on Kawamiya et al. (1995) (referred to as KKYS hereinafter), which is a nitrogen-based model with 6 compartments (phytoplankton; Phy, zooplankton; Zoo, nitrate; NO_3, ammonium; NH_4, Detritus; D, dissolved organic matter; DOM). Four iron compartments were added, separated according to source as shown in Fig.1 (KKYS-Fe), in order to clarify the sources of iron. We assumed that the process of dissolved iron-supply to the Okhotsk Sea are: 1) atmospheric loadings from Northeastern Asia (FE_{AIR}), 2) riverine input from the Amur River (FE_{RIV}), 3) dissolution from sediments (FE_{SED}), and 4) biological regeneration by zooplankton and bacteria (FE_{BIO}). Dissolved iron fraction the source of which cannot be identified is also included in this compartment (FE_{BIO}). We assumed that all dissolved iron is bioavailable and that particulate iron is not bioavailable (and therefore neglected in the model). We also suppose that the phytoplankton and zooplankton have the same iron/nitrogen ratio 0.044 in [nmol : μmol], assuming a carbon/nitrogen ratio of 106: 16 for phytoplankton, based on

Gregg (2002) and Gregg et al. (2003). We used the same iron/nitrogen ratio in the other compartments (Detritus, DOM).

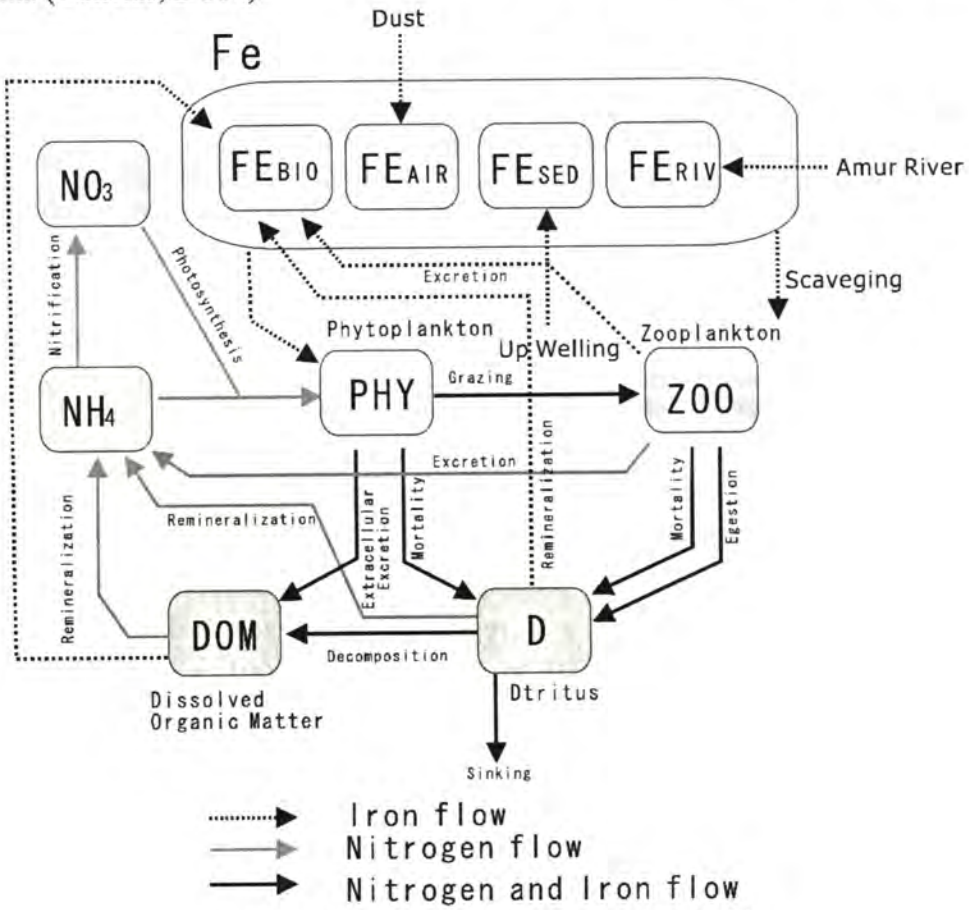

Figure 1: A schematic view of ecosystem model

FORMULATION OF ECOLOGICAL PROCESSES

Time evolution of each compartment is described as follows;

$$\frac{\partial C_i}{\partial t} = -v \cdot \nabla C_i + \nabla(K \nabla C) + (biological\ term) \quad (1)$$

where C_i is arbitrary compartments, v current velocity, and K diffusion tensor. The mathematical formulations for the nitrogen flow followed those of Kawamiya et al., (1995). The new and modified formulations are as follows;

Photosynthesis: Michaelis-Menten formula was adopted for iron uptake by phytoplankton. Noiri et al., (2005) reported that the half-saturation constant for iron is 0.59 nM (at 5 °C) and 0.58 (at 8 °C) for photosynthesis (>10 micro m size fraction) in the western subarctic Pacific. In this model, 0.58 was used for (K_{FFe}). Ammonium inhibition was taken into account (Wroblewski, 1977) in the original KKYS. We modified the half saturation constants (Moore et al., 2002) to account for the increased preference for ammonium under iron limitation. The half-saturation constant for nitrate uptake was increased to as much as 150% of its original value (Eqs.8 and 9) with increasing iron stress. Likewise, the half-saturation constant for

ammonium was decreased to 50% of its original value with increasing iron stress (Eqs. 8 and 9).

$$(\text{Photosynthesis}) = GPP(Phy, NH_4, NO_3, Fe, T, I) = V_{\max}\{\min(LIMITN, LIMETFe)\} \times \exp(kT)\frac{I}{I_{opt}}\exp\left(1-\frac{I}{I_{opt}}\right)Phy \quad (2)$$

$$I = I_0 \exp(-\Lambda|z|) \quad (3)$$

$$\Lambda = \alpha_1 + \alpha_2 \times Phy \quad (4)$$

$$LIMITN = \left\{\frac{NO_3}{NO_3 + K_{NO3}}\right\} \times \exp(-\Psi NH_4) + \frac{NH_4}{NH_4 + K_{NH4}} \quad (5)$$

$$LIMITFe = \frac{TFe}{FFe + K_{Fe}} \quad (6)$$

$$TFe = FE_{AIR} + FE_{RIV} + FE_{SED} + FE_{BIO} \quad (7)$$

$$TFe < K_{Fe} : \begin{matrix} K_{NO3} = K_{NO3} \\ K_{NH4} = K_{NH4} \end{matrix} \quad (8)$$

$$TFe \geq K_{Fe} : \begin{matrix} K_{NO3} = K_{NO3} \times 1.5 \\ K_{NH4} = K_{NH4} \times 0.5 \end{matrix} \quad (9)$$

where T is temperature, z is depth, positive upward (zero at the sea surface), I light intensity, I_{opt} optimum light intensity, I_0 photosynthetically active radiation (PAR) at the sea surface, Λ the light dissipation coefficient, and TFe total dissolved iron concentration. Notation for parameters is given in Table 1 with their values. Parameters used to describe other processes are also given in this table. Here, the fraction of iron uptake from each compartment (FE_{AIR}, FE_{RIV}, FE_{SED}, FE_{BIO}) is defined as follows to simplify later discussion.

$$RAFE = \frac{FE_{AIR}}{TFe},\ RRFE = \frac{FE_{RIV}}{TFe},\ RSFE = \frac{FE_{SED}}{TFe},\ RBFE = \frac{FE_{BIO}}{TFe} \quad (10)$$

Atmospheric iron flux: The main source of dissolved iron to surface water in most areas of the open ocean is dust deposited at the sea surface (Duce and Tindale, 1991). Atmospheric iron flux is added to the first layer of the model at each time step of the ecological calculation. Duce and Tindale (1991) estimated global atmospheric iron flux based on Donaghay et al. (1991), assuming that 3.5% (w/w) of the atmospheric dust contributes as iron flux. Fung et al., (2000) estimated an iron budget for the upper ocean using solubilities of 1% and 10 %. We assumed that 1 % of atmospheric iron is dissolved into the dissolved iron pool. We considered seasonal variation of iron flux by using the Gaussian function after Littmann (1991) .

Iron flux from the Amur River: The Amur River is one of the largest rivers in East and North-East Asia. It supplies significant freshwater to the Okhotsk Sea, is 4440 km long, and drains an area of 1,885,000 km^2. The minimum discharge is about 1,000 m^3 s^{-1} in March. Its discharge starts to increase in April, reaches a maximum (up to 200,000 m^3 s^{-1}) in September, gradually decreases in October, December, and then remains near the minimum level. The major part of the drainage area is underlain by boreal forest, mixed forest and swamps. Dissolved iron concentration of the Amur River is 0.56($\pm$0.17) mg L^{-1} (Shibata, 2005). It is well known that salinity plays important role in the aggregation process of dissolved iron at an estuary. Colloidal iron definitely plays a leading role in controlling the iron behavior in the

mixing process at estuaries, and its flocculation is responsible to the removal of the dissolved iron. Sholkovitz (1976) pointed out that 100% of riverine iron is precipitated by flocculation under the influence of oceanic salinities. On the other hand, about 93% of dissolved iron in Lena River was removed at the mouth of the Laptev Sea (Guieu et al, 1996). Predue *et al.* (1976) found a strong correlation between dissolved organic matter (fulvic acid) and iron concentration in natural waters. Figures *et al.* (1978) reported that organically-bound iron in river water can remain without sinking and is diffused into coastal water. Now, we assumed that 99 % of the riverine iron is lost in the estuary, so that 1 % of the riverine iron was the fluvial iron, and the dissolved iron concentration supplied to the Okhotsk Sea from the Amur River is 100 nM.

PHYSICAL MODEL

POM (Blumberg and Mellor, 1987; Galperina and Mellor, 1990) was used for the ocean model. This model is a three-dimensional, free surface, ocean model with a second moment turbulence closer scheme (Mellor and Yamada, 1982) to provide vertical mixing coefficients. The model domain extends from 34°N to 63°N and from 127°E to 166°E, which does not include the Japan Sea. The Soya and Tsugaru straits are closed, and grids shallower than 30 m depth are masked. The horizontal grid scale is 1/6°. POM uses a sigma coordinate system in the vertical. In deep area, sigma coordinate system cannot resolve adequately near the surface, because the layer thickness becomes large. Therefore, the fixed z-levels coordinate system is used for upper 10 levels, while lower 10 levels are sigma levels.

***Sea ice effect*:** In this study we used the NCAR Climate System Sea ICE Model (Bettge et al., 1996). The momentum dynamics in the above model are based on the model by Flato and Hibler (1992). The thermodynamics of ice growth and melting processes are taken from Semtner (1976), Parkinson and Washington (1979), Harvey (1988), and Pollard and Thompson (1994). Sea ice affects the momentum in the ocean model and the light under ice in the ecological model. The estimated momentum flux and light intensity under ice are as follows.

(Momentum flux under sea ice); Under the existence of sea ice, there is a momentum flux from the atmosphere to the surface water, via the sea ice. Momentum flux in the ocean model is $\tau_x = \tau_a + \tau_i$, τ_a is the moment flux from the atmosphere to surface water, τ_i is the moment flux from sea ice to surface water. Momentum flux from the atmosphere to surface water is described as: $\tau_a = \rho C_d W_x \sqrt{W_x^2 + W_y^2}\,(1 - IC/100)$ (23) where, ρ is sea water density, C_d is drug coefficient W_x is zonal wind speed, W_y is meridional wind speed, and IC is sea ice concentration in per cent. Momentum flux from the sea ice to surface water is described as: $\tau_i = \rho_w C_{Dw} |u_i - u_w| (u_i - u_w)(IC/100)$ (24) where ρ_w is surface water density, C_{Dw} is drug coefficient ($4*10^{-3}$), u_i is sea ice velocity, u_w is surface water velocity.

(Light condition under sea ice): The incident light strength under sea ice (I_d) is described as follows;

$$I_d = I_0(1-r)e^{-\alpha \cdot d} \times (1 - IC/100) \quad (25)$$

where, I_0 is the incident light strength at the surface of sea ice, r is the reflectivity at the sea ice surface, d is thickness of sea ice and α is the extinction coefficient of sea ice. Gilgert and Buntzen (1984) reported that the extinction coefficient in sea ice of 10 cm thickness was 0.025 cm^{-1}. We used this value. Ishikawa et al. (2003) reported the value of 0.04 as the reflectivity at the sea ice surface, and this value is used in our model. The thickness of sea ice is estimated by the sea ice model described above.

MODEL RUN

The simulation was conducted for one year from 1 January, 2001 to 31 December, 2001. In 2001 a large ice-coverage was observed in the Okhotsk Sea; maximum ice area was about 99% in the winter. The momentum fluxes are calculated with the zonal and meridional wind speeds from National Centers for Environmental Prediction and National Center for Atmospheric Research (NCEP / NCAR) reanalysis data (Kalnay et al., 1996). The model can reproduce the seasonal prevalence of sea ice in the Okhotsk Sea in 2001.

RESULTS AND DISCUSSION

Nitrate, Chl-a and iron concentration

Saitoh et al., (1996) showed that the spring bloom usually occurred between April and May in the Okhotsk Sea based on the monthly coastal zone color scanner (CZCS)-chlorophyll (Chl) imagery from 1978 until 1986. Figure 3 shows the time-dependent features of Chl-a concentrations and nitrate concentrations in the surface layer (0-20 m) at five stations (see Fig.2).

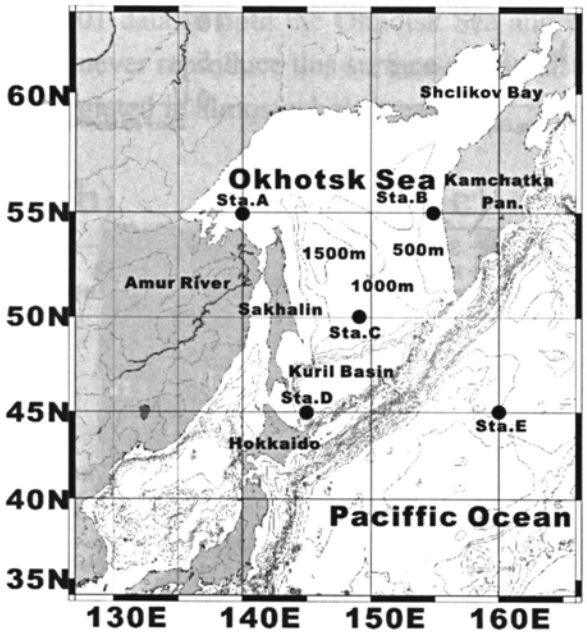

Figure 2: Staions for output of the model

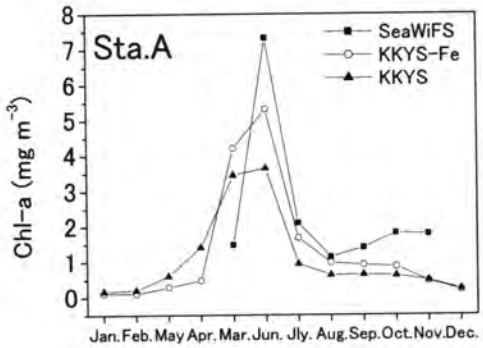
Sta.A
SeaWiFS
KKYS-Fe
KKYS
Chl-a (mg m-3)
Jan. Feb. May Apr. Mar. Jun. Jly. Aug. Sep. Oct. Nov. Dec.

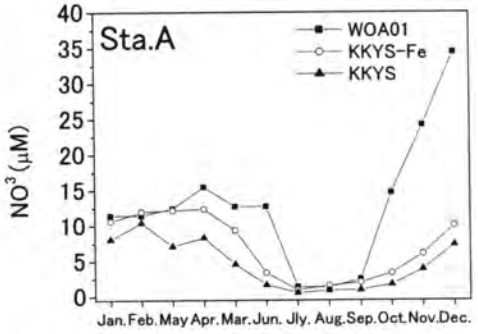
Sta.A
WOA01
KKYS-Fe
KKYS
NO3 (μM)
Jan. Feb. May Apr. Mar. Jun. Jly. Aug. Sep. Oct. Nov. Dec.

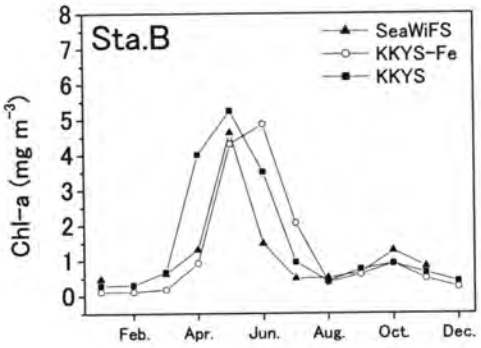
Sta.B
SeaWiFS
KKYS-Fe
KKYS
Chl-a (mg m-3)
Feb. Apr. Jun. Aug. Oct. Dec.

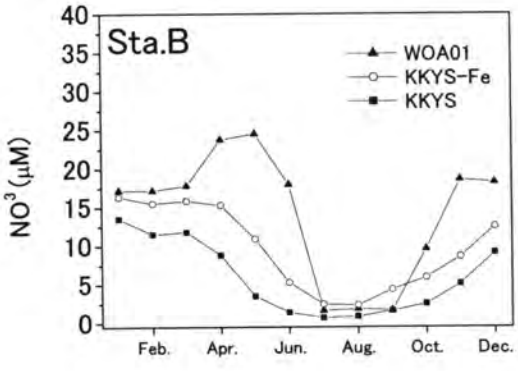
Sta.B
WOA01
KKYS-Fe
KKYS
NO3 (μM)
Feb. Apr. Jun. Aug. Oct. Dec.

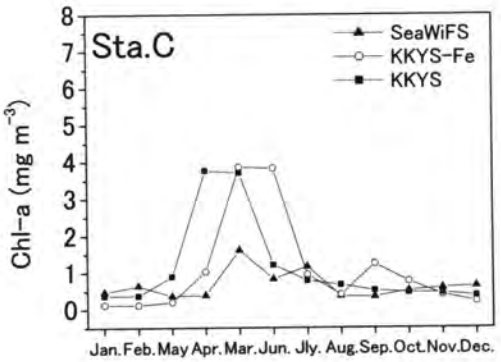
Sta.C
SeaWiFS
KKYS-Fe
KKYS
Chl-a (mg m-3)
Jan. Feb. May Apr. Mar. Jun. Jly. Aug. Sep. Oct. Nov. Dec.

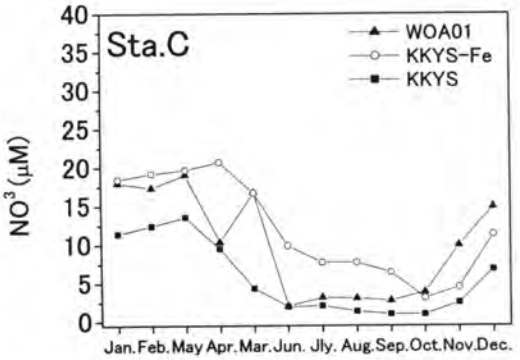
Sta.C
WOA01
KKYS-Fe
KKYS
NO3 (μM)
Jan. Feb. May Apr. Mar. Jun. Jly. Aug. Sep. Oct. Nov. Dec.

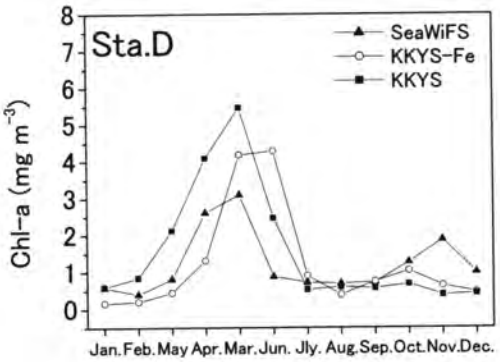
Sta.D
SeaWiFS
KKYS-Fe
KKYS
Chl-a (mg m-3)
Jan. Feb. May Apr. Mar. Jun. Jly. Aug. Sep. Oct. Nov. Dec.

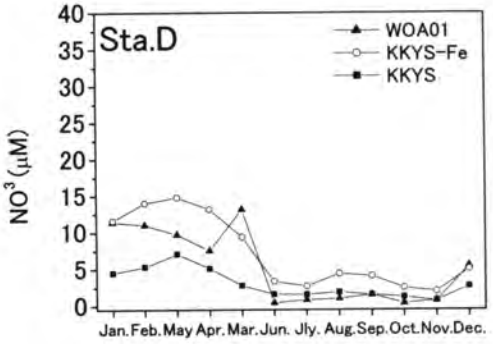
Sta.D
WOA01
KKYS-Fe
KKYS
NO3 (μM)
Jan. Feb. May Apr. Mar. Jun. Jly. Aug. Sep. Oct. Nov. Dec.

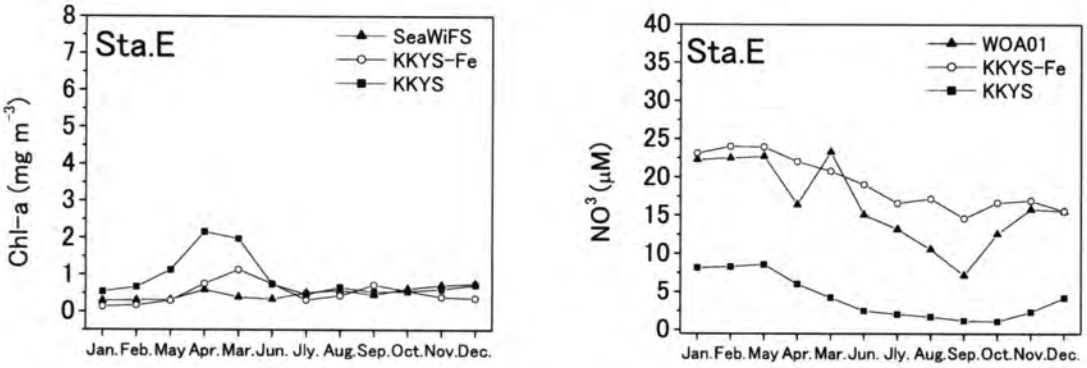

Figure 3: Time-dependent features of Chl-a and nitrate concentrations at the surface layer (20 m) in five study points shown Fig. 1. Left figures show Chl-a concentrations from SeaWiFS data, KKYS-Fe, KKYS. Right figures show nitrate concentrations from World Ocean Atlas data, KKYS-Fe, KKYS

Chl-a concentrations both by KKYS-Fe and by KKYS coincide to the time variation of SeaWiFS features in all stations. But the spring bloom peak by KKYS-Fe occurs slightly later than in SeaWiFS except for Sta. A. Nitrate concentrations by KKYS-Fe and KKYS also agree with the seasonal variation of WOA01's nitrate concentrations in all stations except at Sta.E. At Sta.E (northwestern Pacific) nitrate concentration by KKYS is underestimated, and Chl-a concentration is overestimated during the spring. Fig 4 shows sea surface nitrate distribution simulated by KKYS and KKYS-Fe together with the observed value from WOA 2001 in March. In March, before the spring bloom, results of KKYS-Fe agree well with the observation, but those of KKYS do not in the northwestern Pacific. As shown in Fig. 4 (a, b), nitrate concentration is relatively high in the northwestern Pacific. After the spring boom (July), the sea surface nitrate is depleted in almost all areas of the Okhotsk Sea and remain more than 5nM in the northwestern Pacific (Fig. 5a). KKYS-Fe' (Fig. 5b) shows almost the same features as the WOA 2001 data in both the Okhotsk Sea and the northwestern Pacific. On the other hand, KKYS can never reproduce this surface nitrate distribution either-(Fig. 5c), but the sea surface nitrate is depleted in almost whole areas.

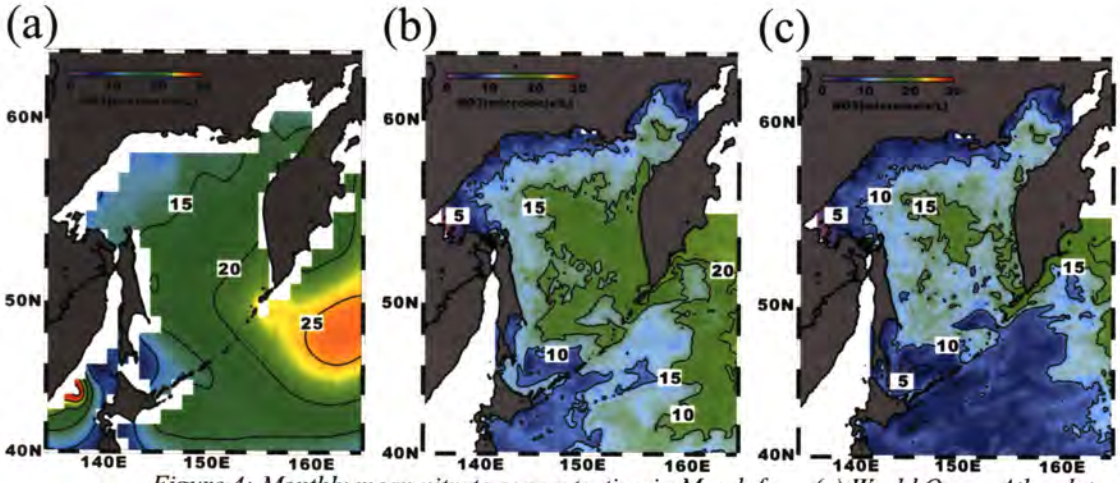

Figure 4: Monthly mean nitrate concentration in March from (a) World Ocean Atlas data, (b) KKYS-Fe and (c) KKYS in surface water (averaged from 0m to 20m).

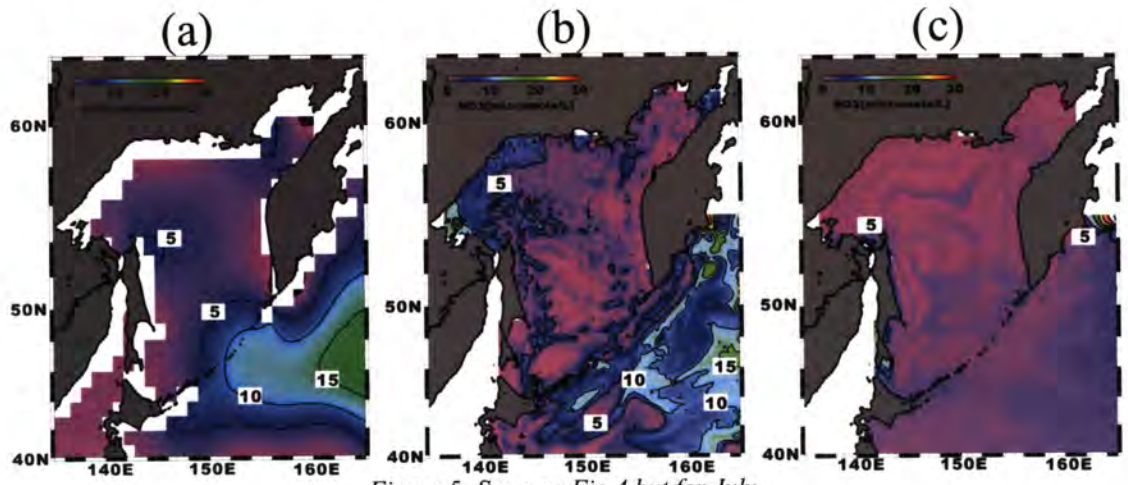

Figure 5: Same as Fig.4 but for July.

CONCLUSION

This study is the first to examine the iron sources in the Okhotsk Sea by using an ecosystem model including iron effect. Our results suggest that atmospheric deposition, iron flux from sediment and biologically regeneration of iron in water column play an important role in maintaining high primary production in the Okhotsk Sea. Contribution of atmospheric deposition of iron for primary production during the spring bloom in the Okhotsk Sea is extremely large, and biologically regenerated iron (FE_{BIO}) is as well through the year.

Table 1. The ecological model parameters values.

V_{max}	Max Photosynthesis Rate at 0℃	0.5	/day
k	k Temperature Coefficient for Photosynthetic Rate	0.063	/℃
I_{opt}	Optimum Light Intensity	80	W/m^2
K_1	Half saturation coefficient for light intensity.	0.0336	W/m^2
α_1	Light Dissipation Coefficient of Sea Water	0.035	/m
α_2	Self Shading Coefficient	0.0281	l/μmolN m
Ψ	Ammonium Inhibition Coefficient	1.5	l/μmol
K_{NO3}	Half Saturation Coefficient for Nitrate	3.0	μmol/l
K_{NH4}	Half Saturation Coefficient for Ammonium	0.5	μmol/l
K_{Fe}	Half Saturation Coefficient for iron	0.58	nmol/l
FENR	Fe/N Ratio to Phytoplankton	0.044	nmol/μmol
M_{P0}	Phytoplankton Mortality Rate at 0℃	0.0281	l/μmolN day
k_{MP}	Temperature Coefficient for Phytoplankton Mortality	0.069	/℃
M_{Z0}	Zooplankton Mortality Rate at 0℃	0.0585	l/μmolN day
k_{MZ}	Temperature Coefficient for Zooplankton Mortality	0.0693	/℃
γ	Ratio of Extracelluler Excretion to Photosynthesis	0.135	-
GR_{max}	Max Grazing Rate at 0℃	0.30	/day
k_g	Temperature Coefficient for Grazing	0.0693	/℃
λ	Ivlev Constant	1.4	l/μmolN
Chl*	Threshold Value for Grazing	0.043	μmolN/l
α	Assimilation Efficiency of Zooplankton	0.7	-
β	Growth Efficiency of Zooplankton	0.3	-
V_{PI0}	Dtritus Decomposition Rate at 0° C (to Inorganic Nitrogen)	0.030	/℃
V_{PIT}	Temperature Coefficient for Dtritus Decomposition (to Inorganic Nitrogen)	0.0693	/day
V_{PD0}	Dtritus Decomposition Rate at 0° C (to DON)	0.030	/℃
V_{PDT}	VPDT Temperature Coefficient for Dtritus Decomposition (to DON)	0.0693	/day
V_{DI0}	VDI0 DON Decomposition Rate at 0° C	0.030	/℃
V_{DIT}	VDIT Temperature Coefficient for DON Decomposition	0.0693	/day
k_{N0}	kN0 Nitrification Rate at 0°C	0.030	/℃
k_{NT}	kNT Temperature Coefficient for Nitrification	0.0693	/day
S	Sinking velocity of Dtritus	10	m/day

REFERENCES

Bettge T. W., J. W. Weatherly, W. M. Washington, D. Pollard, B. P. Briegleb, W. G. Strand Jr., 1996. The NCAR CSM Sea Ice Model, NCAR Technical Note, TN-425+STR, National Center for Atmospheric Research, Boulder, Colorado, 30 pp.

Blumberg, A. F., Mellor G. L., 1987. A description of a three-dimensional coastal ocean circulation model. In: Heaps, N.S., Editor, Three-dimensional Coastal Ocean Models Coastal and Estuarine Sciences vol. 4, AGU, Washington, 1–16

Donaghay, P.L., Liss, P.S., Duce, R.A., Kester, D.R., Hanson, A.K., Villareal, T., Tindale, N.W., Gifford, D.J., 1991. The role of episodic atmospheric nutrient inputs in the chemical and biological dynamics of oceanic ecosystems. Oceanography, 4, 2, 62-70.

Duce, R.A., Tindale, N.W.,, 1991. Atmospheric transport of iron and its deposition in the ocean. Limnology and Oceanography, 36, 17155 - 1726

Figures, G., Martin, J. M., Meybeck, M., 1978. Iron behavior in the Zaire Estuary. Netherlands Journal of Sea Research 12, 329-337.

Flato, G. M. and W. D. Hibler, 1992. Modeling pack ice as cavitating fluid. J. Phys. Oceanogr. 22, 626-651.

Fung, I.Y., Meyn, S.K., Tegen, I., Doney, S.C., John, J.G., Bishop, J.K.B., 2000. Iron supply and demand in the upper ocean. Global Biogeochemical Cycles, 14, 281–291

Galperina, B., Mellor, G. L., 1990. A time-dependent, three-dimensional model of the Delaware Bay and River system. Part 1: Description of the model and tidal analysis. Estuarine, Coastal and Shelf Science, 31, 231-253.

Gilgert, G. D., Buntzen, R. R., 1984. In-situ measurements of the optical properties of arctic sea ice. SPIE Vol.637 Ocean Optics 8, 232-263

Guieu, C., Huang, W-W., Martin, J-M., Yong, Y-Y., 1996. Outflow of trace metal into the Laptev Sea by the Lena River. Marine Chemistry, 53, 255-267

Harvey, L.D.D., 1988. Development of a sea ice model for use in zonally averaged energy balance climate models. J. Clim. 1, 1221-1238.

Ishikawa,N., Takizawa,A., Kawamura,T., Shirasawa,K. and Lepparanta,M., 2003. Changes of the radiation property with sea ice growth in Saroma Lagoon and the Baltic Sea. Report Series in Geophysics, 46, 147-160

Kalnay, E., Kanamitsu, M., Kistler, R., Collins, W., Deaven, D., Gandin, L., et al., 1996. The NCEP/NCAR 40-Year Reanalysis Project, Bull. Am. Meteorol. Soc., 77, 3), pp. 437–470

Kawamiya, M., Kishi, M. J., Yamanaka, Y., Suginohara, N., 1995. An ecological-physical coupled model applied to Station Papa. Journal of Oceanography, 51, 635-664

Littmann, T., 1991. Dust storm frequency in Asia: Climatic control and variability, Int. J. Climatol., 11, 393-412

Mellor, G. L., Yamada, T., 1982. Development of a turbulence closure model for geophysical fluid problems. Rev. Geophys. Space Phys., 20, 851-875

Moore J. K., Doneya, S. C., Kleypasa, J. A., Gloverb, D. M., Fungc, I. Y., 2002. An intermediate complexity marine ecosystem model for the global domain. Deep-Sea Research II, 49, 403–462

Noiri, Y., Kudo, I., Kiyosawa, H., Nishioka, J., Tsuda, A., 2005. Iron and temperature, two factors inXuencing phytoplankton species composition in the westerns subarctic PaciWc Ocean. Progress in Oceanography, 64, 149-166

Parkinson, C. L. and W. M. Washington, 1979. A large-scale numerical model of sea ice. J. Geophys. Res. 84, 311-337.

Pollard, D., and S. L. Thompson, 1994. Sea-ice dynamics and CO_2 sensitivity in a global climate model. Atmosphere-Ocean 32, 449-467.

Predue, E.H., Beck, K. C. and Reuter, J. H., 1976. Organic complexes of iron and aluminum in natural waters. Nature 260, 418-420.

Saitoh, S., Kishino, M., Kiyofuji, H., Taguchi S., Takahashi, M., 1996. Seasonal variability of phytoplankton pigment concentration in the Okhotsk Sea. Journal of the Remote Sensing Society of Japan, 16, 86-92

Semtner, A. J., 1976. A model for the thermodynamic growth of sea ice in numerical investigations of climate. J. Phys. Oceanogr. 6, 379-389

Sholkovitz, E.R., 1976. Flocculation of dissolved organic and inorganic matter during the mixing of river water and seawater. Geochimica et Cosmochimica Acta, 40, 831-845.

Shibata, H., 2005. Process of iron transport from terrestrial ecosystem to river: - Preliminary analysis of spatial and temporal patterns of iron concentration in Amur River -, Proceeding of the Inter national Kyoto Symposium 2005, Report on Amur-Okhotsk Project No.3, December 2005, 97-104.

Wroblewski, J. S., 1977. A model of phytoplankton plume formation during Oregon upwelling. J. Mar. Res., 35, 357–394

アムール・オホーツクプロジェクト会報誌 第４号

Report on Amur-Okhotsk Project No.4

Amur river from Khabarovsk, Aug 2006

Research Institute for Humanity and Nature (RIHN)
Inter-University Research Institute Corporation
National Institutes for the Humanities

Project 2-3
Human Activities in Northeastern Asia and Their Impact to the Biological Productivity in North Pacific Ocean

Edited by : T. SHIRAIWA
Published by : Amur-Okhotsk Project

For further contact :
Amur-Okhotsk Project Office
Research Institute for Humanity and Nature
http://www.chikyu.ac.jp